



SAPIENZA
UNIVERSITÀ DI ROMA

FACOLTÀ DI INGEGNERIA CIVILE E INDUSTRIALE

DIPARTIMENTO INGEGNERIA CHIMICA, MATERIALI E AMBIENTE
Corso di Dottorato in Ingegneria Elettrica, dei Materiali e delle Nanotecnologie
XXXI Ciclo

Tesi di Dottorato:

**SPATIO-TEMPORAL VARIABILITY ANALYSIS
OF TERRITORIAL RESISTANCE AND RESILIENCE
TO RISK ASSESSMENT**

Dottoranda:
Monica Cardarilli

Relatori:
Prof.ssa Mara Lombardi
Prof. Giuseppe Raspa

Correlatore:
Geol. Angelo Corazza

ANNO ACCADEMICO 2018-2019

*“There are two days in the year
that we can not do anything,
yesterday and tomorrow”*

- Mahatma Gandhi -

Abstract

Natural materials, such as soils, are influenced by many factors acting during their formative and evolutionary process: atmospheric agents, erosion and transport phenomena, sedimentation conditions that give soil properties a non-reducible randomness by using sophisticated survey techniques and technologies. This character is reflected not only in the spatial variability of soil properties which differ punctually, but also in their multivariate correlation as function of reciprocal distance.

Cognitive enrichment, offered by the response of soils associated with their spatial variability, implies an increase in the evaluative capacity of contributing causes and potential effects in the field of failure phenomena.

Stability analysis of natural slopes is well suited to stochastic treatment of the uncertainty which characterized landslide risk. In particular, the research activity has been carried out in back-analysis to a slope located in Southern Italy that was subject to repeated phenomena of hydrogeological instability - extended for several kilometres and recently reactivated - applying spatial analysis to the controlling factors and quantifying the hydrogeological susceptibility through unbiased estimators and indicators.

A natural phenomenon, defined as geo-stochastic process, is indeed characterized by interacting variables leading to identifying the most critical areas affected by instability. Through a sensitivity analysis of the local variability as well as a reliability assessment of the time-based scenarios, an improvement of the forecasting content has been obtained.

Moreover, the phenomenological characterization will allow to optimize the attribution of the levels of risk to the wide territory involved, supporting decision-making process for intervention priorities as well as the effective allocation of the available resources in social, environmental and economic contexts.

Preface

The basis of this research originally stems from my passion for developing methodologies concerning natural hazard analysis and risk assessment.

As the world moves further into disaster mitigation and emergency management trying to reduce the potential consequences in term of affected people, damage to critical infrastructure and disruption of basic services, there is the real need to actively contribute giving global society more tools aiming at increasing territorial resistance and resilience as much as reducing the impact of landslides thought a better understanding of its complex variability.

The case study was assigned for its huge extension and massive reactivations over time causing damages to downstream infrastructures as well as the interruption of mobility systems from and to the areas affected by the landslide events.

Following the recent execution of structural interventions along the landslide body and the numerous studies conducted to date by many authors on the same case study, a specific interest has been raised: how much the landslide hazard has been reduced and which areas are more susceptible towards a residual risk management planning.

The project was undertaken in strong collaboration with the Italian Civil Protection Department (DPC), where I undertook a traineeship in which an extensive investigation and data collection of the assigned case study has been accomplished followed by a field trip to the landslide site.

Furthermore, a second traineeship was conducted at the Joint Research Centre (JRC-Ispra) for reducing natural-hazard impacts on critical infrastructures by applying stochastic approaches and quantitative methodologies.

Finally, as member of the 'Young Scientists Programme' of Integrated Research on Disaster Risk (IRDR), the research has acquired a multi-disciplinary character benefiting from a joint network of scientific exchange and professional cooperation.

For these reasons, I would thank you all the supervisors and working groups for their guidance and support during these years without whose cooperation I would not have been able to conduct this research activity.

Contents

Abstract	3
Preface.....	4
Introduction.....	7
Chapter I.....	10
The Factor of Safety (FS)	10
1.1 Safety in Engineering	10
1.2 Slope Stability as Safety Condition.....	10
1.3 Probability of Failure	12
1.4 Slope Stabilization.....	13
Chapter II	16
Characterization of Soil Uncertainty	16
2.1 Sources of Soil Uncertainty.....	16
2.2 Soil Uncertainty Assessment.....	20
Chapter III.....	23
Stochastic Modelling of Soil	23
3.1 Statistical Analysis of Variability	23
3.2 Geostatistical Approach.....	25
3.2.1 Spatial variogram model.....	26
3.2.2 Kriging: spatial prediction method	29
3.3 Reliability Approach.....	32
3.3.1 Random variables	35
3.3.2 Monte Carlo Simulation: random process method.....	36
Chapter IV	38
Case Study: the Landslide of Montaguto (AV).....	38
4.1 Earthflow Phenomenon Description.....	38
4.1.1 Geography and historical activity	40
4.1.2 Geological and hydrological setting.....	42
4.1.3 Soil investigation and monitoring.....	48

4.1.4 Mitigation measures	51
4.2 Soil Characterization	53
4.2.1 Data collection	55
4.2.2 Categorization of data	65
4.2.3 Multivariate analysis	71
4.3 Spatial Variability Modelling	78
4.3.1 Variograms scales	81
4.3.2 Stochastic soil predictions.....	87
4.4 Slope Instability Assessment.....	112
4.4.1 Deterministic slope modelling.....	113
4.4.2 Probabilistic slope failure	120
4.4.3 Sensitivity analysis of variability.....	124
4.5 Stochastic Mapping of Slope Instability	137
4.5.1 Interventions as conditioning elements: Instability Prediction.....	138
4.5.2 Interventions as conditioning elements: Instability Simulation	142
Chapter V	144
Conclusions.....	144
References	149
Appendix 1.....	167
Kolmogorov - Smirnov test	167
Appendix 2.....	169
Regression model with interactions.....	169
Appendix 3.....	171
Statistics and probability distribution of soil properties.....	171
List of Figures	175
List of Graphs	178
List of Tables.....	180

Introduction

Worldwide in the last decade, a new vision and collective sensitivity have been affirmed on disaster risk reduction particularly on stability phenomena (St. Cyr, 2005) thanks to institutions and administrations action in territorial planning in which scientific community and research institutes have been providing fundamental support.

Mitigation policy of the impact of hydrogeological events is essentially based on two parallel and coordinated actions: the organization of interventions which guide social response in emergency contexts and the planning of preventive and protective decisional activities in delayed time (UNISDR, 2017a). In particular, satellite observation technologies of natural phenomena are increasing for a more successful outcome of preventive land management (Quanta Technology, 2009) in quiescent conditions, forecasting the potential effects induced on the areas of interest more accurately.

The increasing availability of data, acquired through modern and sophisticated systems and innovative detection processes, has been associated with application methods and elaborated through numerical modeling aimed at assessing extreme events (Rouaiguia and Dahim, 2013).

The use of new technologies, associated with a growing safety demand of society, makes the development of integrated technical and scientific methodologies necessary to guide predictive spatial planning through a reliable assessment of risk in heterogeneous and dynamic contexts such as those deriving from hydrogeological instability conditions (Ferlisi, 2013) with exogenous - often anthropogenic - origin.

Technological progress and technical-scientific knowledge should lead to improve quantitative analysis by carrying out a reliable probabilistic assessment (Li *et al.*, 2013) for characterizing spatial uncertainty and dynamic evolution of potential risk levels. In the same way, this concerns the need to implement a quantitative procedure for the estimation of the variables affecting scenarios in order to reduce risk to a residual value (Bhattacharya, Chowdhury and Metya, 2017).

These are needs that should meet coordinated investments aiming at synergistic activities to forecast catastrophic events particularly in susceptible territorial contexts (Rossi *et al.*, 2010) either in terms of extension or spatial distribution, considering evolution and duration as well. In fact, enrichment and quantitative cognitive improvement offered by soil response as well as evaluative capacity of

potential causes and expected effects should be adapted to the fragility of the specific area.

The development of applied research and technologies for mitigating “natural” risk in many countries provides wide and useful tools to achieve a more effective disaster risk reduction (Fisher *et al.*, 2014). The use of joint methodologies deriving from multi-disciplinary fields and integrated application methods, would allow to improve planning and safeguarding activities (Marx and Cornwell, 2001), giving a comprehensive risk assessment for natural hazards.

Landslides are among the most potentially manageable of all natural hazards, given the range of approaches and techniques that are available to reduce the level of hazard. There is much scope to reduce their impacts (UNISDR, 2017b). Landslide hazard is a function of susceptibility, as spatial propensity to landslide activity, and temporal frequency of landslide triggers, and its assessment may be done on local (individual slope), regional, national, continental, or even global scales (UNISDR, 2017a). The most appropriate method in each scale depends on the extent of the study area and on the available data (Nadim, Einstein and Roberds, 2005; Nadim *et al.*, 2006; Corominas and Moya, 2008). In any type of landslide hazard assessment, there is a need to consider topography and other factors that influence the propensity to landslide activity (susceptibility factors), as well as landslide triggering factors (precipitation, earthquakes, human activity).

Climate change increases the susceptibility of surface soil to instability because of abandoned agricultural areas, deforestation and other land-cover modifications. Anthropogenic activities and uncontrolled land-use are other important factors that amplify the uncertainty in landslide hazard assessment (Meusburger *et al.*, 2012).

Disasters may catalyse moments of change in risk management aims, policy and practice. Increasingly, the decision-making processes of the authorities in charge of reducing the risk of landslides and other hazards are moving from “expert” decisions to include the public and other stakeholders (Scolobig, Thompson and Linnerooth-Bayer, 2016).

Further, the Hyogo Framework of Action 2005–2015 and the Sendai Framework for Disaster Risk Reduction 2015–2030 emphasise the importance of improved resilience at national and local community level. The concept of resilience is variously defined but covers the capacity of public, private and civic sectors to withstand disruption, absorb disturbance, act effectively in a crisis, adapt to changing conditions, including climate change, and grow over time (Martin-Breen and Anderies, 2011) (Kervyn *et al.*, 2015).

Building resilience not only require accurate hazard estimates that account for spatial distribution, temporal frequency and hazard intensity, but also quantitative assessments of their impacts, as well as the evaluation of current social and cultural structures affecting the territorial vulnerability (Nakileza *et al.*, 2017). This is essential to identify effective adaptation strategies that are cost-effective, technically efficient, culturally acceptable and adapted to the livelihoods of the vulnerable populations.

In this research, a quantitative analysis has been carried out considering the probabilistic distribution of the most influential (Jaksa, 1995) spatial variables identified. In this way may be highlighted the presence of interdependence and potential mutual correlation of the conditioning parameters (Sarma, Krishna and Dey, 2015).

The acquisition of data and territorial information has been performed by considering different geo-environmental elements such as empirical measurements, instrumental monitoring, historical series and statistical databases, integrated to outline a cognitive framework.

A clear advantage is therefore the benefit of a deeper phenomenological knowledge, reorganizing the geo-information to complete implementation of procedures to conduct territorial planning and management as well as coordination of urgent interventions (Cardarilli, Lombardi and Guarascio, 2018).

Common methodologies currently associated with the characterization of instability phenomena of natural soils use semi-probabilistic approaches (Marx and Cornwell, 2001) often neglecting the spatial component. The aleatory uncertainty (Valley, Kaiser and Duff, 2010), belonging to every environmental context, has been recognized as component that may be characterized due to its intrinsic variability, often ignored (F. . Dai, Lee and Ngai, 2002).

To date, spatio-temporal references (Pebesma and Graeler, 2017) concerning mitigation and monitoring are lacking. Planning activities consist of heterogeneous scenarios (Phoon *et al.*, 2006a) and unconditional parametric sequences (Kim and Sitar, 2013) whose predictions do not depend on reliability considerations (Cho, 2013). Essential is therefore the introduction of methodologies which have long been using in mining field - Geostatistics - within hydrogeological context (Meshalkina, 2007).

Chapter I

The Factor of Safety (FS)

1.1 Safety in Engineering

The goal of safety is the preservation of existence of an individual or a community (Ferlisi, 2013). Although the term safety may be found in many laws, this does not necessarily mean that the content of the term is clearly defined (Metya, 2013), so many people have a different understanding of the term (Diamantidis *et al.*, 2006).

Some common descriptions are following presented (Proske, 2008):

- Safety is a state in which no disturbance of the mind exists, based on the assumption that no disasters or accidents are impending;
- Safety is a state without threat;
- Safety is a feeling based on the experience that one is not exposed to dangers;
- Safety is the certainty of individuals or communities that preventive actions will function reliably.

Safety requirements and safety concepts have a long history in some technical fields (Fleming and Leveson, 2015) especially concerning natural slope stability (Cheng, 2004).

1.2 Slope Stability as Safety Condition

A slope is a portion of soil which, for its topographic characteristics, may undergo a movement according to the gravity (Duncan, 1999).

Landslides can be triggered by many, sometimes concomitant causes. Seasonal rainfall is generally responsible of shallow erosion or reduction of shear strength (Kim *et al.*, 2004). In addition, landslides may be triggered by anthropic activities such as adding excessive weight above the slope, digging at mid-slope or at the foot (Kim, Jeong and Regueiro, 2012). Often, more than one triggering factor joins together to generate instability over time, which often does not allow a clear reconstruction of phenomenon evolution.

Causes	Phenomena	Possible Reasons
Increase in stresses	Natural actions	Erosion
		Seismic forces
		Water thrusts, Freezing
	Anthropic actions	Excavations
		Overloading
Decrease in resistances	Increasing pore water pressure	Meteorological events
		Groundwater excursion
	Variation of strength parameters	Changes in hydraulic conditions
		Alteration of rocks
	Soil degradation (softening, creep)	

Table 1 - Causes of soil movement (source: F. Dai, Lee and Ngai, 2002)

The term stability of a slope may be explained as a balance of the shear stresses, induced by the gravity on the mass of soil, to the available soil shear strength before collapsing (Duncan, 1999). In the practice, this equilibrium condition is numerically expressed as Factor of Safety (FS).

$$FS = \frac{\text{Available Soil Shear Strength}}{\text{Equilibrium Shear Stress}} \quad (1)$$

The main interest of slope stability is the assessment of FS along the potential failure slip surface where its results the lowest. According to this, a Factor of Safety equal to 1 indicates that the slope is at limit equilibrium; below 1 indicates an unstable slope that theoretically already should have failed, and consequently greater than 1 indicates stability (Duncan, 2000).

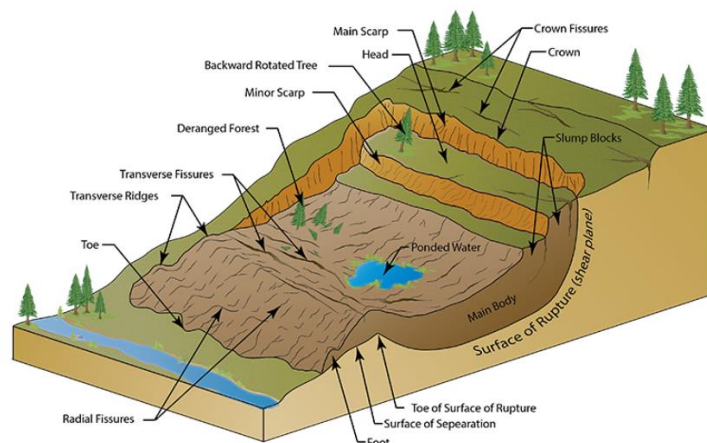


Figure 1 - Slope failure mechanism (source: Wyoming State Geological Survey)

The conventional safety factor depends on physical model, method of calculation, load conditions and soil parameters. Therefore, all these factors with their level of approximation of slope stability conditions, involve uncertainty in FS computation. Another factor concerns also the ability to find the critical slip surface both in term of geometry and position (F. C. Dai, Lee and Ngai, 2002).

In most cases, the most pronounced sources of uncertainty in a slope stability analysis concern soil strength and groundwater levels; a probabilistic evaluation of soil parameters may help in assessing the Factor of Safety (Zhang, 2010).

1.3 Probability of Failure

Engineers are very familiar with uncertainties especially in natural and environmental contexts. This leads to consider uncertainty in a probabilistic way for representing its randomness (Fallis, 2013).

A Probability Density Function (PDF) may be introduced to model the relative likelihood of a random variable. The PDF describes, in fact, the relative likelihood that the variable has a certain value within a range of potential values.

Since soil strength and applied loads are each subject to uncertainties, they may be considered as random variables as well as the Factor of Safety which results from their joint combination (Johari, Fazeli and Javadi, 2013). Based on the PDF of FS, the application of a probabilistic modelling gives also the distribution of FS values then the likelihood of failure.

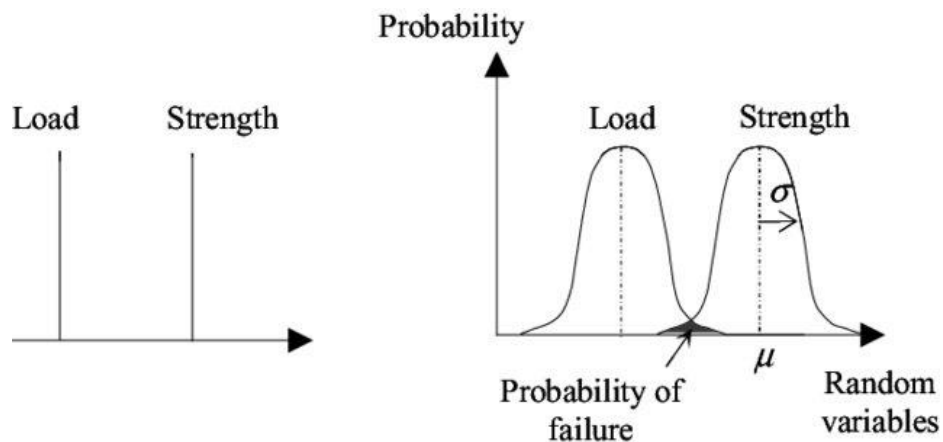


Figure 2 - Deterministic and Probabilistic distributions of Load and Strength
(source: Mustafa, Gelder and Vrijling, 2009)

The advantage of the probability model is that with appropriate considerations and assumptions the PDF extends beyond the information portrayed by the

observed data for the specific site, as well as other related factors. Caution must be exercised, however, to ensure the appropriateness of the PDF in representing the site and state of stability (Hsu, 2013).

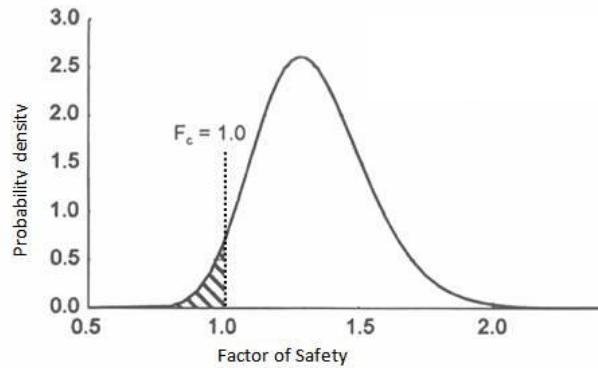


Figure 3 - Probability of Failure P(FS) (source: Johari and Javadi, 2012)

The relative contribution of different factors in slope failure should be kept in mind when a target probability is being selected (Diamantidis *et al.*, 2006). It makes little sense to reduce the computed probability of failure due to slope stability problems if other triggering causes are not addressed at the same time taking also in account past experiences and further studies performed until nowadays (Valley, Kaiser and Duff, 2010).

1.4 Slope Stabilization

Landslide mitigation generally consists of non-structural and structural activities aiming at reducing the probability of occurrence and/or the impact of landslide event on people and goods at risk (Popescu and Sasahara, 2005).

It is possible to consider a subdivision of stabilization interventions in relation to triggering factors and movement mechanism that each measure addresses (Popescu, 2001):

- Geometrical methods, in which the geometry of the slope profile is modified (slope inclination from the horizontal plane);
- Hydrogeological methods, in which an attempt is made to lower the groundwater level or to reduce the water content of the material by draining elements;
- Chemical methods, which increase the shear strength of the unstable mass by introducing internal slope reinforcements through additive materials;

- Mechanical methods, which introduce active external forces (e.g. anchors, or ground nailing) or passive (e.g. retaining walls, piles or reinforced ground) to counteract the destabilizing forces.



Figure 4 - Drainage system (left) and anchorage grid (right)
(sources: Weinstein Construction Corp and Dywidag systems)

Geometrical modification is the most common method that has been used, usually simple and less costly. The changing of the slope angle from steep slope to a gentler slope may increase the stabilization of slope mainly thought roughening, terracing and rounding. Moreover, the angle is usually supported by grass bonding together with soil. Vegetation has, in fact, a beneficial effect on slope stability by the processes of interception of rainfall, and transpiration of groundwater, thus maintaining drier soils and enabling some reduction in potential peak groundwater pressures.

This type of method does not require heavy load resistance and naturally stabilize the slope with the crepey grass surface which requires minimum maintenance.

Drainage concerns one of the slope failure factors: saturation degree and pore water pressure building up in the subsoil. A drainage system may minimize the instability by reducing the surface water and groundwater level with very effective increases of shear strength.

As a long-term solution, however, it suffers greatly because the drains must be maintained if they are to continue to function (Charles and Bromhead, 2008). In general, this method is very common and used in combination with other methods (Glade, Anderson and Crozier, 2012).

Surface drains may discharge more water, especially during heavy rain to avoid the effects of large amounts of water absorption by the slope.

Retaining structures are generally more expensive. However, due to its flexibility in a constrained site, it is always the most commonly adopted method. The principle of this method is to use earth-retaining structures to resist the

downward forces of the soil mass. It also may reduce rainwater infiltration and prevent slope erosion of the slope forming materials.

Over the last several decades, there has been a notable shift forward novel methods such as “internal stabilization” through consolidating additives (lime or concrete), grouting, soil nailing or reinforced grids which increase shear strength. The cost of these remedial measures is considerably lower when compared with the cost of classic structural solutions.

Within the general domain of the structural mitigation measures, they should firstly concern the specific site conditions as well as the economic cost often limited (Song *et al.*, 2014):

- Application of slope;
- Purpose of stabilizing;
- Time available;
- Accessibility of the site;
- Types of construction equipment;
- Cost of repair and maintenance;
- Sustainable environmental impact.

The experience shows that while one remedial measure may be dominant, most landslide repairs involve the use of a combination of two or more of the major categories.

However, the success of corrective slope regrading (fill or cut) is determined not merely by size or shape of the alteration, but also by position on the slope (Popescu and Sasahara, 2005).

Chapter II

Characterization of Soil Uncertainty

2.1 Sources of Soil Uncertainty

Many variables are involved in slope stability analysis as well as in the evaluation of Factor of Safety. It requires physical data on geologic materials and shear strength parameters (i.e. cohesion and angle of internal friction), pore water pressure, geometry of slope, unit weight, etc.

Soil components may affect locally the slope behaviour and globally the geomechanic response but, in addition, they are characterized by variability which leads to uncertainty (Garzón *et al.*, 2015).

The variability associated with soil is uncertain due to many reasons which lead to increasing uncertainty in slope stability as well. The associated uncertainty varies in each analysis and is case specific (Borgonovo, 2007). Soil uncertainties depends mainly on:

- Site topography and stratigraphy;
- Geology and geomorphology;
- Groundwater level;
- In-situ characteristics;
- Properties of materials;
- Mechanical behaviour.

Owing to the nature of soil, it is necessary to individuate and evaluate the uncertainties. Concerning slope stability assessment, the sources may be grouped into three main categories (Phoon *et al.*, 2006a), associated with:

- Measurement (laboratory and field investigations);
- Transformation (indirect relations between soil parameters, modelling);
- Inherent variability of ground conditions at the site (natural soil processes).

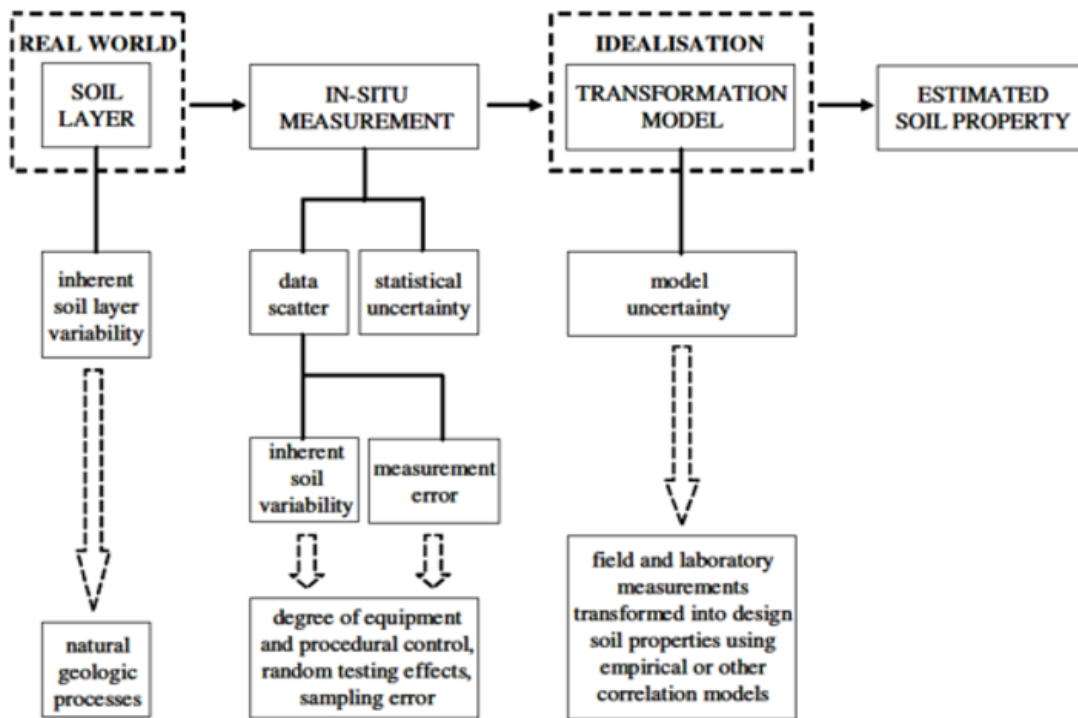


Figure 5 - Uncertainty diagram in soil property estimates (source: Phoon and Kulhawy, 1999)

The first source of uncertainty arises from the difficulty in measuring soil properties (i.e. geological, hydrogeological, geomechanical etc.). Any measurement involves errors due to equipment, procedural/operator sampling process, testing effects. This uncertainty may be minimised increasing tests' density, but it is commonly included within the measurement errors (Phoon, 1999).

Properties such as permeability, compressibility, shear strength, in a soil deposit, may show significant variations, even when located within homogeneous layers. On the other hand, in every investigative campaign, the volume of investigated and sampled soil represents a very small portion of the total volume of soil affected, and global behavior assessments must necessarily be made based on limited, often deficient, information (Phoon and Kulhawy, 1999).

The second one is introduced when field or laboratory measurements are transformed into design soil properties by using empirical or other correlation models. The relative contribution of these uncertainties clearly depends on the precision of the applied models (Phoon *et al.*, 2006a).

To date, the focus on technology has made it possible to increase the efficiency of the technical execution of surveys and to reduce the time of data acquisition as well. It has also improved and integrated the best experiences with empirical transformations of different variables characterizing soils.

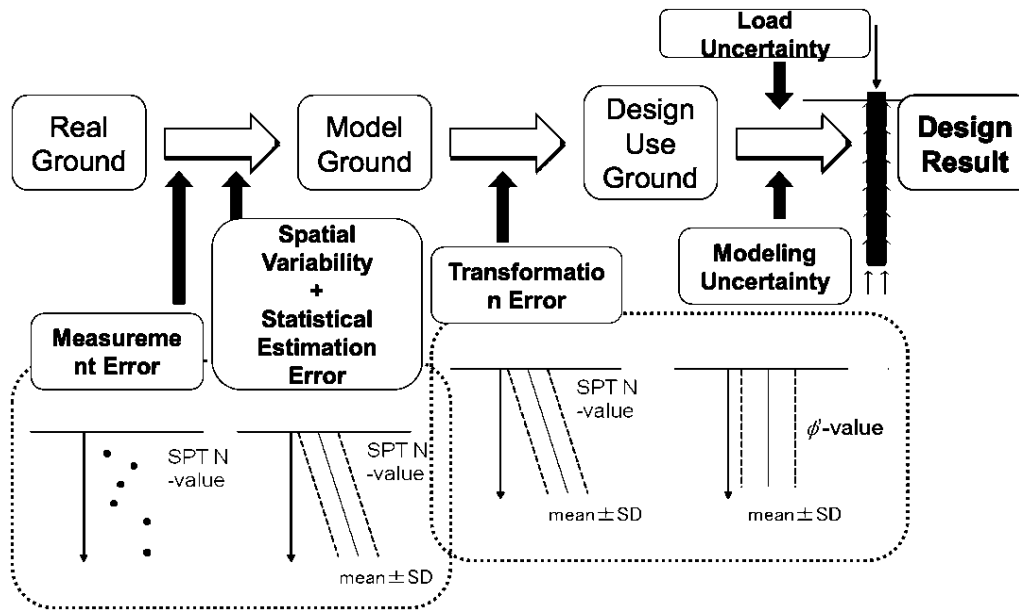


Figure 6 - Uncertainty diagram in geotechnical design process (source: Honjo and Otake, 2011)

Collectively, these two sources may be described as data scatter. Two types of uncertainty were identified. The first one was the *knowledge* or *epistemic* uncertainty which reflects lack of data, lack of information available about events and processes or lack of understanding real phenomena, reducible perfecting survey instruments and knowledge (Riesch, 2013).

Uncertainty due to naturally variable phenomena in time or space: "Uncertainties of nature"	Uncertainty due to lack of knowledge or understanding: "Uncertainties of the mind"
Natural variability	Knowledge uncertainty
Aleatory uncertainty	Epistemic uncertainty
Random/stochastic variation	Functional uncertainty
Objective uncertainty	Subjective uncertainty
External uncertainty	Internal uncertainty
Statistical probability	Inductive probability

Table 2 - Terms used in the literature to describe the duality of meaning for "uncertainty" (source: Muller, 2013)

The third type of uncertainty governs physical properties due to their composition and complex depositional processes over time which are involved in soil formation. The natural inherent character is unknown to designers and must be deduce from limited and uncertain observations.

The term used to define this third uncertainty is *natural* or *aleatory* which means non-reducible (Phoon and Kulhawy, 1996). It represents soil uncertainty over

time for phenomena that take place at a single location (temporal variability), or over space for phenomena which take place at different locations but in a single time (spatial variability), or both (spatial-temporal variability) (Phoon *et al.*, 2006a).

The final objective is the reconstruction of the physical model of the territory, basic for any further step of analysis. In fact, the quality of results obtained is strictly connected to the reliability and uncertainty of the source data.

Mac (2014) considers geological data affected by different estimation error depending on the type of data. This estimation error is connected primarily to a certain data dispersion, due mainly to:

- Intrinsic natural variations;
- System heterogeneity;
- Anisotropy of parameters;
- Sampling difficulties;
- Noise of natural system;
- Calculation system noise.

Therefore, due to the complexity of geological materials, it is important to consider the difficulty of modeling soil. Simplifications and conceptual assumptions are needed to define geotechnical models, trying to be as much effective as possible especially in design practice. The characterization of the reliability degree, however, turns out to be, in some contexts of analysis, indispensable (Johari, Fazeli and Javadi, 2013).

Finally, the factors triggering landslides are, by their nature, subject to a high degree of uncertainty.

Every scale of investigation, characterization and analysis of natural phenomena involves uncertainties that, directly or indirectly, must be considered. In most cases of slope analysis, uncertainty is associated with geotechnical parameters, geotechnical models, frequency, intensity and duration of triggering agents. The importance of different uncertainties depends on size and relevance of the specific site as well as the extension and from the quality of investigations and laboratory tests performed leading to inadequate representativeness of data samples due to time and space limitations. Another source of uncertainty is the temporal variability of parameters such as interstitial water pressure within the slope at different depths and especially along the potential sliding surface.

Ideally, we would like to have perfect knowledge of site conditions, but resources are limited. Expenditures must be commensurate with both the scope of design

and with the potential consequences of using incomplete and imperfect information in making decisions.

Excellent authors (Vanmarcke, 1980; Rethati, 1989; Christian, Ladd and Baecher, 1994; Lacasse and Nadim, 1996; Jaksa, Kaggwa and Brooker, 1999; Phoon and Kulhawy, 2001; Cassidy, Uzielli and Lacasse, 2008; Bond and Harris, 2008; Griffiths, Huang and Fenton, 2009; among others) focused on the need to develop new methods concerning spatial and temporal variability treatment of soil data which aim at optimizing their usage as well as providing a soil characterization and analysis as reliable as accurate.

2.2 Soil Uncertainty Assessment

It is often convenient in risk and reliability analysis to presume that some part of natural uncertainty is due to randomness. This allows to use probabilistic approaches to bear on a problem that might otherwise be difficult to address, incorporating probabilities of both aleatory and epistemic variability (Sarma, Krishna and Dey, 2015).

It is important to point out that the presumed randomness in this analysis is a part of the models, not part of the site geology. The assumption is not being made that site geology is in some way random: once a formation has been deposited or formed through geological time, the spatial distribution of structure and material properties is fixed (Zêzere *et al.*, 2004).

Probabilistic approach results crucial when evaluating, either at quantitative or qualitative level, hazard and consequences of a calamitous event potentially affecting people, environment, infrastructures, local activities and so on (Zhang, 2010).

A probabilistic approach to studying geotechnical issues offers a systematic way to treat uncertainties, especially in soil stability.

Deterministic slope stability analysis uses single value for each variable to calculate the Factor of Safety without evaluating the probability of failure (Alimonti *et al.*, 2017).

Different approaches try to evaluate soil variability. Relatively to the level of “knowledge” or complexity, they may be applied to the treatment of many problems depending on the relevance of design or, in this case, on the consequences of landslide events.

All methods assume soil parameters as variables that may be expressed as Probability Density Function (PDF). As a result, stochastic approaches, based on probabilistic analysis, provide useful and different information. They are

following listed and described according to the level of details provided (Vanmarcke, 1980):

- Semi-probabilistic (Level I);
- Probabilistic simplified (Level II);
- Probabilistic rigorous (Level III).

The first level proposes a probabilistic approach based on characteristic values of each design variables (resistances and loads), conceived as fractiles of the statistical distributions. The characteristic values (respectively R_k and E_k) are defined as lower/upper values which minimise safety, considering volume involved, field extension and laboratory investigations, type and number of samples and soil behaviour (Bond and Harris, 2008).

The second level of soil variability evaluation is the probabilistic simplified approach. In this method, FS may be interpreted in terms of probabilities or of suitable safety indices, leading to defining the probability of failure corresponding to FS less than or equal to 1 (Bond and Harris, 2008).

It assumes soil parameters as aleatory variables that may be expressed with PDF curves. An alternative way of presenting the same information is in the form of Cumulative Distribution Function (CDF), which gives the probability of a variable in having value less than or equal to a selected one.

This method attempts to include the effects of soil property variability giving, in addition to fractile, two more values per each uncertain parameter which characterized the PDF: sample mean value (μ) and sample standard deviation (σ) of the probabilistic distribution function, respectively measuring the central tendency of the aleatory variable and its deviation, the average dispersion of the variable from its mean value (Bond and Harris, 2008).

The normal or Gaussian distribution is the most common type of probability distribution function and respects the distribution of many aleatory variables conform to it (Jiang *et al.*, 2014). It is generally used in probabilistic studies in geotechnical engineering unless there are good reasons for selecting different distributions. Typically, variables which arise as a sum of several aleatory effects are normally distributed (Li *et al.*, 2011).

The problem of defining a normal distribution is to estimate the values of the governing parameters which are the true mean and the true standard deviation. Generally, the best estimates for these values are given by the sample mean and standard deviation, determined from a few tests or investigations. Obviously, it is desirable to include as many samples as possible in any set of observations but, in geotechnical engineering, there are serious practical and economic limitations to the amount of data which may be collected.

Therefore, this approach provides statistical values of soil parameters to stochastically evaluate soil natural variability. The FS obtained is a curve of probability distribution numerically expressing the probability of failure of slope equilibrium condition (Meyerhof, 1994).

The probabilistic rigorous approach performs probabilistic analysis considering not only measured values but also and especially its arrangement within the volume of soil explored. In fact, the claim of this method consists in providing a comprehensive statistical knowledge of all the variables that influence FS: soil parameters evaluated in three-dimensional context (Griffiths, Fenton and Tveten, 2002).

Another feature consists in soil inherent variability considered no more random. Based on probabilistic tools currently available, the analyses aim at a complete understanding of soil spatial laws is not feasible yet, remaining a pure theoretical reference. This underlines as the first two approaches are extremely reductive and approximate in soil characterization then in the evaluation of FS (Griffiths, Huang and Fenton, 2009).

Chapter III

Stochastic Modelling of Soil

Experience with panels of experts suggests that model uncertainty is among the least tractable issues dealt with. The difficult questions about model uncertainty have to do with underlying assumptions, with conceptualizations of physical processes, and with phenomenological issues. Failure processes involve strongly non-linear behaviours in considerations of time rates and sequences.

3.1 Statistical Analysis of Variability

Different types of mathematical models are built using different assumptions about natural phenomena. These different assumptions lead to different limitations in the applicability of models and specified boundary conditions. Thus, each model has an appropriate usage and scope dictated by the underlying assumptions. As the number of assumptions underlying a model increases, the scope narrows and accuracy and relevance of the model decreases (Hsu, 2013).

In natural science, quantitative methods represent the systematic empirical investigation of observable phenomena via statistical, mathematical, or computational techniques. They aim at developing and applying mathematical approach pertaining to natural phenomena, such as slope instability, by including (Huang *et al.*, 2013):

- The generation of models, theories and hypotheses;
- The development of instruments and methods for measurement;
- Experimental control and manipulation of variables;
- Collection of empirical data;
- Modelling and analysis of data.

Quantitative research is often contrasted with qualitative approach, which purports to be focused more on discovering underlying meanings and patterns of relationships (Lari, Frattini and Crosta, 2014), including classifications of types of phenomena and entities without involving numerical expression of quantitative relationships of data and observations.

Hazard Assessment Methods	Qualitative methods (Knowledge driven)	Field analysis	Inventory mapping
		Index or parameter methods	Combination or overlay of index maps
			Logical analytical models
	Quantitative methods (Data driven)	Statistical analysis	Bivariate statistical analysis
			Multivariate statistical analysis
		Mechanistic approaches	Deterministic analysis
			Probabilistic analysis
Neural network analysis			

Table 3 - Scheme of evaluation methodologies (source: Aleotti and Chowdhury, 1999)

Statistical models are the most widely used branch of mathematics in quantitative research. In particular, multivariate statistics starts with studies on causal and interacting relationships by evaluating factors that influence landslide phenomena while controlling other variables relevant to obtain experimental frequency and distribution of outcomes in failure regions.

Empirical relationships and mutual correlations may be examined between any combination of continuous and categorical variables by using some form of general linear model, non-linear model, or by using factor analysis (Pinheiro *et al.*, 2018).

Generally, in this context, to simplify analyses, analytical and transformation models are used to interpret results of site investigation using simplified assumptions and approximations. But, due to the complexity of soil formation and depositional processes, soil behaviour is seldom homogeneous (Svensson, 2014). In addition, the assessment of slope stability is based on approaches based on average/low/high values of soil properties, which may reduce the realistic content of the analyses carried out (Wang, Hwang, Luo, *et al.*, 2013).

Geologic anomalies, inherent spatial variability of soil properties, scarcity of representative data, changing environmental conditions, unexpected failure mechanisms, simplifications and approximations adopted in geotechnical models, as well as human factors (Diamantidis *et al.*, 2006) in stability assessment, are all factors contributing to uncertainty.

Soil components and their properties are inherently variable from one location to another in a three-dimensional space, due mainly to complex processes and effects which influence their formation (Lombardi, Cardarilli and Raspa, 2017).

Therefore, the evaluation of the role of uncertainty necessarily requires the implementation of stochastic methods more accurate (Li *et al.*, 2011).

3.2 Geostatistical Approach

The presence of such a spatial variability is the pre-requisite for the application of Geostatistics and its description is a preliminary step towards spatial prediction (Pebesma and Graeler, 2017). Geostatistics is a mathematical discipline which focuses on a limited number of statistical techniques to quantify, model and estimate the spatial variability of sparse sample data (Meshalkina, 2007). Therefore, it may allow to verify whether the simplified models and hypotheses of soil behaviour, used in the conventional approaches, are well-fitting (Valley, Kaiser and Duff, 2010).

Matheron (1963) stated that the model of spatial variation reflects an inherently random process that has generated the site. Nonetheless, it is convenient to structure the models as if some fraction of the uncertainty we deal with has to do with irreducible randomness and then to use statistical methods to draw inferences about the models applied to that natural variability.

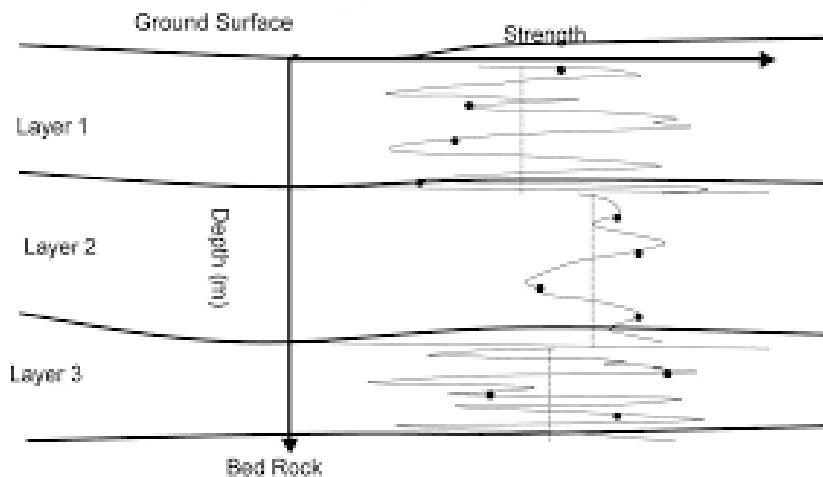


Figure 7 - Variability of soil profile (source: Honjo and Otake, 2011)

Before introducing geostatistical analysis, the concept of regionalised aleatory variable (AV) and Aleatory Function (AF) must be introduced (Matheron, 1963). An AV is a variable that may assume multiple values and whose values are randomly generated according to some probabilistic mechanism. The AV $Z(x)$ is also information-dependent, in the sense that its probability distribution changes as more data about the un-sampled value $z(x)$ become available.

The regionalised value $z(x_0)$ at the specific location x_0 is one realization of the AV $Z(x_0)$, which is itself a member of the infinite family of aleatory variables.

Therefore, the RV measured at each point is one of the possible results of the Aleatory Function: RV is a realization of AF.

This set of functions, given by the spatial nature of the phenomenon, represents the spatial law of AF $Z(x)$.

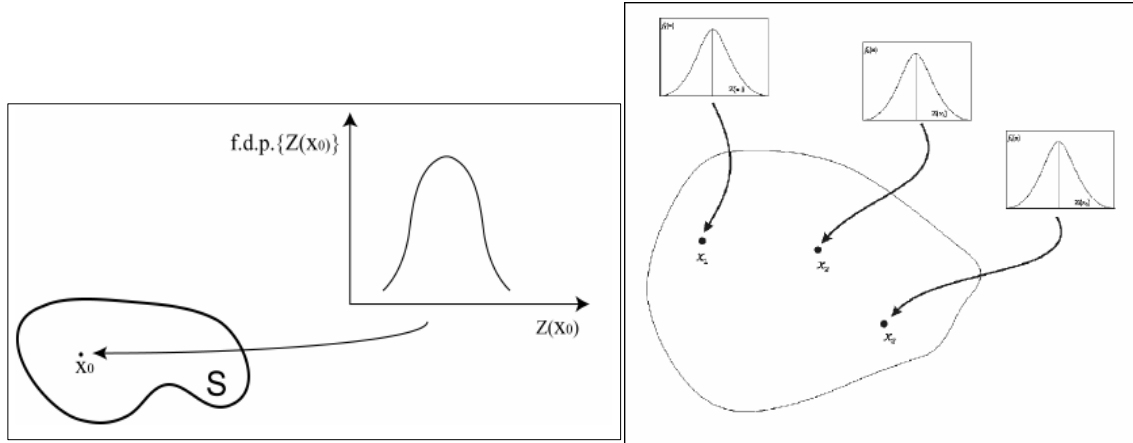


Figure 8 - Description of Aleatory Function in S domain (source: Kasmaeeyazdi *et al.*, 2018)

3.2.1 Spatial variogram model

It is the most common function of Geostatistics, used mainly in applications for characterizing spatial variability of regionalised phenomena (Matheron, 1973).

The variogram is defined as the variance of the increment:

$$[Z(x_1) - Z(x_2)] \quad (2)$$

It is written as:

$$2\gamma(x_1, x_2) = \text{Var} [Z(x_1) - Z(x_2)] \quad (3)$$

The function $\gamma(x_1, x_2)$ is then the semi-variogram.

In particular, weak stationarity models are based on the following two hypotheses:

$$E[Z(x)] = E[Z(x+h)] = m \quad (4)$$

$$\text{Var}[Z(x+h)-Z(x)] = 2\gamma(h) \quad \text{with} \quad \gamma(h) = C(0)-C(h) \quad (5)$$

which respectively mean: constant average value in the whole domain and covariance function invariant by translation. Therefore, the semi-variogram is dependent only on h .

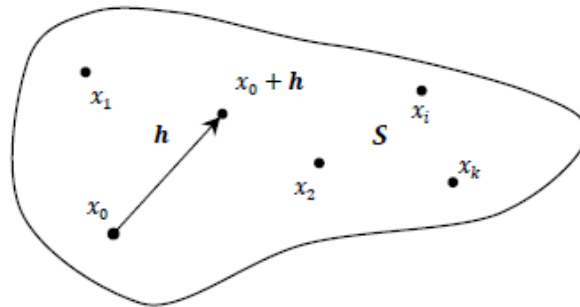


Figure 9 - Schematization of S domain and x_i values (source: Famulari, 2013)

Semi-variogram is the best way to describe spatial correlation for which data at two locations are correlated as function of their distance. It is usually defined *autocorrelation* or *correlation length* because referred to the correlation of a single variable over space (Matheron, 1963).

Generally, the variance changes when the space between pairs of sampled points increases, so near samples tend to be alike. For large spacing, experimental variogram sometimes reaches - or tends asymptotically to - a constant value (*sill*). It corresponds to the maximum semi-variance and represents the variability in the absence of spatial dependence (Guarascio and Turchi, 1977).

The distance after which variogram reaches the sill is the *range* and corresponds to the distance at which there is no evidence of spatial dependence. In case sill is only reached asymptotically, range is arbitrarily defined as the distance at which 95% of the sill is reached (Matheron, 1973).

The behaviour at very detailed scale, near the origin of the variogram, is very meaningful as it indicates the type of continuity of the regionalised variable.

Though the value of the variogram for $h = 0$ is strictly 0, several factors, such as sampling error, short scale variability or geological structures with correlation ranges shorter than the sampling resolution (Meshalkina, 2007), may cause sample values separated by extremely small distances to be quite dissimilar. This causes a discontinuity at the origin of the variogram, which means that the values of the variable change abruptly at the scale of detail. For historical reasons, this type of variogram behaviour is called *nugget effect*. It represents the variability at a point that cannot be explained by spatial structure (Matheron, 1963).

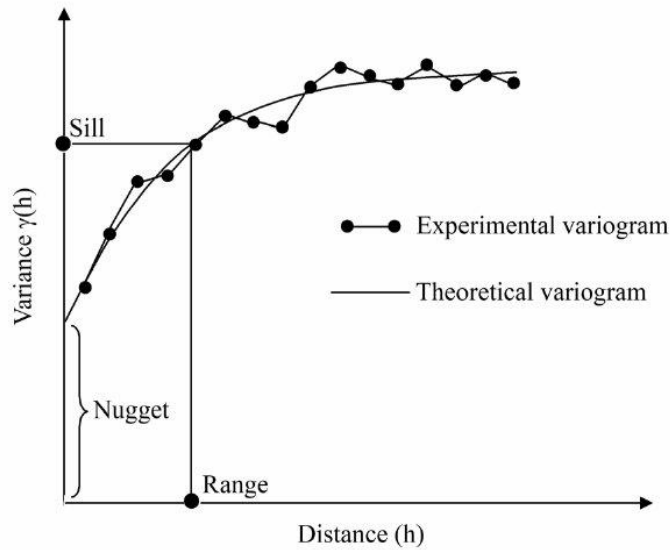


Figure 10 - Variogram parameters and function (source: Loots, Planque and Koubbi, 2010)

In Geostatistics, spatial patterns are usually described by using experimental variogram which measures the spatial dependence (correlation) between measurements, separated by h displacement (lag distance). The variogram is estimated from available values at sample points so it represents the degree of continuity of the soil property at different locations. In nature, generally, the values of a soil property at two close points are more likely similar than those far away from each other (Sidler, Prof and Holliger, 2003).

The description of spatial patterns is rarely a goal. Generally, there is the need to quantify spatial dependence for predicting soil properties at un-sampled locations. Therefore, it is necessary to fit a theoretical function which describes the empirical variogram of the spatial variability of sampled points as well as possible (Jaksa, 1995).

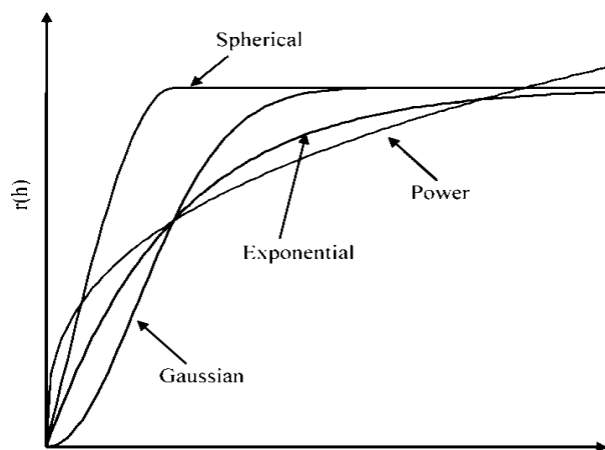


Figure 11 - Theoretical variogram functions (source: gisgeography.com)

Relatively to spatial analysis there is isotropy when the variogram depends on separation distance h between points instead of directional component (Matheron, 1973). If spatial correlation depends on spatial direction (angular direction), then the spatial process assumes anisotropic correlation. This is a common case in most cases concerning soil properties, due to sedimentation (Pebesma and Graeler, 2017) which often gives a preferential layers' orientation (the direction of maximum continuity will most likely be parallel to stratigraphy).

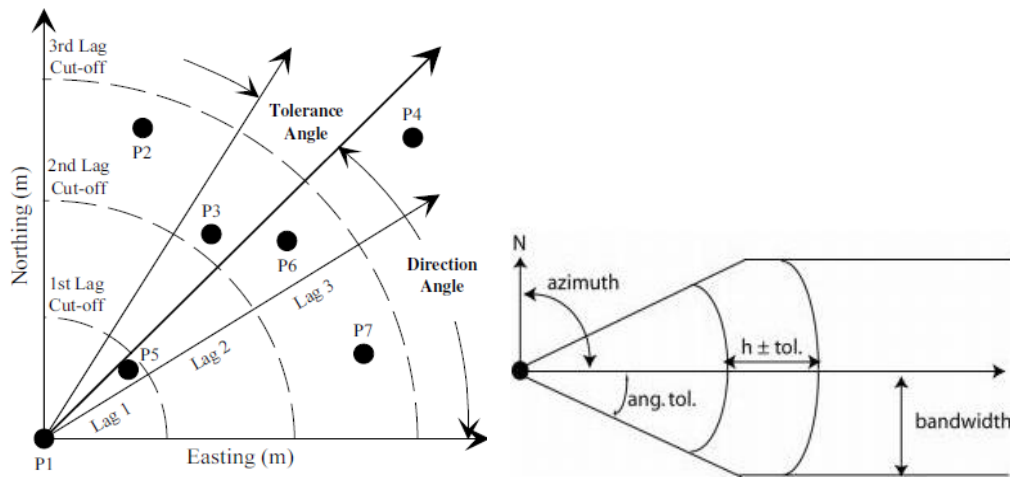


Figure 12 - Anisotropy characteristics and discretization (source: spatial-analyst.net)

3.2.2 Kriging: spatial prediction method

A problem common in site characterization is interpolating among spatial observations to estimate soil or rock properties (Sidler, Prof and Holliger, 2003) at specific locations where they have not been observed.

The main application of Geostatistics is the estimation and mapping of spatial soil properties in the un-sampled areas.

The most obvious way to proceed for spatial prediction at un-sampled locations is simply to take an average of the sample values available and assume that it gives a reasonable prediction at all locations in the region of interest. However, if it is known that the variable of interest tends to be spatially correlated, it would make sense to use a weighted average, with measurements at sampled locations that are nearer to the un-sampled location being given more weight (Matheron, 1963).

Kriging has been defined by Olea (2009) as “a collection of generalised linear regression techniques for minimising an estimation variance defined from a prior model for a covariance”. Kriging is just a generic name for a family of generalised

linear (least-squares) regression algorithms used to define the optimal weighting of measurements points in order to obtain a spatial prediction as much representative as possible at all un-sampled locations (Functions and Geostatistics, 1991). In Kriging the Euclidean distance is replaced by the statistical distance, which depends on the variogram model assumed (Matheron, 1973).

Kriging belongs to the category of stochastic methods, since it is assumed that measurements, both actual and potential, constitute a single realization of an aleatory (stochastic) process. One advantage of this assumption (Meshalkina, 2007) is that measures of uncertainty may be defined and hence, weights may be determined to minimise the measure of uncertainty. Indeed, much of the advantage of using geostatistical procedures, such as Kriging, lies not just in the point and block estimates they provide, but in the information concerning uncertainty associated with these estimates (Zhang *et al.*, 2013).

Kriging fits a mathematical function to a specified number of points, or all points within a specified radius, to determine the output value per each location. Kriging is a multistep process, it includes exploratory statistical analysis of data, variogram modelling, creating a surface and (optionally) exploring the variance surface (Matheron, 1973).

Oliver and Webster (2014) detailed the following key steps involved in Kriging method of geostatistical estimation:

- A structural study defining the semi-variogram;
- Selection of samples to be used in evaluating the elements;
- Calculation of the Kriging system of equations;
- Solution of the equations to obtain optimal weights;
- Use of results to calculate the estimates and the associated estimation variance.

Kriging weights the surrounding measured values for deriving a prediction of un-measured locations (Matheron, 1963). The general formula, applied to original data, consists of a weighted sum of the data:

$$Z^*(x_0) = \sum_{i=1}^n \lambda_i Z(x_i) \quad (6)$$

where:

$Z^*(x_0)$ = the predicted value at x_0 location (Kriging estimation);

$Z(x_i)$ = the measured value at i^{th} location;

λ_i = the unknown weight for the measured value at i^{th} location;

n = the number of measured values.

In Kriging, weights are based not only on Euclidean distance between measured points and prediction locations, but also on the overall spatial arrangement among observed points. These optimal weights depend, in fact, on the spatial arrangement and autocorrelation quantified (Functions and Geostatistics, 1991).

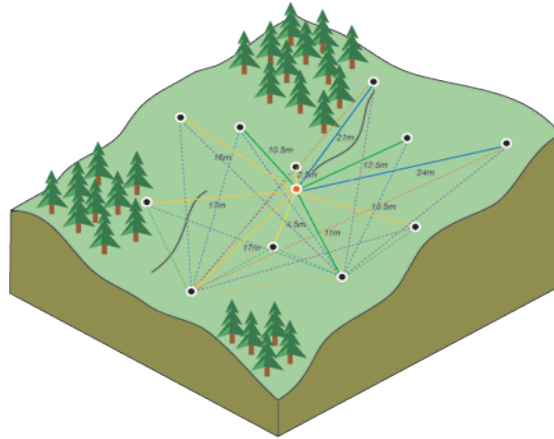


Figure 13 - Spatial prediction between unsampled point (red) and measured values (black)
(source: resources.esri.com)

The Kriging estimation is the best linear unbiased estimator (Viscarra Rossel *et al.*, 2010) of the $Z(x)$ if the properties in Table 4 are hold.

Estimator property	Definition
Unbiasedness	The expected value of $Z(x)$ over all ways the sample might have been realized from the parent population equals the parameter to be estimated
Consistency	$Z(x)$ converges to the parameter to be estimated
Efficiency	The variance of the sampling distribution of $Z(x)$ is minimum
Sufficiency	The estimator $Z(x)$ makes maximal use of the information contained in the sample observations
Robustness	The statistical properties of $Z(x)$ in relation to the parameter to be estimated are not sensitive to deviations from the assumed underlying PDF of Z

Table 4 - Properties of statistical estimators (source: Sigua and Hudnall, 2008)

Kriging is very popular in numerous scientific fields because its estimates are unbiased and have a minimum variance. Furthermore, this interpolation method may estimate errors associated with each prediction and its *correctness*, meaning that in a sampled point the estimated value is equal to the observed one, then the mean estimation error is null (Matheron, 1963). In this way Kriging provides also

the minimum estimation variance of errors, for which it is defined an *accurate* method (Matheron, 1973).

It appears evident that Kriging variance, as measure of precision, relies on the correctness of the theoretical variogram model assumed (Kasmaeeyazdi *et al.*, 2018). However (Sidler, Prof and Holliger, 2003):

- As with any method, if the assumptions do not hold, Kriging interpolation might be not representative of data measurements;
- There might be better non-linear and/or biased methods;
- No properties are guaranteed, when the wrong variogram is used. However typically a 'good' interpolation is still achieved;
- Best is not necessarily good: e.g. in case of no spatial dependence, Kriging interpolation is only as good as the arithmetic mean;
- Kriging provides a measure of precision. However, this measure relies on the correctness of the variogram.

Different Kriging methods for calculating spatial weights may be applied. Classical methods are (Oliver and Webster, 2014):

- Simple Kriging, it assumes stationarity of the first moment over the entire domain with a known zero mean;
- Ordinary Kriging, which assumes constant the unknown mean only over the neighbourhood of x_0 ;
- Universal Kriging, assuming a general polynomial trend model;
- Indicator Kriging, which uses indicator functions instead of the process itself, in order to estimate transition probabilities;
- Disjunctive Kriging, it is a nonlinear generalisation of Kriging;
- Lognormal Kriging, which interpolates positive data by means of logarithms.

Concerning phenomena in which the input is uncertain, also Reliability-based theory deals with stochastic modelling (Jiang *et al.*, 2014).

3.3 Reliability Approach

Reliability approach more widely deals with the estimation, prevention and management of engineering uncertainty and risks of failure (Huang *et al.*, 2013), understanding reliability of parameters and/or system.

Reliability is generally defined as the probability that a component will perform its intended function during a specified period of time under stated conditions (Wu *et al.*, 2013).

To combine the concept of reliability and to retain the advance of convenience for use like the conventional method of Safety Factor, the concept of safety factor of reliability is introduced.

Concerning FS, reliability approach attempts to account explicitly for uncertainties in load and strength and their probability distribution (Kim and Sitar, 2013).

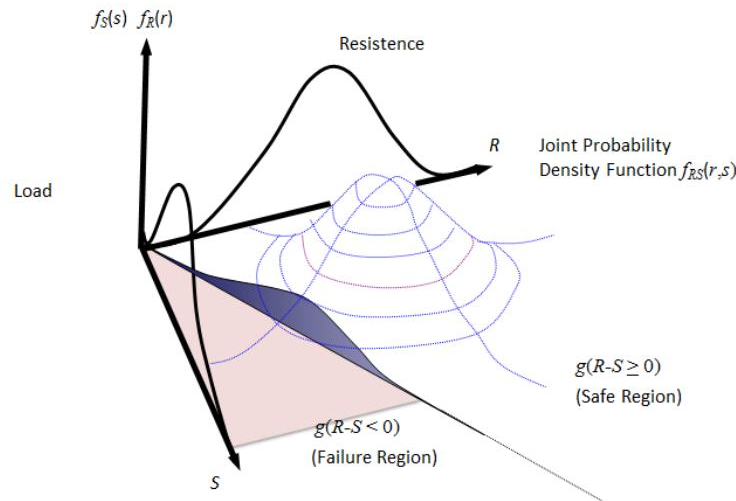


Figure 14 - Three-dimensional joint density function $f(R,S)$
(source: risk-reliability.uniandes.edu.co)

Reliability analysis deals with the relation between the loads a system must carry and its ability to carry those loads. Both the loads (S) and the resistance (R) may be uncertain, so the result of their interaction is also uncertain (Wu, 2013). It is common to express reliability in the form of Reliability Index (β), which may be related to Probability of Failure (p_f).

Failure occurs when $FS < 1$, and the Reliability Index is defined by (Belabed and Benyaghla, 2011):

$$p_f = P[FS < 1] = \phi(-\beta) \quad \beta = \frac{\mu_{FS} - 1}{\sigma_{FS}} \quad (7)$$

β is approximately the ratio of the natural logarithm of the mean FS (which is approximately equal to the ratio of mean resistance over mean load) to the coefficient of variation (COV) of FS (Phoon and Kulhawy, 1999).

A large value of β represents a higher reliability or smaller probability of failure (Usace, 2006). The reliability level associated with a Reliability Index β is approximately given by the Standard Normal Probability Distribution ϕ , evaluated at β , from Table 5.

Analysis Reliability Level	Reliability Index	Probability of Failure
High	5	0.0000003
Good	4	0.00003
Medium High	3	0.001
Medium Low	2.5	0.006
Low	2	0.0023
Unsatisfactory	1.5	0.07
Risky	1	0.16

Table 5 - Typical values of the Reliability Index and Probability of Failure
(source: Usace, 2006)

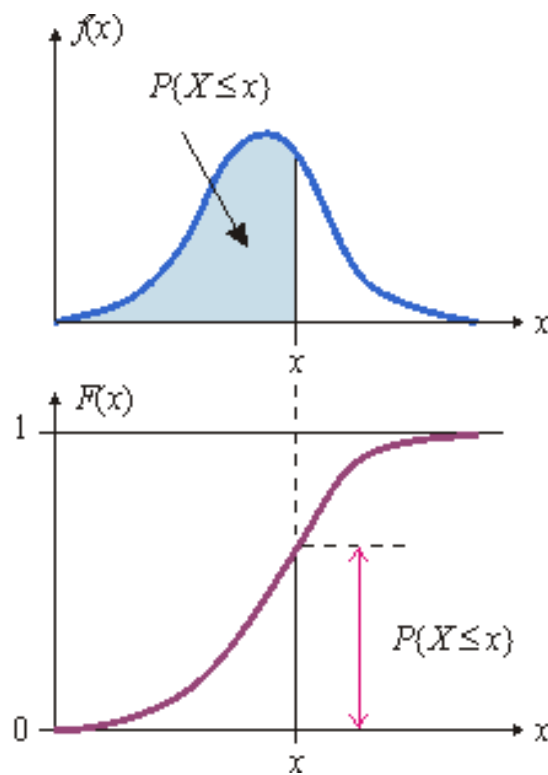


Figure 15 - Probability of exceedance (source: daad.wb.tu-harburg.de)

β index thus expresses the stability condition of a slope; if two slopes have the same FS, with different Reliability Index, they have different Probability of Failure (Manoj, 2016). Therefore, in order to calculate the probability of failure it is necessary to hypothesize, or however to know, the probability distribution of FS (Katade and Katsuki, 2009).

There are several methods in literature for assessing β and p_f , each having advantages and disadvantages (Low, 2003). Among the most widely used there are (Belabed and Benyaghla, 2011):

- The First Order Second Moment (FOSM) method. This method uses the first terms of a Taylor series expansion of the performance function to estimate the expected value and variance of the performance function. It is called a second moment method because the variance is a form of the second moment and is the highest order statistical result used in the analysis.
- The Second Order Second Moment (SOSM) method. This technique uses the terms in the Taylor series up to the second order. The computational complexity is greater, and the improvement in accuracy is not always worth the extra computational effort.
- The Point Estimate method. Rosenblueth (1975) proposed a simple and elegant method of obtaining the moments of the performance function by evaluating the performance function at a set of specifically chosen discrete points.
- The Hasofer–Lind method or FORM. Hasofer and Lind (1974) proposed an improvement on the FOSM method based on a geometric interpretation of the reliability index as a measure of the distance in dimensionless space between the peak of the multivariate distribution of the uncertain parameters and a function defining the failure condition. This method usually requires iteration in addition to the evaluations at $2N$ points.
- Monte Carlo Simulation (van Slyke, 1963). In this approach the analyst creates a large number of sets of randomly generated values for the uncertain parameters and computes the performance function for each set. The statistics of the resulting set of values of the function may be computed and β or p_f calculated directly.

The conventional safety factor depends on the physical model (Bowles, 1979), the method of calculation, and most importantly, on the choice of soil parameters. The uncertainty level associated with the resistance and load is not explicitly considered. Consequently, inconsistency is likely to exist among engineers and between applications for the same engineer. The use of a reliability index β may provide significant improvement over the use of the traditional design safety factor in measuring the reliability component (Abbaszadeh *et al.*, 2011).

3.3.1 Random variables

A random process model describes the generating mechanism of a physical phenomenon in probabilistic terms, from which is described the theoretically “correct” stochastic behavior of the phenomenon (Li *et al.*, 2011). This contrasts with an empirical model that simply fits a convenient, smooth analytical function to observed data with no theoretical basis for choosing the particular function.

A random variable is a mathematical model to represent a quantity that varies (Johari, Fazeli and Javadi, 2013). Specifically, a random variable model describes the possible values that the quantity may take on and the respective probabilities for each of these values (Huang *et al.*, 2013).

A probability is associated with the event that a random variable will have a given value. Random variables for each calculation are needed from a sample of random values (Hsu, 2013) which are based on the selected PDF which well fits the variable. Although these PDFs may take on any shape, normal, lognormal, beta and uniform distributions are among the most favored for analysis (Low, 2003).

The Normal distribution (also known as the Gaussian distribution) is the classic bell-shaped curve that arises frequently in datasets concerning geotechnical aspects and are used to estimate the PDF of FS. Thus, for uncertainties such as the average soil strength with random variations, the Normal pdf is an appropriate model (Papaioannou and Straub, 2012).

In many cases, there are physical considerations that suggest appropriate forms for the probability distribution function of an uncertain quantity. In such cases (Griffiths, Huang and Fenton, 2009) there may be available from which to construct a function cogent reasons for favoring one distributional form over another, no matter the behavior of limited numbers of observed data (Valley, Kaiser and Duff, 2010).

Much work in probability theory involves manipulating functions of random variables (Griffiths, Fenton and Tveten, 2002). If some set of random variables has known distributions, it is desired to find the distribution or the parameters of the distribution of a function of the random variables useful in generating random Normal variables for Monte Carlo Simulation (Danka, 2011).

3.3.2 Monte Carlo Simulation: random process method

Any simulation releasing on random numbers requires that there is some way to generate the random numbers (EPA, 1997). Statisticians have developed a set of criteria that must be satisfied by a sequence of random numbers. The value of any number in the sequence must be statistically independent of the other numbers (Hsu, 2013).

Monte Carlo technique may be applied to a wide variety of problems employed to study both stochastic and deterministic systems. This method involves random behavior and a number of algorithms are available for generating random Monte

Carlo samples from different types of input probability distributions (Harrison, 2010).

The Monte Carlo method is particularly effective when the process is strongly non-linear or involves many uncertain inputs, which may be distributed differently (Enevoldsen and Sørensen, 1994). To perform such a study, it generates a random value for each uncertain variable and performs the calculations necessary to yield a solution for that set of values. This gives one sample of the process. From a set of response realizations, it gives a picture of the response distribution from which probability estimates may be derived (Wu *et al.*, 1997).

The method has the advantage of conceptual simplicity, but it may require a large set of values of the performance function to obtain adequate accuracy. The major disadvantage is that it may converge slowly so it requires a large number of trials directed at either reducing error in sampling process or achieving a desired accuracy. Accurate Monte Carlo simulation depends also on reliable random numbers (Carlo and Galvan, 1992).

Furthermore, the method does not give insight into the relative contributions of the uncertain parameters that is obtained from other methods (Harrison, 2010), each run gives one sample of the stochastic process.

In slope stability context, Monte Carlo simulation produces a distribution of Factor of Safety rather than a single value (Belabed and Benyaghla, 2011). The results of a traditional analysis, using a single value for each input parameter may be compared to the distribution from the Monte Carlo simulation to determine the level of conservatism associated with the conventional design (Danka, 2011). By this procedure, values of the component variables are randomly generated according to their respective PDFs. By repeating this process many times, the Probability of Failure may be estimated by the proportion of times that FS is less than one (EPA, 1997). The estimate is reasonably accurate only if the number of simulations is large; also, the smaller the probability of failure, the larger the number of simulations that will be required (Gustafsson *et al.*, 2012).

Chapter IV

Case Study: the Landslide of Montaguto (AV)

4.1 Earthflow Phenomenon Description

Earth flows are among the most common mass-movement phenomena in nature (Keefer, D.K.; Johnson, 1983).

In Italy, earth flows affect large areas of the Apennine range and are widespread where clay-rich, geologically complex formations outcrop (Del Prete and Guadagno, 1988; Martino, Moscatelli and Scarascia Mugnozza, 2004; Bertolini and Pizziolo, 2008; Revellino *et al.*, 2010). Most of them are reactivations of ancient earth flow deposits; only few events are completely new activations (Martino and Scarascia Mugnozza, 2005; Revellino *et al.*, 2010).

Active earth flows generally manifest a seasonal and long-term activity pattern related to a regional climate pattern (Coe, 2012; Handwerger, Roering and Schmidt, 2013) with a higher susceptibility to movement, in the form of local landslides or major reactivations.

Earth flow response to rainfall or snowmelt, in terms of velocity fluctuations, is often delayed, and in several cases, long periods of cumulated precipitation are required to trigger a reactivation (Kelsey, 1978; Iverson, 1986; Iverson and Major, 1987).

Earth flows are generally identified by an upslope crescent-shaped or basin-shaped scar that is the source area, a loaf-shaped bulging toe that has a long narrow tongue- or teardrop-shaped form (Rengers, 1973; Keefer, D.K.; Johnson, 1983; Bovis, 1985; Cruden and Varnes, 1996; Baum, Savage and Wasowski, 2003; Parise, 2003). Earth flow has characteristic features that make it recognizable on the basis of morphological observation (Keefer, D.K.; Johnson, 1983; Fleming, Baum and Giardino, 1999; Parise, 2003; Zaugg *et al.*, 2016).

The length of an earth flow is commonly greater than its width and its width is greater than its depth.

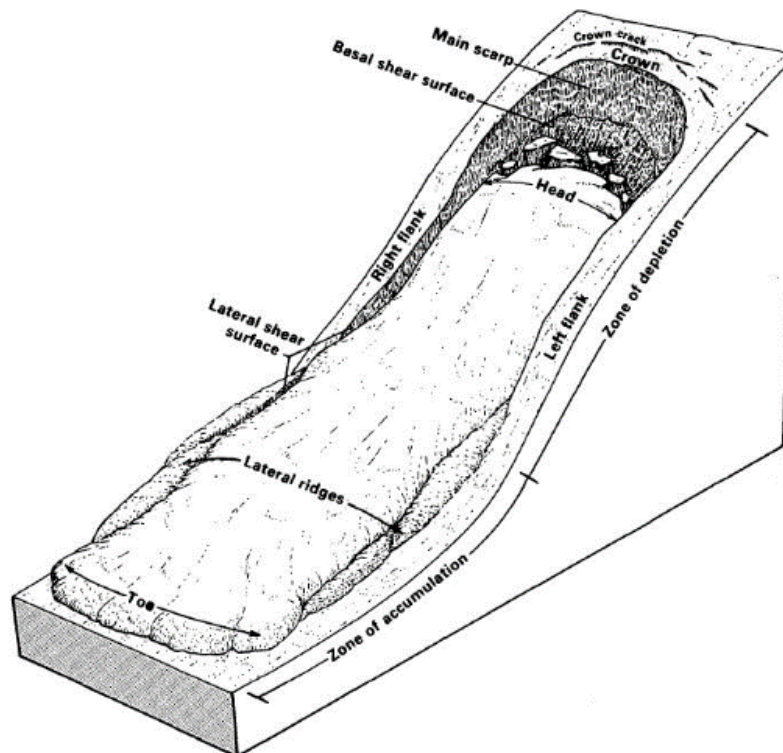


Figure 16 - Earthflow landslide representation diagram (source: Keefer, D.K.; Johnson, 1983)

Some authors observed that weak, low-permeability clay layers, characterizing the basal and lateral shear zones of some earth flows, might effectively isolate the earth flow from adjacent ground. This mechanical and hydrological isolation contributes to the persistent instability of earth flows (Baum, R. L, Reid, M. E., 2000).

Shear strength of the clay layer tends to be significantly lower than both the landslide materials and adjacent ground, helping to perpetuate movement on relatively gentle slopes. The presence of the clay layer causes the landslide to retain water (Habibnezhad, 2014).

The term Earthflow was used by many authors (Cascini *et al.*, 2012; Guerriero *et al.*, 2013; Ferrigno *et al.*, 2017; Bellanova *et al.*, 2018) to describe the Montaguto slope failure because it is composed of predominantly fine-grained material and has a flow-like surface morphology (Keefer, D.K.; Johnson, 1983; Cruden and Varnes, 1996; Hungr, Leroueil and Picarelli, 2014). However, most movement of Montaguto earth flow takes place by sliding along discrete shear surfaces (Guerriero, Revellino, Coe, *et al.*, 2013). The association of the Montaguto landslide with Earth flow phenomenon will be described in more detail afterwards.

4.1.1 Geography and historical activity

The Montaguto landslide is located in the Apennine Mountains of Campania Region in Southern Italy, Province of Avellino (41.2375676 lat, 15.2210359 long). It took the name from the Municipality in which it has been occurred since, at least, 1935 when a first statement reported landslide movement (Guerriero, Revellino, Coe, *et al.*, 2013). Additional information indicates that it was active around 1947 and in 1954 and 1955 when it destroyed farmland and compromised the wheat cultivations (Guerriero, Revellino, Grelle, *et al.*, 2013). Conversely, from 1976 to 1991, it was relatively stable. From 1991 to 2003, the lower part of the landslide was active, and the toe appeared to have expanded. For the period from 2003 to 2005 some residents indicated that the landslide moved again. In June 2005 the entire length of the slope became active and on 26th April 2006 a large remobilization covered and closed the SS90 state road which connects the provinces of Foggia and Avellino (Guerriero *et al.*, 2015).



Figure 17 - Landslide body and run out after the reactivation in 2006
(source: Cascini *et al.*, 2012)



Figure 18 - Landslide toe covering the National Road SS90 after 2006 movement
(source: Guerriero, Revellino, Grelle, *et al.*, 2013)

From October 2007 to July 2009 the landslide activity was concentrated in the source area and near the toe. Between March and November 2008, the movement was minimal. The source area was particularly active in early 2009 when the main head scarp progressed upslope (Terra *et al.*, 2013). On 10th March 2010, another large remobilization occurred. This reactivation covered and closed again the national road SS90 and the Benevento-Foggia railway (Ferrigno *et al.*, 2017).



Figure 19 - Landslide body and run out after the reactivation in 2010
(source: Guerriero, Revellino, Grelle, *et al.*, 2013)



Figure 20 - Landslide toe covering the road SS90 and railway after 2010 movement
(source: Guerriero, Revellino, Grelle, *et al.*, 2013)

4.1.2 Geological and hydrological setting

The Montaguto earthflow is approximately 3 km long and involves 4-6 million of m³ of soil material (Guerriero *et al.*, 2014). The earth-flow width ranges from 75 m of the earthflow neck to 450 m of the upper part of the earth-flow source area. The total elevation difference, from the toe next to the Cervaro River to the top of the 90 m high head scarp, is about 440 m (Luigi Guerriero, Mascellaro, *et al.*, 2016a).

The geological context is tectonically and stratigraphically complex, with a network of faults and folds affecting sedimentary units (Pescatore *et al.*, 1996).

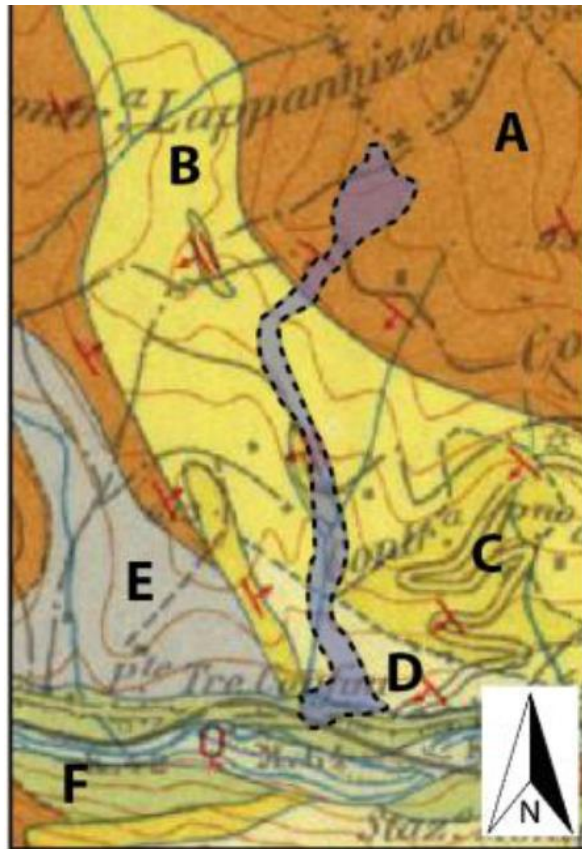


Figure 21 - Geological Sheet No. 174 "Ariano Irpinia" (SGd'I, 1964):
 A - Flysch formation; B - Argillaceous marl unit; C - Arenitic unit; D - Conglomeratic unit;
 E - Ligurid unit; F - Alluvial deposits (source: Pinto *et al.*, 2016)

The morphology and hydrography occur quite articulated with a strong structural control. The outcropping stratigraphic units are mainly three: the Flysch Faeto, the Marne and the clay of the Toppo Capuana, the Altavilla Unit, and the Cervaro river alluvial deposits (Pinto *et al.*, 2016).

The Flysch Faeto formation consists of two main lithofacies. The limestone-marl lithofacies consists of an alternation of turbidite limestones, calcilutites and whitish marls intercalated with greenish clays and bioclastic calcilutites (Guerriero *et al.*, 2014).

The alluvial deposits of the T. Cervaro are characterized by gravel and gravel sandy locally cemented where the thickness of the deposits has been rated not more than 15 m (Guerriero *et al.*, 2015). There are also, widely distributed along the valley bottom, the recent torrential alluvial deposits (Holocene and Present), consisting of gravel and gravel-sandy, with lenses of sand and silt.

The geological complexity of the area controls groundwater flow and spring positions (Diodato *et al.*, 2014). Springs and ponds appeared and disappeared

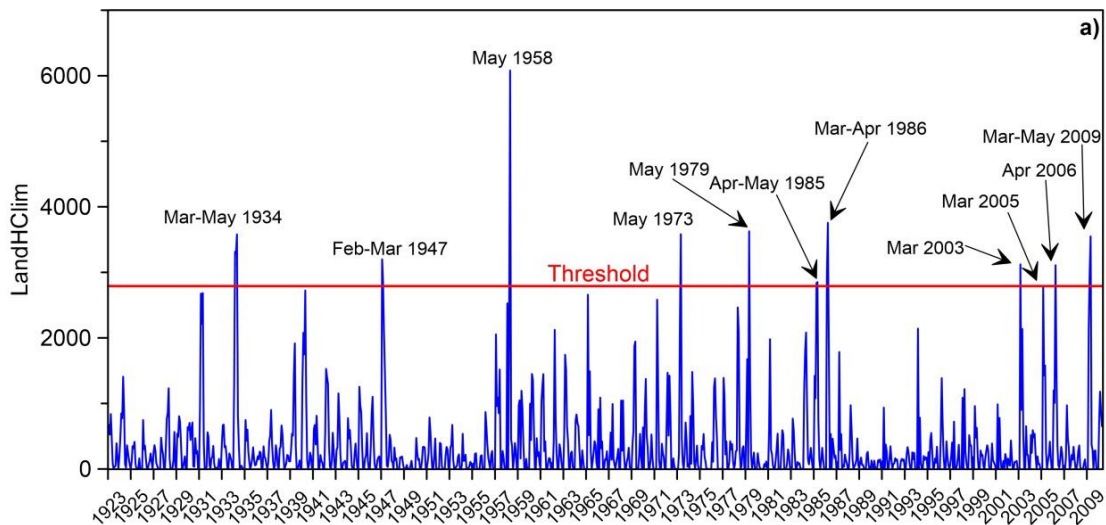
between 1976 and 2010, but their spatial positions stayed in consistent geologic or structural settings.

In the area of the main scarp of the landslide a high number of springs were identified with a total substantial flow rate, its value is around 2.0 l/s. The springs are supplied from the calcareous-clayey complex (Guerriero, Revellino, Coe, *et al.*, 2013). The outflows are channelled within the landslide body.



Figure 22 - Main scarp of Montaguto earthflow (view from the top)
(source: Guerriero *et al.*, 2014)

Cross-correlation analysis performed by Diodato *et al.*, (2014) between spring discharge and precipitation for the yearly cycle shows the existence of a hydrogeological structure with a quasi-fast response to precipitation. A simple statistical model was used to reconstruct spring discharges (Guerriero *et al.*, 2015) by using Landslide Hydrological Climatological indicator (LHC) which analyzed cause-effect relations between documented historical earth flow activity and monthly rainfall data.



Graph 1 - Evolution of the monthly LHC indicator (01/1923 - 05/2010) for the landslide
(source: Guerriero *et al.*, 2015)

The comparative analysis of rainfall data performed by Guerriero *et al.*, (2015) indicates, thus, that the most important landslide reactivations were triggered after at least two consecutive wet hydrologic years¹.

Earth flow response to rainfall or snowmelt is in fact often delayed, and in several cases, long periods of cumulated precipitation are required to trigger a reactivation (Kelsey, 1978; Iverson, 1986; Iverson and Major, 1987). This led to suggest that a cause-effect relationship does exist (Diodato *et al.*, 2014; Guerriero *et al.*, 2015).

Investigation of a large earth flow response to rainfall is particularly challenging due to short-term and seasonal variability of groundwater fluctuation (Coe *et al.*, 2003; Schulz *et al.*, 2009; Doglioni *et al.*, 2012).

However, in hydrogeological complex conditions, groundwater rising caused by rainfall alone cannot be enough to explain earth flow reactivations (Guerriero *et al.*, 2014); local hydrogeological factors and basal slip surface geometry might influence earth flow stability.

At the Montaguto earth flow, previous work by other researchers has documented the evolution of surface topography (Ventura *et al.*, 2011; Giordan *et al.*, 2013) and the influence of basal- and lateral-slip surfaces on long-term earth-flow evolution (Guerriero, Revellino, Grelle, *et al.*, 2013).

Most movement of Montaguto earth flow takes place by sliding along discrete shear surfaces (Guerriero, Revellino, Grelle, *et al.*, 2013). At Montaguto, as at most

¹ A wet hydrologic year is defined as a year where the cumulative rainfall is above the average of two standard deviations.

slope failures, sliding movement is usually concentrated along basal- and lateral-slip surfaces (Hutchinson, 1970; Keefer, D.K.; Johnson, 1983; Baum and Johnson, 1993). The steepness of the basal-slip surface controls differences in flow velocity (from 0.5 m/h up to 4.5 m/h in the upper part of the earthflow), which resulted in local strain.

Cross section profile locations were selected where there were abundant data available to constrain the position of the slip surfaces (Guerriero *et al.*, 2014). Difference DEMs derived from 2006 and 2010 were used to determine the thickness of the basal- and lateral-slip surfaces along a longitudinal-profile and along several cross section profiles (Guerriero *et al.*, 2014).

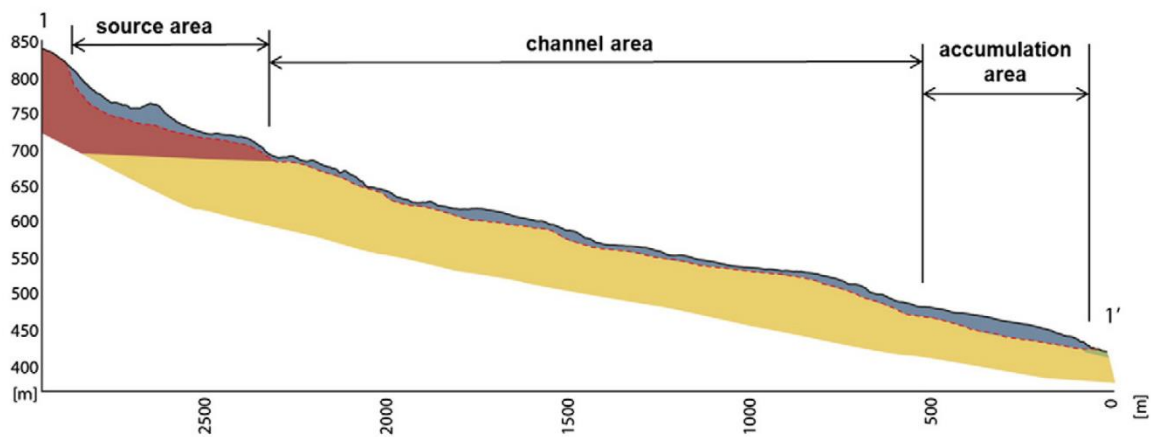


Figure 23 - Geological longitudinal section of the slope in 2006. The Faeto Flysch (brown), the clayey marl unit of Villamaina formation (dark yellow) and the landslide mass (grey).
(source: Guerriero *et al.*, 2014)

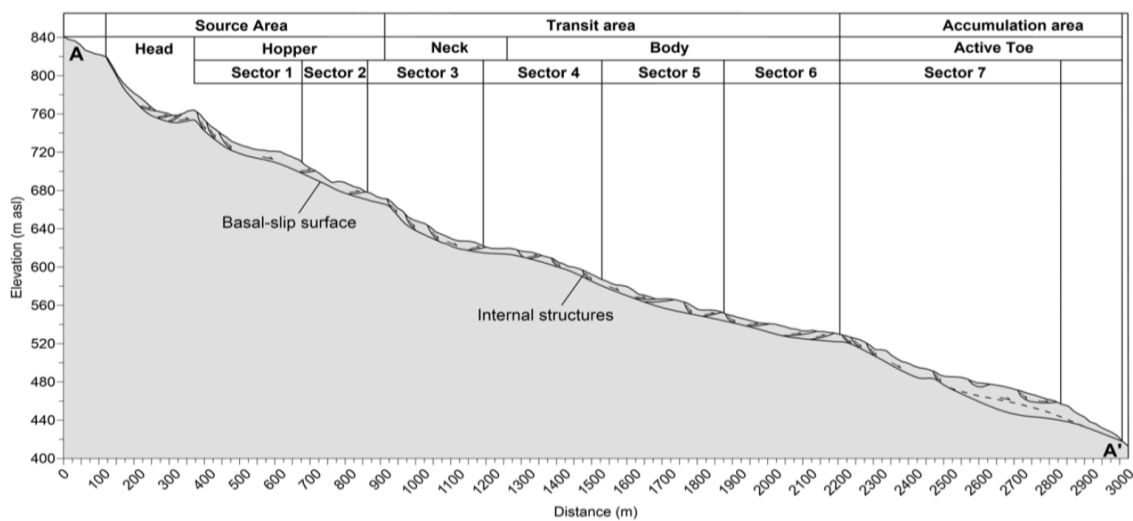


Figure 24 - Longitudinal profile showing the geometry of the basal slip surface of the Montaguto earth flow (source: Guerriero *et al.*, 2014)

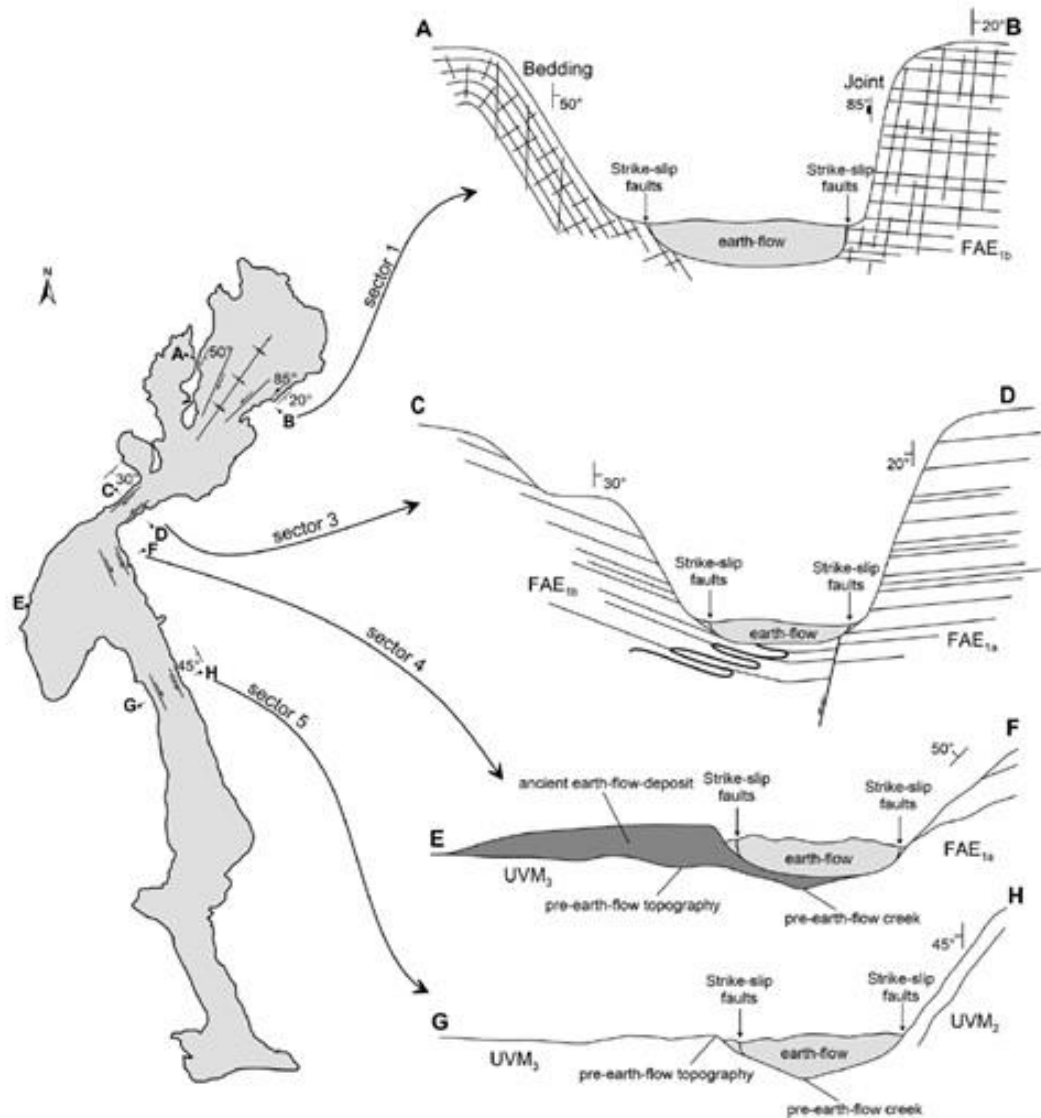


Figure 25 - Slip surface geometry along landslide body
 (source: Pinto *et al.*, 2016)

Overall, the basal-slip surface is a repeating series of steeply sloping surfaces (risers) and gently sloping surfaces (treads).

The implications of these observed and modelled effects are that basal- and lateral-slip surfaces should also control the positions and geometries of surface features (Guerriero *et al.*, 2014).

The direction of earth-flow motion, as well as earth-flow structures with strikes roughly parallel to this direction, was strongly influenced by pre-earth-flow drainages that were controlled by tectonic structures (folds and faults in bedrock) (Giordan *et al.*, 2013). Also, earth-flow deposits (i.e. the inactive toe) influenced

the direction of subsequent earth-flow motion (Guerriero, Revellino, Coe, *et al.*, 2013).

4.1.3 Soil investigation and monitoring

After the first main reactivation occurred in April 2006, hydrogeological and geotechnical surveys were carried out (Pinto *et al.*, 2016). The geo-characterization, performed just after the event, was based on soil investigations both in-situ and in laboratory, consisting of:

- 9 geognostic surveys;
- 22 un-disturbed samples (Direct simple shear and Triaxial tests);
- 15 in-situ penetration surveys (CPT).

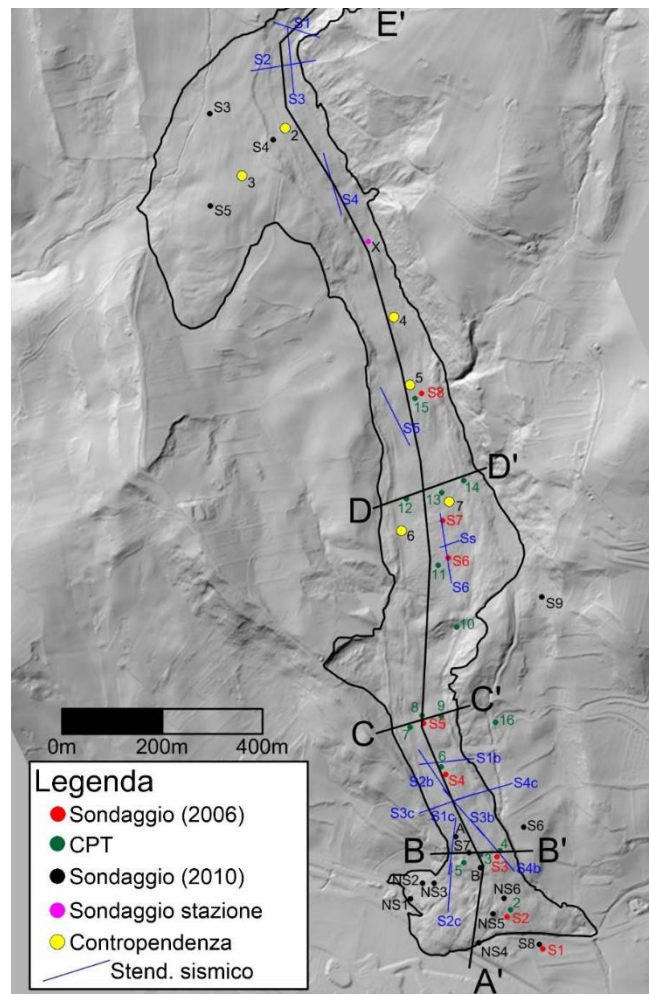


Figure 26 - Geognostic and geotechnical surveys in 2006 (red and green) and 2010 (black and blue) (source: Guerriero *et al.*, 2016b)

Following the second main landsliding event, in March 2010, further surveys campaigns were conducted together with monitoring activity.

Due to the substantial change in the topographic profile occurred during the landslide movement, the monitoring activity was carried out through the integration of different techniques executed by many authors (Denora, Romano and Cecaro, 2013; Allasia *et al.*, 2013; Pinto *et al.*, 2016; Ferrigno *et al.*, 2017), as listed below:

- Ground-based real-time SAR interferometry (DST-UNIFI);
- Laser scanning survey (DST-UNIFI);
- Using of optical and thermal images (DST-UNIFI);
- Robotized total stations (RTSs) monitoring system (CNR-IRPI Turin);
- Geophysical and geognostic surveys (UNI SANNIO).

During the most recent in-situ campaign, other 9 boreholes and 22 samples were performed, reaching the same depths as in 2006, using a rotary drilling apparatus. Overall, the topographic surveys were performed to obtain the following results (Terra *et al.*, 2013):

- Reconstruction of a detailed 3D model (DTM) of the study area;
- Georeferenced map realization for the works location;
- Volumes calculation.

The results of combined investigation techniques and field measurements of the Montaguto earthflow, led to multi-temporal reconstruction of the phenomenon evolution over time (Guerriero, Revellino, Coe, *et al.*, 2013).

Moreover, data from multi-temporal analysis was integrated with a detailed reconstruction of the earth-flow basal-slip surface and geological structures in order to identify the geometrical control exerted by the slip-surface-geometry and bedrock geological structures on earth-flow deformation and movement (Guerriero *et al.*, 2014).

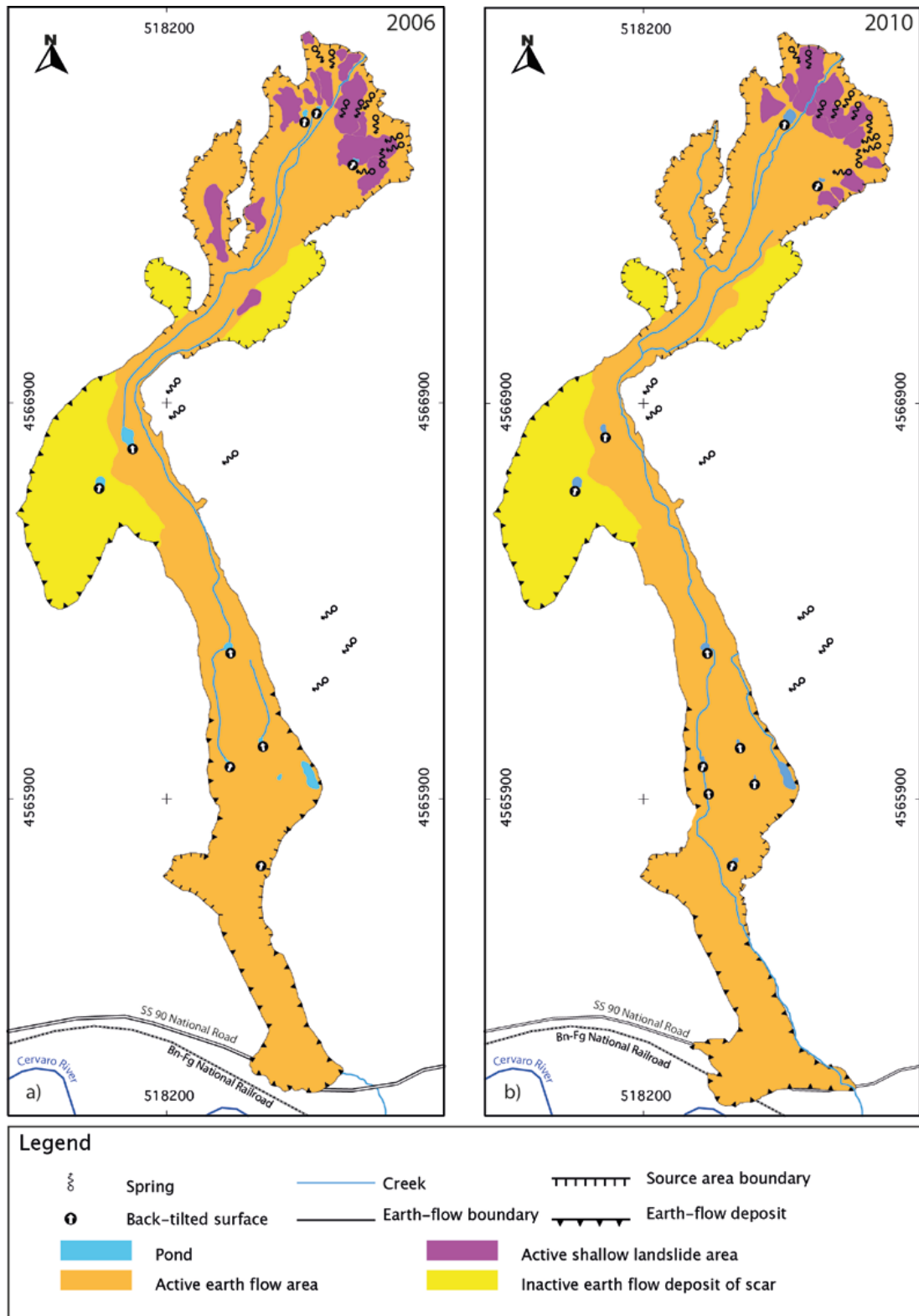


Figure 27 - Maps of the Montaguto Earth flow in 2006 (left) and 2010 (right)
 (source: Guerriero, Revellino, Coe, *et al.*, 2013)

Figure 27 shows the direction of earthflow motion, as well as earthflow structures with strikes roughly parallel to this direction. This one was strongly influenced by pre-earthflow drainages that were controlled by tectonic structures (folds and faults in bedrock). Also, earthflow deposits (i.e. the inactive toe) influenced the direction of subsequent earthflow motion (Guerriero *et al.*, 2014).

4.1.4 Mitigation measures

Many engineering works were realized after the main reactivation in March 2010. They focused on the main triggering factors of the landslide movement. Based on their actions, they may be distinguished in three categories, concerning:

- Shallow and deep drainage systems, lowering groundwater level;
- Topographic reshaping, aims at reducing slope angle of inclination;
- Retaining gabions, which increase stabilization loading on the toe.

Since water was the main engine of the landslide (Diodato *et al.*, 2014), the primary objective of the undertaken actions was to reduce hydraulic pressure applied by groundwater inside and along the boundary of the landslide mass, both from the surface and deeper layers (Pinto *et al.*, 2016).

The restoration of an effective surface circulation has thus been planned, coupled with drainage trenches, able to intercept and divert deep circulation water by a controlled collection.



Figure 28 - Trench channel works

The area affected by the landslide was very large, therefore it has been zoned into 3 different parts, to better plan and carry out the required interventions.

The upper part was characterized by the presence of a system of lakes, whose water, collected into a well by the drainage trenches and superficial channels, is delivered into a watershed located outside the landslide (Guerriero, Revellino, Grelle, *et al.*, 2013).

Superficial channels with bottom hydraulic jumps were carried out in the middle part of the landslide. Furthermore, deep drainage trenches have been dug, allowing deep water to spring at the hydraulic bottom jumps of the channels.

The system of superficial channels coupled with drainage trenches was also repeated at the lower part of the landslide. The water from the lower part and from lateral channel system were conveyed towards a natural watercourse that flows beyond the landslide foot. In this way all the abundant stagnant water within the depressions created by the ground movements has been eliminated, thus reducing water infiltration and contributing to slow the landslide velocity down (Guerriero, Revellino, *et al.*, 2016).

A pilot well has been also drilled upstream the landslide, to intercept the water flowing towards the main scarp; the promising results in terms of water amount and quality suggested a possible water supply (L. Guerriero *et al.*, 2016).



Figure 29 - Retaining gabions on the toe

Secondly, stabilization works were performed along the toe front with the aim of protecting downstream the main elements at risk (Guerriero, Revellino, Grelle, *et al.*, 2013). At first, steel reinforced gabions were installed to build a draining tied wall of considerable size, then the landslide has been reshaped in accordance with the drainage works already carried out.



Figure 30 - Aerial view of the landslide toe after reshaping (source: Google Earth)

Removal of soil material as well as reshaping of the lower part of the landslide were executed as final step. The reduction of the inclination angle tends, indeed, to increase whole slope stability (Low, 2003).

4.2 Soil Characterization

Geological information contained in the maps developed by previous authors (Giordan *et al.*, 2013; Pinto *et al.*, 2016; Guerriero *et al.*, 2016), being based exclusively on lithite - chrono - stratigraphic criteria, are not immediately usable in terms of features techniques for our application purposes. In this sense, the contents of such documents need a phase of "transfer" in quantitative terms (i.e.

characterization in terms of lithological properties, chemical-physical status and geomechanical behaviour).

The definition of the geological factors, competing with the geomorphological susceptibility, needs to operate on differentiated scales and this implies that such transfer "should" be adequate in terms of multiscale hierarchical congruence (Fubelli *et al.*, 2013) through a re-aggregation and recoding of the cartographic data identifying significant lithological systems.

In terms of susceptibility, it is computed from variables such as geology, slope gradient and aspect, elevation, geotechnical properties, vegetation cover, weathering, drainage pattern (Rossi *et al.*, 2010).

Therefore, the geomorphic system has been studied by applying statistical methodologies of coding and aggregation which aim at maintaining the overall behavior deriving from complex interrelations between soil components and conditioning factors of the earthflow.

Slope Aspect	Source of Uncertainty
Geometry	Topography
	Geology / Structures
	Groundwater surface
Properties	Strength
	Deformation
	Hydraulic Conductivity
Loading	In-situ stresses
	Blasting
	Earthquakes
Failure Prediction	Model Reliability

Table 6 - Sources of uncertainty (source: Fischer *et al.*, 2009)

Furthermore, the existence of a correlation between the explanatory variables contributing to the uncertainty may highlight the susceptibility of the landslide system to evolve according to their own modalities barriers identified at scale of detail (Rossi *et al.*, 2010).

For the purpose of this thesis, data derived from 2006 and 2010 soil investigations and survey campaigns were used to determine spatial characteristics of the landslide mass based on documentation given by previous authors (Giordan *et al.*, 2013; Pinto *et al.*, 2016; Guerriero *et al.*, 2016). Data acquisition from each survey campaign conducted in 2006 and 2010 was collected and analyzed separately for a better understanding and soil characterization.

4.2.1 Data collection

Geognostic surveys allow the subsurface exploration for the reconstruction of stratigraphic profile and lithological description and layers depths by taking soil samples – carrots - to be submitted to subsequent investigations for characterizing soil material (Bergman, 2012). The objectives of any subsurface investigation are to determine the following (Kim, 2011):

- Nature and sequence of the subsurface strata (geologic regime);
- Groundwater conditions (hydrologic regime);
- Physical and mechanical properties of the subsurface strata.

Boreholes are among the most common in-situ samples for geotechnical characterization of earth flow material (Guerriero *et al.*, 2014). They are generally drilled inside and outside of the instable area, allowing a precise localization of the basal slip surface through stratigraphic and geotechnical analyses of the resulting core samples.

In 2006 no. 9 drills were carried out up to the maximum depth of 60 m below ground surface (b.g.s.). A summary table following shows identification code, maximum sampling depth, number of undisturbed samples taken and groundwater level b.g.s.. The water table was measured from 2 to 25 m depth which highlights a huge spatial variation.

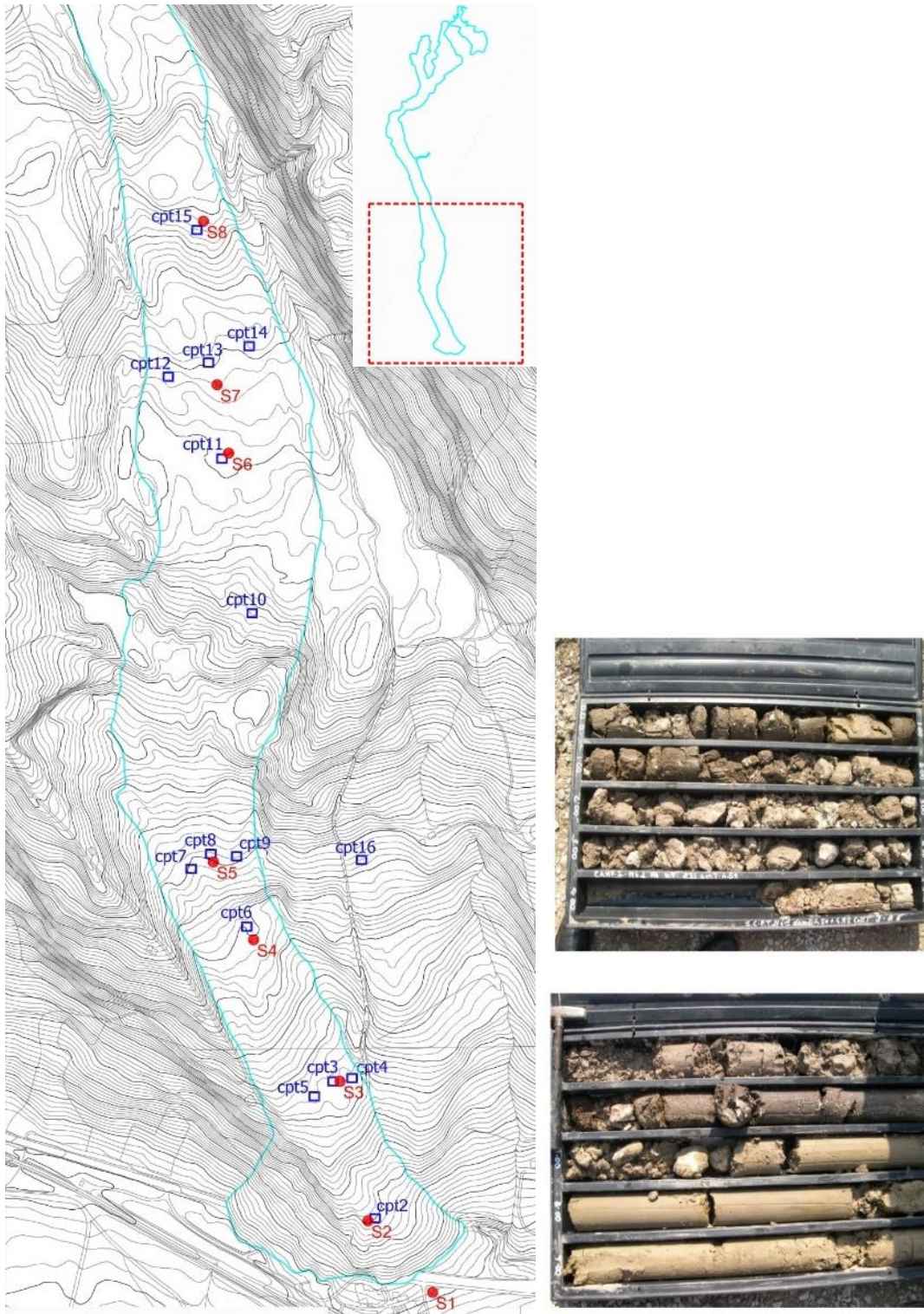


Figure 31 - Survey area in 2006 at 1:5000 scale (left): CPT tests (in blue), geognostic surveys (in red). Carrots extracted during on-site tests up to 10 meters of depth (right)

ID code	Max sampling depth (m b.g.s.)	Undisturbed sample	Groundwater level (m b.g.s.)	Saturat. (%)	Plast. Index (%)	Consist. Index (-)
S1	30	C1	12	89.93	/	/
S2	60	C1	18	83.28	28	0.1
		C2		82.86	/	/
		C3		81.12	27	1.06
		C4		48.28	20	1.4
S3	29.5	C1	4.8	86.77	/	/
		C2		72.71	26	1.17
S4	40	C1	3.5	88	25	0.77
		C2		84.78	24	0.71
		C3		/	/	/
S5	30	C1	2	92.38	30	0.71
		C2		81.41	30	0.71
		C3		/	/	/
S6	60	C1	25	76.55	28	0.72
		C2		/	/	/
S6bis	30.5	C1	19.5	90.43	/	/
S7	40	C1	15.2	92.35	44	0.78
		C2		/	30	0.76
		C3		/	/	/
S8	40	C1	10.2	88	25	0.41
		C2		/	31	0.8
		C3		/	/	/

Table 7 - Details of geognostic samples in 2006

In 2010, other new 9 drills were performed to compare data information to the previous survey campaign. The same maximum depth of 60 m from the ground was reached as well as 22 undisturbed samples were taken by soil carrots. No information on groundwater level was provided at that time.

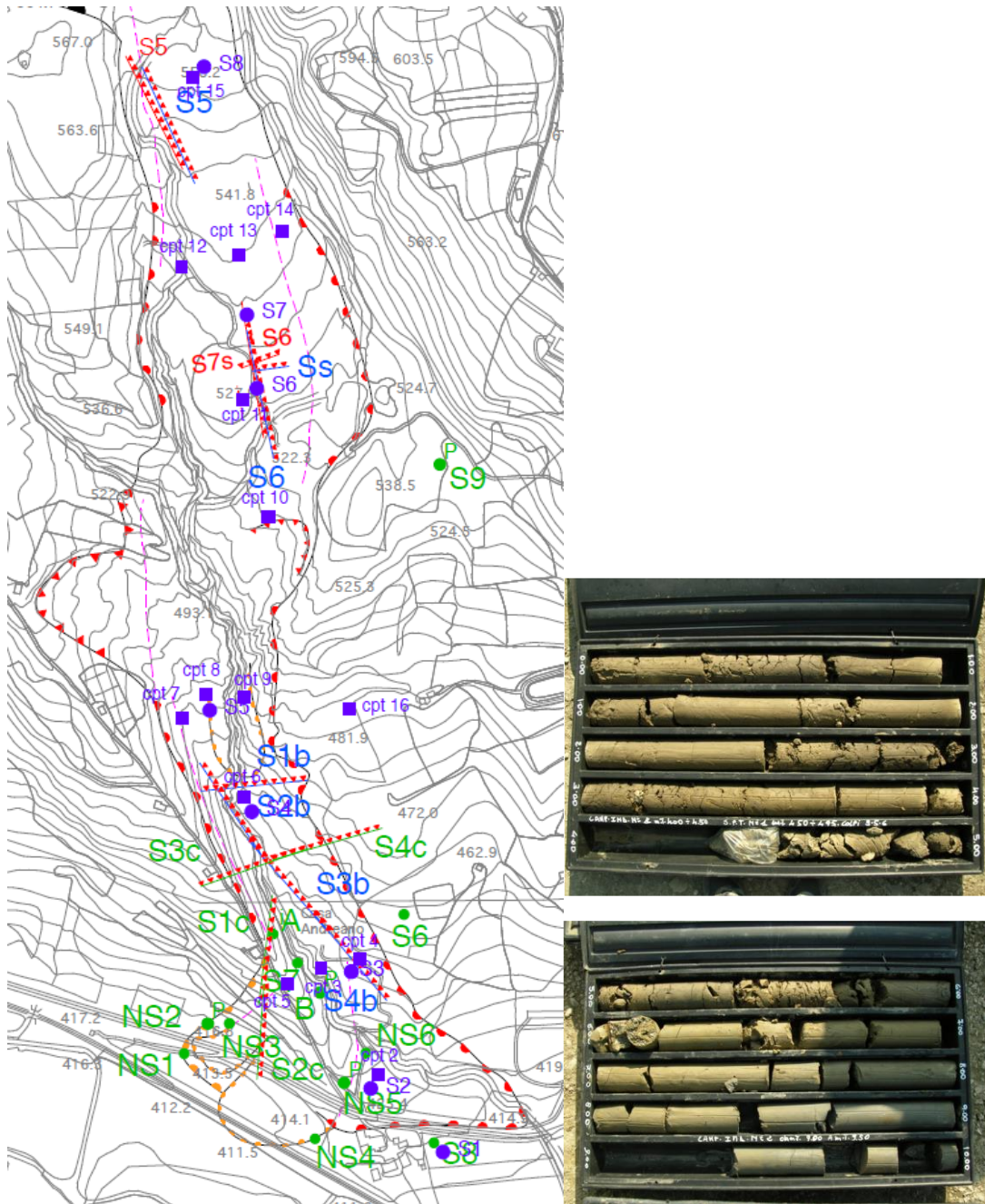


Figure 32 - Survey area at 1:5000 scale (left): old surveys executed in 2006 (in blue), new geognostic surveys in 2010 (in green). Carrots extracted during on-site tests up to 10 meters of depth (right)

ID code	Soil type	Undisturbed sample	Sampling depth (m b.g.s.)	Saturat. (%)	Plast. Index (%)	Fine Content (%)
S7	Landslide deposits	C1	4	96	31.72	64.69
		C2	10	76	28.73	/
		C3	19.5	82	20.55	38.73
S9	Alluvial and/or colluvial deposits	C1	4	88	30.64	38.4
S6	Deposits of Villamaina Unit - altered part	C1	4	90	15.25	/
S5		C1	4	/	/	/
S6	Deposits of Villamaina Unit - substrate	C2	9	82	21.5	37.41
		C3	15	89	16.84	/
		C4	23	88	19.49	27.27
S8		C1	18	96	17.5	/
		C2	20	73	18.95	33.82
S9		C2	10	86	35.51	/
		C3	18	83	35.15	37.35
		C4	23.5	85	20.04	/
S8		C3	23.5	92	18.79	/
S2		Faeto Flysh deposits	C1	13	75	19.49
	C2		17.5	83	13.75	/
	C3		27.5	81	19.97	42.03
	C4		62	75	15.11	/
S5	Ancient landslide deposits	C2	13.5	78	34.49	/
		C3	17	82	31.31	44.57
		C4	25	78	39.78	/

Table 8 - Details of geognostic samples in 2010

From 2006 to 2010 the portion of the soil involved in the landslide in this area has declined, probably due to the sliding of the material downwards.

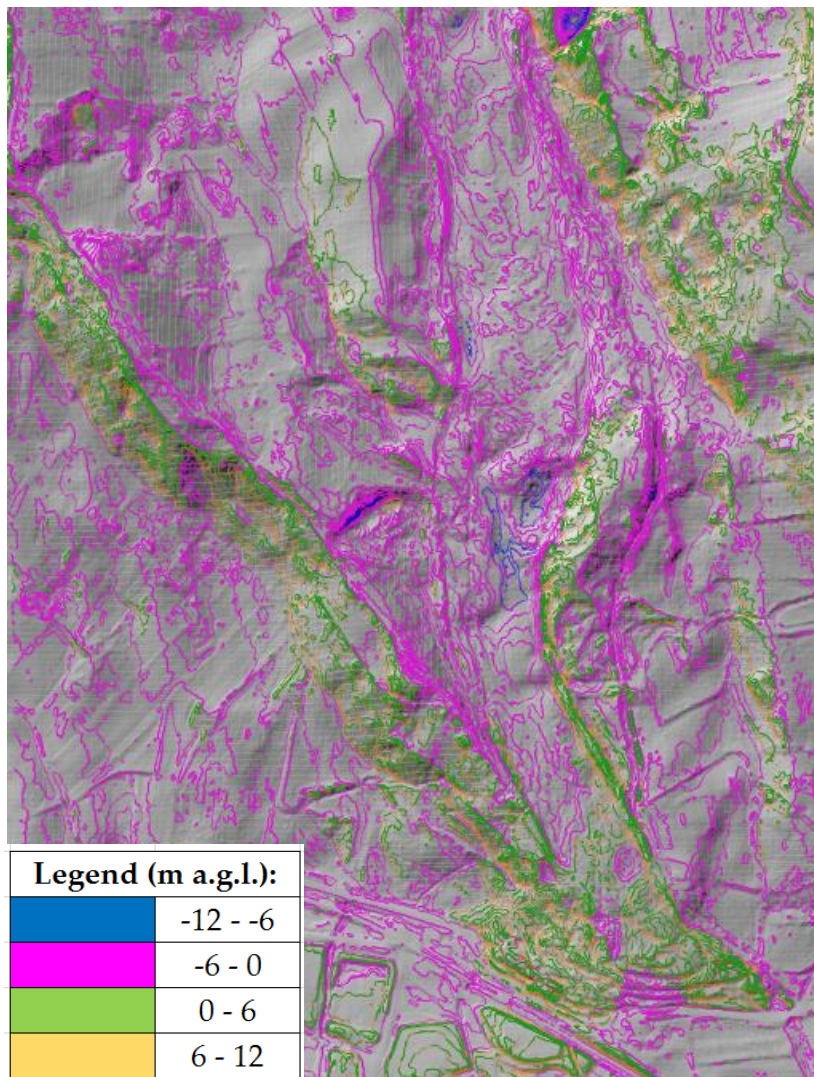


Figure 33 - Differences in elevation by comparing 2006 and 2010 reactivations

Since no geological surveys were carried out before 2006, no information on landslide thickness evolution may be used for spatial-temporal comparison.

Regarding geotechnical surveys, they were carried out only during the survey campaign in 2006.

CPT code	Sampling depth (m b.g.s.)
2	15.4
3	16.6
4	5.4
5	7.4
6	14.2
7	14.4
8	15.8

9	4.8
10	16.2
11	7
12	6.4
13	11.2
14	5.4
15	9.2
16	16.4

Table 9 - Details of CPT surveys in 2006

The undisturbed samples, taken at site both in 2006 and 2010, were analyzed in order to identify physical-volumetric and mechanical characteristics of the lithotypes forming the subsoil along the vertical. In particular, the following parameters were evaluated:

- General characteristics: water content (W_n), specific gravity of grains (γ_s), weight of natural volume (γ_n), through which dry weight weight (γ_d), grade of saturation (S), index of voids (e) and porosity (n);
- Granulometric curve through granulometric analysis by sieving / sieving and/or sedimentation;
- Determination of Atterberg limits;
- ϕ (internal friction angle) and c (cohesion) by direct shear tests with estimation of the "residual" break parameters;
- ϕ (internal friction angle) and c (cohesion) by triaxial compression test consolidated non-drained.



Figure 34 - Sample used for laboratory tests (silt with clayey sand)

A number of 15 Cone Penetration Tests (CPTs) with mechanical point² were performed to determine geotechnical properties of soils and to delineate soil type which is used to obtain geotechnical sections and profiles. On average, the depth reached was about 12 m from the ground level, with maximum value of 16.20 m

² Penetrometer type PAGANI 10/20 tons. Penetrometer characteristics: Begemann tip of 10 cm² (tip area) and 150 cm² side sleeve.

and minimum depth between 5 and 9.4 m. The following parameters were measured during the survey (Begemann, 1965; AGI, 1977):

- q_c = unit tip friction (kg/cm^2);
- f_s = unit sleeve friction (kg/cm^2);
- F_s = friction ratio (%) of the above ones.

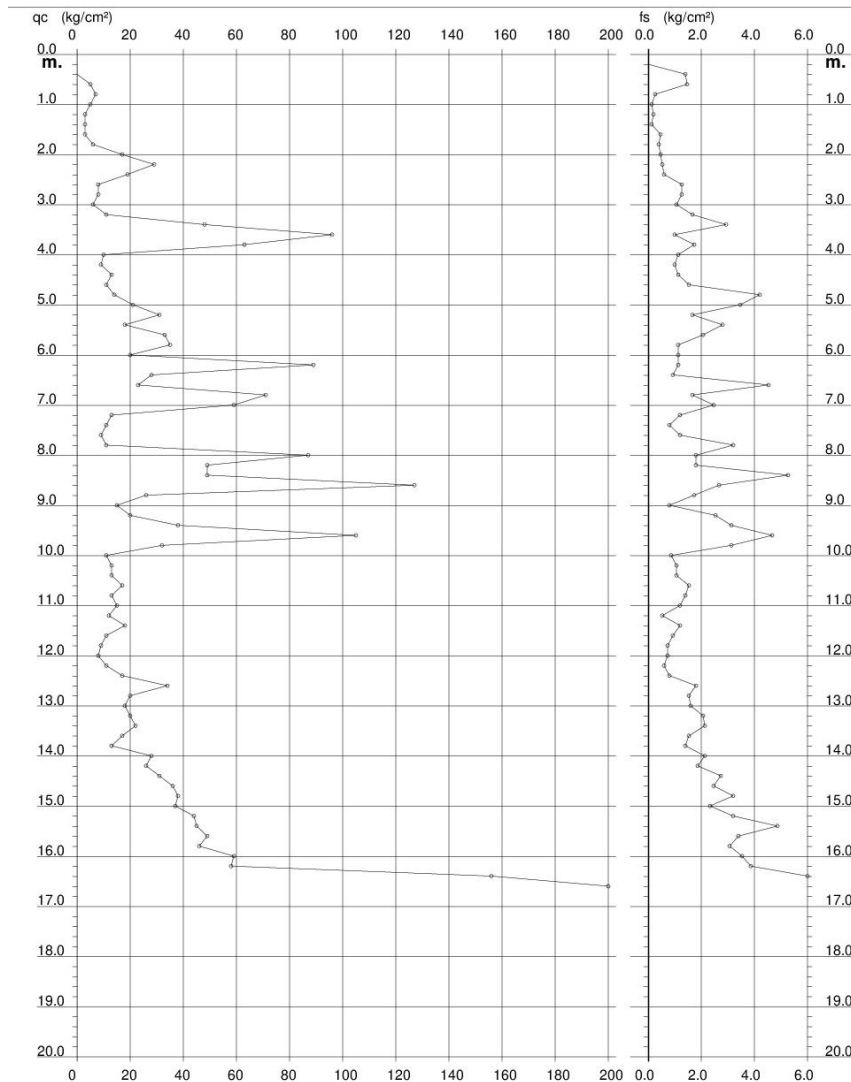


Figure 35 - A CPT profile: f_s (left) and q_c (right) with depth

They represent strength parameters describing geomechanical properties of soil layers along the vertical profile.

This has typically been accomplished using charts that link cone parameters to soil type. One of the more common CPT-based methods to estimate soil profiling and soil type is the chart suggested by Robertson (2010) based on friction ratio F_s .

Typically, the cone resistance is high in sands and low in clays, and the friction ratio is low in sands and high in clays (Resume and Robertson, 2006). The CPT cannot be expected to provide accurate predictions of soil type based on physical characteristics, such as, grain size distribution but provide a guide to the mechanical characteristics (strength, stiffness, compressibility) of the soil, or the Soil Behaviour Type (SBT) (Robertson, 2010). CPT data provides a repeatable index of the aggregate behaviour of the in-situ soil in the immediate area of the probe. Hence, prediction of soil type based on CPT is referred to as Soil Behaviour Type (SBT) normalized respect to increasing effective stresses along depth (Robertson, 2016).

Jefferies and Davies (1993) identified that a Soil Behaviour Type Index, I_{SBT} , might represent the SBTn zones in the normalized³ chart where, I_{SBT} is essentially the radius of concentric circles that define the boundaries of soil type. I_{SBT} may be defined as follows:

$$I_{SBT} = [(3.47 - \log(Q_t))^2 + (\log Ft + 1.22)^2]^{0.5} \quad (8)$$

where:

Q_t = normalized cone penetration resistance (dimensionless);

F_t = normalized friction ratio (%).

Zone	Soil Behavior Type	I_{SBTn}
1	Sensitive, fine grained	NA
2	Organic soils - clay	> 3.6
3	Clays - silty clay to clay	2.95 - 3.6
4	Silt mixtures - clayey silt to silty clay	2.60 - 2.95
5	Sand mixtures - silty sand to sandy silt	2.05 - 2.60
6	Sands - clean sand to silty sand	1.31 - 2.05
7	Gravelly sand to dense sand	< 1.31
8	Very stiff sand to clayey sand ⁴	NA
9	Very stiff, fine grained ²	NA

Table 10 - SBTn zones per Normalized CPT Soil Behavior Type (SBTn)

(source: Robertson, 2010)

Empirical relations are often used in geotechnical engineering to correlate soil properties. The purpose is to estimate soil parameters needed for analysis and

³ Normalized to vertical overburden stresses.

⁴ Heavily overconsolidated or cemented

design by using some indirect properties that are relatively cheaper and easier to obtain although empirical relations add further uncertainty.

Based on the lithological estimations, further parameters may be derived using relations suggested by scientific literature (Robertson, 2009; Robertson, 2010; Robertson, 2016).

An approximate estimate of hydraulic conductivity or coefficient of permeability, k , of soil may be made from an estimate of soil behaviour type using the CPT SBT charts. It describes the rate of the water flows through a unit cross section of soil mass under a unit gradient of pore pressure (Robertson, 2016). Lunne, Robertson and Powell, (1997) propose the following relationship for estimating hydraulic conductivity (k) based on Normalized SBTn:

$$1.0 < I_{SBT} \leq 3.27 \quad k = 10^{(0.952 - 3.04 I_{SBT})} \quad \text{m/s} \quad (9)$$

$$3.27 < I_{SBT} < 4.0 \quad k = 10^{(-4.52 - 1.37 I_{SBT})} \quad \text{m/s} \quad (10)$$

Zone	I_{SBTn}	Range of k (m/s)
1	NA	3×10^{-10} to 3×10^{-8}
2	> 3.6	1×10^{-10} to 1×10^{-8}
3	2.95 - 3.6	1×10^{-10} to 1×10^{-9}
4	2.60 - 2.95	3×10^{-9} to 1×10^{-7}
5	2.05 - 2.60	1×10^{-7} to 1×10^{-5}
6	1.31 - 2.05	1×10^{-5} to 1×10^{-3}
7	< 1.31	1×10^{-3} to 1
8	NA	1×10^{-8} to 1×10^{-3}
9	NA	1×10^{-9} to 1×10^{-7}

Table 11 - Estimated soil permeability (k) based on the CPT SBTn
(source: Robertson, 2010)

The above relationships may be used to provide an approximate estimate of soil permeability (k) and to show the likely variation of soil permeability with depth from a CPT sounding.

Since the normalized CPT parameters (Q_t and F_t) respond to the mechanical behaviour of the soil and depend on many soil variables, the suggested relationship between k and I_{SBTn} is approximate but may provide a guide to variations of possible permeability (Robertson, 2010).

4.2.2 Categorization of data

To characterize soils, textural characters, prevailing lithology, genesis and stratigraphic relationships, thickness and degree of cementation and alteration must be identified.

In addition, a general characterization of soil must be formulated for geological-applicative purposes, evaluating all parameters considered necessary, such as weaving, plasticity, the potential for swelling-contraction, density, the existence of cemented or hardened horizons, permeability, degree of saturation and position of the possible phreatic surface or the presence of small suspended slopes, presence of drainage difficulties, acclivity and stability, depth of substrate, angle of friction etc.

Soils must be represented according to permeability ranges or, when possible, according to classes of intrinsic vulnerability, where by intrinsic vulnerability we mean the set of characteristics of the hydrogeological complexes which constitute their specific susceptibility (Aleotti and Chowdhury, 1999).

In particular, geognostic surveys were used to classify lithology types by the composition of the following soil classes: clay, silt, sand and gravel, and calibrated through the results produced by laboratory tests (undisturbed samples) performed during the same survey campaign.

In this way it was possible to associate categorical variables with soil classes (Tedesco and Sociale, 2016).

Soil texture refers to the relative percentage of clay, silt, sand and gravel in a soil. Natural soils are comprised of soil particles of varying sizes. They are found in aggregated form (Li *et al.*, 2013).

Arrangement of these soil particles on certain defined patterns is called soil structure (Vardanega and Bolton, 2015). The natural structure of soil particles also reveals the colour, texture and chemical composition of soil aggregates. Soil structure is influenced by air moisture, organic matter, micro-organisms and root growth. When many particles are aggregated into cluster, a compound particle is formed (Li *et al.*, 2013).

The following chart is adapted from fraction system of U.S.D.A. (Whitney, 1911). If relative percentages of soil separates are known, the soil may be given textural name. For this purpose, equilateral triangles are used. The most widely used Equilateral triangles are international equilateral triangle and the one used by USDA. These consist of three angles and its area is divided into twelve groups representing twelve different textural classes. Each group covers definite range of percentages of sand, silt, and clay. In the triangles, left side line represents the

clay percentage, right side line represents percentage of silt and base represents percentage of sand (Whitney, 1911).

Each side of the triangle is divided into ten divisions representing soil separate percentage. These divisions are further divided into ten small divisions; each small division represents one per cent of soil separate. The percentages of sand, silt, and clay obtained after mechanical analysis of the given soil are read on the equilateral triangle (Whitney, 1911).

In using the diagram as indicated the percentages of silt and clay should be located on silt and clay lines respectively. The line in case of silt is then projected inward parallel to clay side of the triangle and in case of clay it should be projected parallel to the sand side. The three lines; one representing sand percentage, other representing silt percentage and the third clay percentage meet at a point in the triangle (Whitney, 1911). The compartment in which the point falls indicates textural name for the given soil sample. The knowledge of soil texture is of great help in the classification of soil and in determination of degree of weathering of rock.

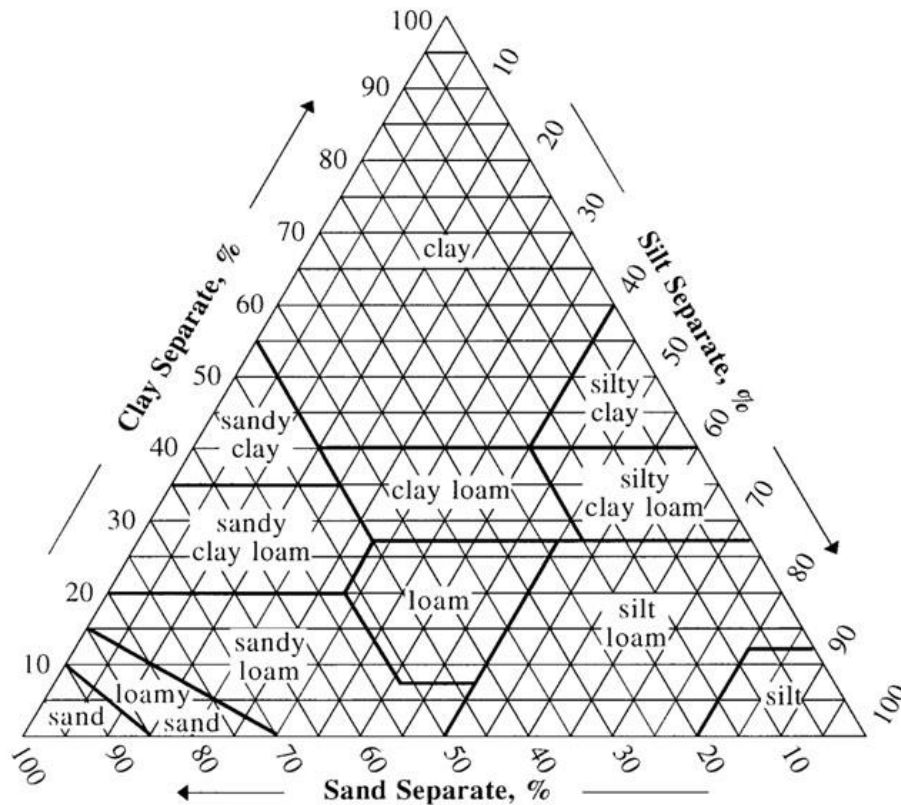


Figure 36 - Soil texture triangle of soil classes (source: Whitney, 1911)

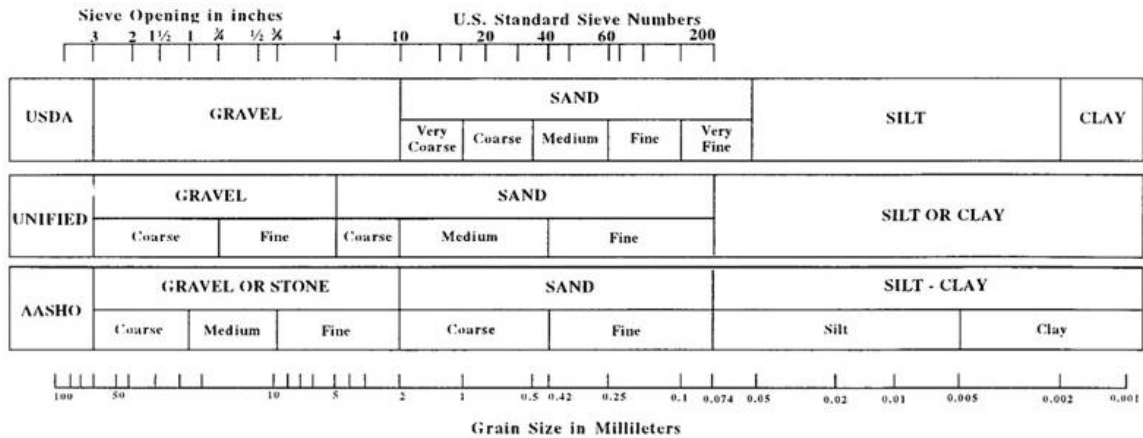


Figure 37 – Comparison of particle size scales (source: Whitney, 1911)

Texture names are given to soils based upon the relative proportion of each of the four soil granulometries based on their preponderant percentage content (Clay, Silt, Sand and Gravel).

As the soil is a mixture of various sizes of soil separates, it is therefore, necessary to define limits of variation among soil fractions to group them into textural classes. These classes are recognized based on relative percentage of separates; sand, silt and clay, as shown below:

Common name	Texture	Basic soil textural class name
Sandy soils	Coarse	Sandy
		Loamy sands
		Sandy loam
Loamy soils	Moderately coarse	Fine sandy loam
		Very fine sandy loam
	Medium	Loam
		Silt loam
		Silt
	Moderately fine	Clay loam
		Sandy clay loam
		Silty clay loam
	Clayey soils	Fine
Silty clay		
Clay loam		

Table 12 - Textural class names (source: Whitney, 1911)

Textural group	Sand	Silt	Clay
Sand	80 - 100	0 - 20	0 - 20
Sandy loam	50 - 80	0 - 50	0 - 20
Loam	30 - 50	30 - 50	0 - 20
Silt loam	0 - 50	50 - 100	0 - 20
Sandy clay loam	50 - 80	0 - 30	20 - 30
Silty clay loam	0 - 30	50 - 80	20 - 30
Clay loam	20 - 50	20 - 50	20 - 30
Sandy clay	50 - 70	0 - 20	30 - 50
Silty clay	0 - 20	50 - 70	30 - 50
Clay	0 - 50	0 - 50	30 - 100

Table 13 - Soil texture classes and percentage content of sand, silt, clay separates
(source: Whitney, 1911)

Considering laboratory classification ranges used to define consistency (coherent soils), density (granular soils) and saturation degree, the following comparison was applied:

Consistency (coherent soils)	Density (granular soils)	Saturation condition
No consistency	No density	Dry
Low consistency	Low density	Low humidity
Moderate consistency	Moderate density	Humid
Consistent	Dense	High humidity
High consistency	High density	Wet

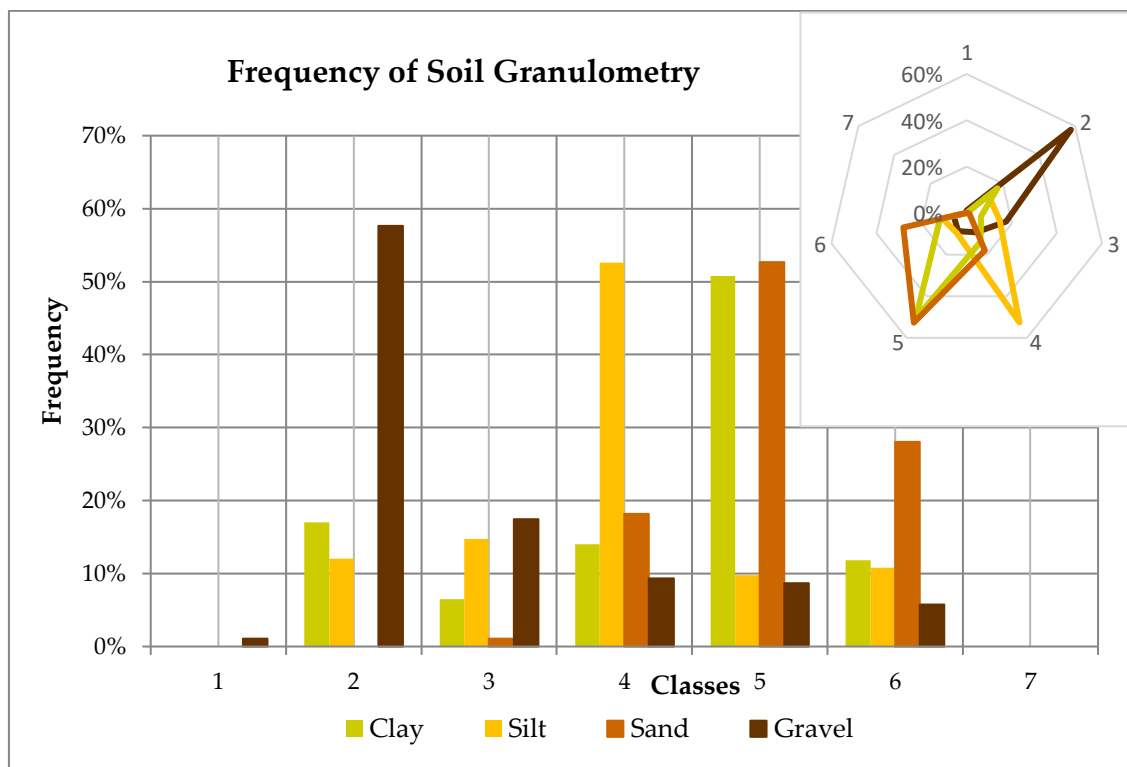
Table 14 - Range of values based on physical characteristics

Soil Texture (C-Si-Sa-G)	Density (D)	Consistency (Co)	Saturation (S)	Code
0	0-0.2	0-0.5	0-0.2	1
0-0.05	0.2-0.4	0-0.75	0.2-0.4	2
0-0.15	0.4-0.6	0.5-0.75	0.2-0.6	3
0.15-0.25	0.6-0.8	0.5-1	0.4-0.6	4
0.25-0.35	0.8-1	0.75-1.5	0.4-0.8	5
0.35-0.5	NA	1-1.5	0.8-1	6
0.50-0.75	/	NA	NA	7

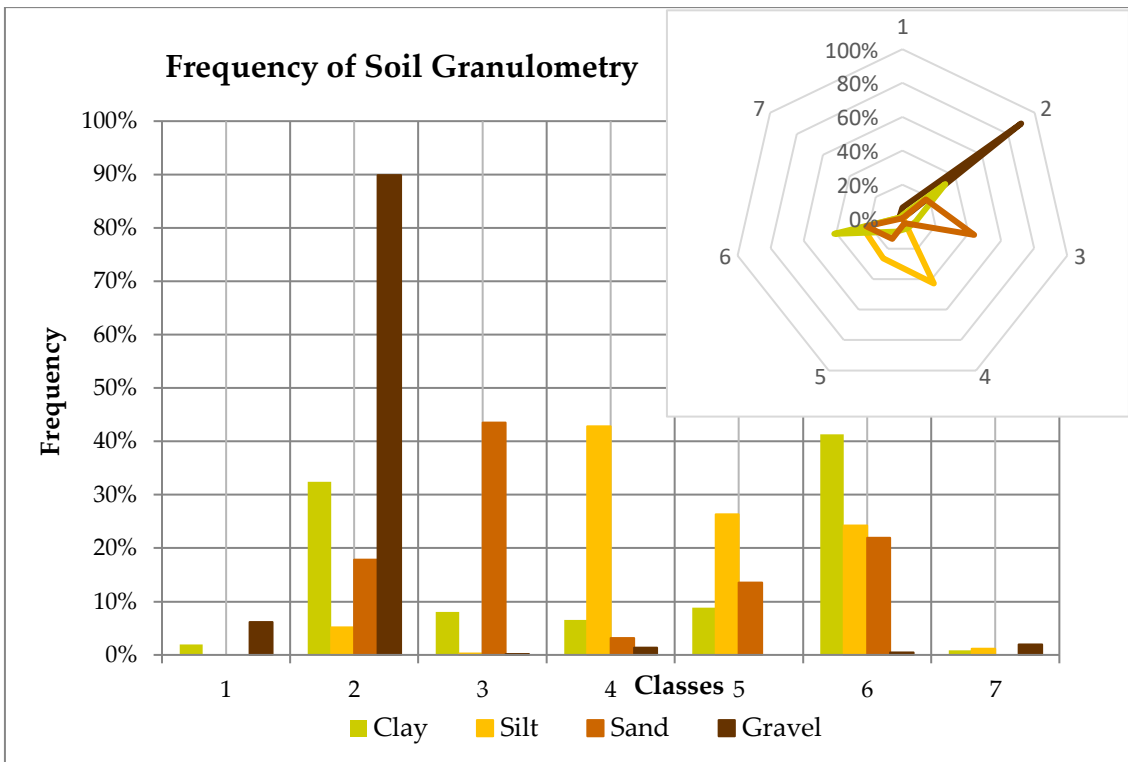
Table 15 - Soil parameters and percentage content converted to numerical coding

As for geognostic surveys and laboratory samples, the same classification was done for geotechnical parameters, but as already numeric values, no categorical association was performed.

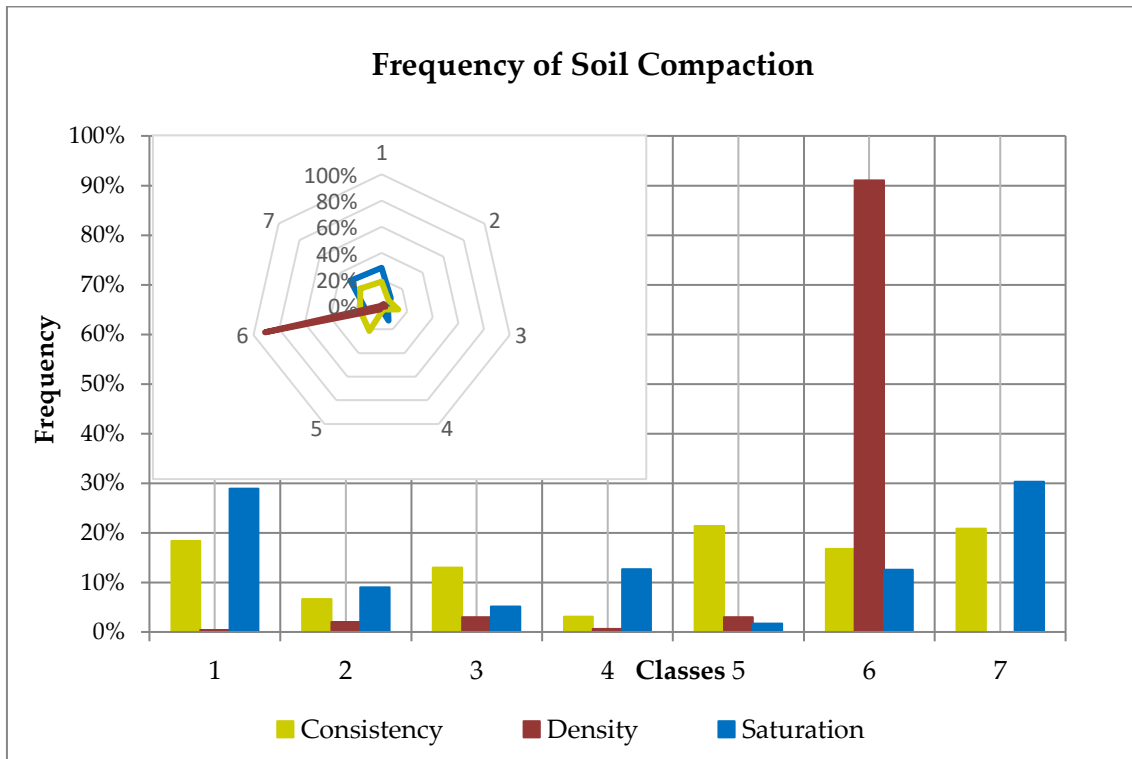
The following graphs represent the distribution of the frequencies related to soil classes, corresponding respectively to soil texture and soil compaction of the soil profiles sampled during the execution of 2006's and 2010's investigations.



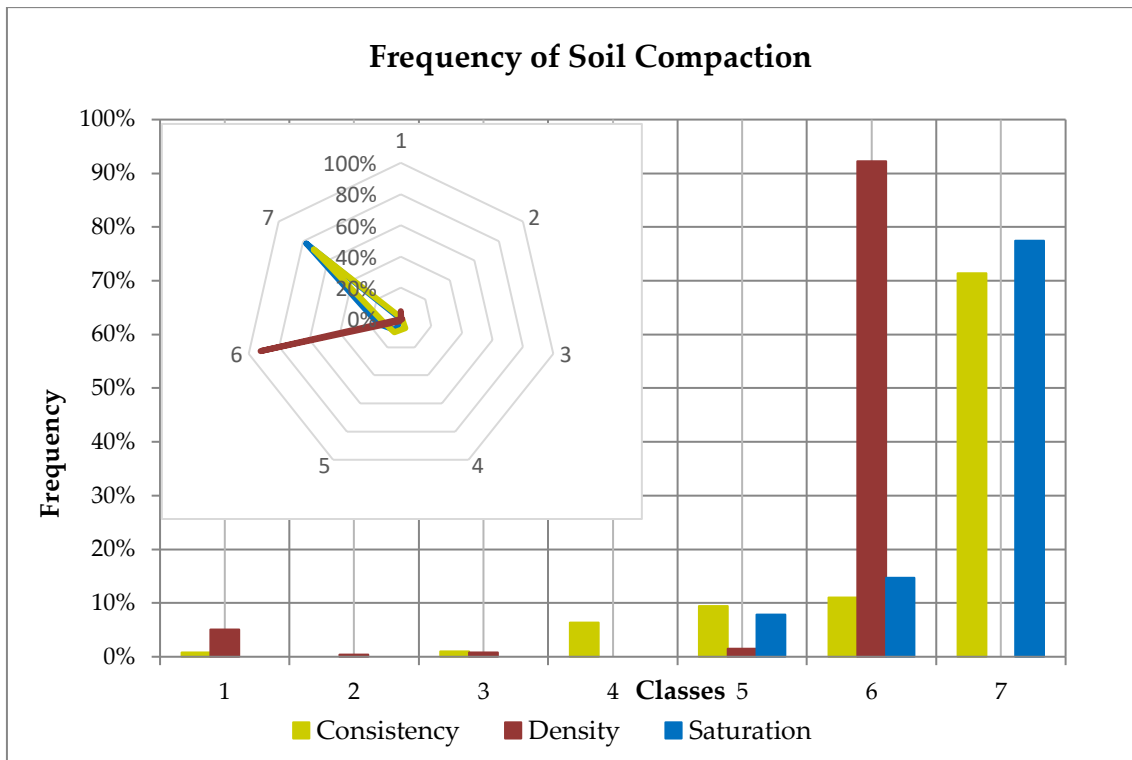
Graph 2 - Frequency of soil texture from surveys in 2006



Graph 3 - Frequency of soil texture from surveys in 2010



Graph 4 - Frequency of soil compaction from surveys in 2006



Graph 5 - Frequency of soil compaction from surveys in 2010

The scatterplots (Graphs 2-5) describe the distribution of the parameter along depth. Frequency of occurrence in each histogram interval is obtained by dividing the number of occurrences by the total number of data points.

	Fs (-)	k (m/s)
MIN	0.409277	3.73E-11
MAX	268.6329	1.25E-01

Table 16 - Range of values for friction ratio and soil permeability by CPTs in 2006

Table 16 shows the minimum and maximum interval within which friction ratio values and permeability, sampled from CPTs in 2006, fall.

4.2.3 Multivariate analysis

Index and classification properties easily measure attributes useful in categorizing soils, making rough forecasts of mechanical properties based on correlations among measures (Bowles, 1979).

Soil characterization consists in a qualitative as well as quantitative description of the heterogeneity and distribution of soil parameters in a specific site (Marx and Cornwell, 2001).

The elaboration of the predisposing parameters to obtain quantitative soil indices allows to relate the geo-environmental factors for the determination of the susceptibility level and therefore the propensity to landslide hazard (Denora, 2013).

In this study, for each conditioning factor, a numerical weighting value has been associated with each class, based on the grade, assessed qualitatively, with which this contributes to the triggering of the phenomenon.

The first step was the statistical description of soil properties was based on soil sample analysis which gives quantitative measure of their variability.

Features of interest include the central tendency of the data, dispersion or scatter in the data, skewness in the data, and correlation or dependence between data points. Based on the above tables, the following outcome was obtained for the specific site:

Lithology	Clay	Silt	Sand	Gravel	Consistency	Saturation	Density	I _{CSiSaG}	I _{CoDS}
slightly weakly clayey loamy silty sand (very thick and humid)	0-0.15	0.15-0.25	0.35-0.5	0-0.15	1-1.5	0.4-0.6	NA	0.02	0.53
fine clay sand (not consistent and slightly saturated)	0.25-0.35	0.15-0.25	0.35-0.5	0-0.15	0.5-0.75	0.8-1	NA	0.11	0.50
coarse sands (on average consistent)	0-0.05	0-0.05	0.35-0.5	0.25-0.35	0.5-0.75	NA	NA	0.22	0.46
medium-coarse sand with weakly silty gravel (not very thick and moderately thickened, humid)	0-0.05	0-0.15	0.35-0.5	0.25-0.35	0-0.5	0.4-0.6	0.4-0.6	0.30	0.40
sandy gravel (low consistent and humid)	0-0.05	0-0.05	0.25-0.35	0.15-0.25	0-0.5	0.4-0.6	NA	0.44	0.54
sandy silty	0-0.05	0.15-0.25	0.25-0.35	0-0.05	NA	NA	NA	0.54	0.39

fine sand, slightly weak clay (inconsistent and not very consistent, humid and very humid)	0.15-0.25	0-0.15	0.15-0.25	0.35-0.5	0-0.5	0.4-0.8	NA	0.64	0.46
fine sandy clays (very thick, slightly humid and dry)	0.35-0.5	0.15-0.25	0.15-0.25	0-0.05	1-1.5	0-0.2	NA	0.72	0.61

Table 17 - Correspondence between some soil lithologies and I_{CSISaG} classes in 2006

Lithology	Clay	Silt	Sand	Gravel	Consistency	Saturation	Density	I _{CSISaG}	I _{CoDS}
weakly cemented sand	0-0.05	0-0.05	0.35-0.5	0-0.05	NA	NA	0.4-0.6	0.04	0.47
sandy silt	0-0.05	0.35-0.5	0.25-0.35	0-0.05	NA	NA	NA	0.10	0.43
cemented silt	0-0.15	0.35-0.5	0-0.05	0	0.75-1.5	0.8-1	NA	0.21	0.75
Silty sandy	0-0.05	0.25-0.35	0.15-0.25	0-0.05	NA	NA	NA	0.31	0.43
clayey silt soil	0.25-0.35	0.35-0.5	0-0.15	0-0.05	1-1.5	0.8-1	NA	0.43	0.69
silty clay	0.35-0.5	0.25-0.35	0-0.15	0-0.05	NA	NA	NA	0.58	0.43
clay and weakly silty and sandy clay	0.5-0.75	0.15-0.25	0.15-0.25	0-0.05	NA	NA	NA	0.63	0.43
clay	0.5-0.75	0-0.15	0-0.05	0	NA	NA	NA	0.99	0.43

Table 18 - Correspondence between some soil lithologies and I_{CSISaG} classes in 2010

The most common measure of dependence among uncertain quantities is the Correlation Coefficient. It measures the degree to which one uncertain quantity varies linearly with another uncertain quantity (Phoon and Kulhawy, 1999), as following shown:

$$\rho_{X,Y} = \frac{cov(X,Y)}{\sigma_X \sigma_Y} = \frac{E[(X - \mu_X)(Y - \mu_Y)]}{\sigma_X \sigma_Y} \quad (11)$$

The correlation coefficient (ρ) varies within $[-1,+1]$, with the higher bound implying a strict linear relation of positive slope and the lower bound a strict linear relation of negative slope. The higher the magnitude, the more closely the data fall on a straight line. Zero correlation coefficient implies no (linear) association between the two variables.

It expresses the degree to which two parameters (X and Y) vary together in linear relationship:

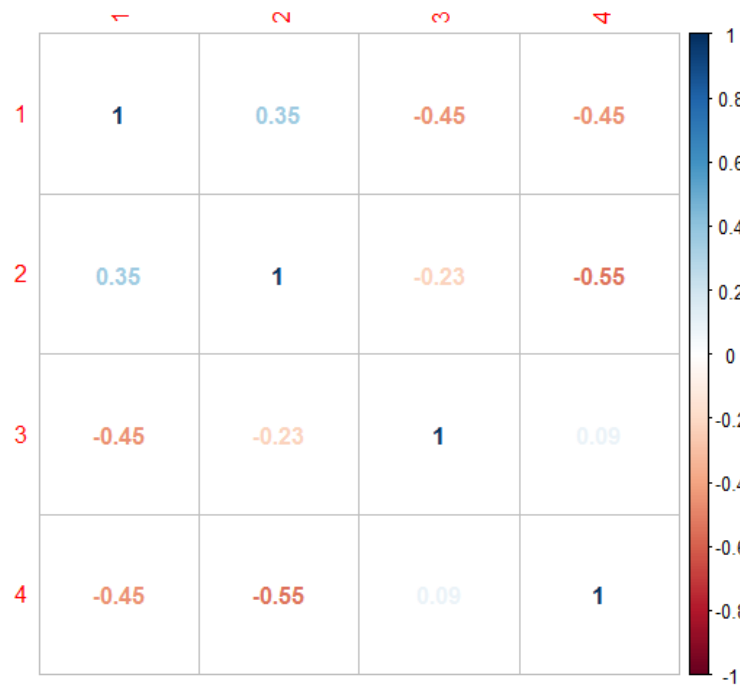


Figure 38 - Correlation among soil texture components in 2006: clay (1), silt (2), sand (3), gravel (4)



Figure 39 - Correlation among soil texture components in 2010: clay (1), silt (2), sand (3), gravel (4)

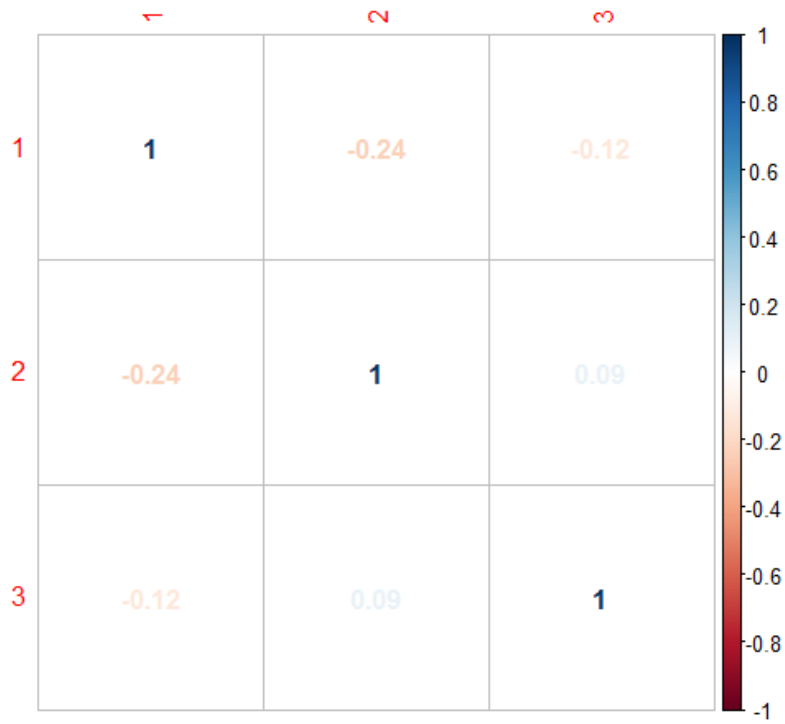


Figure 40 - Correlation among soil texture components in 2006: consistency (1), density (2), saturation (3)

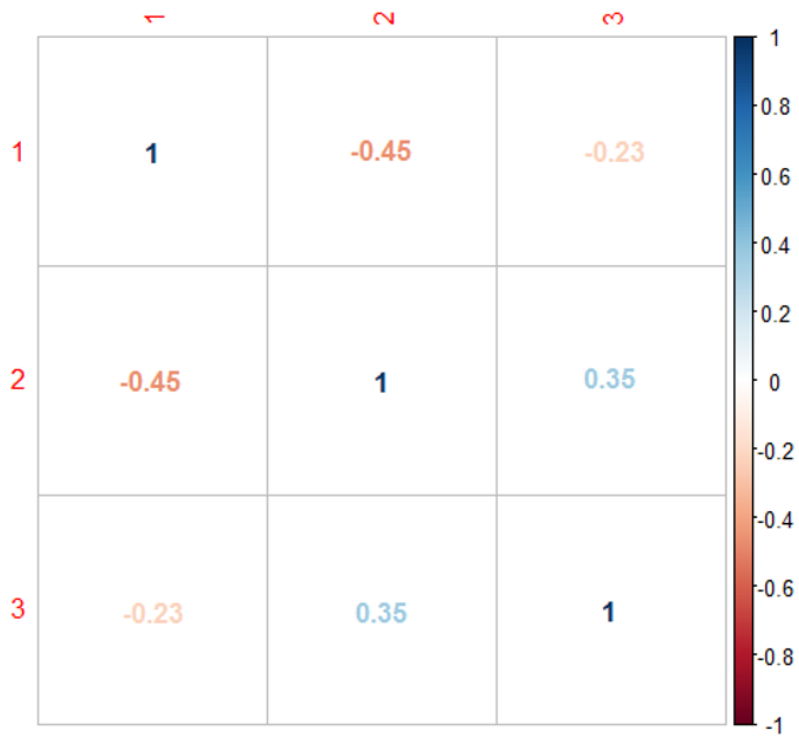


Figure 41 - Correlation among soil texture components in 2010: consistency (1), density (2), saturation (3)

It is often the case that soil properties or other variables are related to one another along the depth (Matheron, 1973). What we need is a mathematical relationship that captures this correlation among the variables with vertical depth. In our case, more than two variables correlation would be explored.

A multivariate statistical analysis was then carried out for groups of homogeneous variables (granulometric characteristics, densimetric and saturation conditions, mechanical behavior, etc.) through the application of an interacting regression model (Pinheiro *et al.*, 2018) according to vertical depth in order to evaluate how each category of soil influences the others based on sampling location.

A categorization treatment was carried out based on the geomorphological and hydrogeological characteristics by weighting (Coulton and Chow, 1993) the quantitative values that considered the lithological characteristics and the respective propensity towards a potential site-specific triggering phenomenon and/or in reference to technical-scientific literature (Zêzere *et al.*, 2004).

The regression analysis was applied among the *clay-silt-sand-gravel* soil classes obtaining the I_{CSiSaG} index which represents the lithological-geological composition index; and through the application of the variables, the I_{CoDS} index obtained from the regressive analysis of the *consistency-density-saturation* degree as an explanatory index of soil thickening.

Multiple Linear Regressions (MLR) have been widely used (Coulton and Chow, 1993; Keough & Quinn, 1995; Kelley and Bolin, 2013) to predict the response of a dependent variable from a set of independent variables, as a function of the correlations between them (Loh, 2002). The MLR algorithm was calculated using the 'logistic model' (Gortmaker, Hosmer and Lemeshow, 1994), with stepwise (backward) analysis, which fits the model by removing variables according to the confidence level (95%).

All the variables have been standardized before applying the regression model to avoid the presence of biased trends (Loh, 2002) according to density distributions which best fitted their empirical frequencies, making the results comparable (Gortmaker, Hosmer and Lemeshow, 1994).

The approximation through least-squares was used to validate and constitute the best linear unbiased estimators of the regression parameters (William D. Berry & Stanley Feldman, 1985). This study focused on prediction of soil classes (sand, silt, and clay) and their content in the soil layer as well as in degree of compaction (consistency and density) and saturation relationship.

Following the linear regression equation applied to obtain the I_{CSiSaG} index, considering both the multivariate and the conditioned component of interdependence among the soil variables.

$$I_{CSiSaG[xyz]} = \beta_0 + \beta_1 C + \beta_2 Si + \beta_{12} CSi + \dots + \beta_{123} CSiSa + \dots + \beta_{1234} CSiSaG \quad (12)$$

where:

β_i = regression coefficient at i^{th} location,

$x^T \beta$ = linear predictor,

$x_i x_j$ = mutual interaction between parameters at i^{th} and j^{th} locations.

The soil index I_{CSiSaG} is found by multiplying the discriminant weights associated with each factor by the corresponding factor values and summing over the thus weighted factors forming linear combinations of the original ones.

Simple correlations among the variables, according to regression function (Korup 2004), made it possible to calculate the coefficient of determination R^2 which represents their correlation index ranging from 0 to 1 (Tedesco and Sociale, 2016). The higher is R^2 value, the higher is the correlation and goodness of the regression with highlights the presence of an estimation error in term of systematic biases (Uzielli, 2008).

	$R^2_{I_{CSiSaG}}$	$R^2_{I_{CoDS}}$
2006	0.8326	0.9122
2010	0.8131	0.7265

Table 19 - Goodness of the regressions applied to soil parameters in 2006 and 2010

The indices thus obtained were normalized in order to make them comparable with those related to the mechanical strength of soil (i.e. the friction ratio F_s) and to the permeability k obtained from CPTs and empirical relations of literature (Robertson, 2010).

The geo-mechanical parameters, as quantitative values obtained from in-situ surveys, were analyzed only by applying probabilistic approaches to perform the best fitted density distribution for standardization purpose as already numerical variables (Robertson and Campanella, 1983).

Since in 2006 geognostic surveys and CPT tests were performed at minimum inter-distance (Helton *et al.*, 2006) from each other and since there are not

particular litho-geological discontinuities in technical maps, so as their outcomes are spatially comparable.

However, in 2010 only geognostic investigations were conducted, then composite index I_{geo} has been defined based on geological composition (i.e. granulometric characteristics, densimetric and saturation conditions) in order to make a comparison between 2006 and 2010 survey results.

Overall, the combination of predisposing factors along depth indicates their temporal contribution to susceptibility (Zêzere *et al.*, 2004) both locally, within a geo-defined unit, and globally, at whole landslide area.

4.3 Spatial Variability Modelling

In geological field, besides the importance of the numerical value of the parameter to be studied, the position that the data has in space is fundamental. The classical statistical methods do not take into account the spatial information proper to the geological data (Wu *et al.*, 1997).

Geostatistics offers a way to exploit spatial information, allowing also to study spatial continuity as an essential aspect of many geological phenomena and for which the correlation between two values is as greater as the reciprocal spatial distance is smaller (Matheron, 1963).

Uncertainty in mapping arises when it is necessary to infer (Myers, 2005) the type of soil material that exists at unobserved points from data obtained at points of observation (Daneshkhah, 2004).

To study the effect of correlation, observe first that soil samples collected adjacent to each other are likely to have properties that are similar to each other compared with the relationships between those collected at large distances apart (Matheron, 1973). Also, soil specimens tested by the same device will likely show less scatter in the measured values than if they were tested by different devices in separate laboratories.

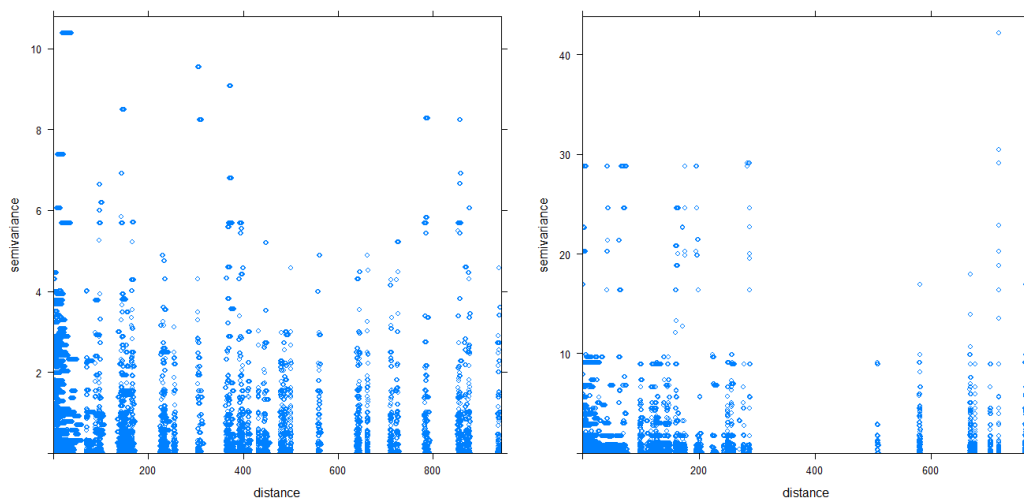
The degree of correlation as a function of separation distance between soil samples depends on the specific soil type and deposit characteristics and on the property considered (Matheron, 1963). Nevertheless, the more erratic the variation - less correlated - of the soil property with distance and the larger the soil domain considered, the larger the reduction in the variability of the average property will be.

This phenomenon is a result of the increasing likelihood that unusually high property values at some points will be balanced by low values at other points;

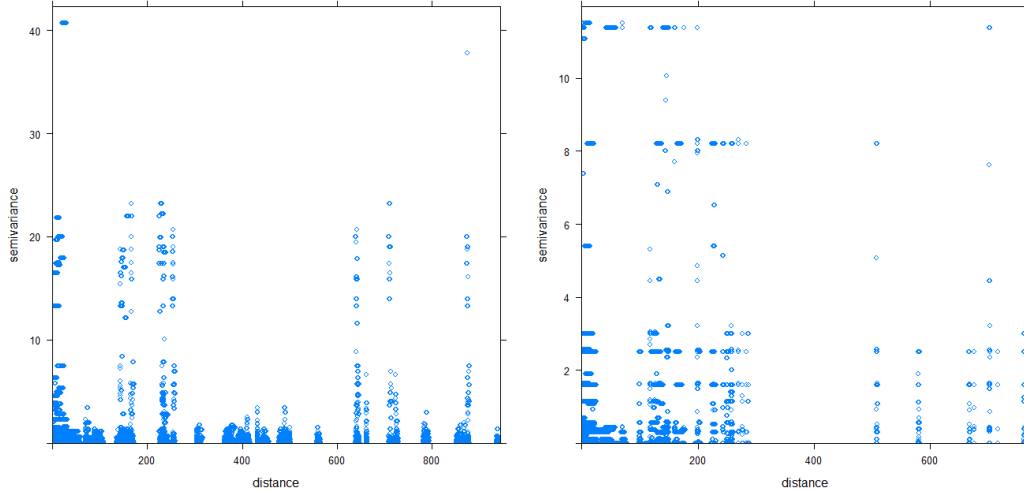
therefore, the average property is less likely to take on exceptionally high or low values (Sidler, Prof and Holliger, 2003).

Second, the in-situ soil property at incipient failure is not necessarily duplicated by the sampling and testing procedure performed on the soil specimen. Some of the causes of variance are sample disturbance, different stress conditions, and macro features that may not be well represented by a small specimen. Hence (Kim and Sitar, 2013), a bias may exist that needs to be analysed and incorporated into the overall (Phoon *et al.*, 2006b) spatial variability evaluation.

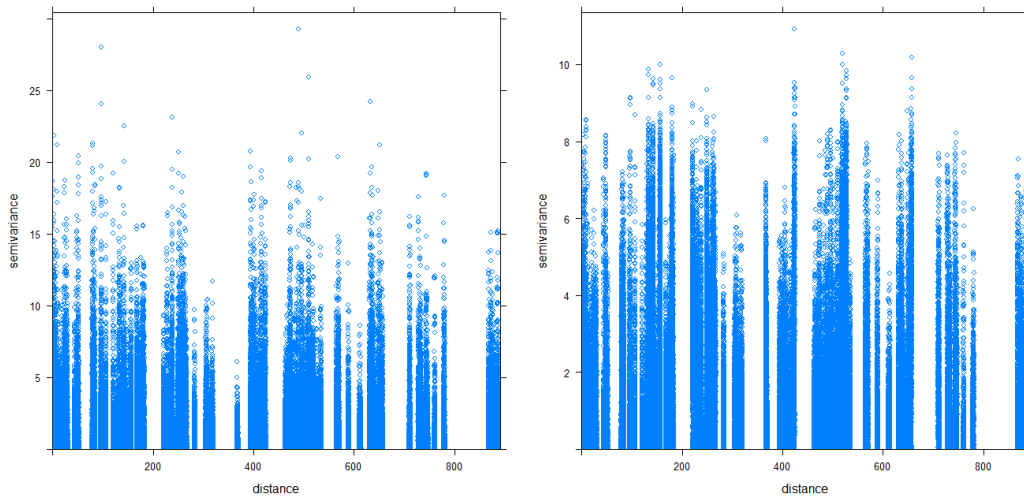
To characterize the entire variability of soil indices, *variogram clouds* have been graphed. They represent the diagram of pairs of values as a function of the sample distance and the different variability scale related to both horizontal and vertical directions necessary to determine the empirical variograms (Oliver and Webster, 2014).



Graph 6 - Variogram clouds of ICSISaG in 2006 (left) and 2010 (right)



Graph 7 - Variogram clouds of I_{CoDS} in 2006 (left) and 2010 (right)



Graph 8 - Variogram clouds of I_{Fs} (left) and I_k (right) in 2006

In the geo-applications, due to the sedimentary nature of a flat soil deposit, two locations separated by vertical distance are more likely to have different properties than two locations separated by the same distance but in the horizontal direction (Matheron, 1963). The application problem, when trying to model experimental variograms on data, consists in the different sampling scales for the vertical and horizontal directions due to the sedimentary nature of a flat soil deposit; for instance, the information along a vertical well bore is indeed on a 'scale of detail', the horizontal information between wells is on a 'scale of area' (Phoon and Kulhawy, 1996). In particular, as show the above graphics, the locations separated by vertical distance are in order of few meters (scale of detail) while the distances in the horizontal direction are representative of the scale of

area. Thus, it is easy to construct a vertical spatial relationship, but difficult to construct the horizontal one.

When more scales (Jaksa, 1982) of the same variable are not recognised - generally the smallest - experimental variogram does not show a clear structure near the origin of axes: this may be unjustly associated with a nugget effect as measurement error (no spatial relationship) for small extents. It is therefore essential to make an experimental variogram that changes with the distance (width); its tolerance and the number of lags, over which the variogram will be calculated, allow to appreciate adequately the spatial variability (Cressie, 1989). Hicks and Samy (2004) observed that scale of fluctuation in horizontal direction is much larger (less variability), due to natural processes, than in vertical direction.

4.3.1 Variograms scales

To underline the presence of spatial correlation between sampled values, they have been analysed in two different variability scales corresponding to the horizontal and the vertical ones.

As first step the omnidirectional variogram (Cressie, 1989) was calculated: an isotropic analysis which includes all data pairs regardless of their directions.

In particular it is found to be a correlation which decreases increasing the separation distance. Practically, this means that the values of the sampled points at distances close to each other, are most correlated (with small variance) while increasing the distance it decreases to settle to a constant value.

Subsequently, it was investigated the presence of directional anisotropy (Cressie, 1989) or if there are directions such that the spatial correlation is greater or lesser than the others. To do this, two angular directions were used:

- alpha (α): the angle in the horizontal plane;
- beta (β): the angle in vertical direction.

The analyses on horizontal plane have not shown the presence of directional anisotropy rotating every 90 degrees the variogram plotting. This means that they have an isotropic correlation distance: at equal spatial distance the variance does not vary for different investigated directions.

Therefore, omnidirectional variograms may be considered representative of the all variability characterizations, then evaluated for each soil index.

At this point, theoretical variogram modelling is required to represent the behaviour of each spatial variable in term of variability degree (sill) and autocorrelation distance (range). This aims at estimating soil variability in unsampled locations (Goovaerts, 1999).

The theoretical model of three-dimensional variograms have been built for each soil indices considering spatial correlation parameters in all directions.

Since a difference in range values has been detected between the two scales (Jaksa, Kaggwa and Brooker, 1999) of fluctuation (i.e. vertical and horizontal), this means that fitted variogram model along horizontal as well as vertical directions must be evaluated separately.

The models which best fitted the variability scales (horizontal and vertical) of every index have been applied and following graphed (Graphs 9-11).

The Exponential model has been used as theoretical variogram based on the goodness of fitting to empirical values. It has the following formula (Chiles and Delfiner, 1999; Cressie, 1993):

$$\gamma(h) = c_0 + c_1[1 - e^{-(h/\alpha)}] \quad (13)$$

where:

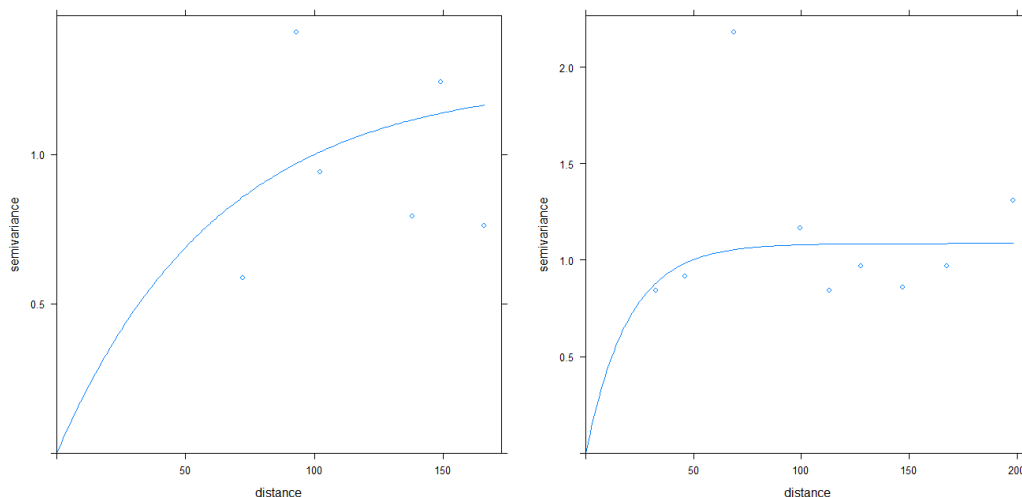
h = distance between i^{th} and j^{th} locations;

$\gamma(h)$ = semi-variance at distance h ;

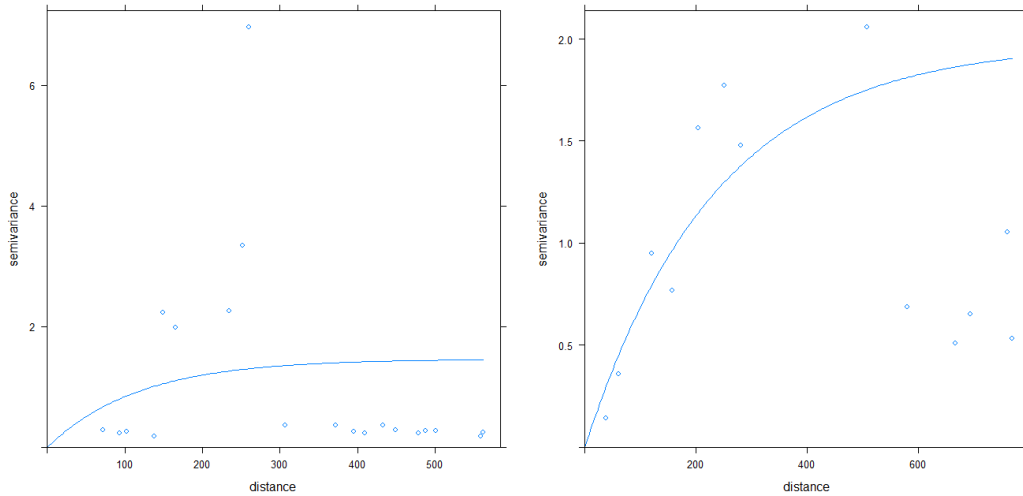
c_0 = nugget effect;

c_1 = partial sill;

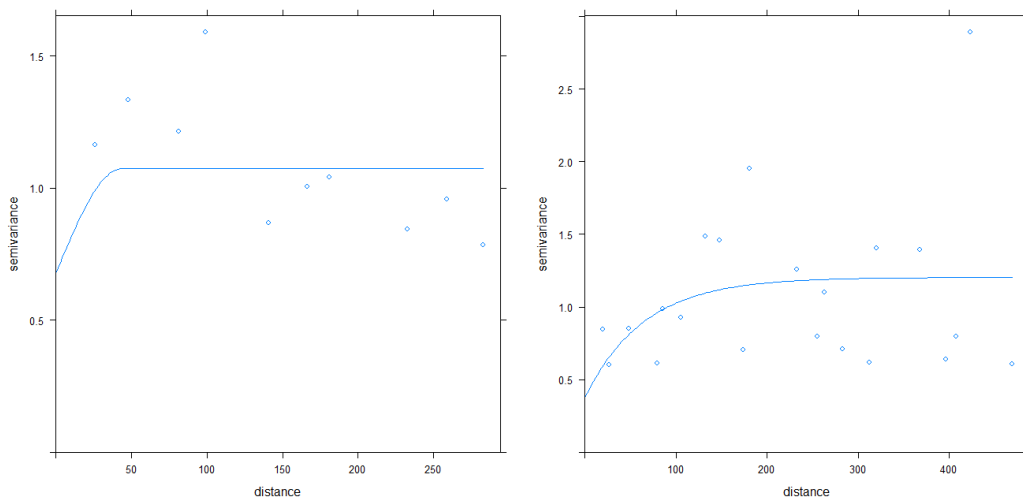
α = range at which the variogram is of 95% of the sill.



Graph 9 - Horizontal variograms and theoretical models for ICsisaG in 2006 (left) and 2010 (right)



Graph 10 - Horizontal variograms and theoretical models for I_{CoDS} in 2006 (left) and 2010 (right)



Graph 11 - Horizontal variograms and theoretical models for I_{Fs} (left) and I_k (right) in 2006

F_s and k values show in Graph 11 a structure near the origin of the axes: this may be unjustly associated with a nugget effect as measurement error (no spatial relationship) for small extents. It happens when more scales of the same variable are not recognised and it is generally associated to the smallest one (Matheron, 1963).

The following coding has been used respectively to describing:

- Calculation step: distance (h_{lag}) and distance tolerance ($tol.h_{lag}$);
- Angular parameters: alpha (hor), alpha tolerance ($tol.hor$), beta ($vert$), beta tolerance ($tol.vert$);

- Nugget effect: partial sill (Nug_psill) and range (Nug_range);
- Theoretical parameters: partial sill (Exp_psill) and range (Exp_range).

The choice of this parametric representation is based on the best characterization of the dataset and defined after the application of attempting procedures.

	I _{CSiSaG}	I _{CoDS}	I _{Fs}	I _k	
h_lag	20	20	30	20	m
tol.h_lag	10	10	15	10	m
alpha	0	0	0	0	°
tol.hor	180	180	180	180	°
beta	0	0	0	0	°
tol.vert	89	89	89	89	°

Table 20 - Empirical values of horizontal variograms for I_{CSiSaG}, I_{CoDS}, I_{Fs}, I_k in 2006

	I _{CSiSaG}	I _{CoDS}	
h_lag	20	45	m
tol.h_lag	10	22.5	m
alpha	0	0	°
tol.hor	180	180	°
beta	0	0	°
tol.vert	89	89	°

Table 21 - Empirical values of horizontal variograms for I_{CSiSaG} and I_{CoDS} in 2010

	I _{CSiSaG}	I _{CoDS}	I _{Fs}	I _k
Nug_psill	0	0	0.67	0.37
Nug_range	0	0	0	0
Exp_psill	1.25	1.46	0.39	0.82
Exp_range	62.59	117.59	43.23	65.03

Table 22 - Theoretical values of horizontal variograms for I_{CSiSaG}, I_{CoDS}, I_{Fs}, I_k in 2006

	I _{CSiSaG}	I _{CoDS}
Nug_psill	0	0
Nug_range	0	0
Exp_psill	1.08	1.97
Exp_range	19.48	235.31

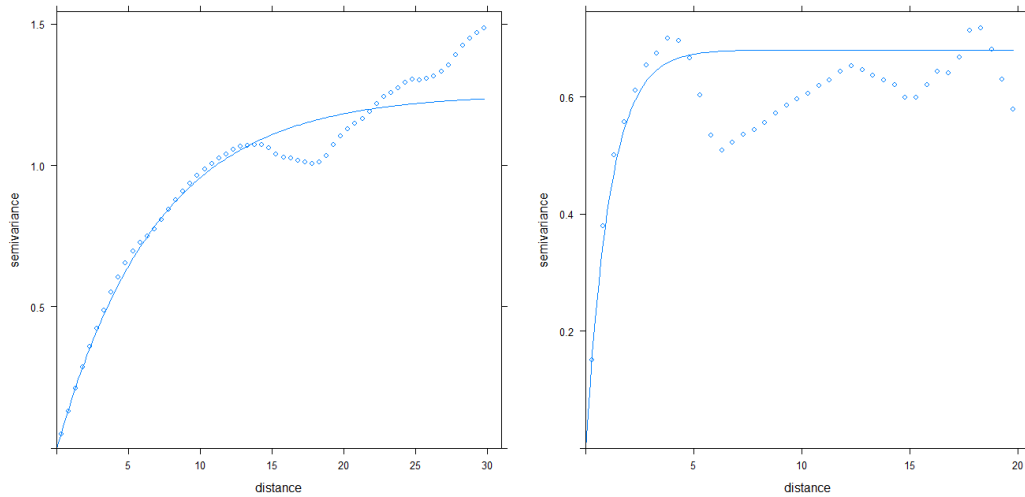
Table 23 - Theoretical values of horizontal variograms for I_{CSiSaG} and I_{CoDS} in 2010

In our case, for distances greater than 20-30m, on average, the autocorrelation tends to remain at a constant value of the sill.

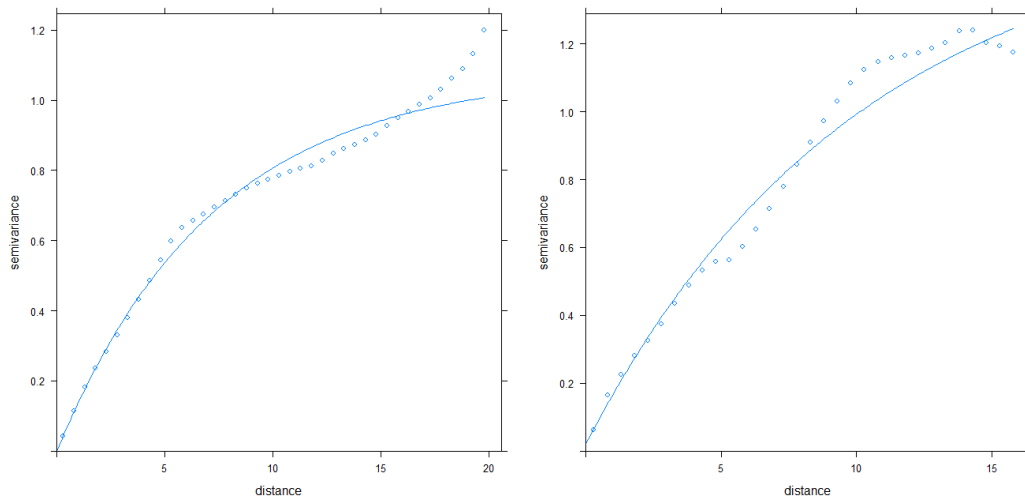
Now, the variability at the detailed scale will be evaluated such as along depth (vertical direction).

Since the depth constitutes a single direction and not a plane, the variogram at the scale of detail is unique; anisotropy condition is thus not applicable (Cressie, 1989).

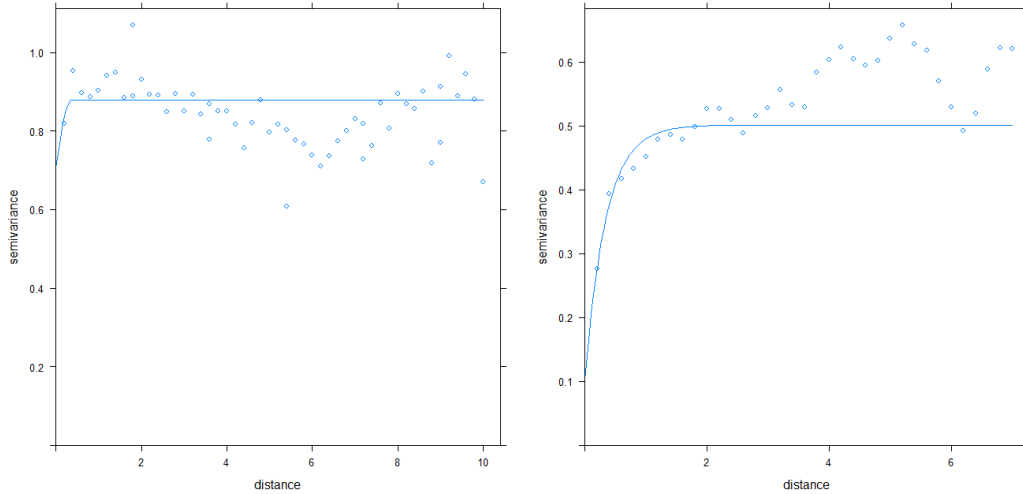
The Exponential model has been used again as theoretical variogram based on the goodness of fitting of empirical values and profiles.



Graph 12 - Vertical variograms and theoretical models for IC_{SisaG} in 2006 (left) and 2010 (right)



Graph 13 - Vertical variograms and theoretical models for ICo_{DS} in 2006 (left) and 2010 (right)



Graph 14 - Vertical variograms and theoretical models for I_{Fs} (left) and I_k (right) in 2006

	I_{CSiSaG}	I_{CoDS}	I_{Fs}	I_k	
h_lag	0.5	0.5	0.09	0.09	m
tol.h_lag	0.25	0.25	0.045	0.045	m
alpha	0	0	0	0	°
tol.hor	180	180	180	180	°
beta	90	90	90	90	°
tol.vert	0	0	0	0	°

Table 24 - Empirical values of vertical variograms for I_{CSiSaG} , I_{CoDS} , I_{Fs} , I_k in 2006

	I_{CSiSaG}	I_{CoDS}	
h_lag	0.5	0.5	m
tol.h_lag	0.25	0.25	m
alpha	0	0	°
tol.hor	180	180	°
beta	90	90	°
tol.vert	0	0	°

Table 25 - Empirical values of vertical variograms for I_{CSiSaG} and I_{CoDS} in 2010

	I_{CSiSaG}	I_{CoDS}	I_{Fs}	I_k
Nug_psil	0	0	0.7	0.1
Nug_range	0	0	0	0
Exp_psil	1.25	1.07	0.17	0.39
Exp_range	6.92	7.23	0.35	0.34

Table 26 - Theoretical values of vertical variograms for I_{CSiSaG} , I_{CoDS} , I_{Fs} , I_k in 2006

	I _{CSiSaG}	I _{CoDS}
Nug_p sill	0	0
Nug_range	0	0
Exp_p sill	0.68	1.55
Exp_range	1.1	10.17

Table 27 - Theoretical values of vertical variograms for I_{CSiSaG} and I_{CoDS} in 2010

It should be noted, from the first distances, that presence of systematic variability, such as trends, is not evident (Lacasse and Nadim, 1996). This means that there is not a structural variability due essentially to stratigraphic processes.

All experimental variograms along depth show as the spatial correlation progressively reaches a sill remaining constant after 0.5m.

Finally, in order to make a spatial estimation of the soil indices among the slope, DEM layers of surface topography in 2006 and 2010 were used. From the ground surface, deeper layers were also extrapolated: slip-surface layer (Guerriero *et al.*, 2014) and one more at middle depth between the two previous ones.

4.3.2 Stochastic soil predictions

Geostatistics studies the natural phenomena that develop on a spatial basis starting from information deriving from their sampling by studying the spatial variability of the parameters that describe the aforementioned phenomena extracting the rules in a reference modeling framework and using them to carry out the operations aimed at giving a solution to specific problems concerning the characterization and estimation of the phenomena themselves (Murty, 2005).

Peculiarity of Kriging regression is the possibility of having, for each estimate, a value which gives a reliability degree to spatial prediction in term of minimal variance of estimation (Matheron, 1973). This allows to define a confidence interval by identifying the areas in which it is necessary to increase the density of investigations.

Linear spatial regression analysis was performed by applying Kriging as the best stochastic predictor (Oliver and Webster, 2014). Kriging considers each observation as a single realization of an aleatory variable whose statistical properties are defined by a variogram function (Sidler, Prof and Holliger, 2003). Starting from available observations, theoretical models have been realized which define spatial variability as well as auto-correlation of the predisposing factors in all three dimensions according to their mutual distance.

A 3D variogram model has been implemented to all indices conditioning soil instability. Therefore, Universal Kriging (UK) regression model (Pebesma and Graeler, 2017) has been applied to the variables providing spatial predictions of the values in points without surveyed information (unknown data). The following predictive maps have been obtained by multiplying values of spatial variability to soil index, as in Eqs (12) and (13).

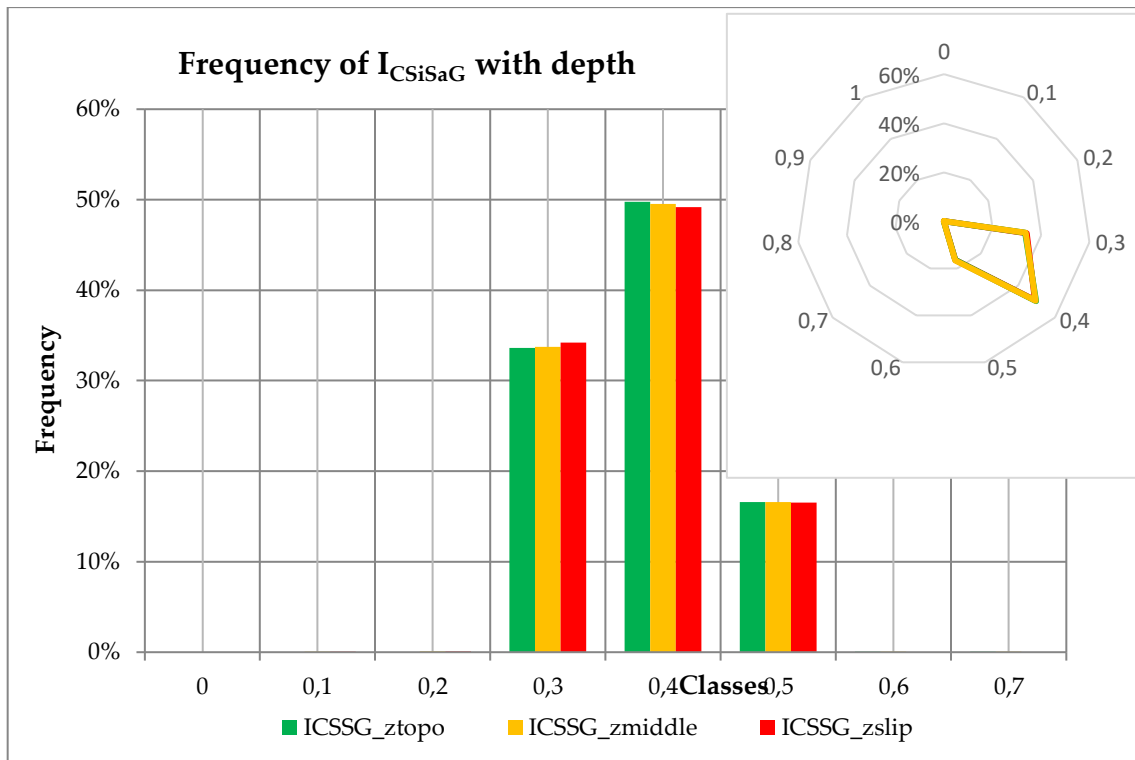
$$I_{soil}(\text{predicted})_{[xyz]} = I_{CSiSaG} * I_{CoDS} * I_{Fs} * I_k = I_{geo} * I_{Fs} * I_k \quad (14)$$

$$I_{soil}(\text{variance of prediction})_{[xyz]} = var_{CSiSaG} * var_{CoDS} * var_{Fs} * var_k \quad (15)$$

The geostatistical approach provides not only an estimate of the unknown value, but also an estimate of the uncertainty referred to a specific spatial location (Goovaerts, 1999) of the predicted value: the *Kriging variance*.

The three-dimensional spatial maps below illustrate the spatial distribution of soil spatial predictions and errors of estimate associated to them by using Universal Kriging model as well as their distribution in term of frequency classes. The predicted values were normalized (from 0 to 1) in order to make them comparable.

The graphs illustrate the frequency and distribution of the values through both histogram plots and radar charts.



Graph 15 - Frequency of I_{CSiSaG} index at different vertical depths in 2006

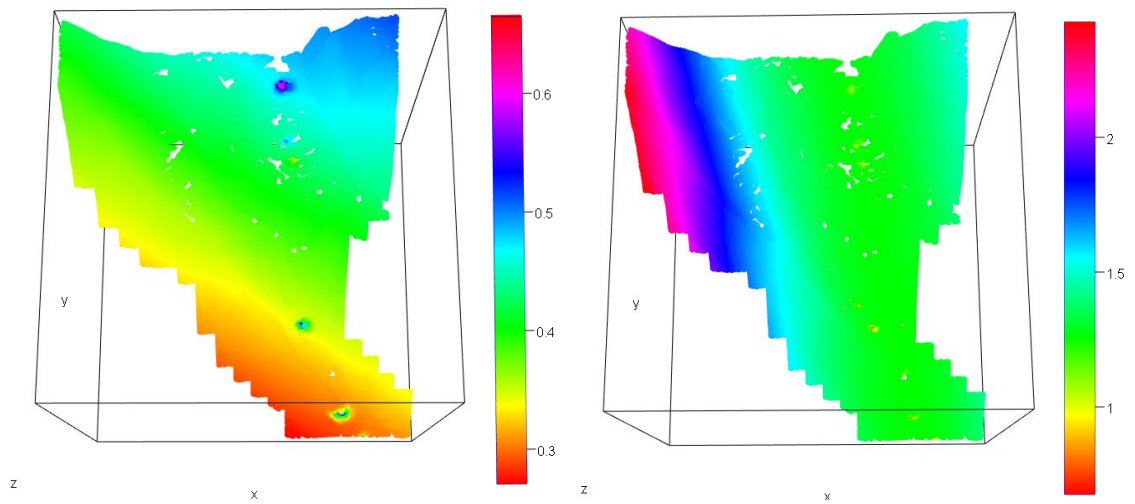


Figure 42 - Variability maps of spatial predictions (left) and variances (right) of I_{CSiSaG} at ground surface in 2006

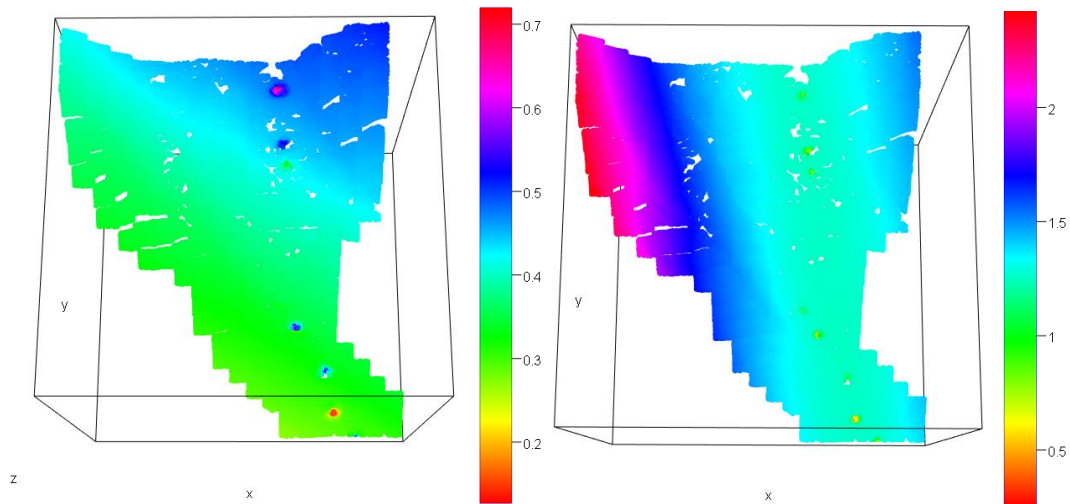


Figure 43 - Variability maps of spatial predictions (left) and variances (right) of ICsIsaG at middle surface in 2006

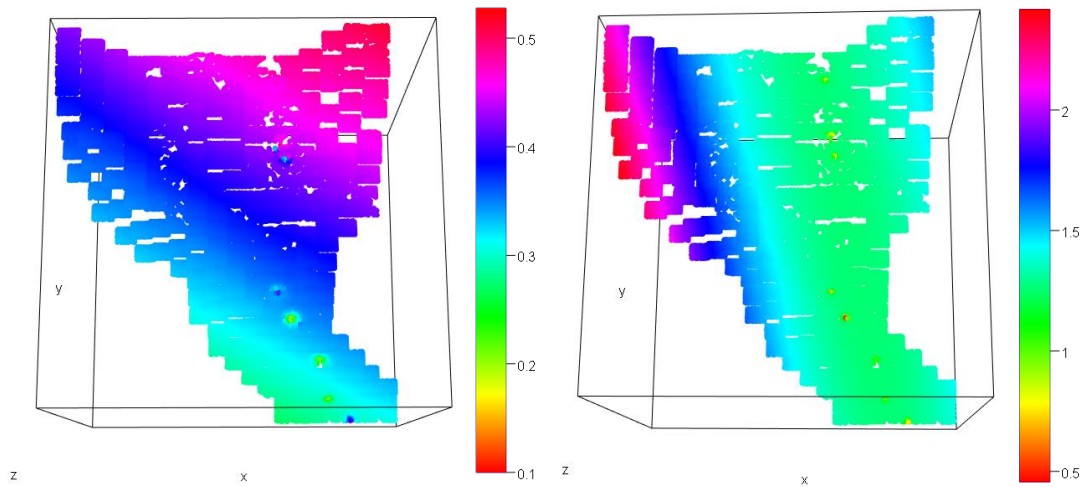
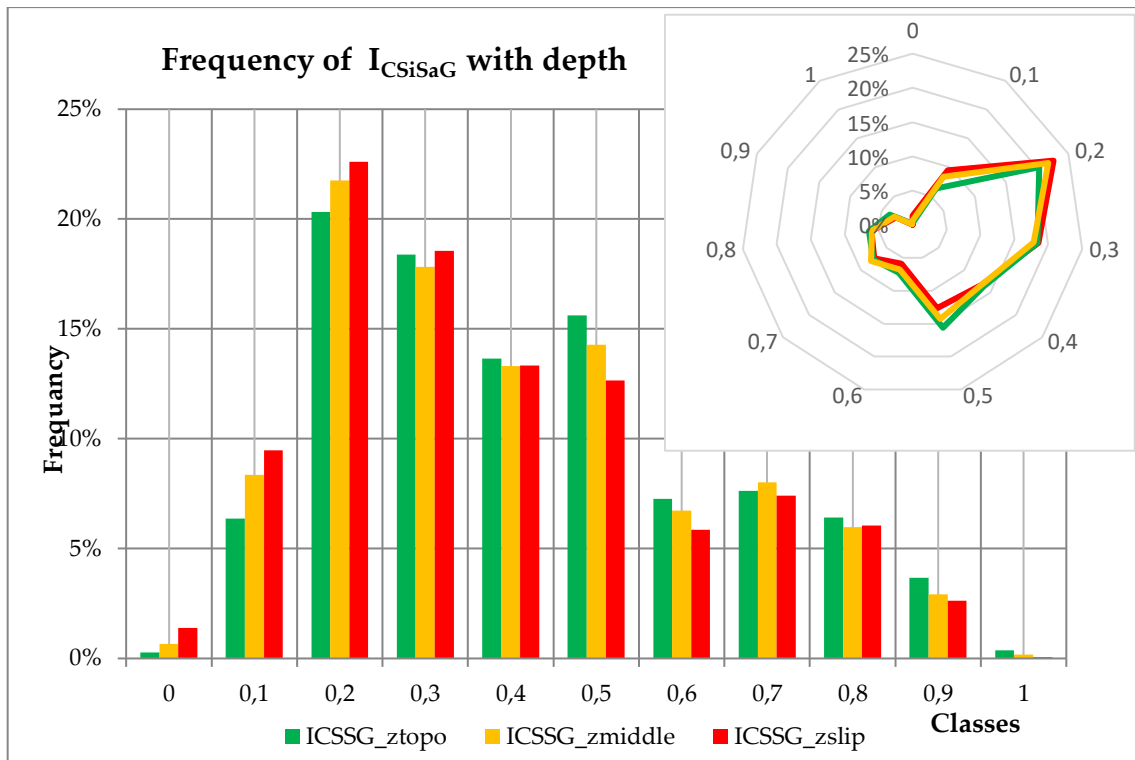


Figure 44 - Variability maps of spatial predictions (left) and variances (right) of ICsIsaG at slip surface in 2006

In 2006, Kriging maps show values close to zero downstream of the topographic surface, growing upwards. Compared to the topographical level, the intermediate surface and even more the critical surface tend to have more uniform and homogeneous values. The predictions are characterized by a greater variance of estimation along the left end of the slope, while in the central band, corresponding to the landslide area, the values are between 1 and 1.5 for all three depths.



Graph 16 - Frequency of I_{CSiSaG} index at different vertical depths in 2010

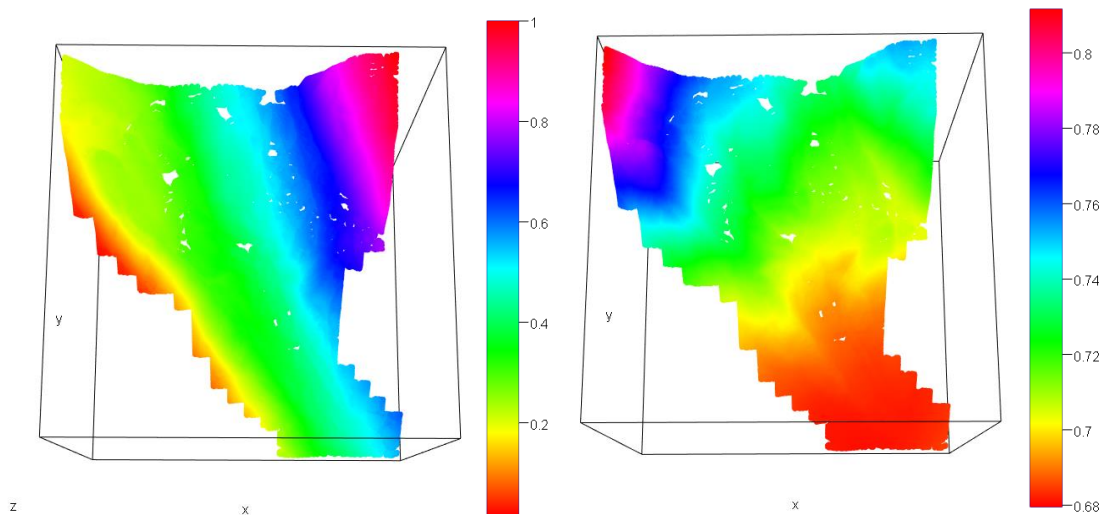


Figure 45 - Variability maps of spatial predictions (left) and variances (right) of I_{CSiSaG} at ground surface in 2010

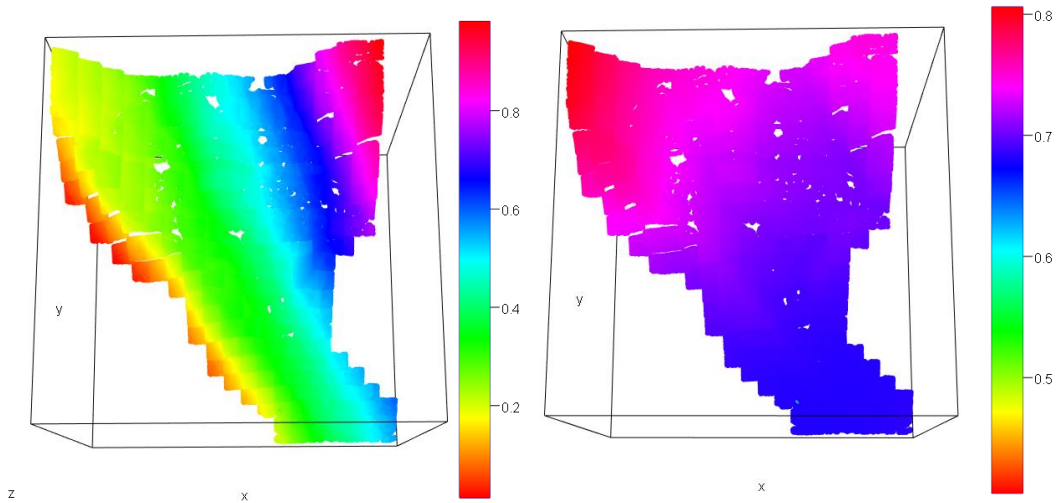


Figure 46 - Variability maps of spatial predictions (left) and variances (right) of I_{CSiSaG} at middle surface in 2010

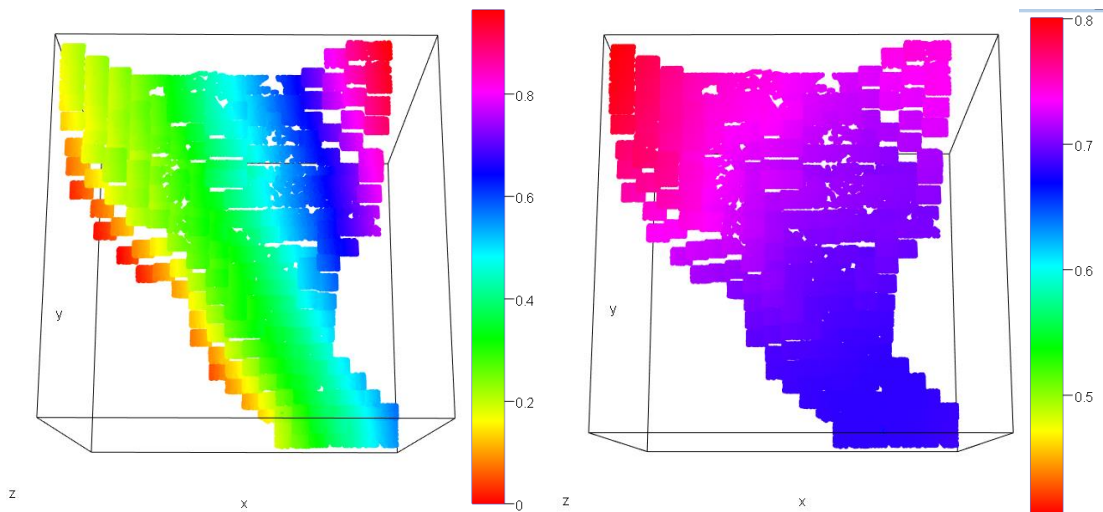
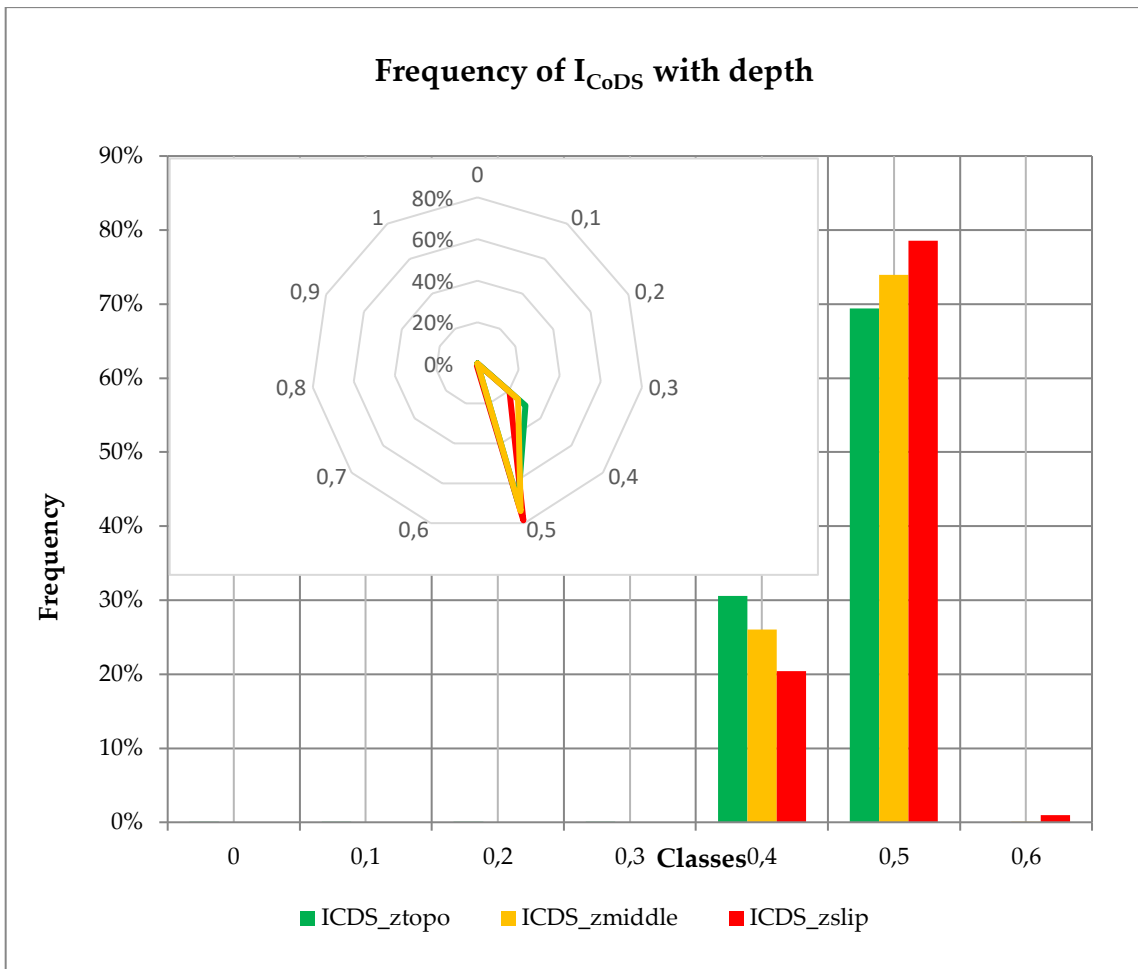


Figure 47 - Variability maps of spatial predictions (left) and variances (right) of I_{CSiSaG} at slip surface in 2010

In 2010 the frequencies for the granulometric index are characterized by a greater heterogeneity, presumably due to the reactivation of the landslide area with consequent mixing and redistribution of the granulometries present with respect to the more homogeneous condition of 2006.

Along the vertical profile the granulometries are constant, a considerable variability is present between upstream and downstream parallel to the geometry of the landslide. The estimate variance changes with increasing depth, but maintaining minimum values in the downstream area.



Graph 17 - Frequency of I_{CoDS} index at different vertical depths in 2006

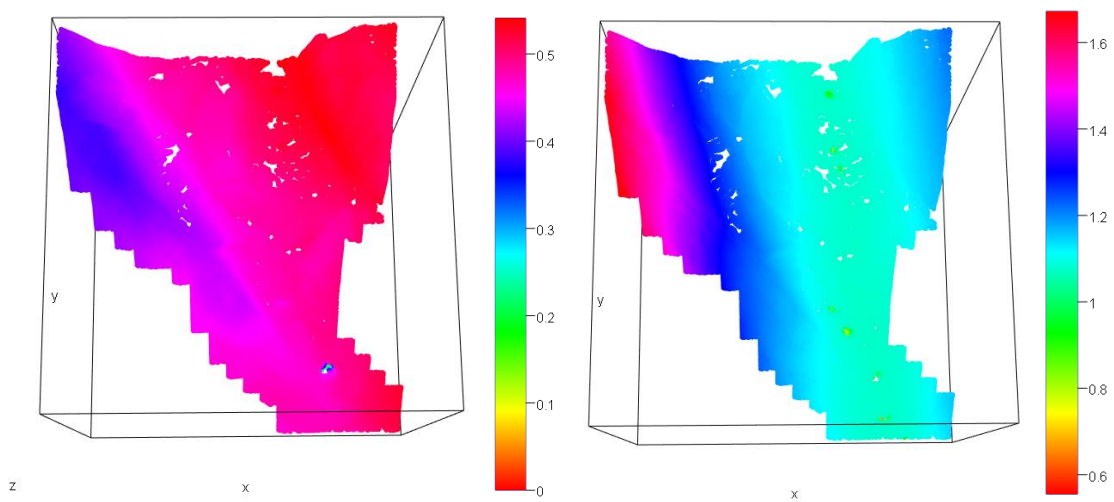


Figure 48 - Variability maps of spatial predictions (left) and variances (right) of I_{CoDS} at ground surface in 2006

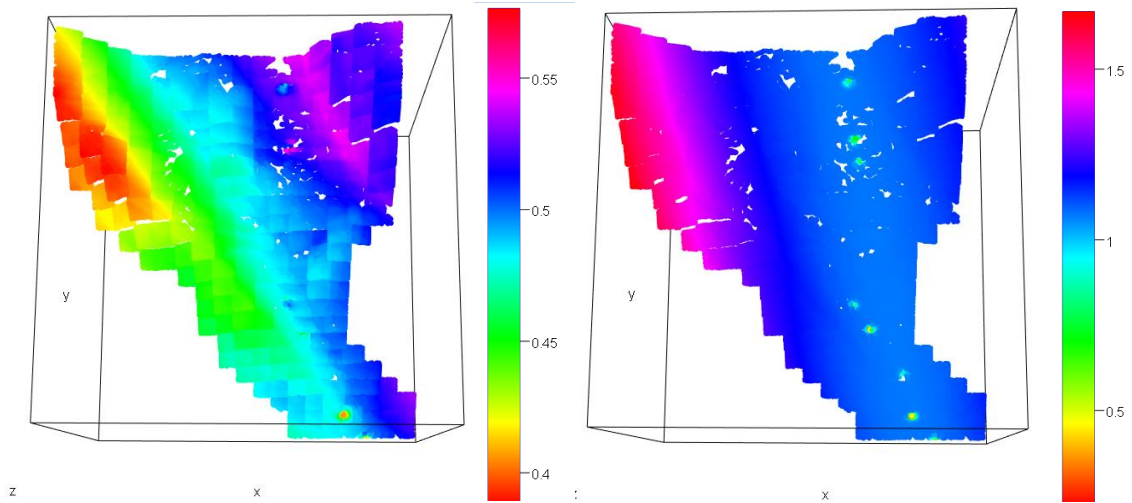


Figure 49 - Variability maps of spatial predictions (left) and variances (right) of I_{CoDS} at middle surface in 2006

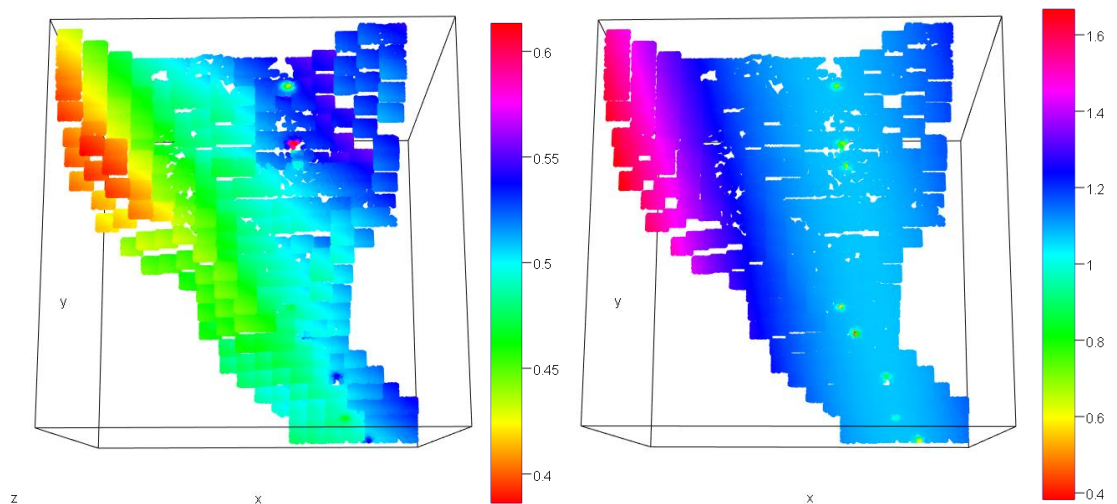
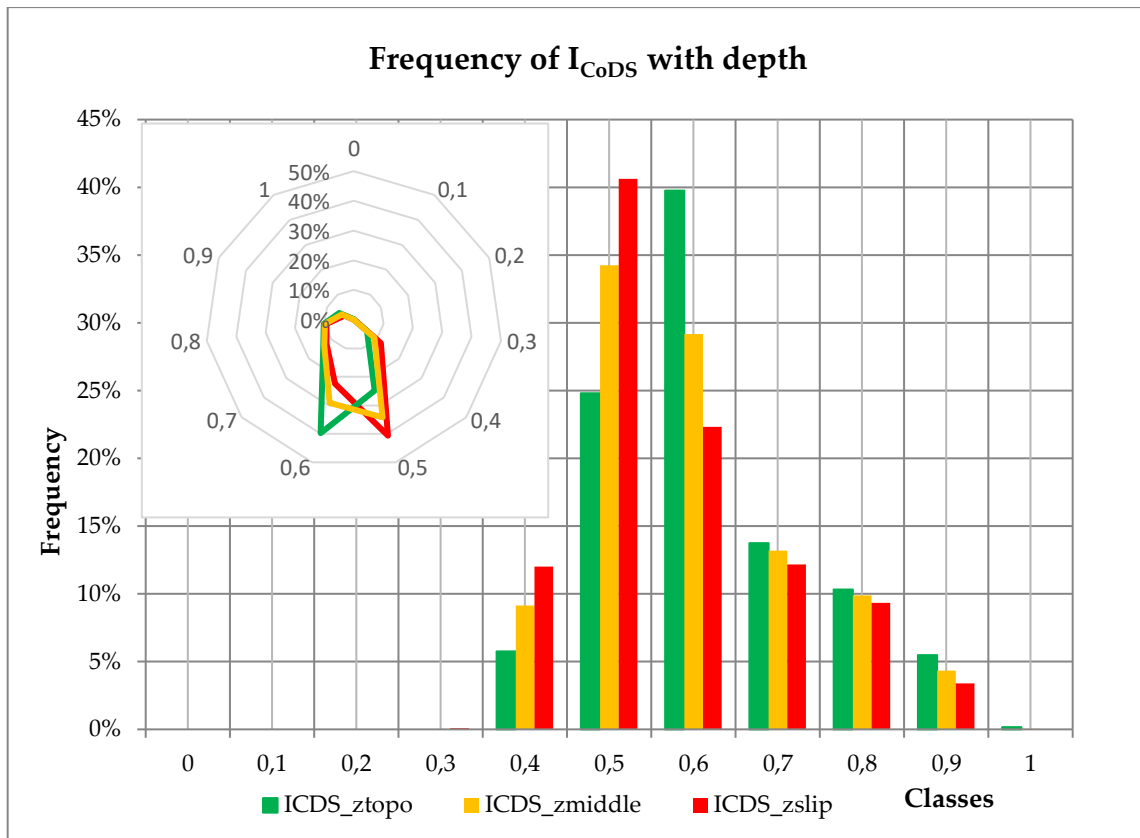


Figure 50 - Variability maps of spatial predictions (left) and variances (right) of I_{CoDS} at slip surface in 2006

Regarding soil compaction index, despite a homogeneity distribution along the topographic surface, the layers at greater depth reveal a high spatial heterogeneity, sign of a variability that grows in the right area corresponding to moderate variance values, suggesting a good reliability of the estimates.



Graph 18 - Frequency of I_{CoDS} index at different vertical depths in 2010

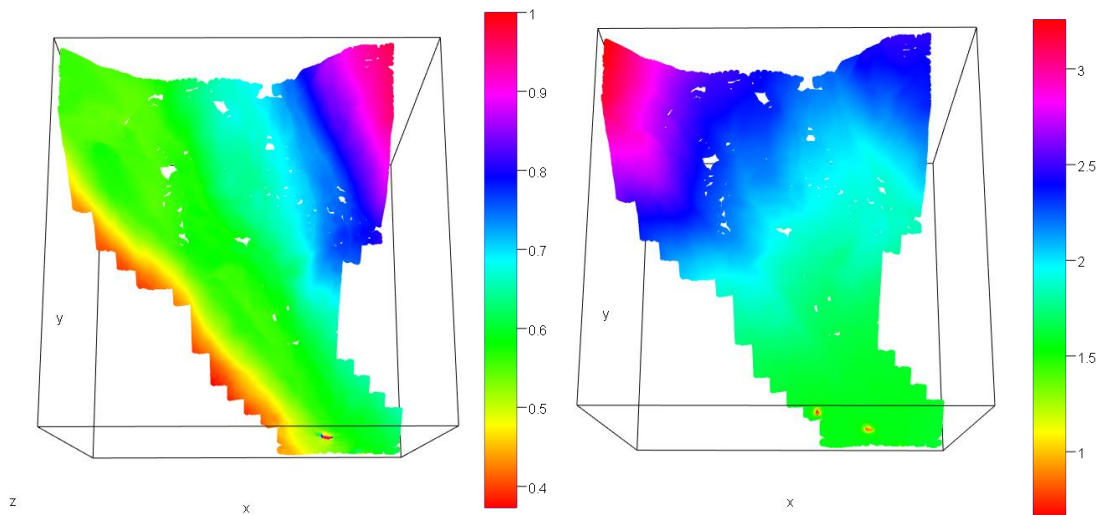


Figure 51 - Variability maps of spatial predictions (left) and variances (right) of I_{CoDS} at ground surface in 2010

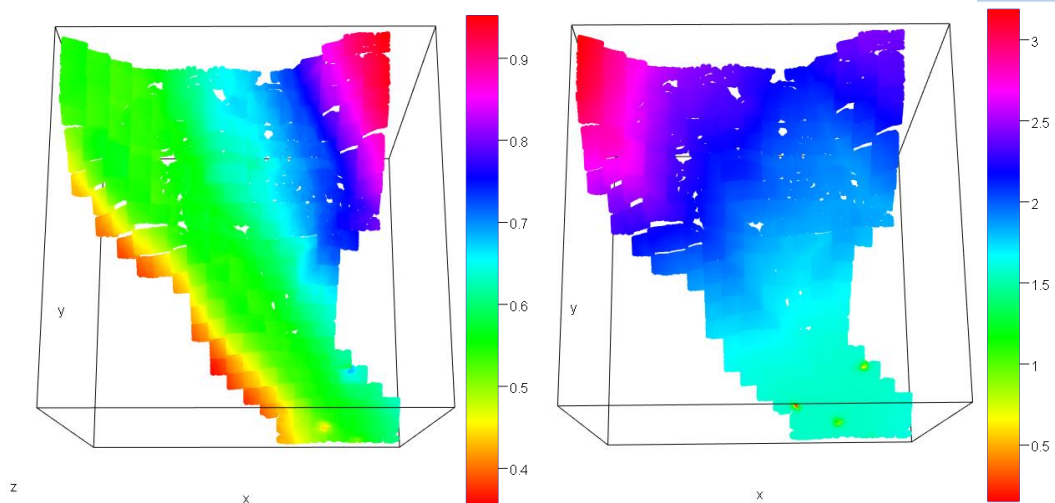


Figure 52 - Variability maps of spatial predictions (left) and variances (right) of I_{CoDS} at middle surface in 2010

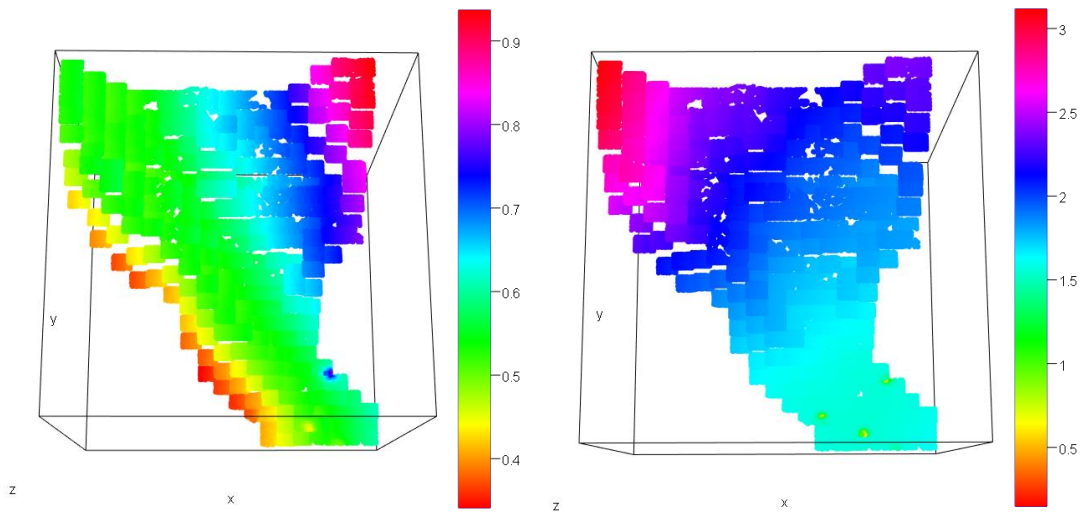
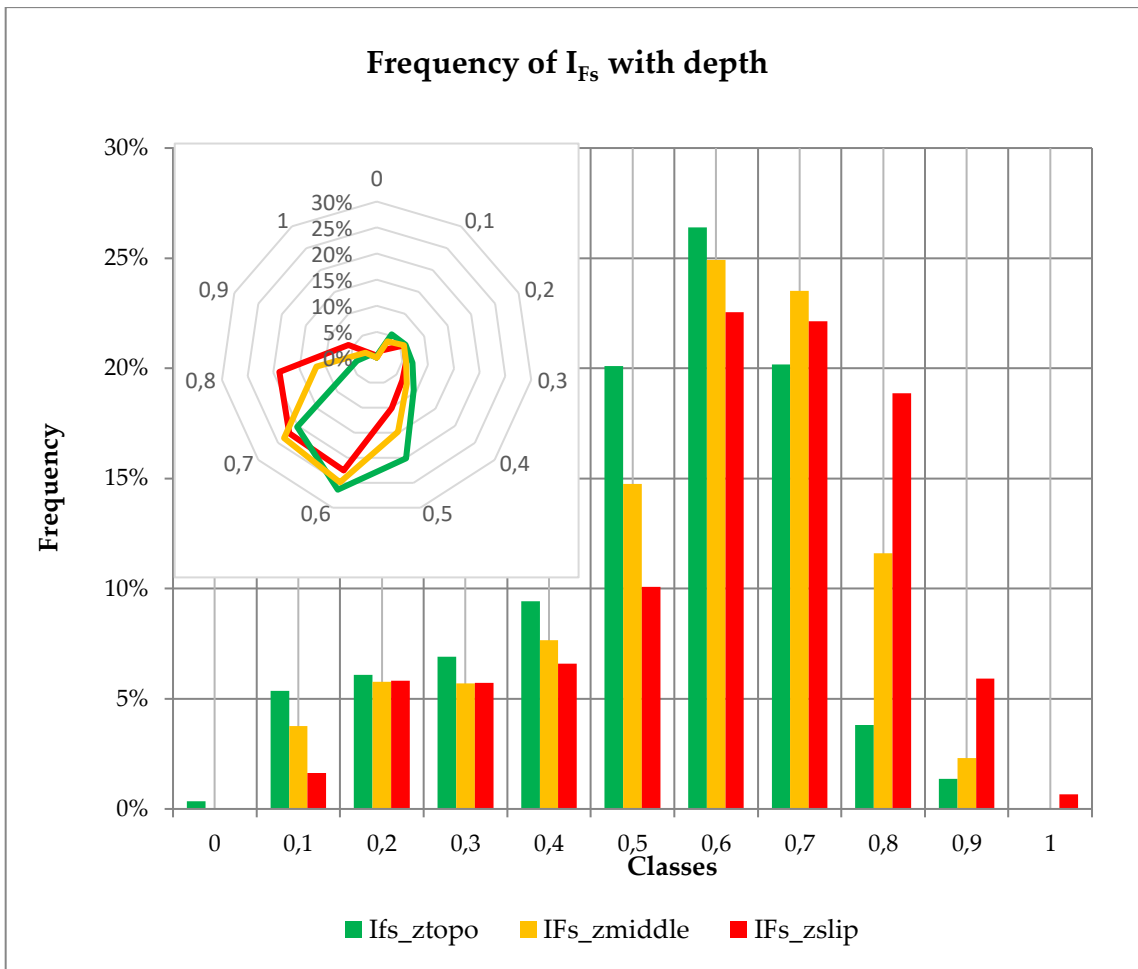


Figure 53 - Variability maps of spatial predictions (left) and variances (right) of I_{CoDS} at slip surface in 2010

Once again, 2010 shows a variability of frequency classes that suggests a greater heterogeneity of the level of soil compaction. Moderate values characterize the left side of the slope, while lower frequency classes are on the side with greater topographic elevation. Finally, the variances of the valley are attested on the value 1.5 in all the topographical levels maintaining therefore the same reliability of estimate.



Graph 19 - Frequency of I_{Fs} index at different vertical depths in 2006

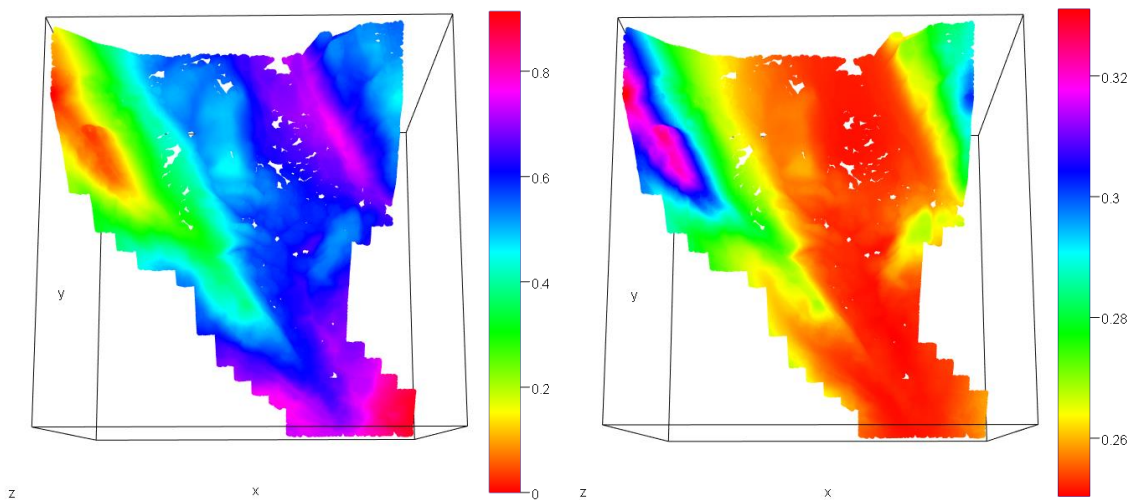


Figure 54 - Variability maps of spatial predictions (left) and variances (right) of I_{Fs} at ground surface in 2006

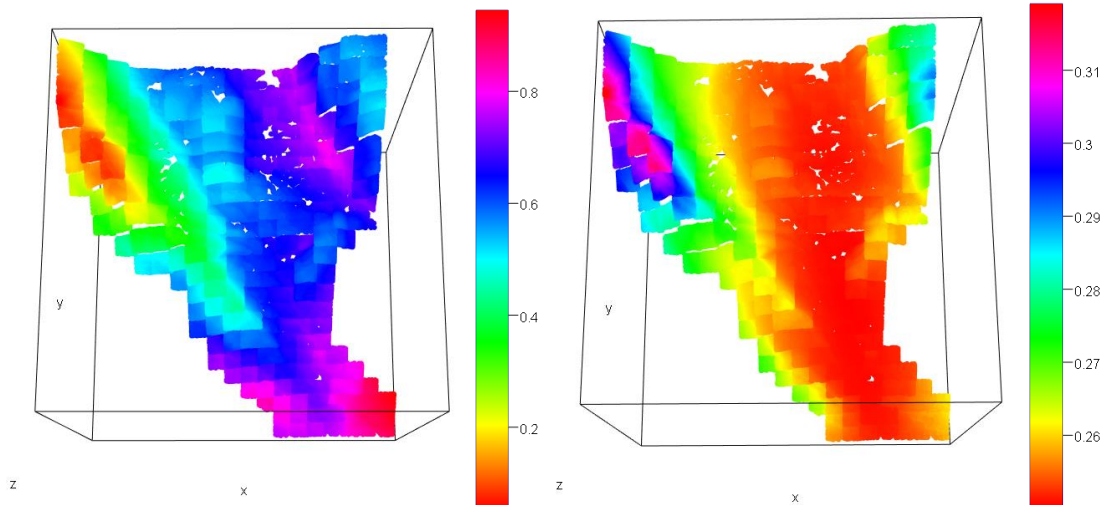


Figure 55 - Variability maps of spatial predictions (left) and variances (right) of I_{Fs} at middle surface in 2006

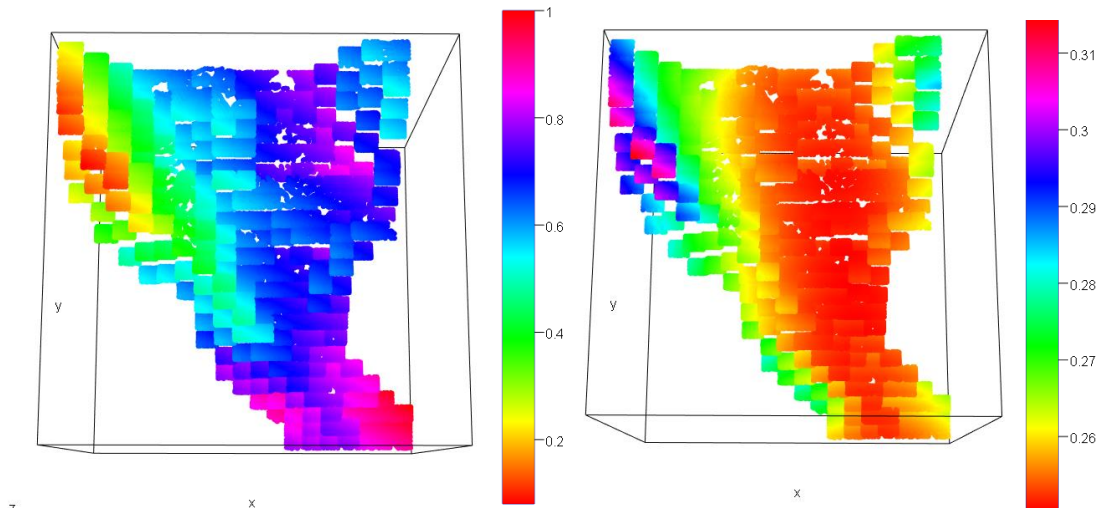
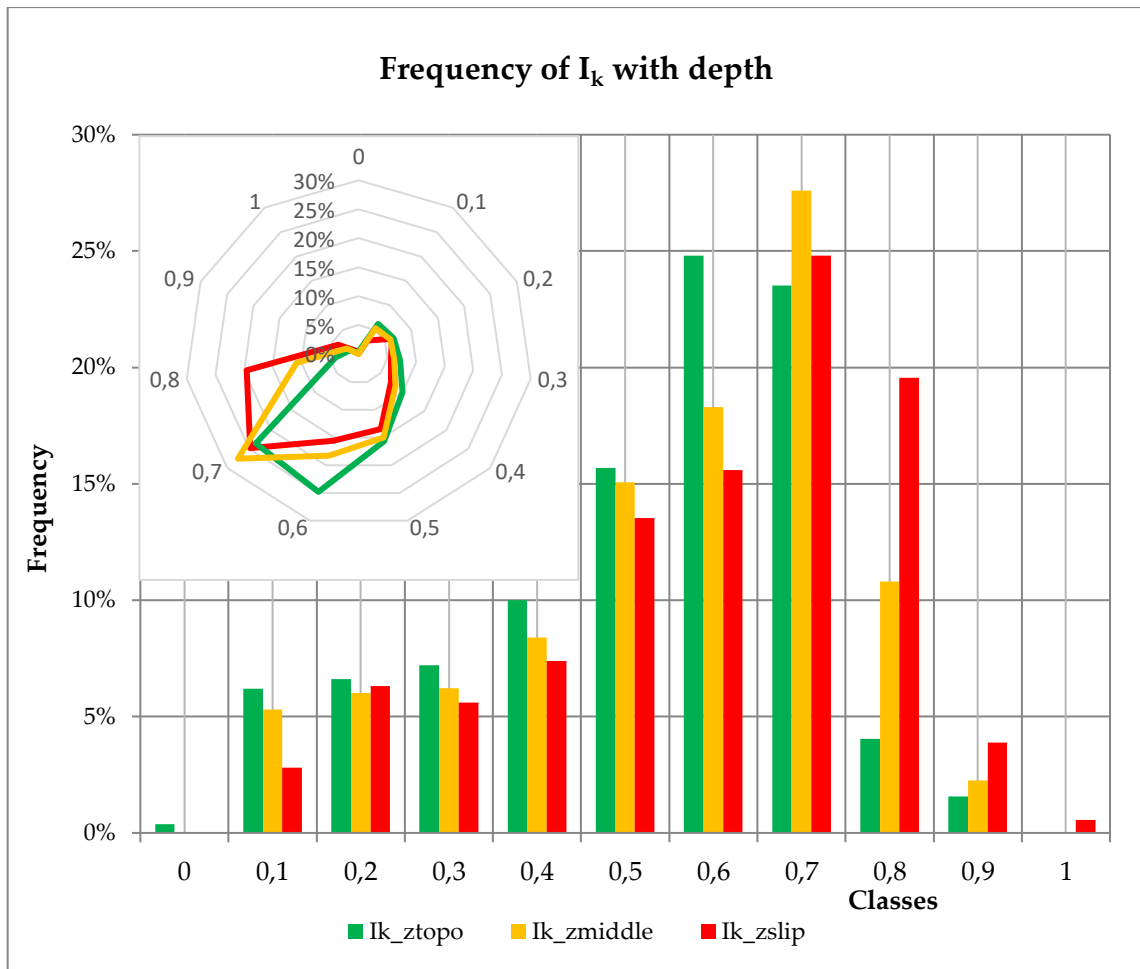


Figure 56 - Variability maps of spatial predictions (left) and variances (right) of I_{Fs} at slip surface in 2006

As far as the spatial variability of the friction ratio is concerned, no particular heterogeneity comes at deeper layers; maximum values are in the valley area, tending to zero along the western slope profile. The variance shows in the central area a homogeneity of values that attest around zero.



Graph 20 - Frequency of I_k index at different vertical depths in 2006

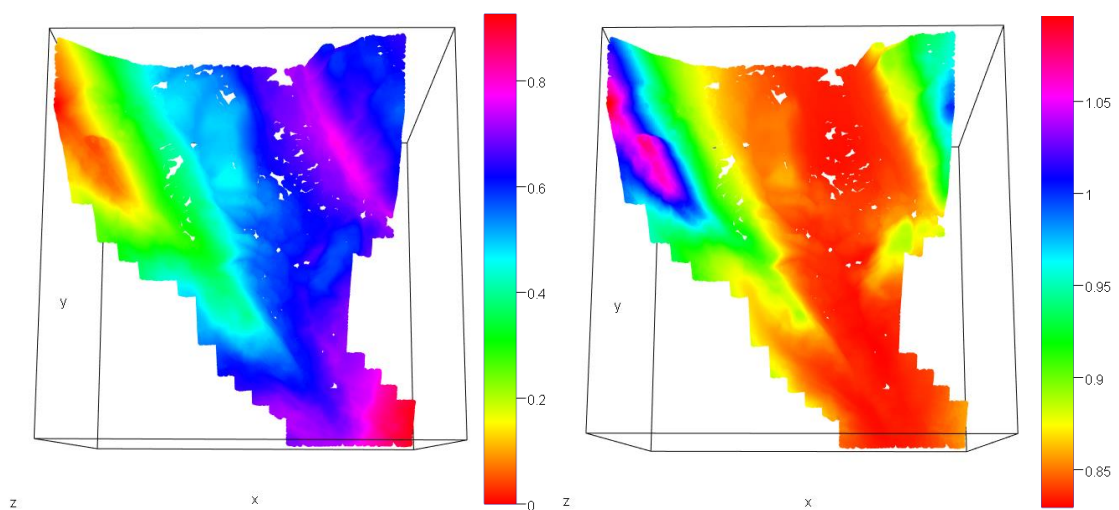


Figure 57 - Variability maps of spatial predictions (left) and variances (right) of I_k at ground surface in 2006

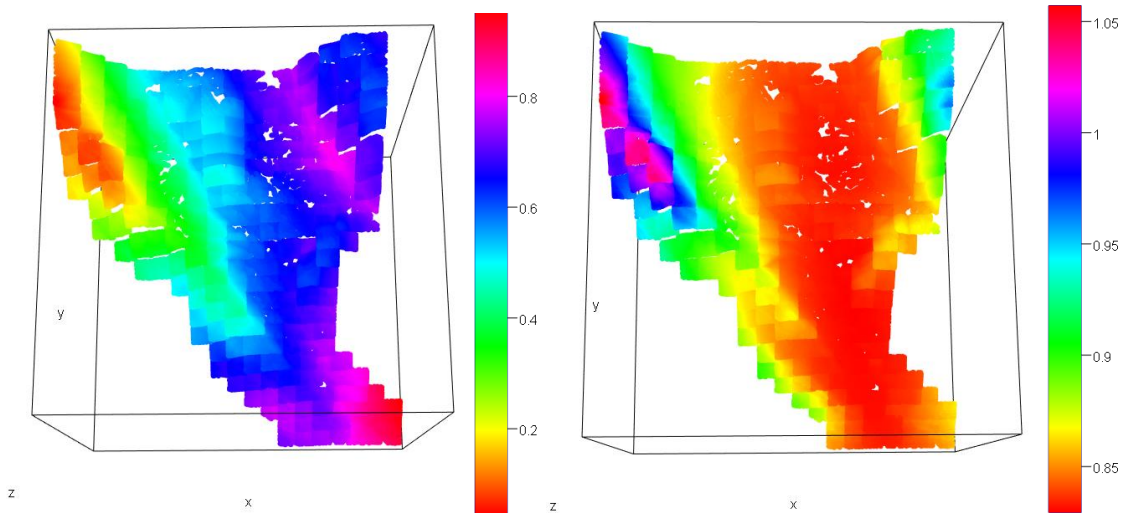


Figure 58 - Variability maps of spatial predictions (left) and variances (right) of I_k at middle surface in 2006

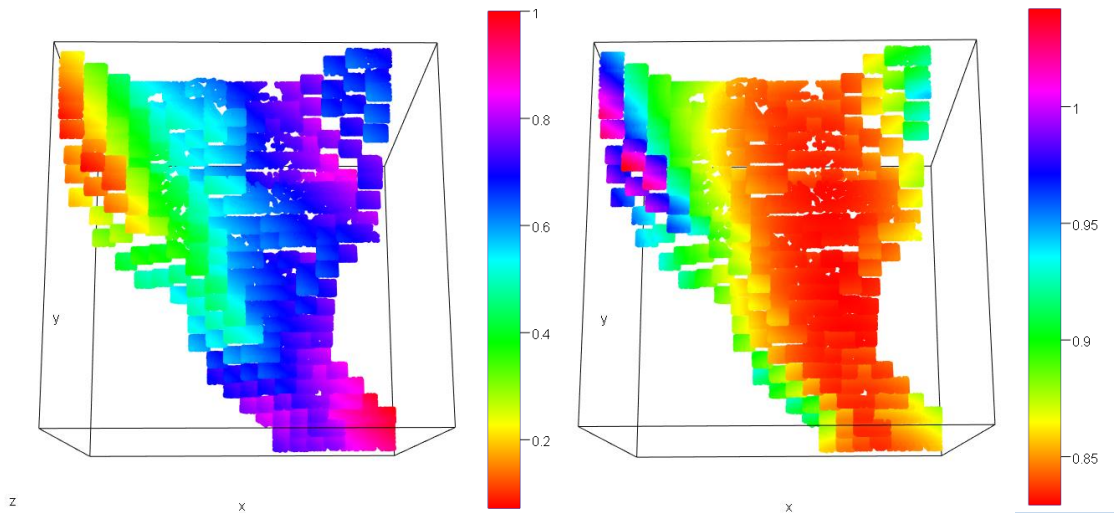
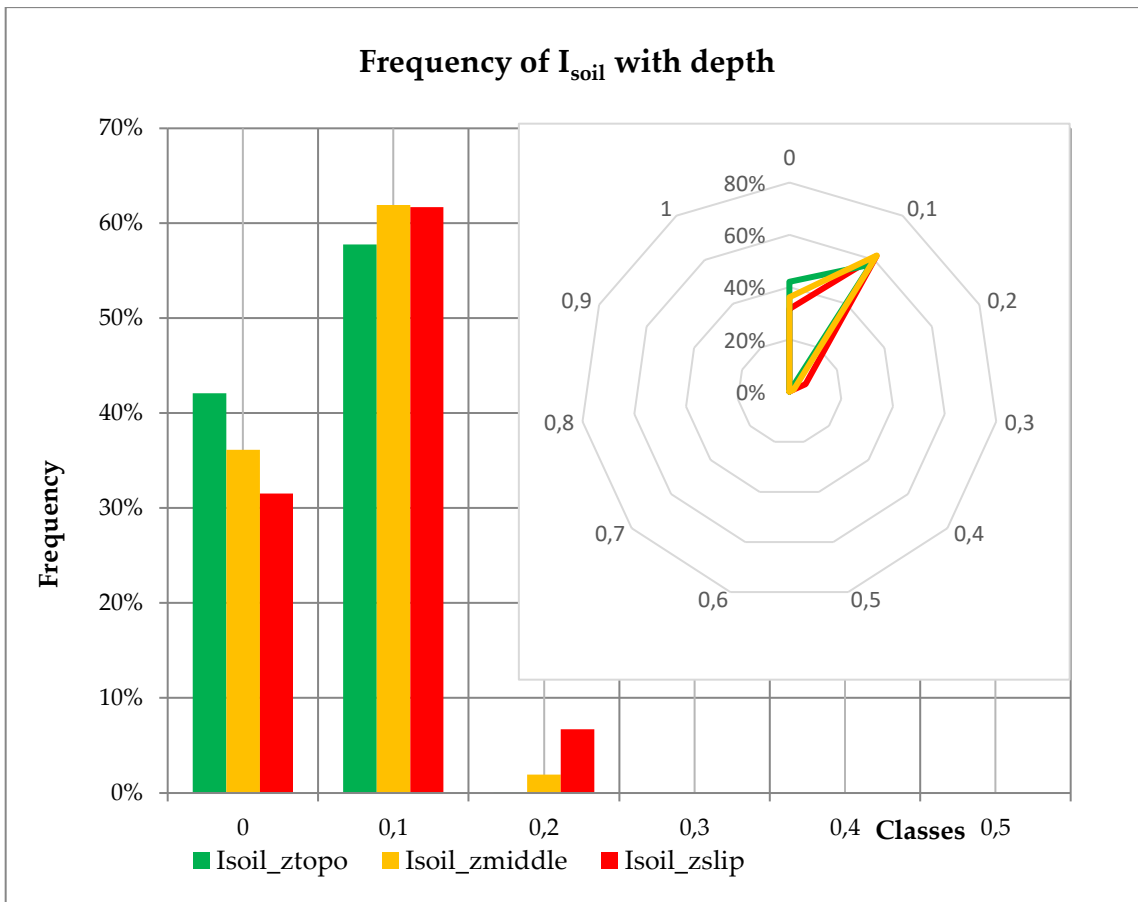


Figure 59 - Variability maps of spatial predictions (left) and variances (right) of I_k at slip surface in 2006

The permeability values are widely distributed in all frequency classes identified, giving the soil a wide variety of filtration rates. Along the vertical profile there are no particular variations in hydraulic conductivity, while along the horizontal planes there is a great heterogeneity that particularly affects the landslide area, with values ranging between 0.6 and 1.

The estimate variance grows with increasing elevation but tends to minimum values along the landslide profile.



Graph 21 - Frequency of I_{soil} index at different vertical depths in 2006

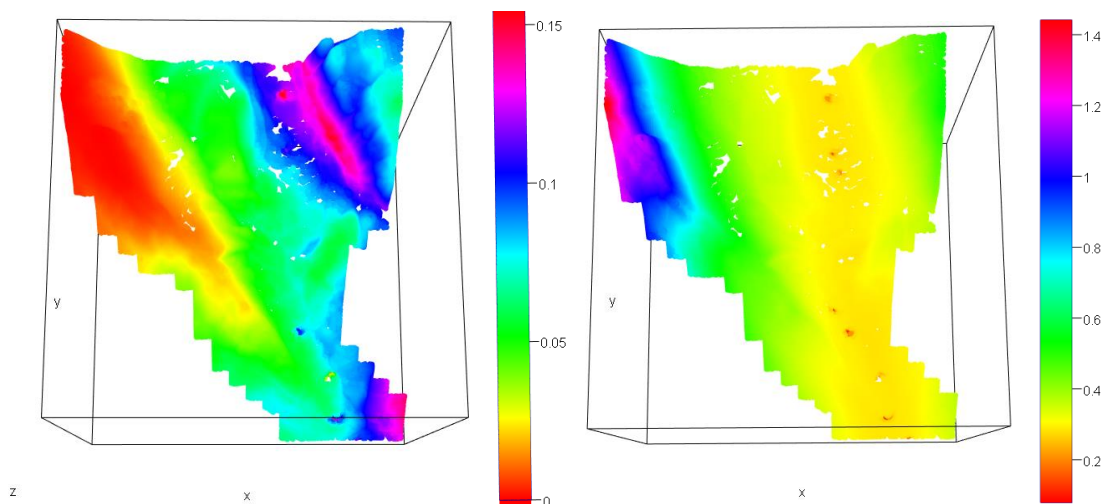


Figure 60 - Variability maps of spatial predictions (left) and variances (right) of I_{soil} at ground surface in 2006

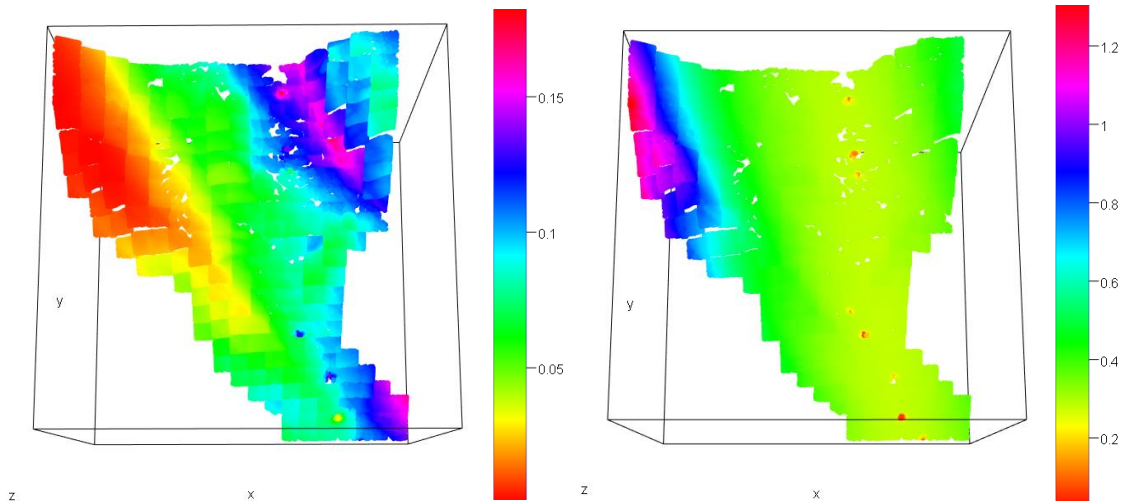


Figure 61 - Variability maps of spatial predictions (left) and variances (right) of I_{soil} at middle surface in 2006

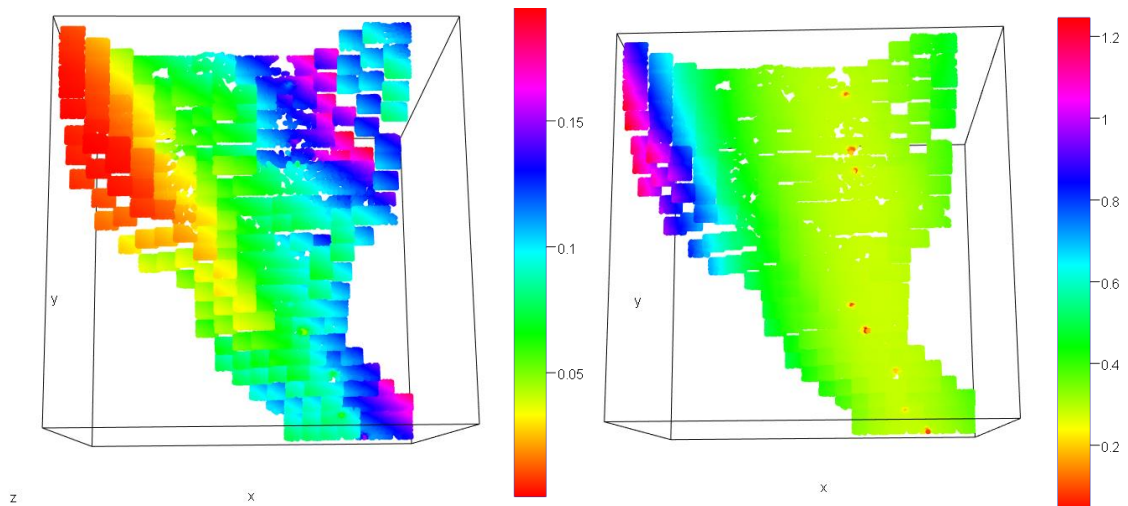
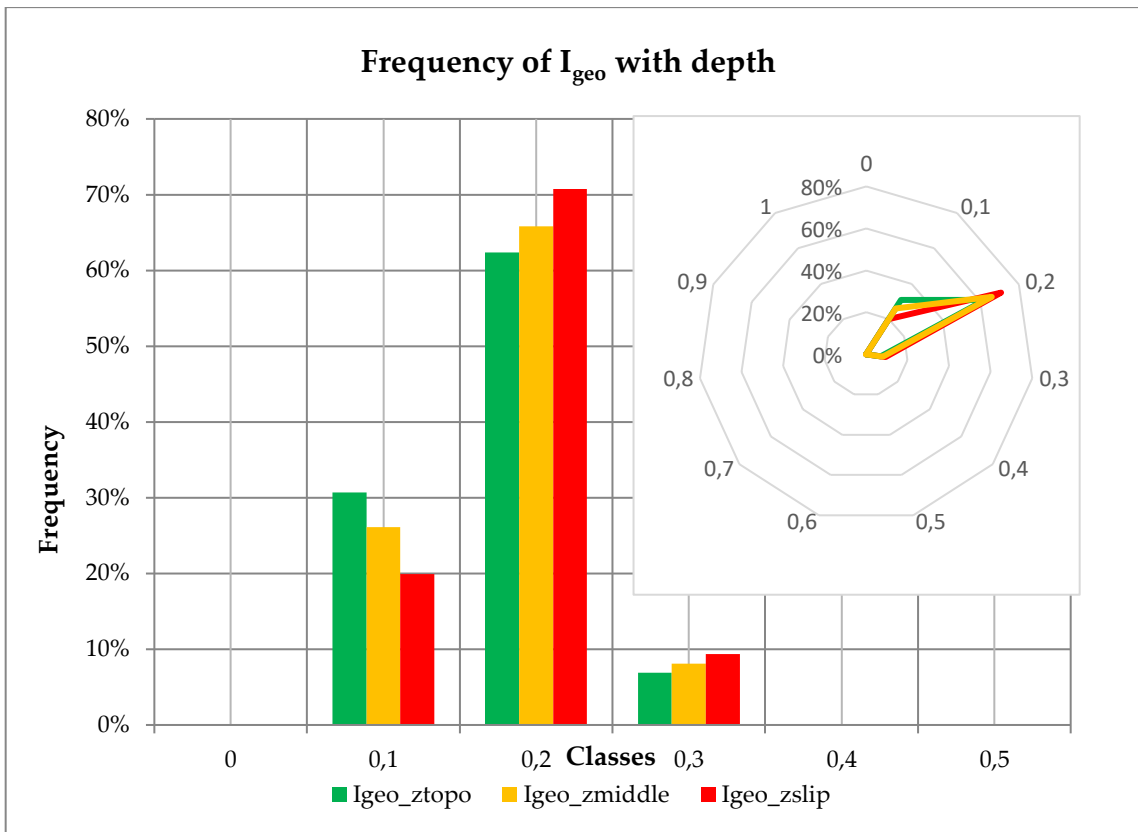


Figure 62 - Variability maps of spatial predictions (left) and variances (right) of I_{soil} at slip surface in 2006

In order to have an overview of the soil given by mutual interaction between the various components and soil indices, the above maps show the variability of soil index both in terms of spatial predictions and estimation variances. A considerable variability is located between the right side and the left, affecting in particular the toe of the slope. In fact, the values range highlighting areas of minimum and maximum value along the entire slope.

The variances of the three layers are overall moderate and evenly distributed, as proof of the overall goodness of the estimate.



Graph 22 - Frequency of I_{geo} index at different vertical depths in 2006

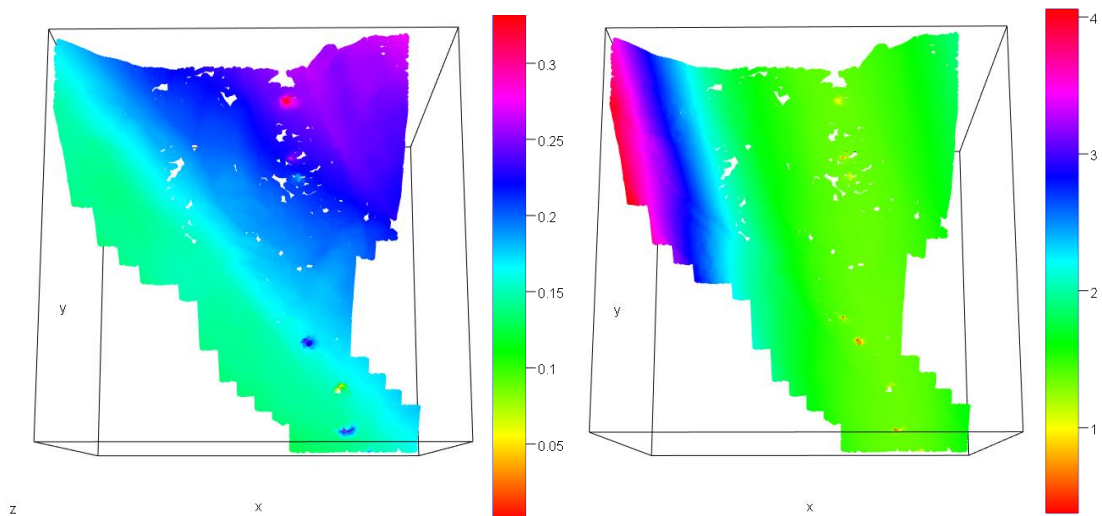


Figure 63 - Variability maps of spatial predictions (left) and variances (right) of I_{geo} at ground surface in 2006

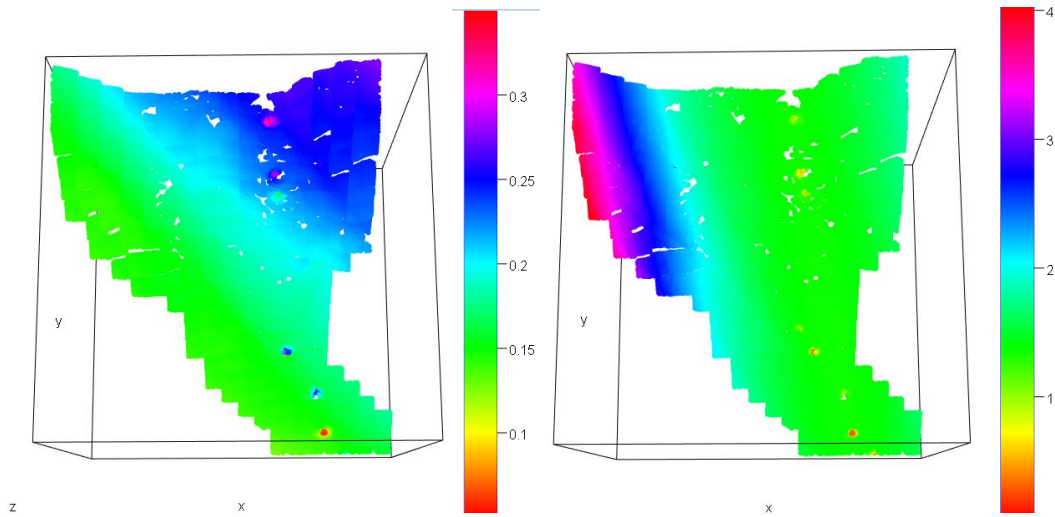


Figure 64 - Variability maps of spatial predictions (left) and variances (right) of I_{geo} at middle surface in 2006

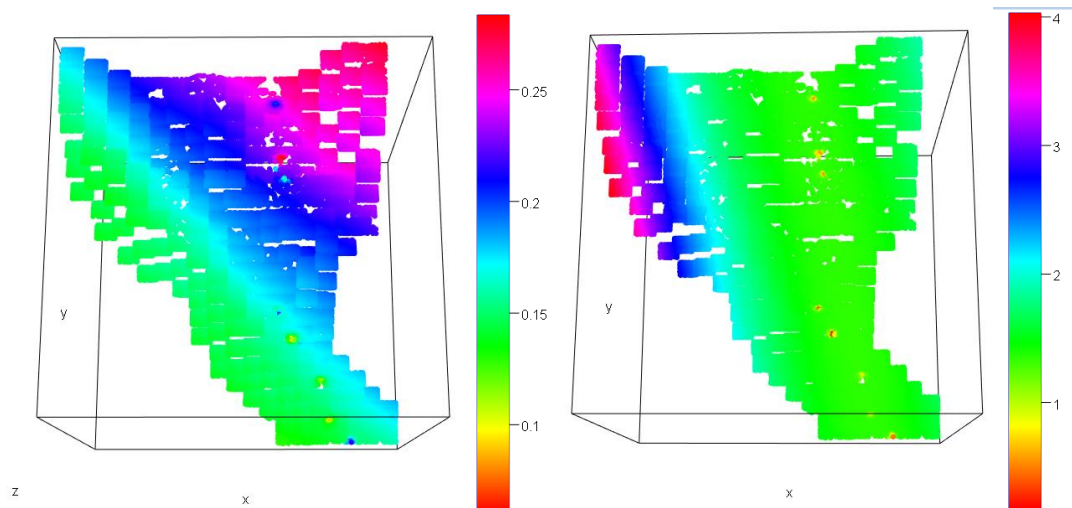
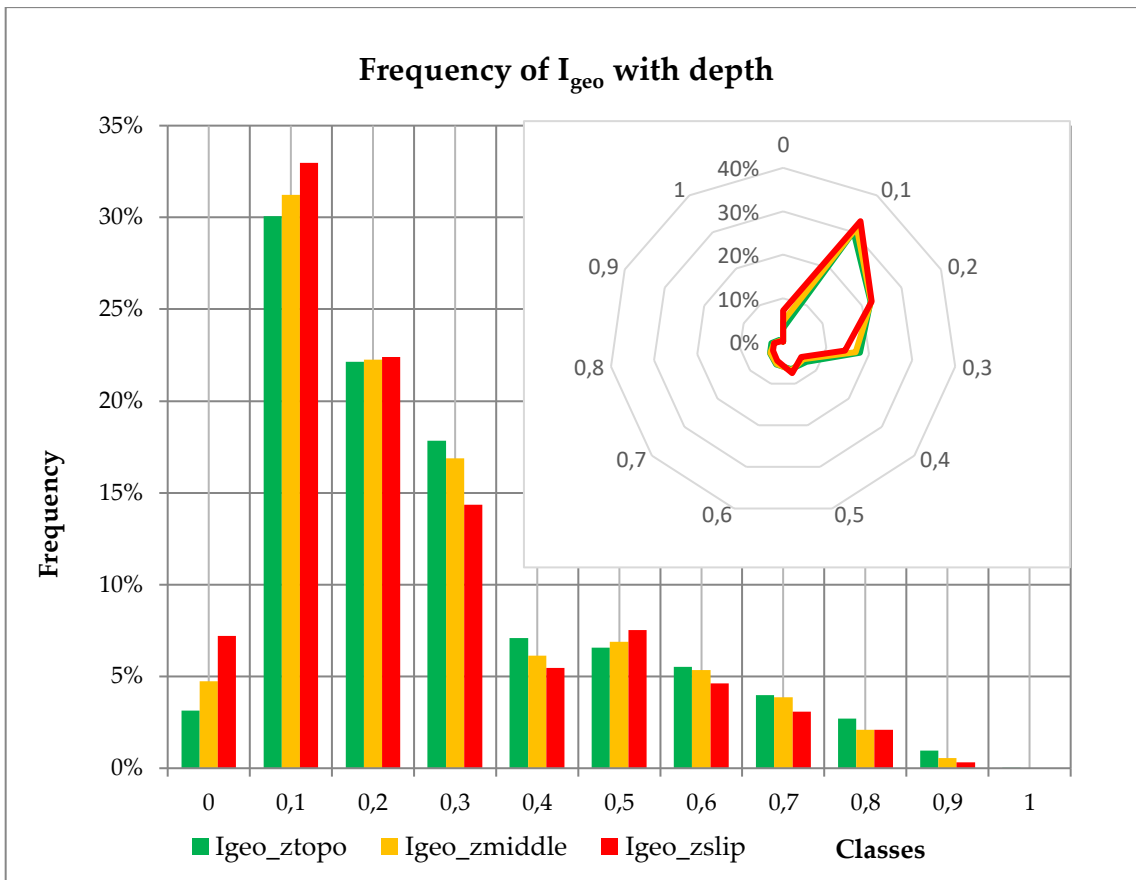


Figure 65 - Variability maps of spatial predictions (left) and variances (right) of I_{geo} at slip surface in 2006

By comparing soil indices for both the reactivations, the partial I_{geo} index has been spatially reproduced, taking into account only the information obtained from the geognostic surveys.

The color difference shows a longitudinal variability that crosses the slope from upstream to downstream despite the frequency classes being limited to a few categories. The variance is instead kept constant along the vertical profile with values that are around the 1 along the landslide body.



Graph 23 - Frequency of I_{geo} index at different vertical depths in 2010

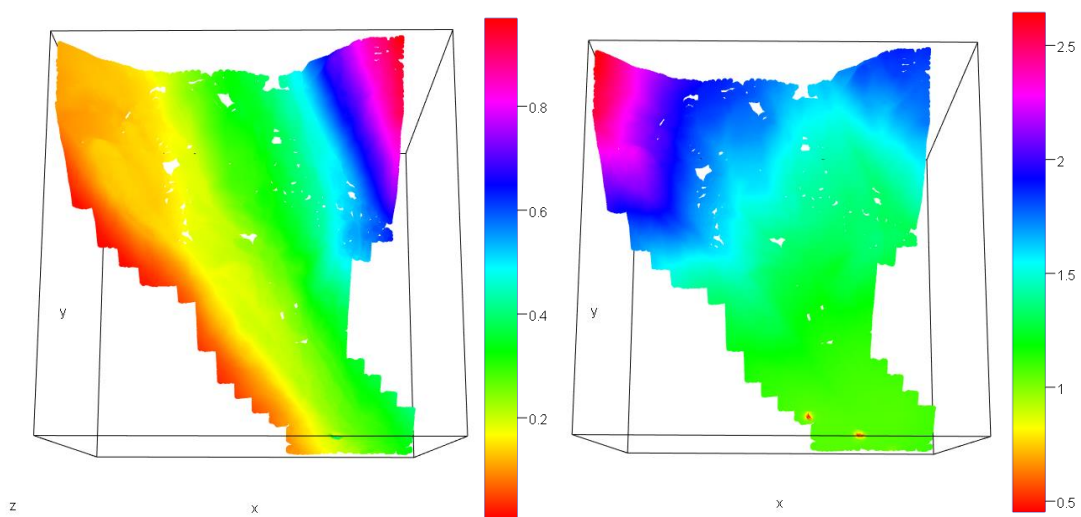


Figure 66 - Variability maps of spatial predictions (left) and variances (right) of I_{geo} at ground surface in 2010

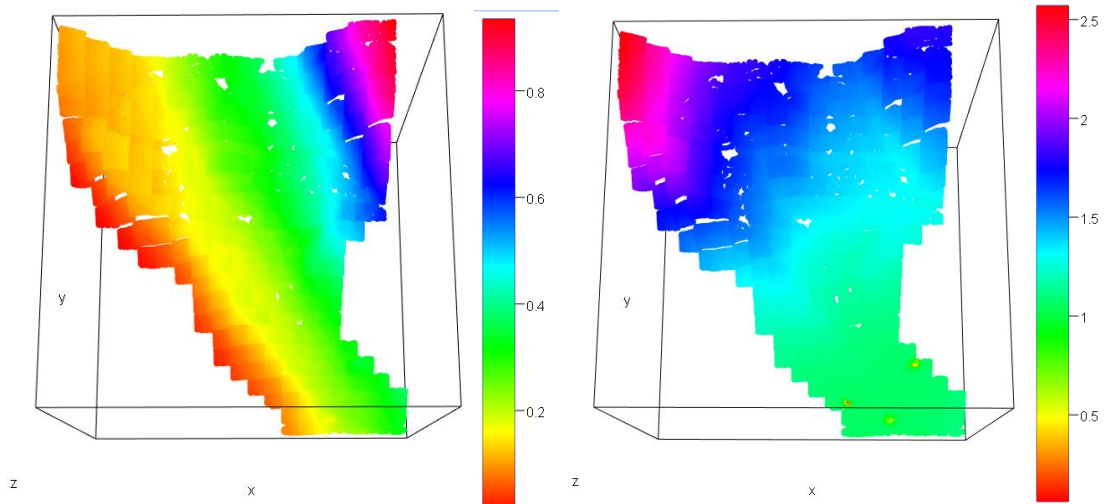


Figure 67 - Variability maps of spatial predictions (left) and variances (right) of I_{geo} at middle surface in 2010

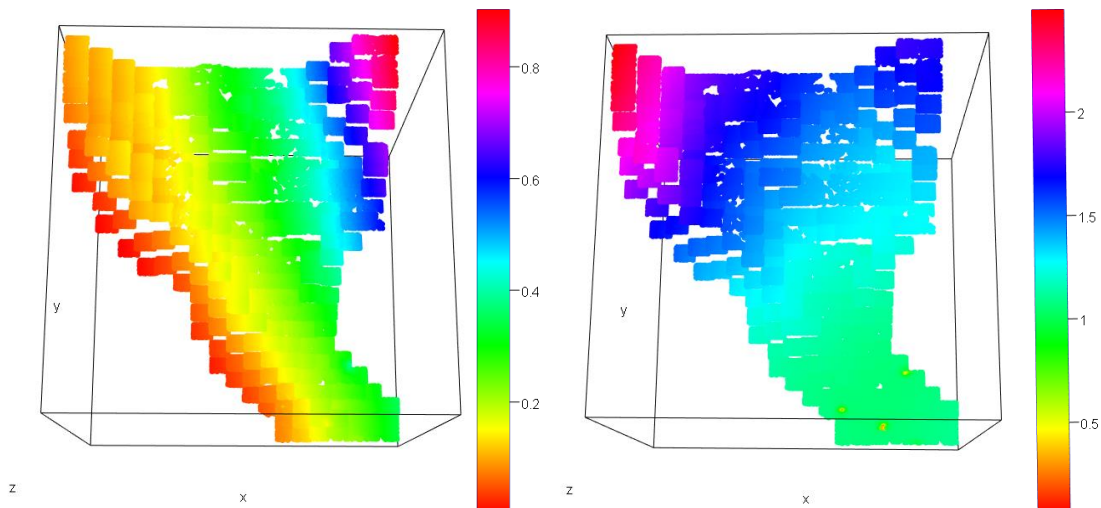
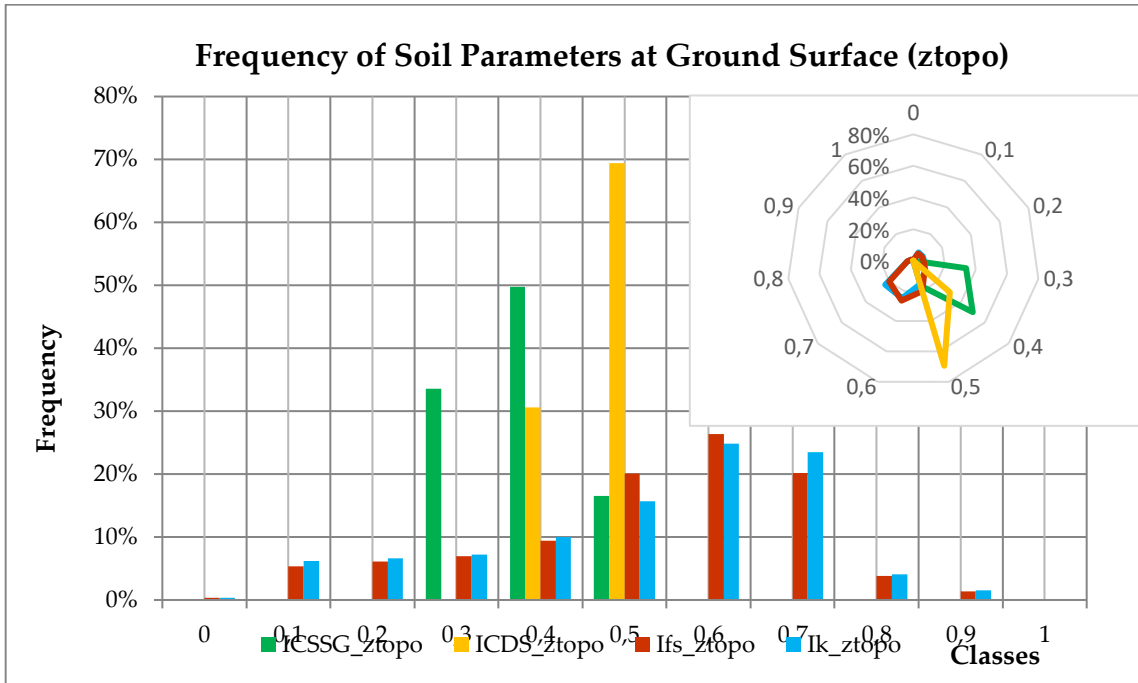


Figure 68 - Variability maps of spatial predictions (left) and variances (right) of I_{geo} at slip surface in 2010

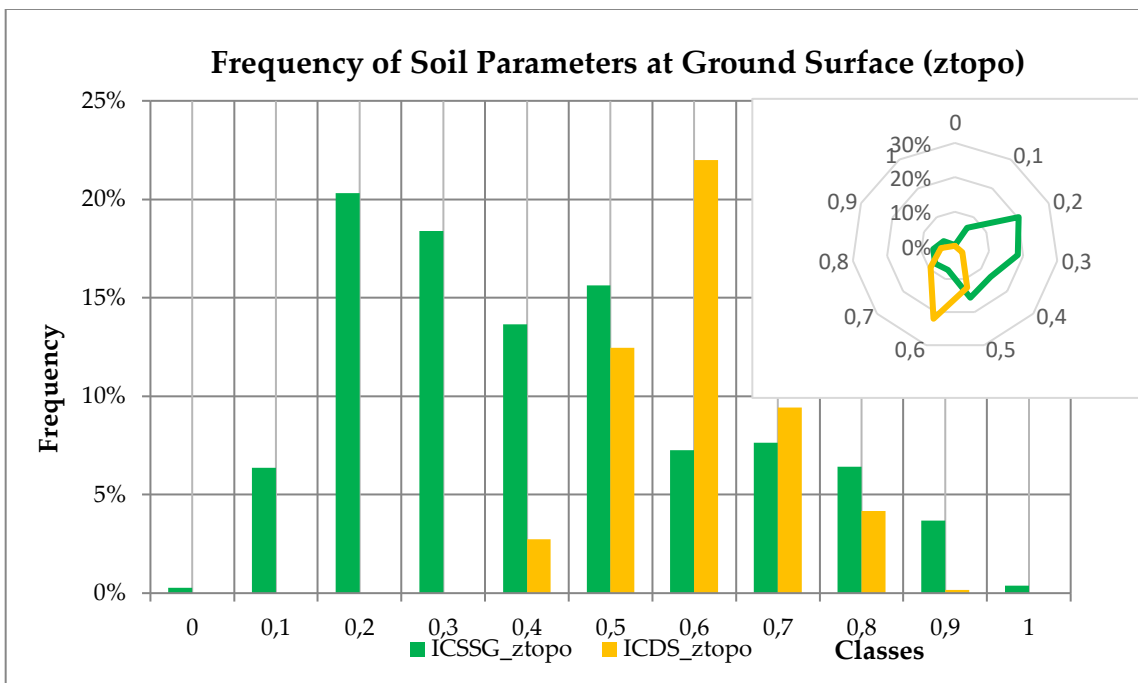
The maps show, both in 2006 and in 2010, clear contours and distinct values as the elevation increases, keeping partly the heterogeneity already found in I_{soil} . This enhances the role that particle size composition and degree of compaction and saturation have on the overall soil variability for different depths investigated and predictions obtained.

The above maps illustrate how the increase of the variance values of the predicted locations at the edge of the interesting area, reflects the increasing of distance from measured points. So the estimation variance allows to evaluate the ability of the Kriging method to estimate uncertainty accurately with respect to the true data (Matheron, 1963). Thus the UK approach provides a very accurate ranking of the spatial distribution of the estimation uncertainty.

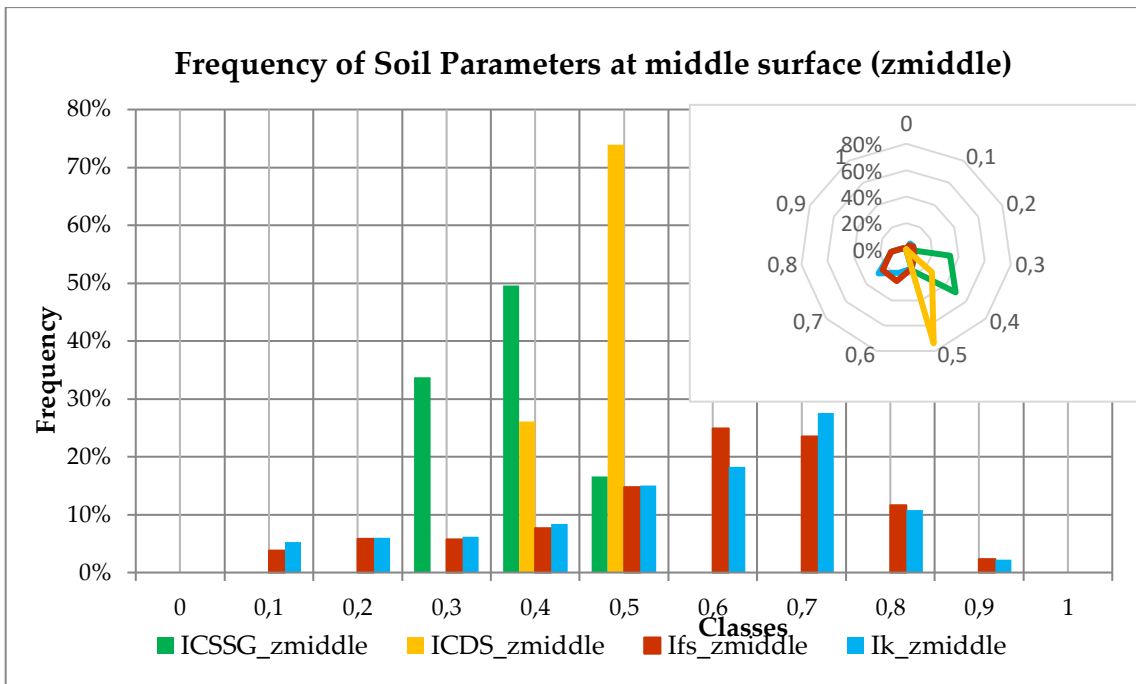
Following, the empirical frequencies have been plotted and grouped at the same depth to better highlight anisotropies and spatial variability.



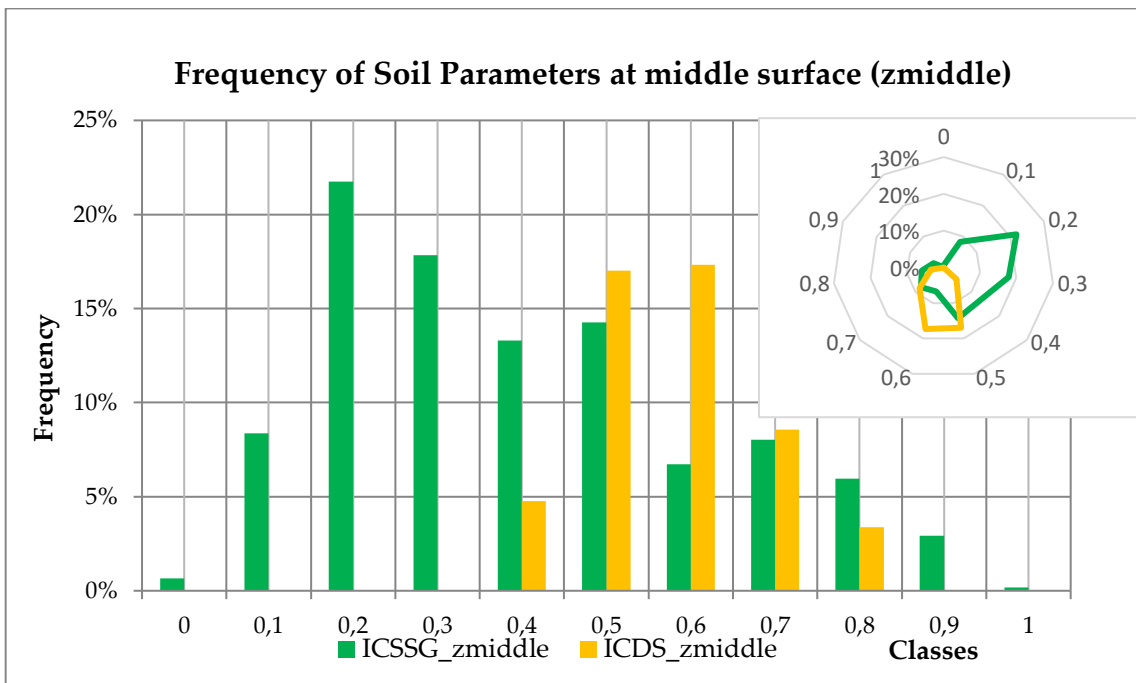
Graph 24 - Frequency of soil indices at ground surface (z_topography) in 2006



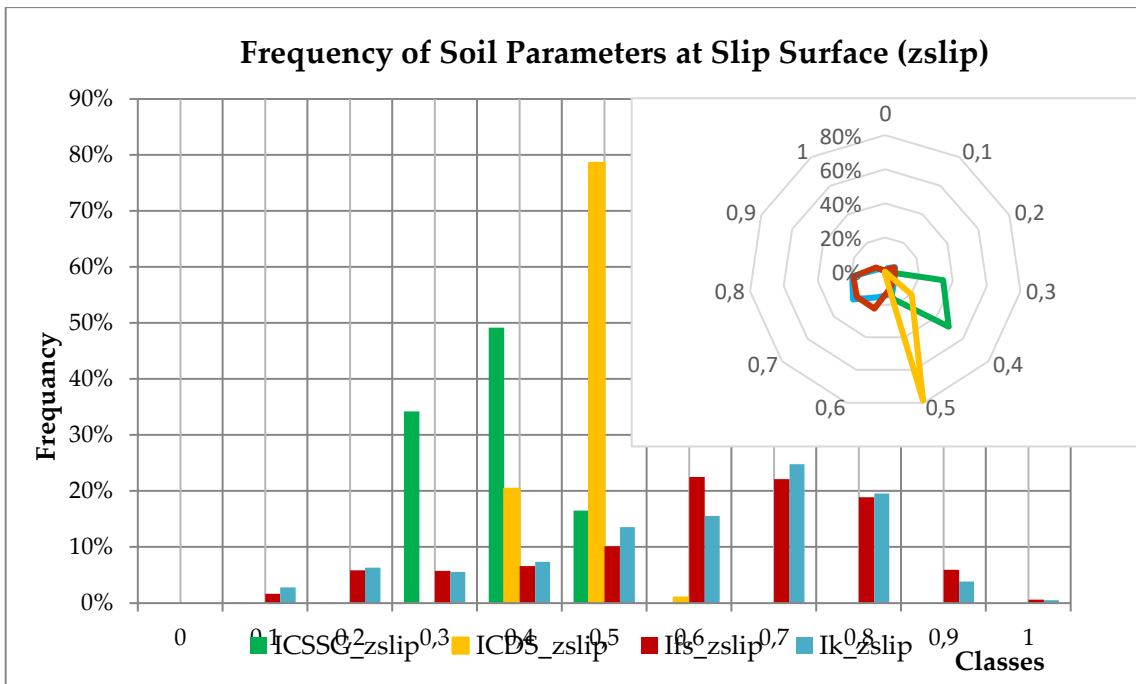
Graph 25 - Frequency of soil indices at ground surface (z_topography) in 2010



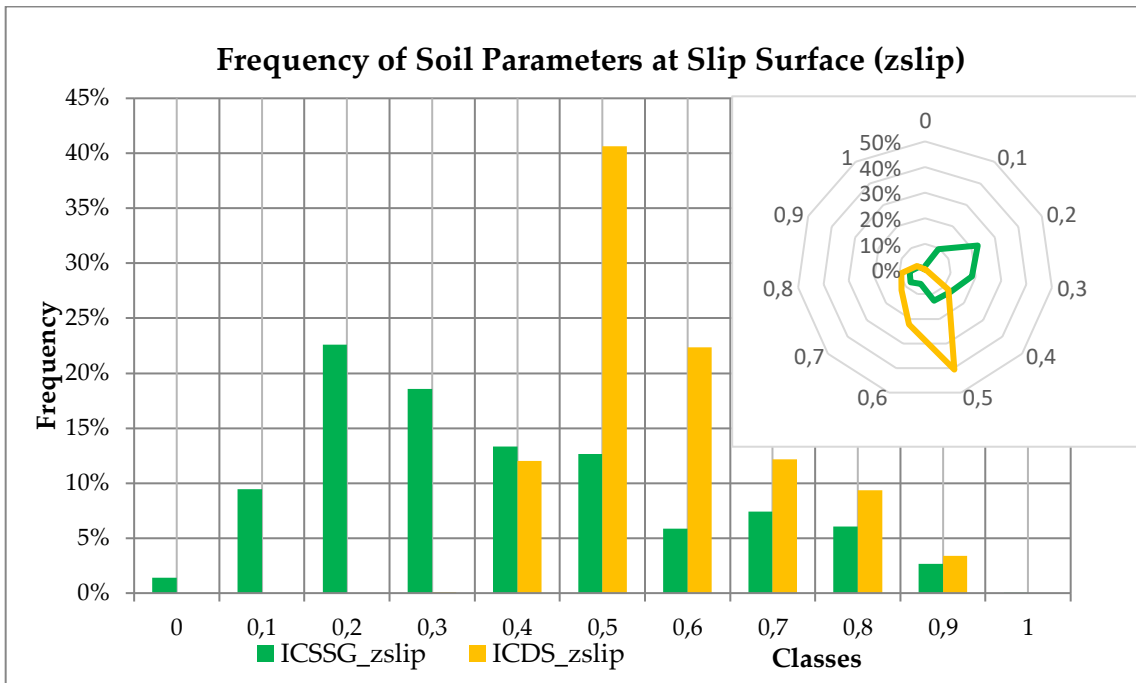
Graph 26 - Frequency of soil indices at middle surface between ground and slip surfaces (z_middle) in 2006



Graph 27 - Frequency of soil indices at middle surface between ground and slip surfaces (z_middle) in 2010



Graph 28 - Frequency of soil indices at critical surface (z_slip surface) in 2006

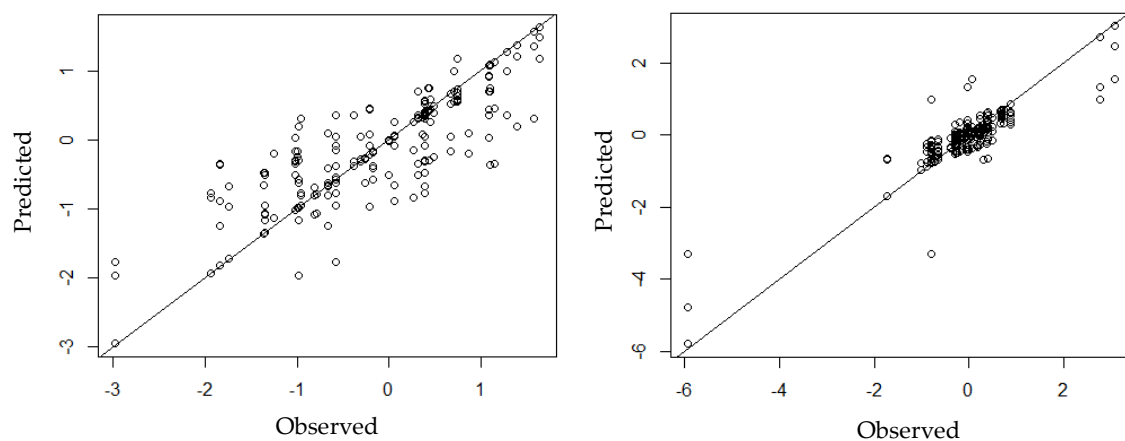


Graph 29 - Frequency of soil indices at critical surface (z_slip surface) in 2010

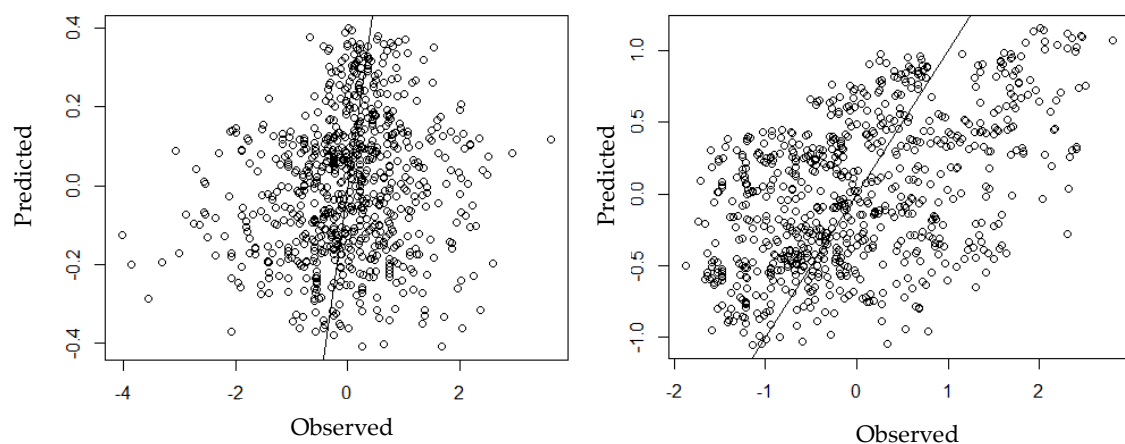
Several measures may be used to compare the goodness of theoretical fitting methods applied to data measurements (Wu, 2013).

Cross-Validation (CV) is a method which allows to establish how well theoretical model predicts values at unknown locations by measuring the discrepancy between measured and estimated values (Meshalkina, 2007). It removes each data location and predicts the associated value using remaining data in other locations. Thus, iterating this step in every measured point, CV compares predicted values to observed values obtaining useful information about the quality of predictions. It validates the goodness of fitted variogram model, parameters and neighbourhood (Oliver and Webster, 2014).

A comparison between the original data of the indices, and the relative estimated output values is following shown:



Graph 30 - Scatterplot between observed and estimated values of the indices I_{CSiSaG} (left) and I_{CoDS} (right) in 2006

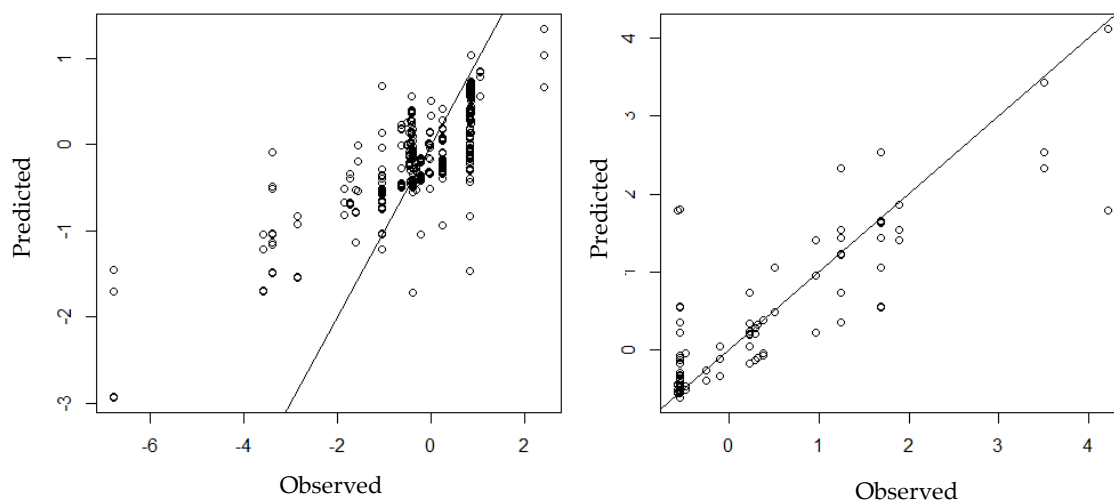


Graph 31 - Scatterplot between observed and estimated values of the indices I_{Fs} (left) and I_k (right) in 2006

In Graphs 30-32, the combination of data by a weighted linear sum tends away from low and high estimates. The characteristic to note is the *smoothing effect*

(Wackernagel, 2003): Kriging surface will basically be as smooth as possible given the constraints of the data thus, the estimated maps represent smoother outputs than real variable (Heuvelink *et al.*, 2016).

In particular, the Graphs 30-31 relative to the estimates of the values measured in 2006 show good approximations for I_{CSiSaG} and I_{CoDS} indices, while they deviate more for I_{Fs} and I_k . This is due to the limited adaptability of the theoretical variogram model used with respect to the first two indices.



Graph 32 - Scatterplot between observed and estimated values of the indices I_{CSiSaG} (left) and I_{CoDS} (right) in 2010

In particular, the results of the CV show that the *smoothness of Kriging* has involved an appreciable overestimation of low soil indices and a slight underestimation of higher values. But, largely, the spatial distributions are quite heterogeneous and asymmetric.

The scatterplots of the predictions of the values observed in 2010 show again good approximations for I_{CSiSaG} and I_{CoDS} indices. This confirms the adequacy of the model and its predictions (Pebesma and Graeler, 2017).

	I_{CSiSaG}	I_{CoDS}	I_{Fs}	I_k
MAE	0.02	0.032	0.12	0.17
RMSE	0.13	0.12	0.58	0.61

Table 28 – Performance criteria between predicted and observed values of the indices in 2006

	I_{CSiSaG}	I_{CoDS}
MAE	0.09	0.035
RMSE	0.28	0.14

Table 29 - Performance criteria between predicted and observed values of the indices in 2010

Root-Mean-Squared-Error (RMSE) and The Mean-Absolute-Error (MAE) are two of the most common metrics used to measure accuracy for continuous variables. RMSE is a quadratic scoring rule that also measures the average magnitude of the error. It is the square root of the average of squared differences between prediction and actual observation.

MAE, instead, measures the average magnitude of the errors in a set of predictions, without considering their direction. They may be used together to diagnose the variation in the errors of predictions (Willmott and Matsuura, 2005). Each of them may range from zero to infinity: lower values indicate better model performance so for this case study the comparative error assessment gives acceptable results (Chai and Draxler, 2014).

The results globally indicate that for relatively uniform, dense sampling locations, methods appear to be optimal. We hypothesize that it is a consequence of the relatively large number of observations, which lessens the influence of extreme values on model calibration and spatial interpolation.

The task of the estimated variability from experimental data is thus very challenging indeed and it allows to appreciate each contribution to the overall spatial variability for indicative values of critical soil strength conditions both local and global.

The analysis of the uncertainty may have possible effects on the same stability assessment for the individuation of the failure conditions, based on accurate, correct and local estimated un-sampled values.

Thus, to highlight the presence of soil values particularly critical, the assessment of the overall stability has been performed.

4.4 Slope Instability Assessment

Evaluative analyses of slope stability allow a quantitative estimate of landslide susceptibility (Aleotti and Chowdhury, 1999).

These methods assume that ground does not deform until it breaks and that, under conditions of breakage, shear strength remains constant and independent (Baba *et al.*, 2012) from deformations (a rigid behavior, perfectly plastic, of soil is assumed). From these hypotheses it follows (Fredlund, Krahn and Pufhal, 1981):

- Breakage occurs along a net separation surface between landslide mass and stable ground;
- Landslide mass is a rigid block in roto-translational motion;

- Resistance mobilized along the sliding surface in limit equilibrium conditions is constant over time and everywhere equal to the shear strength. It is independent of deformations and landslide movements;
- It is not possible to determine deformations preceding the break, nor the extent of the movements of the landslide block, nor the phenomenon speed.

Concerning conditioning factors, the uncertainties in slope stability analysis belong in three main groups (Gustafsson *et al.*, 2012):

- Uncertainties on strength parameters and geometry (angle of internal friction, cohesion, slope angle);
- Uncertainties on loads (surface loads, soil weight, pore pressure);
- Uncertainty in critical breaking mechanism, which may be slightly different from that one identified in the analysis.

4.4.1 Deterministic slope modelling

Generally, different Limit Equilibrium Methods (LEMs) typically divide soil mass into many slices and assume different interslice normal and shear forces in order to achieve a statically determine solution: there is only one constant factor of safety along the potential slip surface (Griffiths and Lane, 1999).

LEMs may analyze undefined slopes and slopes of limited height (Fredlund, Krahn and Pufhal, 1981).

Infinite slope is a LEM that allows to divide the slope in slices long enough to be considered with a constant inclination, according to characteristics of landslide (Barbosa, Morris and Sarma, 1989).

A slope is considered infinite when the depth of the critical breaking surface is small compared to slope length. This length may therefore be assumed as 'infinite'. So, infinite slope pattern well fits long sliding landslides (Griffiths, Huang and Fenton, 2011).

The stability of alluvial deposits, debris or alteration of small thickness than landslide length, placed on a rigid rocky layer (i.e. bedrock), is normally referred to infinite slope model (Park, Lee and Woo, 2013)

For modelling the Montaguto earthflow, infinite slope method (Lollino, Giordan and Allasia, 2014) was considered based on landslide movement and basal-slip surface.

It has been used in order to represent and develop two approaches, through back-analysis procedure, for evaluating the main reactivations effects on the middle-low part of the landslide:

- Deterministic analysis, to verify the slope instability conditions after 2006 and 2010 reactivations;
- Probabilistic analysis, in order to calculate the probability of failure in 2006 and 2010, after the main reactivations' occurrence.

Based on 2D infinite slope model, the following assumptions were considered for evaluating FS:

- The soil is homogeneous (or layered) with a sliding surface parallel to the ground surface;
- The piezometric surface is parallel to the ground surface: filtration motion has parallel flow lines to the ground surface;
- The interfaces are in the same condition, so the tangential forces along the vertical planes are the same and do not affect the balance of acting forces.

The undrained condition (has been applied using the following formula for calculating the Factor of Safety per each slice (Skempton and Delory, 1957):

$$FS = \frac{c' + (\gamma z - \gamma_w z_w) \cos^2 \beta \tan \phi'}{\gamma z \sin \beta \cos \beta} \quad (16)$$

where:

c' = cohesion of the soil,

ϕ' = angle of internal friction of the soil,

γ = unit weight of the soil,

γ_w = unit weight of water,

β = inclination of the slope to the horizontal,

z = depth below the ground surface,

z_w = depth of the water table below the ground surface.

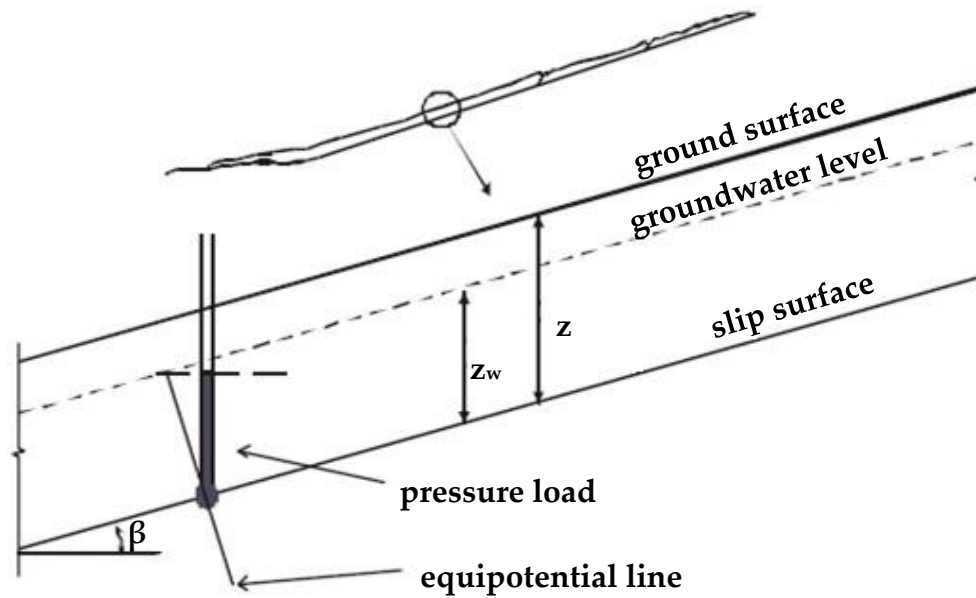


Figure 69 - Translational sliding diagram, infinite slope geometry and parameters
(source: Mater *et al.*, 2010)

The slope angle was extracted by DEM files realized by previous authors on the site during the two motions occurrences.

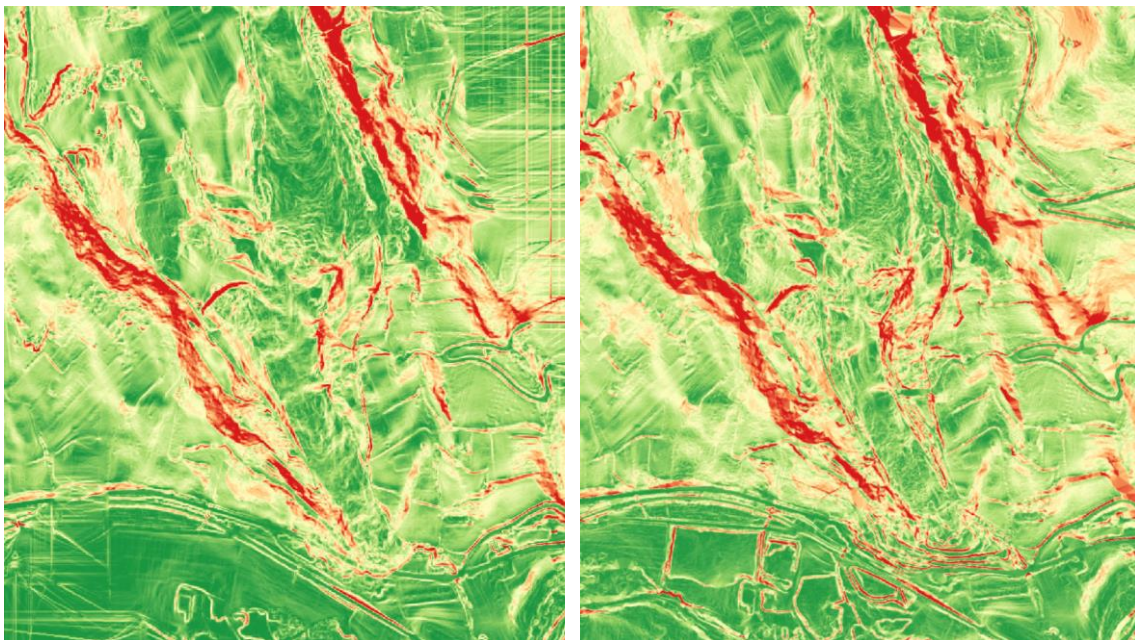


Figure 70 - Slope terrain models (β) in 2006 (left) and 2010 (right). Chromatic classes range from 0 degrees (green) up to over 45 degrees (red)

The study area was divided in 23 tiles (50mx50m) with strength (friction angle (ϕ), cohesion (c')) and geometrical (slope inclination (β), slip surface (z), groundwater level (z_w)) parameters constant for each longitudinal slice. Each

conditioning factor represent the average value along the landslide width at the same slice latitude.

γ	20 kN/m ³
γ'	10 kN/m ³
γ_w	10 kN/m ³

Table 30 - Constant slope parameters for all tiles

ID_tile	z (m)	β (°)	ϕ' (°)	c' (kPa)	z _w (m)	FS
1	12	28	28	11	11.13	0.65
2	17	29	29	10	16.97	0.57
3	22	26	30	8	16.97	0.77
4	21	29	31	6	8.72	0.89
5	22	26	28	7	8.72	0.91
6	20	30	29	7	6.28	0.85
7	20	30	29	9	6.28	0.86
8	15	28	26	8	3.98	0.86
9	14	30	28	9	3.98	0.86
10	15	32	29	10	4.25	0.84
11	16	32	29	9	4.25	0.83
12	16	26	29	9	9.85	0.86
13	19	26	27	9	9.85	0.83
14	11	26	27	9	11.13	0.63
15	14	26	28	10	15.07	0.59
16	11	26	26	10	11.13	0.62
17	10	26	26	12	10.22	0.65
18	18	26	26	11	18.04	0.58
19	11	26	28	9	11.13	0.65
20	9	26	24	10	9.43	0.60
21	7	25	28	9	7.32	0.74
22	12	24	30	11	10.55	0.85
23	11	22	29	11	10.55	0.86

Table 31 - Soil parameters and values in 2006 per tile

	z (m)	β (°)	ϕ' (°)	c' (kPa)	z _w (m)
MEAN	14.91	27.17	28	9.30	12.29
SD	4.38	2.47	1.62	1.45	5.97
COV	29%	9%	6%	16%	49%

Table 32 – Statistical values of soil parameters in 2006

ID_tile	z (m)	β (°)	ϕ' (°)	c' (kPa)	z _w (m)	FS
1	12	27	28	11	11.13	0.66
2	17	28	29	10	16.97	0.58

3	22	25	30	8	16.97	0.79
4	21	29	31	6	8.72	0.89
5	22	25	28	7	8.72	0.93
6	20	29	29	7	6.28	0.87
7	20	29	29	9	6.28	0.88
8	15	27	26	8	3.98	0.89
9	14	29	28	9	3.98	0.90
10	15	30	29	10	4.25	0.89
11	16	30	29	9	4.25	0.88
12	16	24	29	9	9.85	0.92
13	19	23	27	9	9.85	0.92
14	11	24	27	9	11.13	0.67
15	14	24	28	10	15.07	0.63
16	11	24	26	10	11.13	0.64
17	10	24	26	12	10.22	0.68
18	18	24	26	11	18.04	0.62
19	11	24	28	9	11.13	0.67
20	9	24	24	10	9.43	0.60
21	7	24	28	9	7.32	0.74
22	12	22	30	11	10.55	0.90
23	11	20	29	11	10.55	0.92

Table 33 - Table 19 - Soil parameters and values in 2010 per tile

	z (m)	β (°)	ϕ' (°)	c' (kPa)	z_w (m)
MEAN	14.91	26.09	28	9.30	12.29
SD	4.38	2.66	1.62	1.45	5.97
COV	29%	10%	6%	16%	49%

Table 34 - Statistical values of soil parameters in 2010

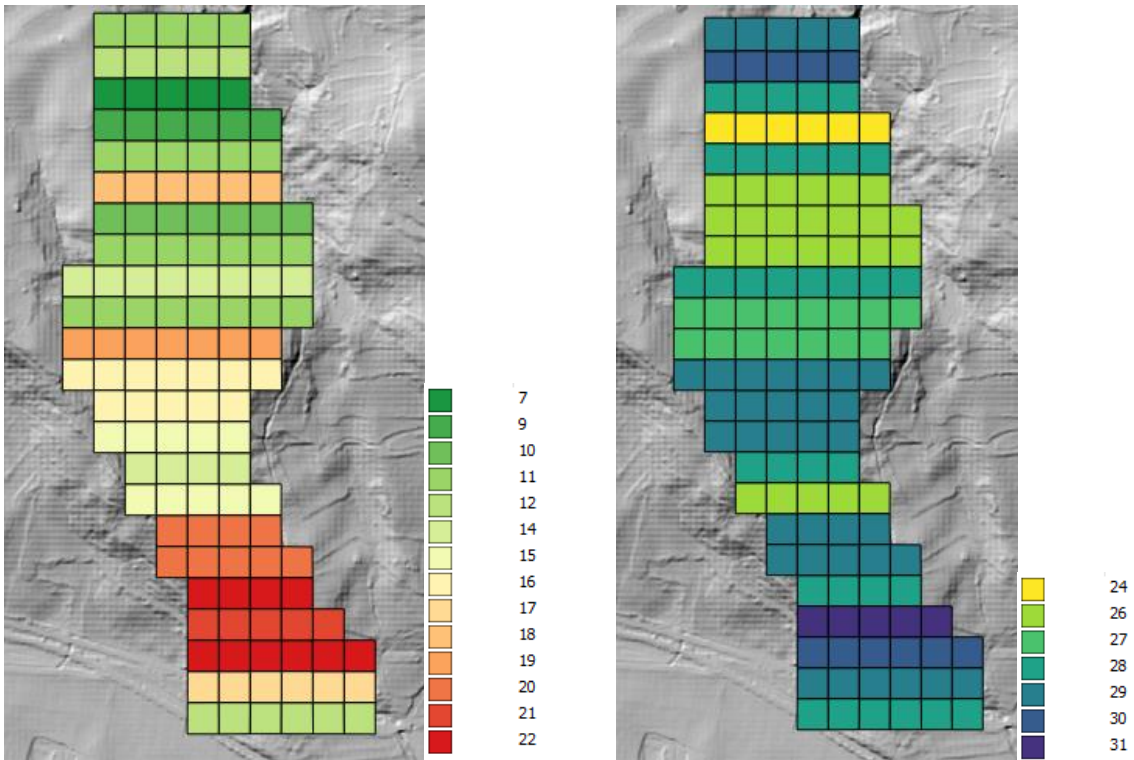


Figure 71 - Spatial values of slip surface (left) and friction angle (right) in 2006 and 2010

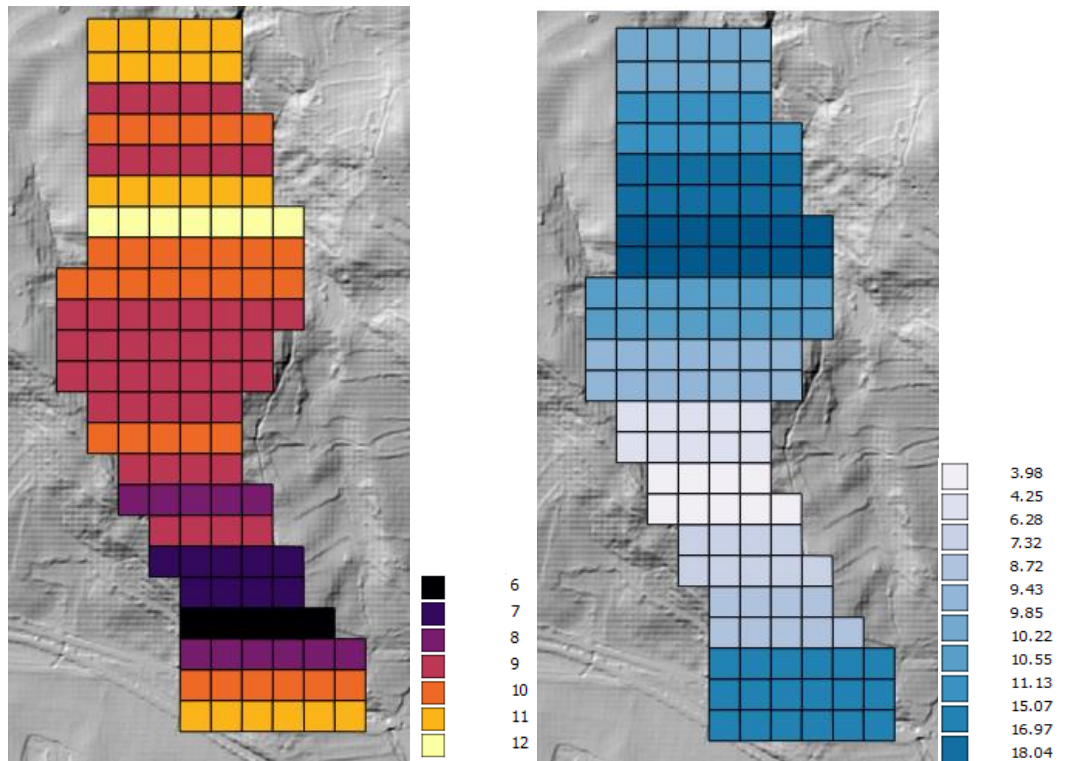


Figure 72 - Spatial values of cohesion (left) and groundwater surface (right) in 2006 and 2010

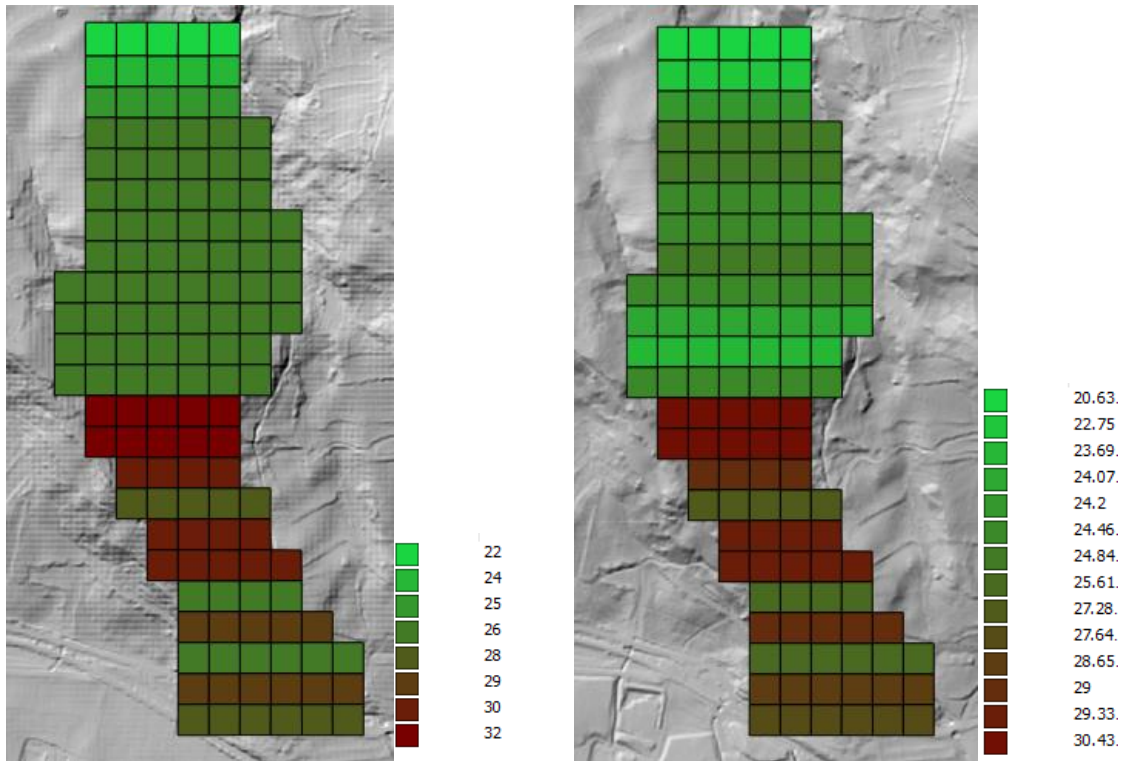


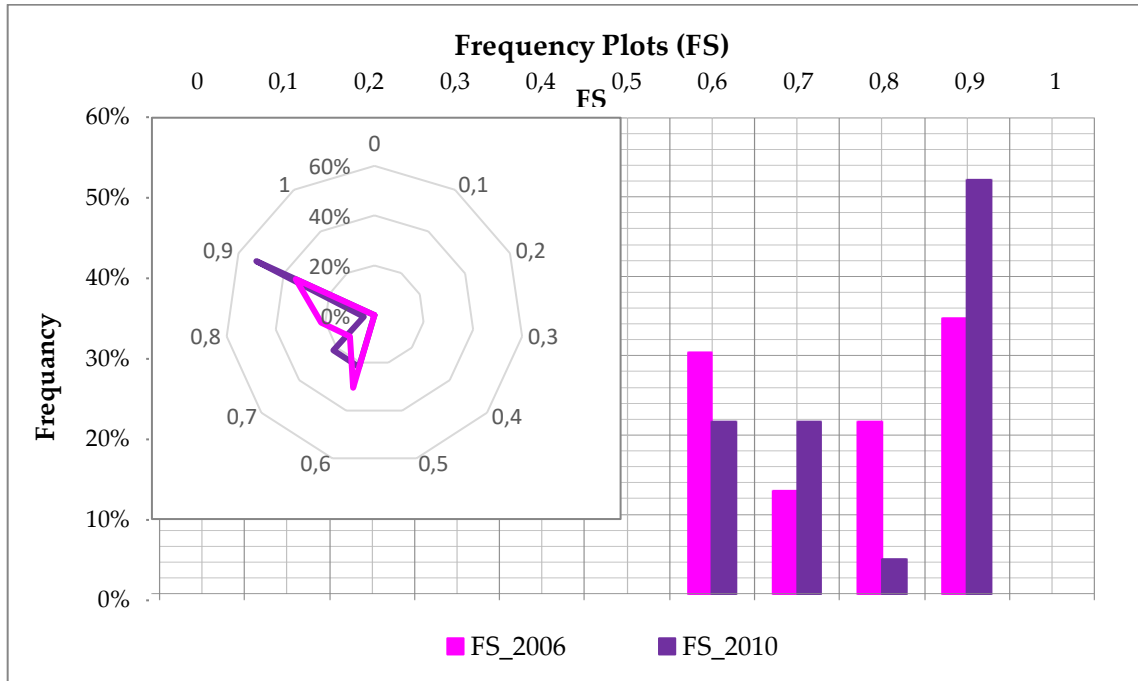
Figure 73 - Spatial values of slope angle in 2006 (left) and in 2010 (right)

According with the tables above, the FS function along the slope has been considered dependent on 5 variables with spatial variability (slope angle, friction angle, cohesion, water level z_w and depth of slip surface z) while other parameters were considered constant, such as soil weight, immersed soil weight and water weight. FS values were calculated and plotted in order to evaluate how stable was the middle and toe area compared to the safety condition ($FS \geq 1$).

FS_Frequency Classes	FS_Relative Freq_2006	FS_Relative Freq_2010
0	0%	0%
0.1	0%	0%
0.2	0%	0%
0.3	0%	0%
0.4	0%	0%
0.5	0%	0%
0.6	30%	22%
0.7	13%	22%
0.8	22%	4%
0.9	35%	52%
1	0%	0%

Table 35 - Empirical Frequency of FS in 2006 and 2010

All data were obtained by soil investigations and survey campaigns performed in 2006 and 2010 after the two main landslide movements.



Graph 33 - Empirical Frequency plots of FS in 2006 and 2010

4.4.2 Probabilistic slope failure

Considering the heterogeneity and uncertainty in material properties, together with changes and variability in geometry and loading factors, a probabilistic evaluation of slope stability is required (Griffiths, Huang and Fenton, 2011).

For some component events, engineering models are available for predicting behaviour (Zhang *et al.*, 2014). In these cases, reliability analysis may be used to assess probabilities associated with the components (Christian, Ladd and Baecher, 1994).

Reliability analysis propagates uncertainty in input parameters to uncertainties in predictions of performance. The assessment problem is changed from estimating probabilities of adverse performance directly to estimating probabilities for the input parameters (Johari, Fazeli and Javadi, 2013).

Once probabilities for the input parameters are assessed, any of a variety of simple mathematical techniques may be used to calculate probabilities associated with performance (Cadini, Agliardi and Zio, 2017).

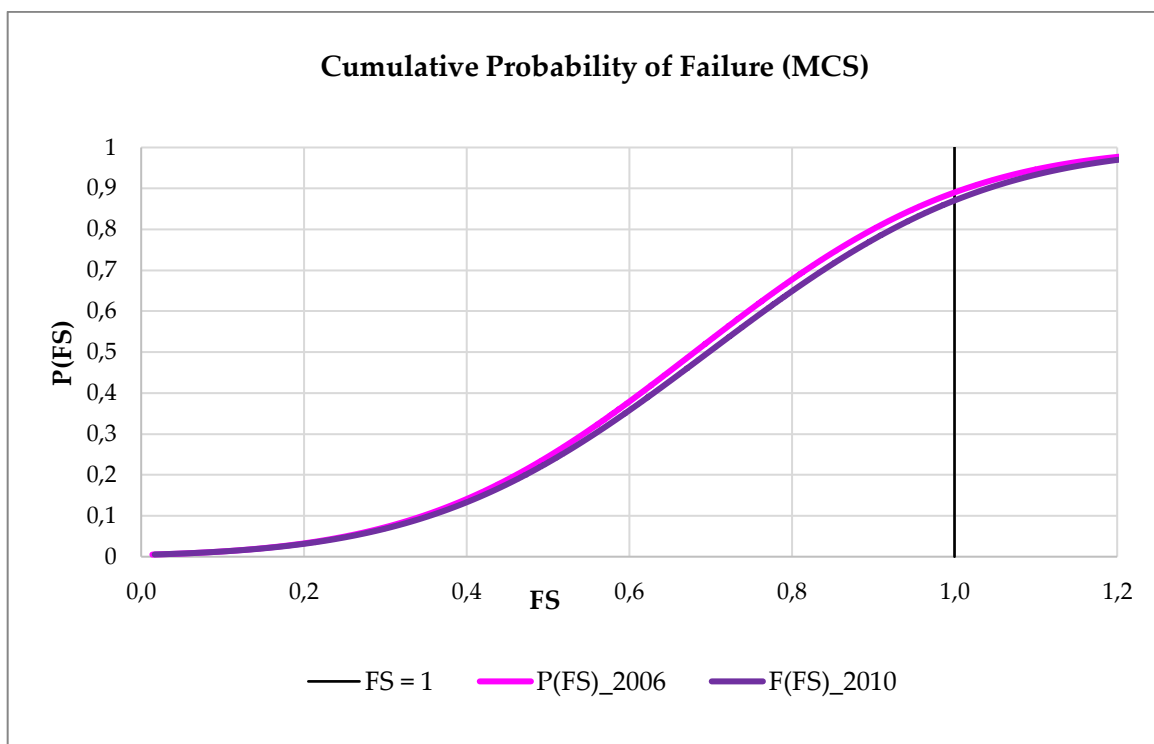
Among these are First-Order Second-Moment approximations, advanced Second-Moment techniques, Point-Estimate calculations, or Monte Carlo Simulation (MCS) as seen in previous chapters.

In our case, the Monte Carlo Simulation was carried out with 1000 samples (Papaioannou, Breitung and Straub, 2013).

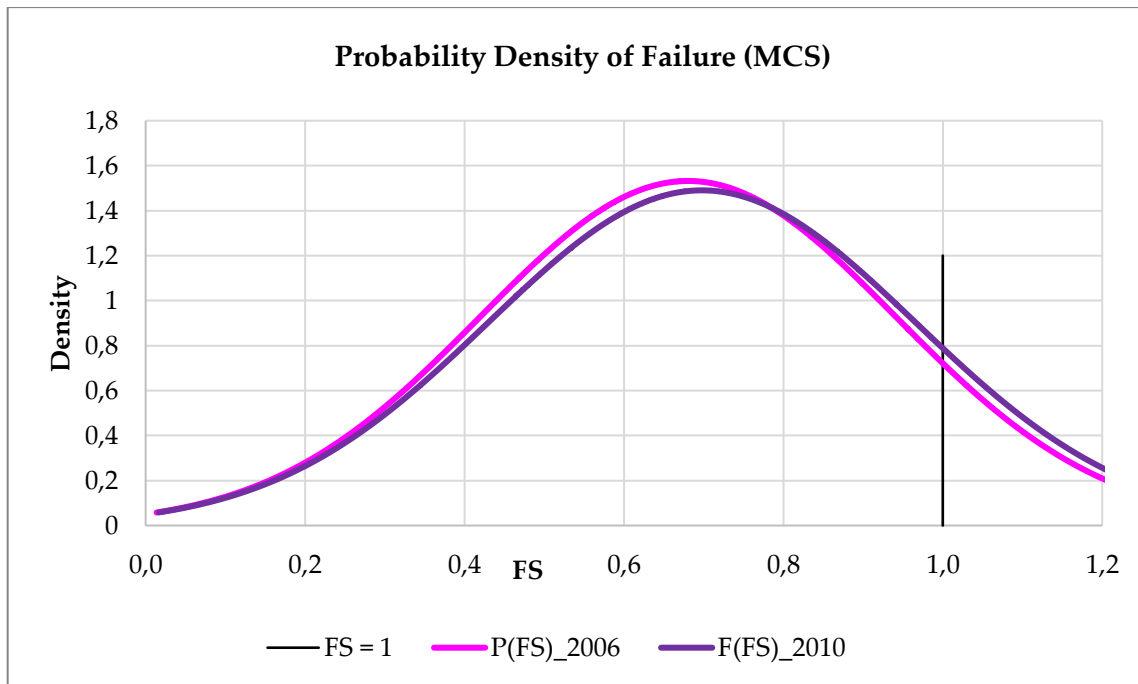
For the sake of consistency, every conditioning factor with local variation (strength and geometrical parameters) was considered in the random process (Hsu, 2013). Remaining variables were kept at their mean values (i.e. soil weight, immersed soil weight and water weight).

All the identified parameters affecting slope stability were considered as random variables in such a way as to respect the assumed probability distribution curves (Sofianos, Nomikos and Papantonopoulos, 2014).

The component input parameters (Zaman *et al.*, 2011) in stability analysis were thus modelled randomly and used to estimate the PDF of the Factor of Safety in term of Probability of Failure.



Graph 34 - Cumulative distributions of FS in 2006 and 2010



Graph 35 - Probability density curves of FS in 2006 and 2010

The above graphs give the results for one set of runs (1000 iterations). In each plot the solid lines are the result of the Monte Carlo simulation both in term of cumulative distribution and density function of FS in 2006 and 2010.

Following, the Reliability Index (β) has been calculated, based on MSC assumptions and FS moments (mean and standard deviation), by using the Eq. 7:

	FS_2006	FS_2010
μ_{FS}	0.68	0.70
σ_{FS}	0.26	0.27
β_{FS}	-1.23	-1.13
$P_{f_{FS}}$	0.62	0.64

Table 36 - Statistical and Reliability values of FS in 2006 and 2010

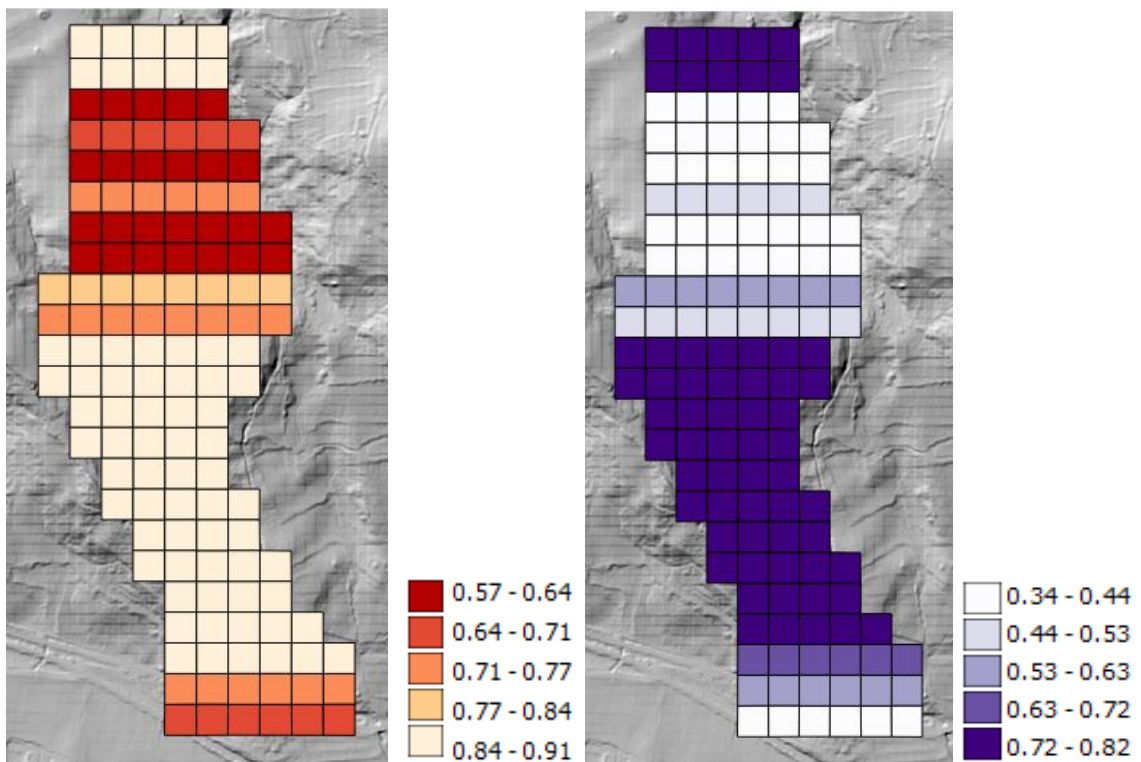


Figure 74 - Spatial values of FS and P(FS) in 2006

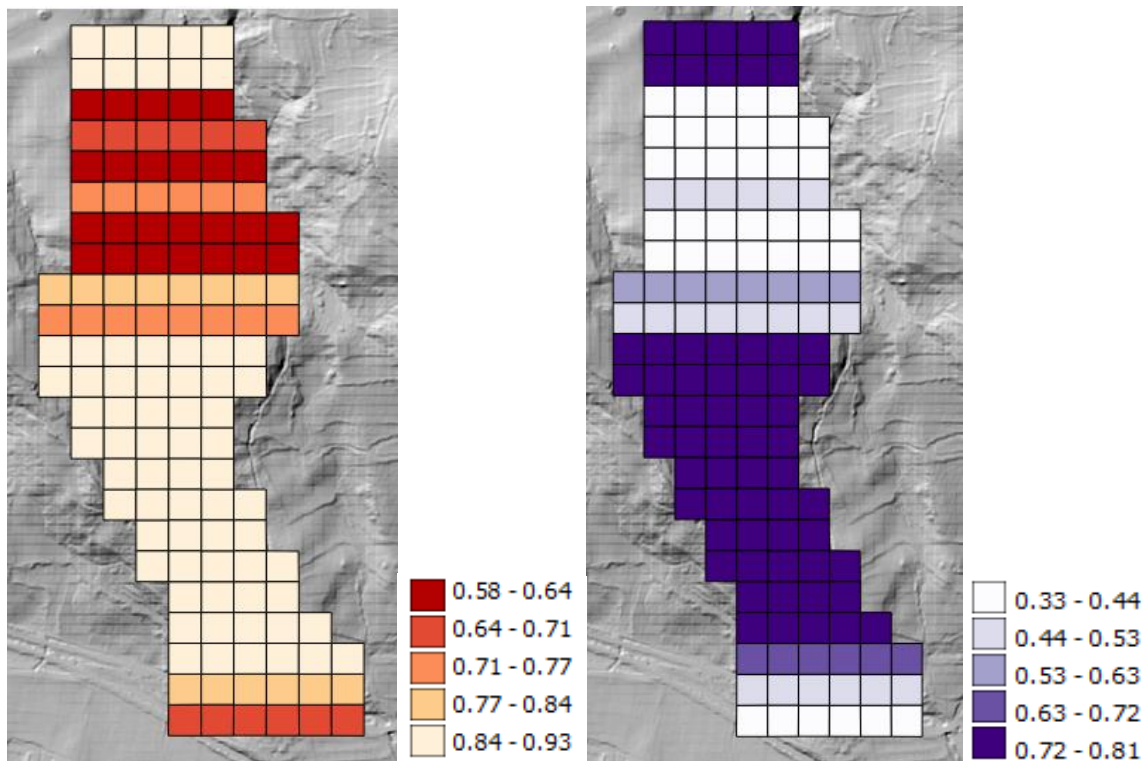


Figure 75 - Spatial values of FS and P(FS) in 2010

Figure 74 and 75 show FS and the Probability of Failure after the reactivation in 2006 and 2010. They are everywhere less than 1. It's not surprising that the landslide was still moving until 2010.

The results showed the presence of strength values particularly critical and locally circumscribed representing the likely predisposing factor the instability condition of the slope that has really occurred implying the soil failure with landslide downstream.

Calculation for both 2006 and 2010 slope stability analyses were carried out based on empirical means and variances for every variable as the first step for estimating their uncertainty. In this case, uncertainty includes both aleatory and epistemic components as no information was given on sampling errors as well as on estimation errors committed by previous authors concerning the methodologies they applied on the case study (i.e. slip surface depth, water level, shear strength values etc.).

4.4.3 Sensitivity analysis of variability

In traditional slope stability analysis, single fixed values (typically, mean values) of representative samples or strength parameters or slope parameters are used (Mustaffa, Gelder and Vrijling, 2009b). The factor of safety is generally calculated for a slope to assess its stability by using single value of soil properties and slope parameters. The deterministic analysis is unable (Alimonti *et al.*, 2017) to account for variation in slope properties and parameters and other variable conditions so that a probabilistic analysis has been performed.

Anyway, in reality, each parameter has a range of values which may differently affect the whole slope stability (Johari, Fazeli and Javadi, 2013).

The reliability analysis and reliability sensitivity analysis are two important steps in engineering design (Cui, Lu and Wang, 2011). In many practical applications of reliability analysis, there is the interested in knowing the sensitivity of the probability of failure for optimization purposes (Haukaas and Der Kiureghian, 2003; Krzykacz-Hausmann, 2006; Guo and Du, 2009).

The objective of reliability sensitivity analysis is to determine input variables that mostly contribute to the variability of the failure probability. Moreover, it is based on a perturbation of the original probability distribution of the input random variables, quantifying their effects on model outputs. The objective is to determine the most influential input variables and to analyze their impact on the failure probability (Papaioannou, Breitung and Straub, 2013).

Parameter sensitivities are obtained in terms of the sensitivity of the respective probability approximation (Krzykacz-Hausmann, 2006).

In this research independent sensitivity measure has been based on a perturbation of the initial probability density independently for each input variable. The variables providing the highest variation of the original failure probability are settled to be more influential. These variables will need a proper characterization in terms of uncertainty influencing the probability of failure.

It investigates the robustness (Wang, Hwang, Juang, *et al.*, 2013) of a study when the study includes some form of mathematical modelling. It increases understanding or quantification of the system (e.g. understanding relationships between input and output variables) especially when input variables are subject to many sources of uncertainty such as errors of measurement, absence of information and poor or partial understanding of the driving forces and mechanisms (Zaman *et al.*, 2011).

The sensitivity analysis is able to account for variation (Jiang *et al.*, 2014) in slope properties and different geotechnical conditions. The stability of a slope depends on many factors such as water pressure, slope height, slope angle, shear strength, etc. These factors not only help in designing the slope but also help in understanding the failure mechanism.

The proposed method is based on Monte Carlo Simulation (MCS). The Monte Carlo method is a simple and robust technique, independent of system complexity. Also, the efficiency of the Monte Carlo method in its standard form does not depend on the dimension of the random variable space (Danka, 2011).

Most of the existing reliability sensitivity analysis methods assume that all the probabilities and distribution parameters are precisely known (Christian, Ladd and Baecher, 1994; Griffiths, Huang and Fenton, 2009; Wang *et al.*, 2012). That is, every statistical parameter involved is perfectly determined. However, geological, geotechnical and geometrical properties of a slope may differ from those one measured during survey investigation within a range of values (Krzykacz-Hausmann, 2006) which may greatly affect the probability of failure.

As discussed in previous chapters, there are two types of uncertainties: epistemic and aleatory that may not be perfectly determined in engineering practices. In this study, both epistemic and aleatory uncertainties were considered in reliability sensitivity analysis (Guo and Du, 2007).

Since no reference has been given by previous researchers on any uncertainty component, all the following were considered (Phoon *et al.*, 2006a):

- Measurement (laboratory and field investigations);

- Transformation (indirect relations between soil parameters, modeling);
- Inherent variability of ground conditions at the site (natural soil processes).

From a reliability perspective, the uncertainties of site geometry may be equally important to those of material properties, as discussed by (Dowding, 1979).

The approach is to evaluate FS for the values of the parameters at the different condition and then to change each of the parameters in turn by a small amount and re-evaluate FS. The variations provide estimates of FS numerical changes as far as conditioning factors vary. The magnitude of this effect may be expressed quantitatively. This leads to identifying the spatial distribution of FS values and which areas are more affected by instability.

The uncertainty in a random variable may be investigated through its first two moments (Cassidy, Uzielli and Lacasse, 2008), i.e. the mean (a central tendency parameter) and variance (a dispersion parameter).

Second-moment descriptive and inferential modelling (Loh, 2002) of soil parameters are widely used in the geotechnical literature (Phoon and Kulhawy, 1999; Cassidy, Uzielli and Lacasse, 2008; Zaman *et al.*, 2011) because of their efficiency in transmitting important properties of data sets.

The sample coefficient of variation is obtained by dividing the sample standard deviation by the sample mean. It provides a concise measure of the relative dispersion of data around the central tendency estimator (Phoon *et al.*, 2006b)

Therefore, Reliability sensitivity analysis is used to find the rate of change in the probability of failure (or reliability) due to the changes in distribution parameters (Cui, Lu and Wang, 2011).

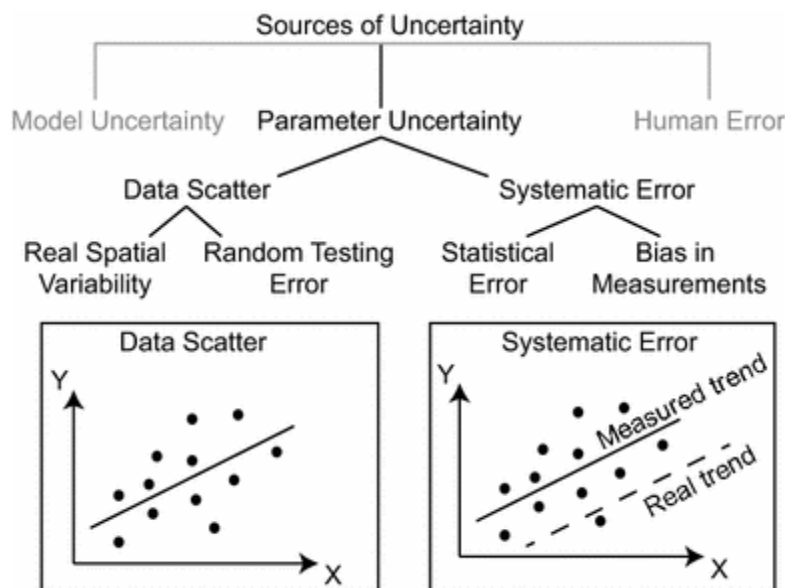


Figure 76 – Type of uncertainties in soil parameters (source: Vardanega and Bolton, 2015)

The uncertainty in the values of the soil properties is a major contributor to the uncertainty in the stability of slopes. It consists of two portions: scatter and systematic error.

The structure of the spatial variation may be used to estimate the level of random noise in soil property data and to eliminate it from the calculation of reliability index. The effects of the spatial variability on the computed reliability index are further reduced because the variability is averaged over a region or failure surface, and it is only its average contribution to the uncertainty that is of interest. The strength of the reliability analysis is not that one may get a better estimate of each of these uncertainties, but that one may deal with them explicitly and coherently.

Uncertainties in soil properties yield a lower bound estimate of the probability of failure, not the absolute probability of failure. However, for most practical applications the calculation of relative probability of failure is enough for parametric analysis.

Sensitivity analysis is an interactive process (Xiao *et al.*, 2011) adopted to simulate slope instability more realistically and determine the influence of the different parameters on the Factor of Safety. It indicates which input parameters may be more critical to the assessment of slope stability, and which input parameters are less influencing it (Sarma, Krishna and Dey, 2015).

Therefore, how much each parameter affects the whole stability, of the middle-low part of the earthflow, has been evaluated. The sensitivity analysis was based on the following statistical moments (Lu, Shen and Zhu, 2017):

- Variance values, possibly due to sampling errors, modeling approximations, inherent soil variability.

The first sensitivity analysis was carried out based on variance variability of geological and geotechnical survey campaigns performed in 2006.

A second one was performed based on 2010 soil investigations. It focused instead on central tendency of variability, as follows:

- Mean value, as degree (slope inclination, friction angle), depth meters (slip surface, groundwater level), etc.

Based on that, the reliability sensitivity analysis with respect to distribution parameter of random variable may be derived to evaluate the effect of distribution parameter on the new reliability index under stochastic perturbations (Lu, Shen and Zhu, 2017).

The reason of the last sensitivity analysis concerns the interest in evaluating, in back analysis, either how much reducing or increasing each parameter, it increases slope stability. This would be useful for decision-making process as well as for identifying the most effective mitigation measures and priorities.

Conditioning factors of slope stability are not exactly known because of scarcity or lack of data, assumptions made by experts in modelling, presence of inherent variability (Phoon and Kulhawy, 1996).

These uncertainties are introduced by sampling errors during soil investigations, the relative inadequacy of the conceptual models, numerical approximations and completeness uncertainty difficult to assess or quantify (Phoon *et al.*, 2006a). However, it is possible to minimize the effect of uncertainty (Phoon and Kulhawy, 1999) by carrying out sensitivity studies on the model assumptions thus the effect on the model output.

The focus here is on the uncertainties regarding the variability and distribution of the parameters sampled in 2006.

The Coefficient of Variation (COV) is commonly used in geotechnical variability analyses (Phoon and Kulhawy, 1996). The advantages are that it is dimensionless and provides a more physically meaningful measure of dispersion relative to the mean, it is the ratio between standard deviation and mean value. Coefficients of variation of the same physical properties at sites worldwide vary within a relatively narrow range; moreover, they are thought to be independent of the geological age of the soil (Phoon *et al.*, 2006a).

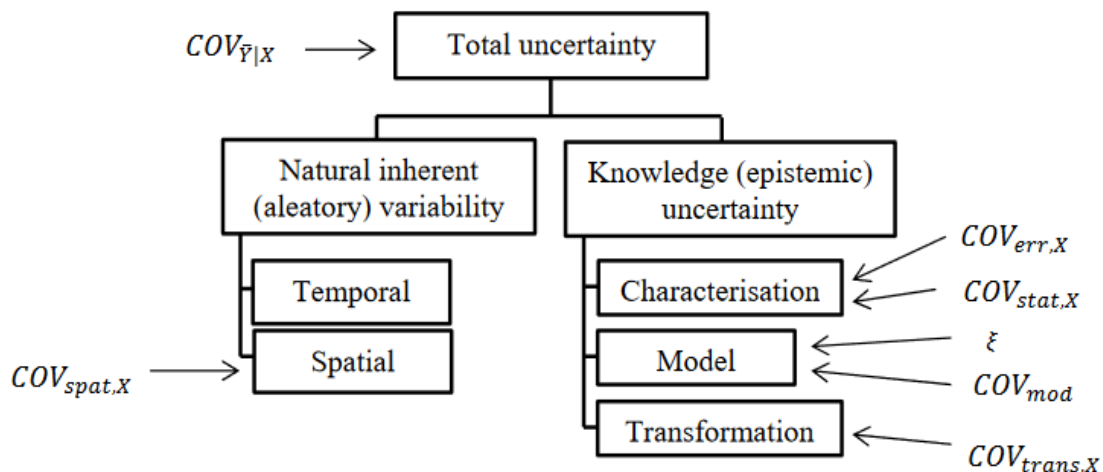


Figure 77 - Main components contributing to the total uncertainty of soil properties
(source: Muller, 2013)

In sensitivity analysis, a common approach is that of changing one-factor-at-a-time (Phoon *et al.*, 2006a), to see what effect this produces on the FS output. This appears a logical approach as any change observed in the output will unambiguously be due to the single factor changed. Furthermore, by changing one factor at a time one may keep all other factors fixed to their central or baseline value. This increases the comparability of the results (all ‘effects’ are computed with reference to the same central point in space) and minimizes the chances of computer program crashes, more likely when several input factors are changed simultaneously (Johari, Fazeli and Javadi, 2013).

Sensitivity analysis involves a series of calculations in which each significant parameter is varied systematically over its maximum credible range (Tsompanakis *et al.*, 2010) in order to determine its influence upon the Factor of Safety.

Literature review (Phoon, 1999; Phoon and Kulhawy, 1999; Phoon *et al.*, 2006a) was conducted to estimate the typical COV values of inherent soil variability. However, this task was complicated because most COVs reported in the geotechnical literature are based on total variability analyses (F. C. Dai, Lee and Ngai, 2002).

Harr (1987) provided a “rule of thumb” by which coefficients of variation below 10% are considered to be “low”, between 15% and 30% moderate”, and greater than 30%, “high” (Phoon *et al.*, 2006b).

Based on literary research (see Appendix 3) and COVs observed by soil data in 2006- ranging from 6% to 50% - the following COVs values of total variability were considered: 10%, 25%, 50% then applied to each conditioning parameter.

ID_tile	FS	P(FS)	P(FS_10%)	P(FS_25%)	P(FS_50%)
2	0.570	0.336	0.133	0.320	0.388
18	0.578	0.346	0.147	0.332	0.398
15	0.594	0.370	0.185	0.361	0.419
20	0.597	0.375	0.193	0.367	0.424
16	0.615	0.401	0.240	0.400	0.447
14	0.626	0.417	0.272	0.420	0.461
19	0.649	0.452	0.344	0.462	0.492
1	0.652	0.457	0.355	0.469	0.496
17	0.652	0.457	0.356	0.469	0.496
21	0.738	0.587	0.658	0.629	0.609
3	0.773	0.639	0.766	0.691	0.653
11	0.832	0.720	0.896	0.781	0.722
13	0.834	0.722	0.899	0.784	0.725

10	0.836	0.724	0.902	0.786	0.726
6	0.850	0.742	0.922	0.805	0.742
22	0.850	0.743	0.923	0.806	0.742
23	0.858	0.752	0.932	0.816	0.751
12	0.858	0.752	0.933	0.816	0.751
8	0.860	0.755	0.935	0.818	0.753
7	0.861	0.756	0.936	0.820	0.754
9	0.864	0.760	0.940	0.824	0.757
4	0.893	0.792	0.965	0.857	0.786
5	0.914	0.816	0.978	0.879	0.806

Table 37 – Sensitivity of FS in 2006 with different COVs

In Table 37, for low initial values of P(FS) the probability of failure increases by increasing the variance while for high initial values of P(FS), the probability of failure increases as much as the variance decreases.

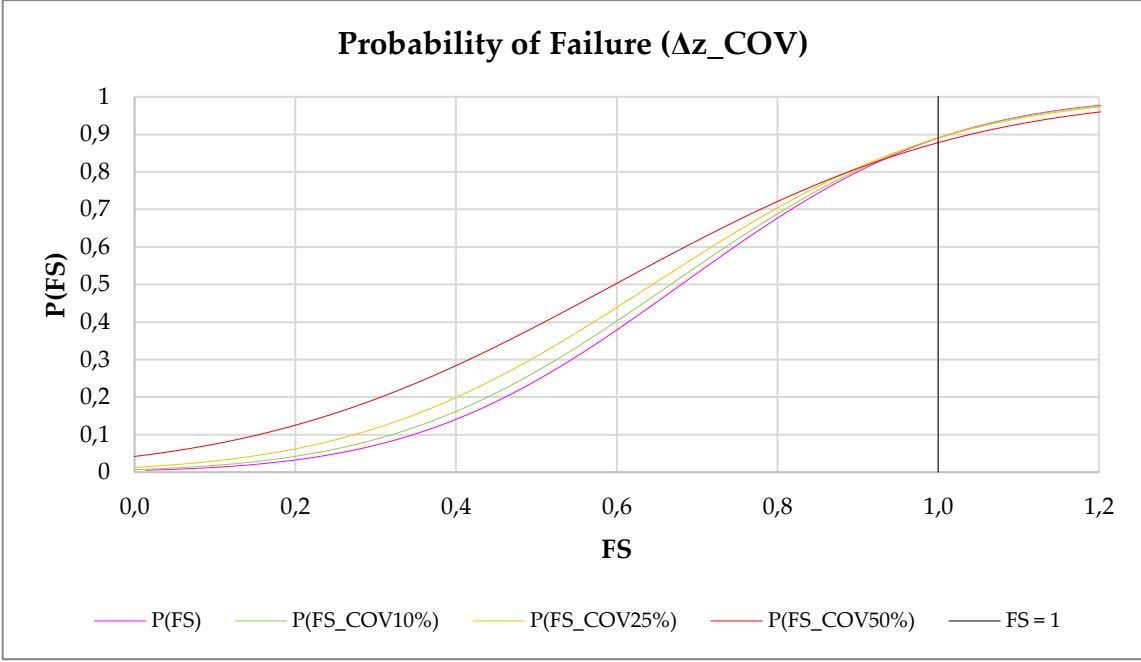
This is potentially due to sampling errors, modelling approximations and/or inherent soil variability.

	FS	FS_10%	FS_25%	FS_50%
μ_{FS}	0.68	0.66	0.64	0.59
σ_{FS}	0.26	0.27	0.28	0.34
β_{FS}	-1.23	-1.23	-1.23	-1.16
$P_{f_{FS}}$	0.62	0.62	0.62	0.64

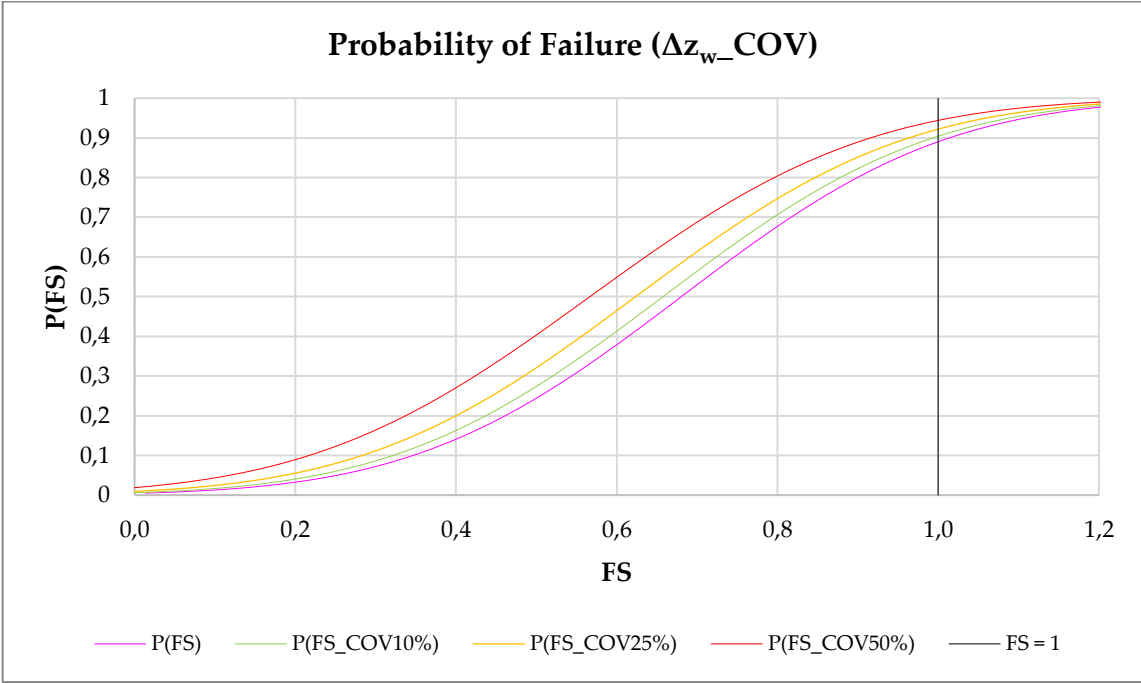
Table 38 – Statistical and Reliability values of FS for different COVs in 2006

The current practice is the use of Monte Carlo simulation to propagate uncertainties by increasing the coefficient of variation.

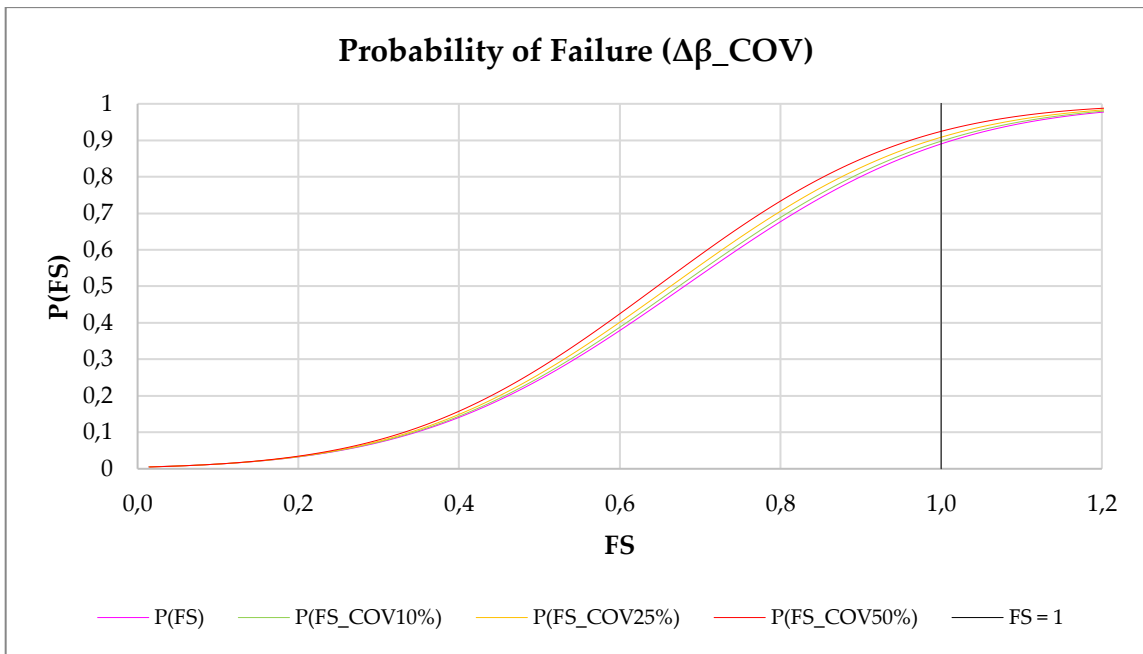
Therefore, by assuming the above target coefficients of variation, the probability of failure has been estimated by Monte Carlo Simulation. Again, each parameter has been treated as random variable at each sample of the sensitivity estimate.



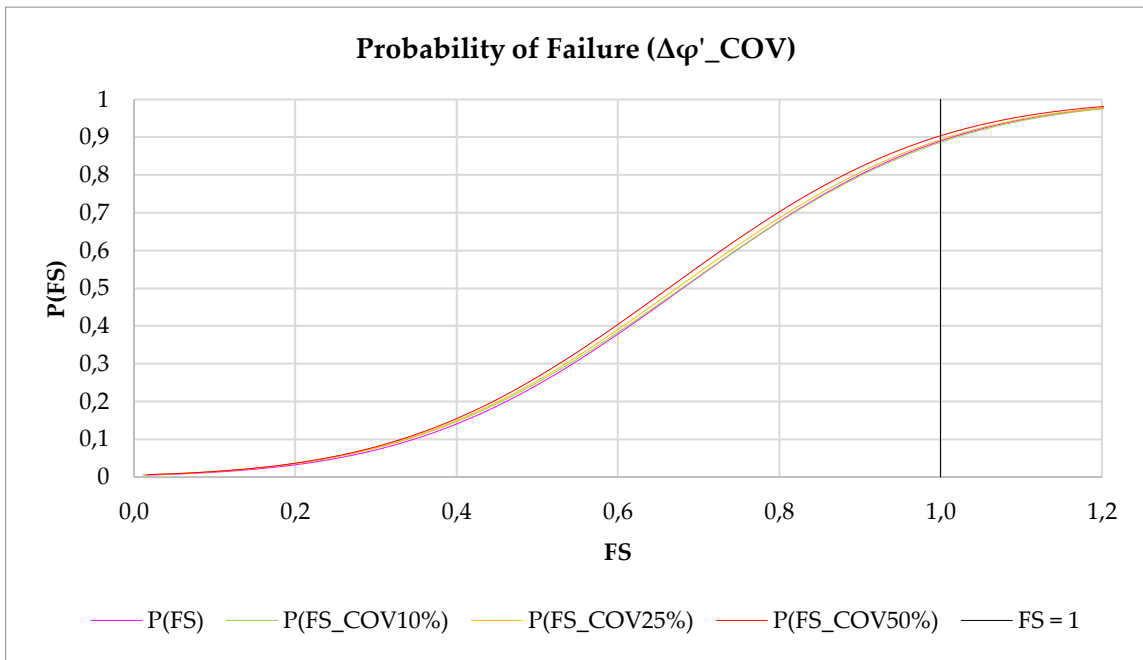
Graph 36 - Sensitivity of FS in 2006 with different COVs for slip surface



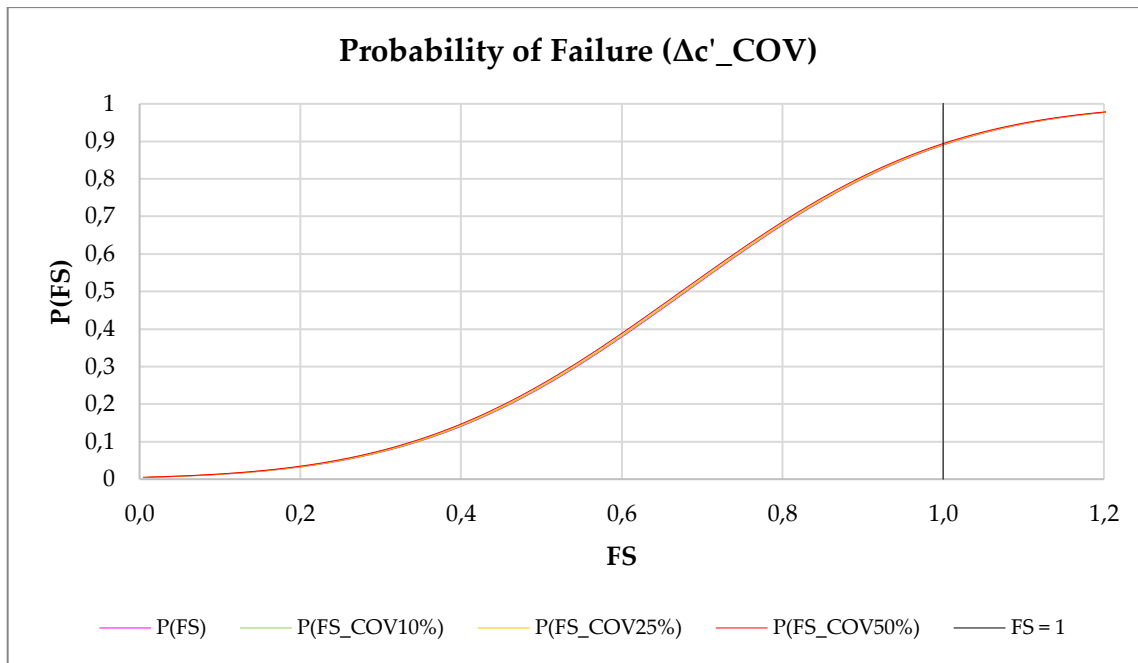
Graph 37 - Sensitivity of FS in 2006 with different COVs for groundwater depth



Graph 38 - Sensitivity of FS in 2006 with different COVs for slope angle



Graph 39 - Sensitivity of FS in 2006 with different COVs for friction angle



Graph 40 - Sensitivity of FS in 2006 with different COVs for cohesion

The parametric curves above (Graphs 36-40) show how the variance of each parameter changes FS. In particular, a large increase in FS is given by the variation in the depth of the sliding surface and the groundwater level, followed by the inclination of the profile, and by the parameters of shear strength.

Statistical parameters used to model a random field are generally uncertain and statements regarding probabilities are equally uncertain (Cui, Lu and Wang, 2011). That is, because of the uncertainty in estimates of mean properties, statements regarding the probability of failure of a slope, for example, cannot be regarded as absolute.

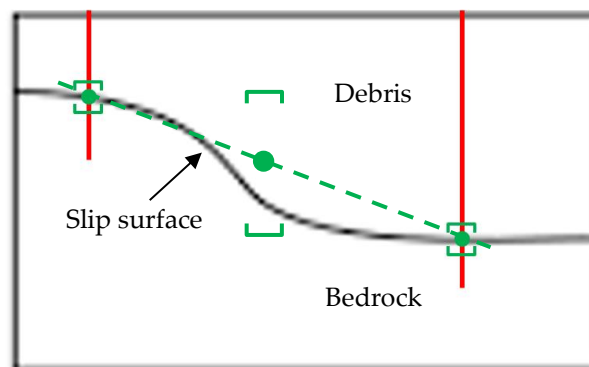


Figure 78 - Uncertainty in mean values of depth (green) by using survey investigations (red).

In many geotechnical problems, the parameter of interest is the soil property or geometry averaged over a length, a surface or a volume. Vanmarcke (1980)

showed that one of the effects of spatial averaging is to reduce the variability of the averaged parameter (e.g. shear strength) compared to the variability of the data considered separately. The reason for this reduction is the averaging of the variability over a length, surface or volume, and then only the averaged contribution to the uncertainty is of interest (Nadim, 2016).

ID_tile	FS	P(FS)	P(FS_10%)	P(FS_25%)	P(FS_50%)
2	0.578	0.327	0.176	0.055	0.023
20	0.604	0.362	0.193	0.060	0.024
18	0.616	0.380	0.202	0.063	0.025
15	0.634	0.406	0.215	0.067	0.025
16	0.640	0.414	0.219	0.068	0.026
1	0.656	0.438	0.232	0.072	0.026
14	0.673	0.463	0.245	0.077	0.027
19	0.675	0.465	0.246	0.077	0.027
17	0.683	0.479	0.253	0.079	0.028
21	0.736	0.557	0.298	0.095	0.030
3	0.786	0.630	0.343	0.111	0.032
6	0.873	0.743	0.427	0.144	0.037
11	0.882	0.755	0.436	0.148	0.038
7	0.884	0.757	0.438	0.149	0.038
8	0.886	0.758	0.440	0.149	0.038
10	0.886	0.759	0.440	0.149	0.038
4	0.893	0.767	0.447	0.152	0.038
9	0.899	0.773	0.453	0.155	0.039
22	0.900	0.775	0.454	0.155	0.039
23	0.918	0.794	0.472	0.163	0.040
12	0.918	0.795	0.472	0.163	0.040
13	0.925	0.801	0.479	0.166	0.040
5	0.930	0.807	0.484	0.169	0.040

Table 39 – Sensitivity of FS in 2010 with different mean values

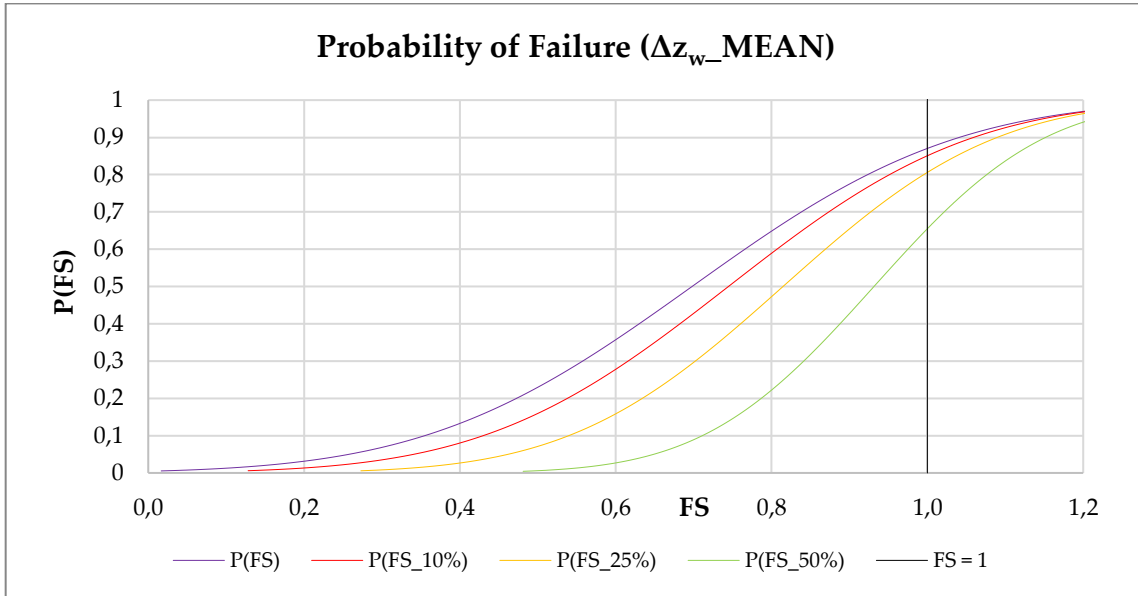
In Table 39, for initial values of P(FS) both low and high, the probability of failure decreases by halving/doubling respectively the mean value of the corresponding parameter.

The variation of the central tendency influences the probability of failure without considering its initial value.

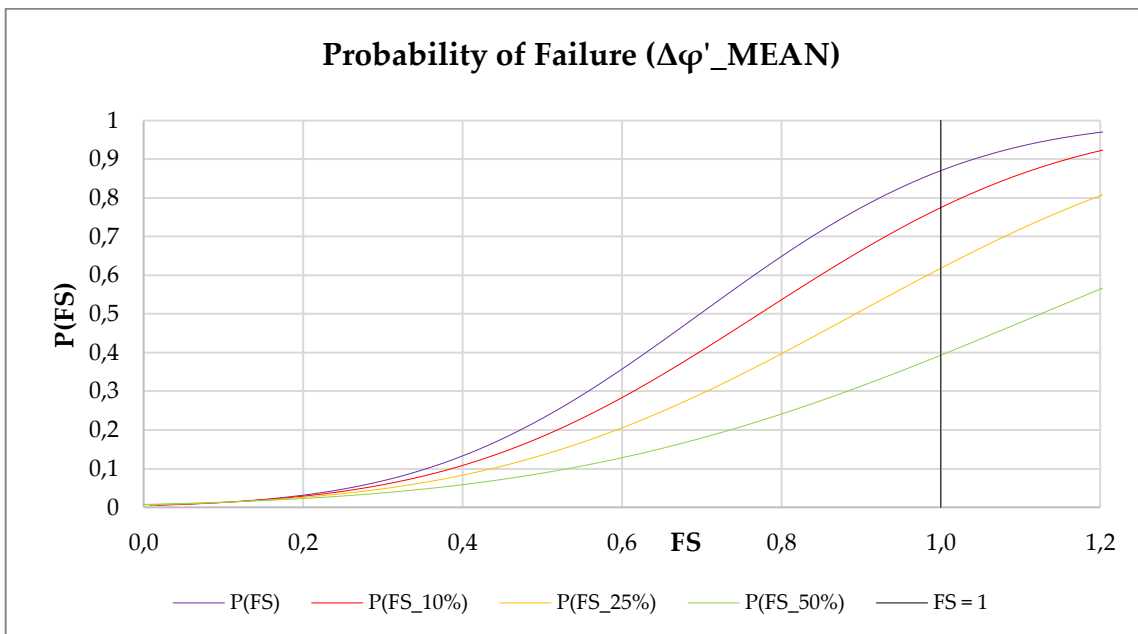
	FS	FS_10%	FS_25%	FS_50%
μ_{FS}	0.69	0.94	1.45	3.41
σ_{FS}	0.26	0.39	0.54	1.42

β_{FS}	-1.13	-0.14	0.83	1.70
$P_{f_{FS}}$	0.64	0.7	0.18	0.04

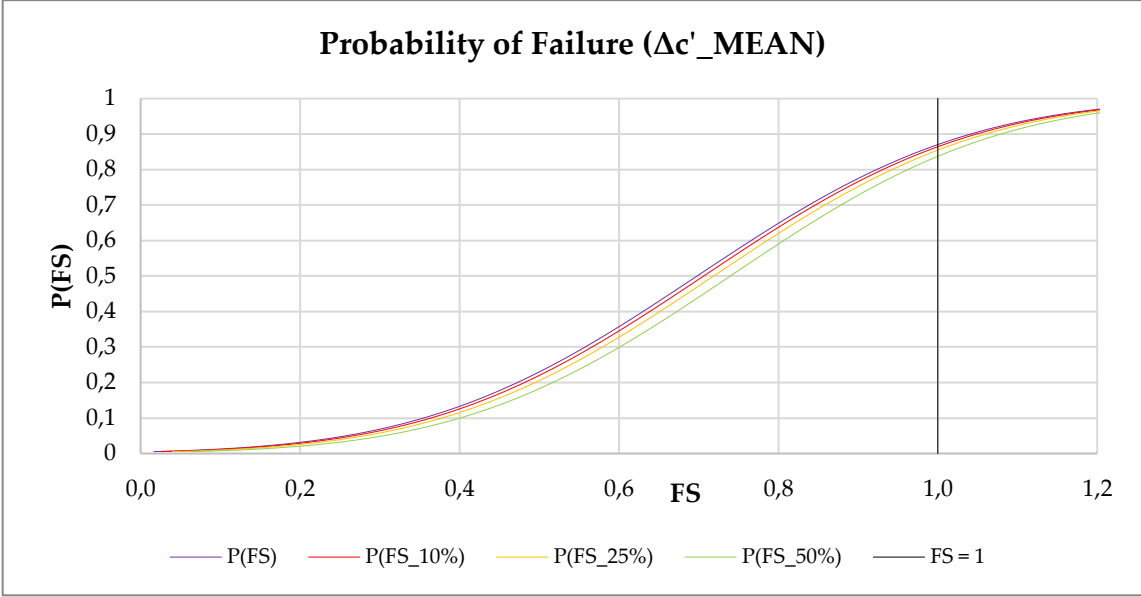
Table 40 – Statistical and Reliability values of FS for different mean values in 2010



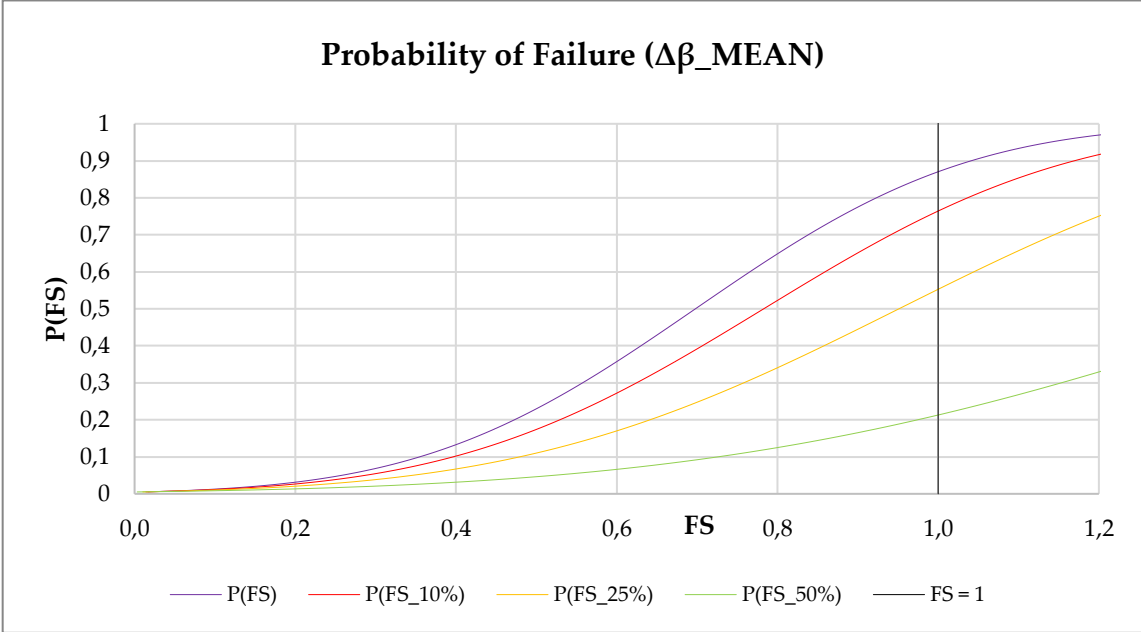
Graph 41 - Sensitivity of FS in 2010 with different groundwater depths



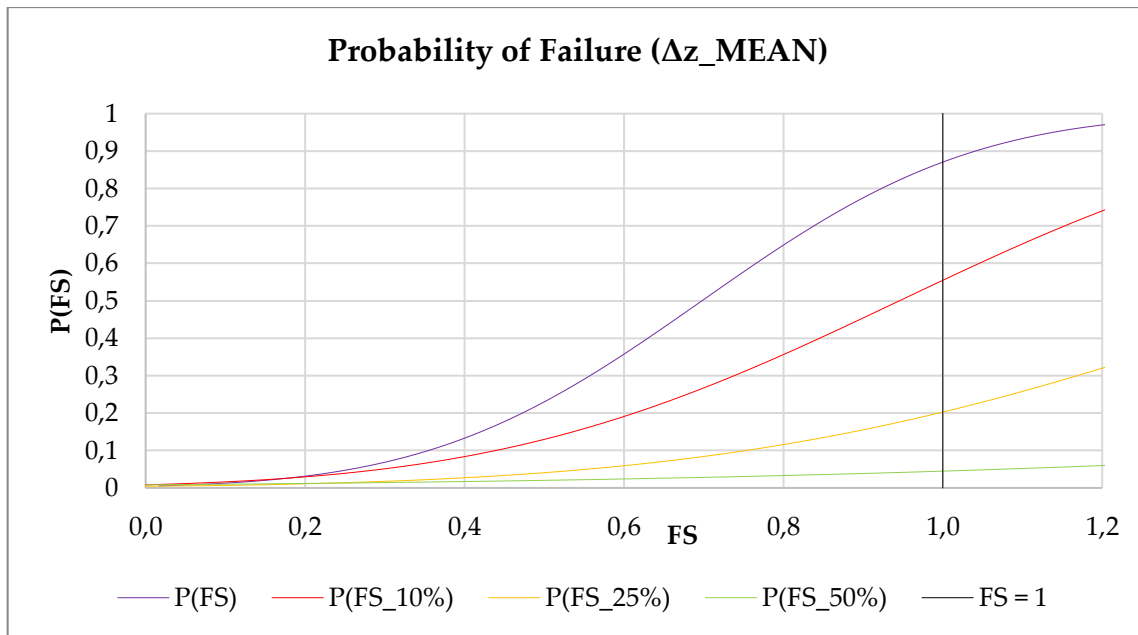
Graph 42 - Sensitivity of FS in 2010 with different friction angles



Graph 43 - Sensitivity of FS in 2010 with different cohesion values



Graph 44 - Sensitivity of FS in 2010 with different slope angles



Graph 45 - Sensitivity of FS in 2010 with different ground surfaces

The curves above (Graphs 41-45) show how the variation of each average parameter changes FS. In particular, a large increase in FS is given by the variation of groundwater depth and slope inclination, followed by shear strength parameters.

4.5 Stochastic Mapping of Slope Instability

Among the most basic tasks of quantitative characterization is to map local and regional geo-information with spatial continuity along the study area even when soil parameters are discrete (Hammah, Yacoub and Curran, 2009).

Mapping attempts to divide the three-dimensional area into layers or strata. It identifies and characterizes features that might be difficult to notice without a spatial vision of the whole site (Lombardi, Cardarilli and Raspa, 2017). It helps to observe each surface, looking for potential spatial correlations distributed either locally, in a single map, or at scale of area by combining more realizations.

Such mapping includes the probabilities of unlikely as well as likely composition and distribution, assigning each point to the most probable class (with minimum variance) and associating with it a probability of misclassification (estimation variance), directly informing on the reliability assessment as well (Rossi *et al.*, 2010).

The thematic mappings based on uncertainties in soil components and instability system would try to satisfy four requirements (Mancini, Ceppi and Ritrovato, 2010):

- be simple to conceive and use;
- be able to assign subjective prior probabilities to its components;
- be reliable or give a measure of the reliability degree (i.e. estimation error);
- be directly useful in design decisions.

As shown in previous chapters, every component conditioning slope stability has been mapped at different location: at the ground surface, at the slip surface depth, and at an intermediate depth between them. It has been made regarding both discrete than continuous parameters grouping each one in several ranges. By classifying them in chromatic categories, faster detection and easier understanding may be carried out by any stakeholder involved.

4.5.1 Interventions as conditioning elements: Instability Prediction

The interventions carried out after the reactivation of 2010 made it possible to assess the applicability of the method based on the variations induced by the works on the stability of the slope analyzed.

In particular, interest has been focused on reshaping of the longitudinal profile and the collection of surface water made respectively through excavations/backfills and draining trenches.

Concerning reshaping profile, the upper part was reduced to 14 degree from the horizontal plane, while the middle and toe area respectively to 10 and 20 degree. These values have been defined based on natural inclinations and spatial location.

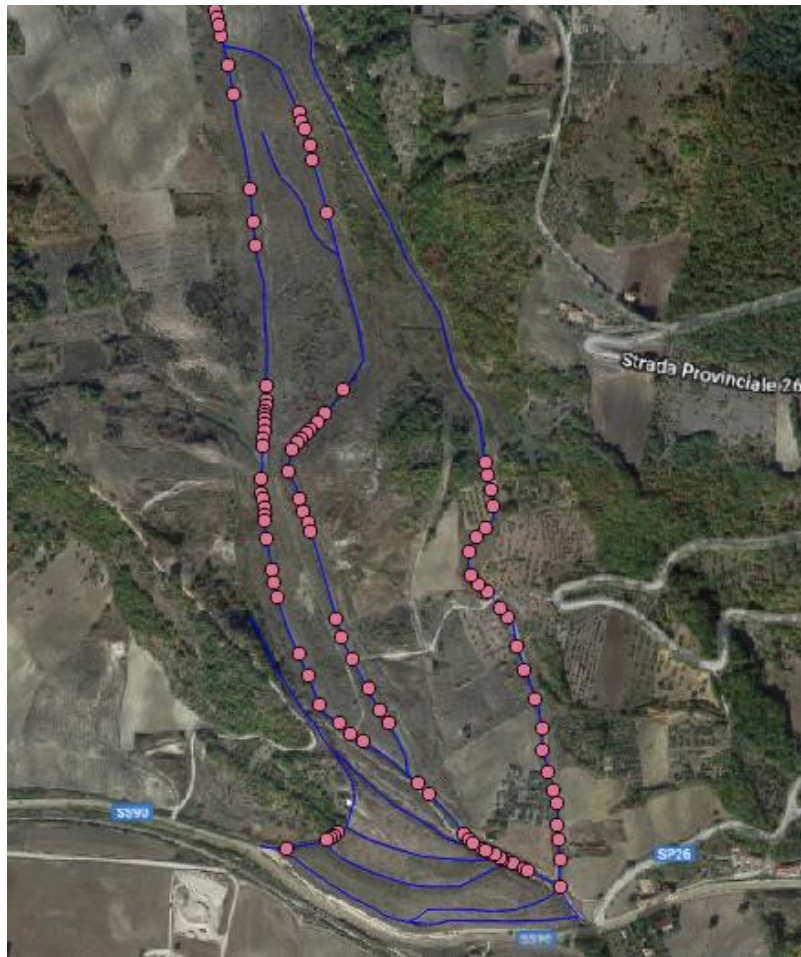


Figure 79 - Longitudinal profile of the landslide area with stabilization works: draining trenches (pink points) and drainage channels (blue lines)

As groundwater surface, sub-superficial drainage network was realized reducing the depth from 1m to 2m. For the aim of the study it has been considered 10% on average.

Based on these new considerations, the variability of FS has been analyzed and estimated with the geostatistical approach, as follows:

	FS	
h_lag	100	m
tol.h_lag	50	m
alpha	0	°
tol.hor	180	°
beta	0	°
tol.vert	89	°

Table 41 - Empirical values of FS variogram in 2010

	FS
Nug_psill	0.01
Nug_range	0
Exp_psill	0.17
Exp_range	512.97

Table 42 - Theoretical values of FS variogram in 2010

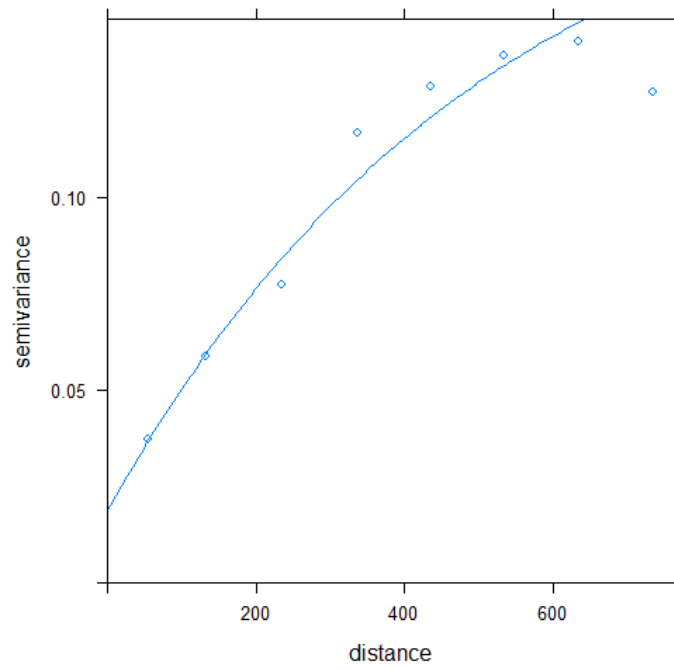


Figure 80 - Variogram and theoretical model for FS and 2010

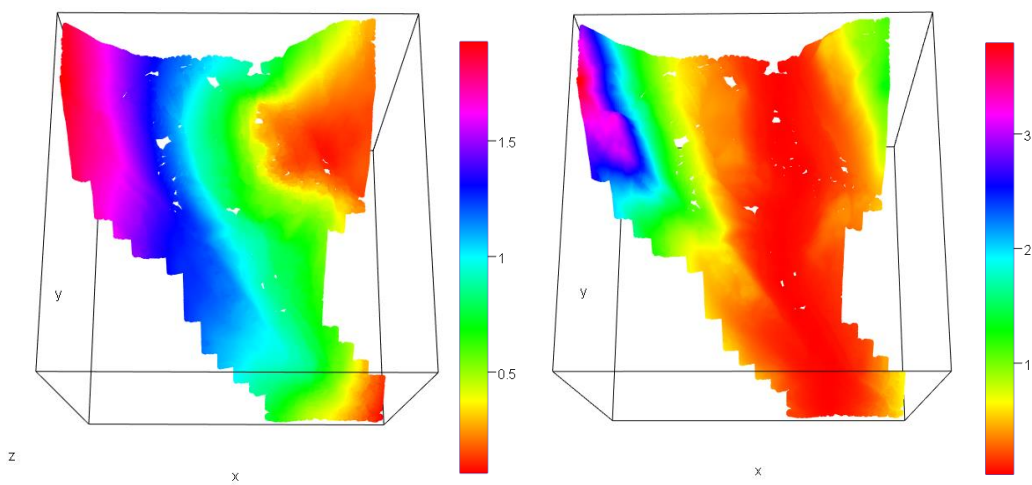
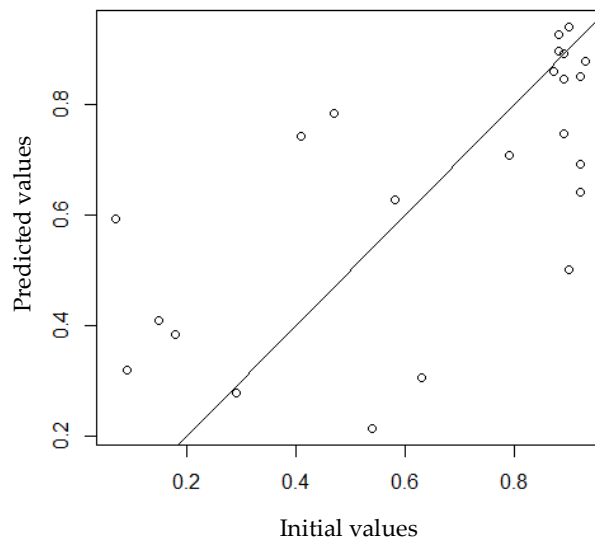


Figure 81 - Variability maps of spatial predictions (left) and variances (right) of FS in 2010

In order to have an overview of the spatial variability of FS, predictions and variances have been estimated.

A considerable variability is located between the right side and the left, affecting in particular the toe of the slope. On the left, colour distribution shows a longitudinal variability that crosses the slope from upstream to downstream, highlighting the landslide area and the eastern side of the slope at minimum values.

The variance is instead kept constant along the longitudinal profile with values that are around the 0 along the landslide body.



Graph 46 - Scatterplot between initial and estimated values of FS in 2010

The scatterplot (Graph 46) relative to the estimates of FS shows good approximations for higher values, while it deviates more for the lower ones. In particular, the results show that the smoothness of Kriging has involved an appreciable overestimation of low values and a slight underestimation of higher values.

RMSE and MAE below, quantify the variation of the errors. As the values are close to zero, it indicates a good model performance giving acceptable results.

	FS
MAE	0.17
RMSE	0.22

Table 43 - Performance criteria between predicted and observed values of FS in 2010

4.5.2 Interventions as conditioning elements: Instability Simulation

The same new considerations about FS after the stabilization works have been made with the reliability approach. The variability of FS and P(FS) has been analyzed and simulated, as following shown:

ID_tile	z (m)	β (°)	ϕ' (°)	c' (kPa)	z_w (m)	FS	P(FS)
1	12	14	28	11	10.02	0.97	0.85
2	17	14	29	10	15.27	1.35	0.99
3	22	14	30	8	15.27	1.59	1.00
4	21	14	31	6	7.85	2.02	1.00
5	22	14	28	7	7.85	1.82	1.00
6	20	14	29	7	5.65	1.98	1.00
7	20	14	29	9	5.65	2.00	1.00
8	15	14	26	8	3.58	1.84	1.00
9	14	14	28	9	3.58	2.00	1.00
10	15	10	29	10	3.83	2.94	1.00
11	16	10	29	9	3.83	2.93	1.00
12	16	10	29	9	8.87	2.44	1.00
13	19	10	27	9	8.87	2.35	1.00
14	11	10	27	9	10.02	1.35	0.99
15	14	10	28	10	13.56	1.76	1.00
16	11	10	26	10	10.02	0.82	0.69
17	10	10	26	12	9.20	0.71	0.51
18	18	10	26	11	16.24	1.51	1.00
19	11	10	28	9	10.02	0.86	0.61
20	9	10	24	10	8.49	0.92	0.80
21	7	10	28	9	6.59	0.74	0.57
22	12	20	30	11	9.50	1.10	0.93
23	11	20	29	11	9.50	1.02	0.89

Table 44 - Soil parameters and values after interventions per tile

The maps below (Figure 82) represent FS and P(FS) obtained from the use of input data altered by the realization of the works. FS assumes values that are significantly higher than the stability condition, except for some areas upstream which maintain critical conditions with respect to stability. The probability vice versa is attested to low values in those areas, meaning that the forecast does not have a high potential for occurrence.

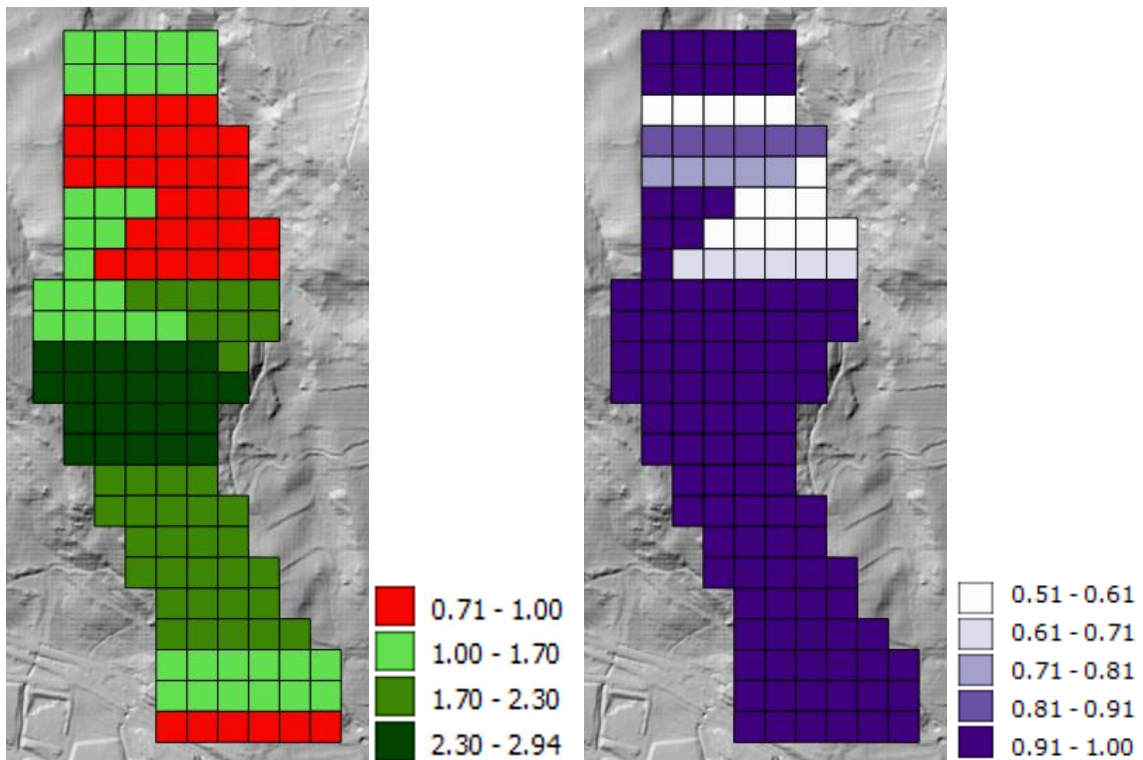


Figure 82 – Spatial values of FS and P(FS) after stabilization works

Probability theory and statistics may aid this process of geological mapping in at least two ways. First, they may be used to make inferences about the geology of unobserved parts of a site (or region) that are more powerful than those based on intuition, and those inferences may be associated with measures of precision and accuracy. Second, they may be used to optimize the way exploration effort is allocated across a site or among different means of collecting data, balanced against competing investments in sampling for material properties or finding geological anomalies.

Nonetheless, probability theory and statistics have been relatively little used in rationalizing how we do this mapping, and the undertaking is often viewed as more art than science. Therefore, there are fewer tangible results in the literature on quantitative mapping than on other aspects of quantitative site characterization. This is a shame, and it is likely to change, because increasing use of remote sensing, global positioning, and other sensing technologies has generated an abundance of data on geology that might feed more rational and efficient approaches to mapping.

Chapter V

Conclusions

In determining the probability that a mass movement is activated, it is fundamental to consider the conditions that cause this situation of instability. Conditioning variables, such as geology, geometry, height, groundwater level, soil geotechnical properties, i.e. those factors that predispose a slope to instability and make it susceptible to failure, were considered, analyzed and evaluated. Afterwards, loading factors as triggering variables, such as soil and water weight were included in the study, bringing the slope from a marginal stability condition to a state of instability to failure.

Stochastic analysis on empirical variables and their theoretical distribution have been performed using quantitative methods, such as multivariate Statistics, Geostatistics and Reliability approaches, depending on how the predisposing factors were considered and related to local and regional effect within the landslide area.

Stability analysis and data processing, together with those of surveying, monitoring and modelling processes, were performed to verify the effectiveness of an integrated use of different approaches.

Thanks to the effectiveness and versatility shown by these approaches to the landslide system, the possibilities of wider applications of statistics and probabilistic tools and the integration of further quantitative modelling, would provide complementary information for assessing slope instability phenomena. Furthermore, the stochastic assessment might allow to establish the efficiency of stabilization works or to guide planning of new mitigation measures and their position. Anyway, it should be remembered that, the efficiency of the undertaken activities must be evaluated by observing the time history of the velocity recorded at critical points, not considered within the study.

Soil characterization of the Montaguto earth flow has revealed the existence of heterogeneous conditions (Terra *et al.*, 2013) and isotropic spatial correlation likely due to continuous soil mixing for reactivation activity. Indeed, the landslide is characterized by complex morphology and different activation times (Terra *et al.*, 2013).

Slope stability assessment has led to identify the presence of more unstable areas representing the most critical portion of the slope to failure; these areas match

perfectly with those highlighted by conditioning soil parameters so then by the Factor of Safety maps.

Sectors and unstable zones are characterized by a low value of strength and non-smoothness of geometries.

Probability of failure increases more in some area than in other sectors or/and at different period of times (i.e. years).

Changes in landslide activity, however, are only reflected in the temporal sensitivity as the susceptibility is not changed for the scenarios (Terra *et al.*, 2013).

A clear model advantage is the nature of the slope stability model. The model simulates changes in landslide susceptibility, which might arise from adaptations in the morphology and the soil properties of a slope under temporal sensitivity variations.

The awareness of having, at least in part, achieved the goal was represented by a clear correspondence in terms of temporal-space evolution and distribution of the most unstable areas, observed between the developed stochastic models and the measurements obtained through investigation and monitoring.

There are several advantages in using a reliability-based approach versus the traditional approach. It allows to quantify the reliability, and load and resistance components to achieve consistent levels of reliability among different potential scenarios.

By quantifying reliability, it is possible to perform cost-benefit analyses to balance mitigation costs against the risk of slope failure.

The model was calibrated using measured time series and observed earth flow activity and might be re-calibrated for application at other slope instabilities.

The application of these innovative-methodological mapping and interpretative approaches, and predictive models at the Montaguto earth flow permitted to obtain further information about landslide characteristics and instability evolution of the earth flow complementary to those provided by past researches.

The model has reached a higher validation degree as the input data were acquired through measurements taken at sampling rates (geological and geotechnical parameters). All output is basically composed of stacks of maps, reported at each time step (year) and main interesting depths.

The model validity is affected by random and systematic errors. Random errors represent statistical fluctuations (in either direction) in the measured data due to inherent variability component and usually to the precision limitations of the measurement instruments as well. Systematic errors, by contrast, are reproducible inaccuracies that are consistently in the same direction. Systematic

errors are often due to a problem which persists throughout the entire experiment.

A reduction of random errors may be done by averaging over a large number of observations while systematic errors are difficult to detect.

The results of second-moment statistics in the form of mean value, coefficient of variation and coefficients of correlation between properties, as well as suitable probability distributions of conditioning parameters, should not be used uncritically in design purposes. It is due to statistics of those geo-information which are related to in-situ state then significantly dependent upon the site.

For these parameters, it is difficult to identify *typical* values. Also, in geo-engineering it is often possible to measure the same parameter using two or more testing methods and/or procedures. Different testing procedures are generally characterised by different testing uncertainty. Moreover, using more than one testing procedure will result in different measured values because the measurement occurs in a different way (Denora, Romano and Cecaro, 2013). Hence, the testing method should be specified when reporting statistics from a source site.

Lastly, it is generally not possible to evaluate the degree of homogeneity in the soil units from which the statistics are calculated. If such information is not provided, descriptive and inferential statistics will be misleading (Popescu, Prevost and Deodatis, 1998).

Therefore, main limitations concern rounding errors and data limitations that originate from the heterogeneous distribution of soil investigations as well as discretisation of slope stability model.

Certainly, we highlight the effective integrated modelling system, obtained by analyzing the results of every surveys campaigns and by the comparison between them in term of spatial variability and distribution. This was made possible thank to previous information from past studies on the site as well.

Finally, future predictions should not be deterministic. They should be probabilistic.

The current practice in forward-prediction modelling is to research several historical events similar to the target event over a range of physical characteristics. These historic events are then individually back-analysed, using expert judgement to select the best-fit rheologies and parameters.

By recommending a specific set of parameters based on the physical characteristics of an event, the preliminary hazard map may be rapidly produced, reducing the cost to make landslide analysis a more accessible tool for decision makers. The recommended parameters also provide context-specific starting

parameters so that an expert practitioner may fine-tune model parameters in the usual iterative process for parameter selection in the construction of a more detailed hazard map.

This thesis is highly dependent on the accuracy of reported observations, from the recorded soil characteristics to accurate maps of pre- and post-event topography. No attempt was made to verify or reinterpret reported observations.

Recommendations and Further Developments

The paper provides an overview of selected techniques for modelling the spatial and temporal variability of soils. A perspective as practical as possible was pursued, with wide reference to available literature.

Examples from probabilistic slope stability analyses were illustrated to highlight the benefits and limitations of approaches with various levels of complexity.

Most statistics available in the literature are strongly site- and case-specific, and the data should be examined with caution if they are to be applied at other sites.

Research may help simplify the use of variability-modelling techniques, thus assisting the practitioner. However, even the most powerful modelling technique may yield unreliable results if input data are insufficient in quantity and quality. Geological and geotechnical practice makes use of data sets which invariably indicate variability in any soil property. The variability information is often lost in the characterisation and design processes. A first step towards an uncertainty-based approach might be the explicit reporting of properly obtained data statistics and probabilistic information.

At present, research efforts focus on a variety of aspects of soil variability modelling but the gap between research and practice needs to be narrowed.

Therefore, the joint effort of researchers and practitioners should aim towards a full recognition of the benefits of such development.

More research should be completed to improve the characterization of Montaguto earth flow especially related to using quantitative data for stability analysis.

Possible future research, might improve or grow from these results, developing the following aspects, or at least some of them:

- A comparative analysis of geotechnical parameters in FS evaluations, should be carried out using different values in 2006 and 2010. It would be a more realistic assumption as the landslide occurred in the period between the two.
- A geostatistical analysis should be applied for each parameter used in the calculation of FS, to have a more accurate spatial comparison: a Sensitivity

analysis based on the “real” spatial distribution of soil parameters, not in the random one.

- Sensitivity analysis should also be done on the Coefficient of Correlation for a comparison between 2006 and 2010 soil values and stochastic modelling.
- The application of numerical methods that also consider the deformability of materials, in this case certainly high as well as variable, could allow an interesting back-analysis of the reactivations which occurred in 2006 and 2010.

Doing so, the theme of research might be improved on in the future. The methods and approaches might be also successfully applied elsewhere for improving knowledge of landslide phenomena and their relation to environmental drivers with spatial and temporal variability.

References

(EPA), U. S. E. P. A. (1997) 'Guiding Principles for Monte Carlo Analysis', *Us Epa*, (March), pp. 1–35. doi: EPA/630/R-97/001.

Abbaszadeh, M. *et al.* (2011) 'Uncertainty and Reliability Analysis Applied to Slope Stability: A Case Study From Sungun Copper Mine', *Geotechnical and Geological Engineering*, 29(4), pp. 581–596. doi: 10.1007/s10706-011-9405-1.

AGI (1977) 'Raccomandazioni sulla programmazione ed esecuzione delle indagini geotecniche'.

Aleotti, P. and Chowdhury, R. (1999) 'Landslide hazard assessment: Summary review and new perspectives', *Bulletin of Engineering Geology and the Environment*. doi: 10.1007/s100640050066.

Alimonti, C. *et al.* (2017) 'Reliability Analysis Applied on Land Subsidence Effects of Groundwater Remediation: Probabilistic vs. Deterministic Approach', *Water Resources Management*, 31(6). doi: 10.1007/s11269-017-1596-7.

Allasia, P. *et al.* (2013) 'ADVICE: A new approach for near-real-time monitoring of surface displacements in landslide hazard scenarios', *Sensors (Switzerland)*. doi: 10.3390/s130708285.

Baba, K. *et al.* (2012) 'Slope Stability Evaluations by Limit Equilibrium and Finite Element Methods Applied to a Railway in the Moroccan Rif', *Open Journal of Civil Engineering*, 02(01), pp. 27–32. doi: 10.4236/ojce.2012.21005.

Barbosa, M. R., Morris, D. V. and Sarma, S. K. (1989) 'Factor of safety and probability of failure of rockfill embankments', *Géotechnique*, 39(3), pp. 471–483. doi: 10.1680/geot.1989.39.3.471.

Baum, R. L, Reid, M. E. (2000) 'Ground water isolation by low-permeability clays in landslide shear zone', *In: Bromhead EN, Dixon N, Ibsen ML. Proc. 8th Int Symp on Landslide. Cardiff, Wales*, Landslide, p. 139–144,.

Baum, R. L. and Johnson, A. M. (1993) 'Steady movement of landslides in fine-grained soils; a model for sliding over an irregular slip surface', *United States Geological Survey Bulletin 1842-D*. doi: 10.1024/0040-5930/a000430.

Baum, R., Savage, W. and Wasowski, J. (2003) 'Mechanics of earth flows', in *Proceedings of the International Conference FLOWS, Sorrento, Italy*.

- BEGEMANN, H. K. S. (1965) 'The friction jacket cone as an aid in determining the soil profile.', *Proceedings of the 6th International Conference on Soil Mechanics and Foundation Engineering, ICSMFE*.
- Belabed, L. and Benyaghla, H. (2011) 'Reliability Analysis in Geotechnical Engineering', *6th International Advanced Technologies Symposium, (May)*, pp. 25–30.
- Bellanova, J. *et al.* (2018) 'Electrical resistivity imaging for the characterization of the Montaguto landslide (southern Italy)', *Engineering Geology*, 243(February), pp. 272–281. doi: 10.1016/j.enggeo.2018.07.014.
- Bergman, N. (2012) 'Characterization of strength variability for reliability-based design of lime-cement columns'.
- Bertolini, G. and Pizziolo, M. (2008) 'Risk assessment strategies for the reactivation of earth flows in the Northern Apennines (Italy)', *Engineering Geology*. doi: 10.1016/j.enggeo.2008.03.017.
- Bhattacharya, G., Chowdhury, R. and Metya, S. (2017) 'Residual factor as a variable in slope reliability analysis', *Bulletin of Engineering Geology and the Environment*. Bulletin of Engineering Geology and the Environment, pp. 1–20. doi: 10.1007/s10064-017-1085-5.
- Bond, A. and Harris, A. (2008) *Decoding Eurocode 7, Notes*. doi: 10.1017/CBO9781107415324.004.
- Borgonovo, E. (2007) 'A new uncertainty importance measure', *Reliability Engineering and System Safety*. doi: 10.1016/j.res.2006.04.015.
- Bovis, M. J. (1985) 'Earthflows in the Interior Plateau, southwest British Columbia', *Canadian Geotechnical Journal*. doi: 10.1139/t85-045.
- Bowles, J. E. (1979) 'Physical and geotechnical properties of soils', p. 478.
- Cadini, F., Agliardi, G. L. and Zio, E. (2017) 'A modeling and simulation framework for the reliability/availability assessment of a power transmission grid subject to cascading failures under extreme weather conditions', *Applied Energy*. Elsevier Ltd, 185, pp. 267–279. doi: 10.1016/j.apenergy.2016.10.086.
- Cardarilli, M., Lombardi, M. and Guarascio, M. (2018) 'Preventive planning model for rescue priority management in seismic emergency', *International Journal of Safety and Security Engineering*, 8(2). doi: 10.2495/SAFE-V8-N2-307-319.
- Carlo, M. and Galvan, R. (1992) 'La simulazione Monte Carlo: appunti integrativi 1', pp. 1–10.
- Cascini, L. *et al.* (2012) 'SPH propagation modelling of an earthflow from Southern Italy', p. 2012.

- Cassidy, M. J., Uzielli, M. and Lacasse, S. (2008) 'Probability risk assessment of landslides: A case study at Finneidfjord', *Canadian Geotechnical Journal*. doi: 10.1139/T08-055.
- Chai, T. and Draxler, R. R. (2014) 'Root mean square error (RMSE) or mean absolute error (MAE)? -Arguments against avoiding RMSE in the literature', *Geoscientific Model Development*. doi: 10.5194/gmd-7-1247-2014.
- Charles, J. A. and Bromhead, E. N. (2008) 'Contributions to *Géotechnique* 1948–2008: Slope stability and embankment dams', *Géotechnique*. doi: 10.1680/geot.2008.58.5.385.
- Cheng, P. F. K. (2004) 'Assessment of Landslide Risk of Natural Hillsides', *GEO Special Project Report*, (July), pp. 1–13.
- Cho, S. E. (2013) 'First-order reliability analysis of slope considering multiple failure modes', *Engineering Geology*. Elsevier B.V., 154, pp. 98–105. doi: 10.1016/j.enggeo.2012.12.014.
- Christian, J. T., Ladd, C. C. and Baecher, G. B. (1994) 'Reliability Applied to Slope Stability Analysis', *Journal of Geotechnical Engineering*. doi: 10.1061/(ASCE)0733-9410(1994)120:12(2180).
- Coe, J. A. *et al.* (2003) 'Seasonal movement of the Slumgullion landslide determined from global positioning system surveys and field instrumentation, July 1998-March 2002', *Engineering Geology*. doi: 10.1016/S0013-7952(02)00199-0.
- Coe, J. A. (2012) 'Regional moisture balance control of landslide motion: Implications for landslide forecasting in a changing climate', *Geology*. doi: 10.1130/G32897.1.
- Corominas, J. and Moya, J. (2008) 'A review of assessing landslide frequency for hazard zoning purposes', *Engineering Geology*. doi: 10.1016/j.enggeo.2008.03.018.
- Corotis RB, Azzouz AS, K. R. (1975) 'Statistical evaluation of soil index properties and constrained modulus', *proceedings of the 2nd International Conference on Applications of Statistics and Probability in Soil and Structural Engineering, Aachen, September 15–18*, pp. 273–294.
- Coulton, C. and Chow, J. (1993) 'Interaction Effects in Multiple Regression', *Journal of Social Service Research*. doi: 10.1300/J079v16n01_09.
- Cressie, N. (1989) 'Geostatistics', *American Statistician*. doi: 10.1080/00031305.1989.10475658.
- Cruden, D. M. and Varnes, D. J. (1996) 'Landslide Types and Processes', in *Landslides Investigation and Mitigation; Transportation Research Board*. doi: Fact Sheet 2004-3072.
- Cui, L., Lu, Z. and Wang, P. (2011) 'Reliability sensitivity analysis with mixture of random and fuzzy variables', in *ICQR2MSE 2011 - Proceedings of 2011 International*

Conference on Quality, Reliability, Risk, Maintenance, and Safety Engineering. doi: 10.1109/ICQR2MSE.2011.5976739.

St. Cyr, J. F. (2005) 'At Risk: Natural Hazards, People's Vulnerability, and Disasters', *Journal of Homeland Security and Emergency Management*, 2(2). doi: 10.2202/1547-7355.1131.

Dai, F. ., Lee, C. . and Ngai, Y. . (2002) 'Landslide risk assessment and management: an overview', *Engineering Geology*, 64(1), pp. 65–87. doi: 10.1016/S0013-7952(01)00093-X.

Dai, F. C., Lee, C. F. and Ngai, Y. Y. (2002) 'Landslide risk assessment and management: An overview', *Engineering Geology*. doi: 10.1016/S0013-7952(01)00093-X.

Daneshkhah, a R. (2004) 'Uncertainty in Probabilistic Risk Assessment: A Review Aleatory and Epistemic Uncertainties in Probabilistic Risk', *The University Of Sheffield, August*. doi: 10.1016/S0951-8320(96)00070-1.

Danka, J. (2011) 'Probability of failure calculation of dikes based on Monte Carlo simulation', *Geotechnical Engineering: New Horizons*. Available at: [http://www.kiviniria.nl/eygec/papers/30 DEP Danka.pdf](http://www.kiviniria.nl/eygec/papers/30_DEP_Danka.pdf).

Denora, D. (2013) 'Landslide Science and Practice', (September 2013), pp. 4–9. doi: 10.1007/978-3-642-31445-2.

Denora, D., Romano, L. and Cecaro, G. (2013) 'Terrestrial laser scanning for the montaguto landslide (Southern Italy)', in *Landslide Science and Practice: Early Warning, Instrumentation and Monitoring*. doi: 10.1007/978-3-642-31445-2-4.

Diamantidis, D. *et al.* (2006) 'On the Acceptable Risk for Structures Subjected to Geohazards', *Proceedings Geohazards Engineering Conferences International Year*, p. 9. Available at: <http://dc.engconfintl.org/geohazards/32>.

Diodato, N. *et al.* (2014) 'Predicting Monthly Spring Discharges Using a Simple Statistical Model', *Water Resources Management*, 28(4), pp. 969–978. doi: 10.1007/s11269-014-0527-0.

Dogliani, A. *et al.* (2012) 'Evolutionary polynomial regression to alert rainfall-triggered landslide reactivation', *Landslides*. doi: 10.1007/s10346-011-0274-8.

Dowding, C. H. (1979) 'Perspectives and challenges of site characterization', *Site Chara*, pp. 10–38.

Duncan (1999) 'Factors of safety and reliability', *The seventh Spencer J. Buchanan Lecture*, pp. 1–38. doi: 10.1061/(ASCE)1090-0241(2000)126:4(307).

Duncan, J. M. (2000) 'F Actors of S Afety and Reliability', *Journal of Geotechnical and Geoenvironmental Engineering*, 126(4), pp. 307–316. doi: 10.1227/01.NEU.0000249269.11074.CA.

- Enevoldsen, I. and Sørensen, J. D. (1994) 'Reliability-based optimization in structural engineering', *Structural Safety*. doi: 10.1016/0167-4730(94)90039-6.
- Fallis, A. . (2013) 'Uncertainty in Civil Engineering', *Uncertainty in Civil Engineering*, pp. 1–21. doi: 10.1017/CBO9781107415324.004.
- Famulari, A. M. (2013) 'Tecniche regionali di stima della portata di progetto : impatto della correlazione spaziale tra le serie di osservazioni', *Thesis*.
- Fasano, G. and Franceschini, A. (1987) 'A multidimensional version of the Kolmogorov-Smirnov test', *Monthly Notices of the Royal Astronomical Society*. doi: 10.1007/s10342-011-0499-z.
- Ferlisi, S. (2013) 'The SafeLand project The FP7 SafeLand project • SafeLand (Living with landslide risk in Europe : Assessment , effects of global change , and risk research project in EU ' s 7 th Framework Programme . Europe , and collaborates with several organisations', (November 2012), pp. 1–69.
- Ferrigno, F. *et al.* (2017) 'GB-InSAR monitoring and observational method for landslide emergency management: The Montaguto earthflow (AV, Italy)', *Natural Hazards and Earth System Sciences*, 17(6), pp. 845–860. doi: 10.5194/nhess-17-845-2017.
- Fischer, L. *et al.* (2009) 'Slope instabilities on perennially frozen and glacierised rock walls: multi-scale observations, analyses and modelling', *Department of Geography*. doi: 10.5167/uzh-31038.
- Fisher, D. *et al.* (2014) 'International Disaster Law Course', (May), pp. 1–4.
- Fleming, C. H. and Leveson, N. (2015) 'Integrating Systems Safety into Systems Engineering during Concept Development', *25th INCOSE International Symposium*, pp. 989–1003. doi: 10.1002/j.2334-5837.2015.00111.x.
- Fleming, R. W., Baum, R. L. and Giardino, M. (1999) 'Map and description of the active part of the Slumgullion landslide, Hindsdale County, Colorado', *Geologic Investigations Series*.
- Fredlund, D. G., Krahn, J. and Pufhal, D. E. (1981) 'The relationship between limit equilibrium slope stability methods', *Proceedings of the International Conference on Soil Mechanics and Foundation Engineering (Vol 3)*, pp. 409–416. doi: 10.1016/0148-9062(84)91799-6.
- Fubelli, G. *et al.* (2013) 'Holocene aggradation/erosion of a tufa at Triponzo (Central Italy)', *Geografia Fisica e Dinamica Quaternaria*. doi: 10.4461/GFDQ.2013.36.21.
- Functions, F. P. A. and Geostatistics, I. (1991) 'Agterberg, F. P. (1970). Autocorrelation Functions in Geology. In', (1970), pp. 821–828.

- Garzón, L. X. *et al.* (2015) 'Physical modelling of soil uncertainty', *International Journal of Physical Modelling in Geotechnics*, 15(1), pp. 19–34. doi: 10.1680/ijpmg.14.00012.
- Giordan, D. *et al.* (2013) 'Morphological and kinematic evolution of a large earthflow: The Montaguto landslide, southern Italy', *Geomorphology*. Elsevier B.V., 187, pp. 61–79. doi: 10.1016/j.geomorph.2012.12.035.
- Glade, T., Anderson, M. and Crozier, M. J. (2012) *Landslide Hazard and Risk, Landslide Hazard and Risk*. doi: 10.1002/9780470012659.
- Goovaerts, P. (1999) 'Geostatistics in soil science: State-of-the-art and perspectives', *Geoderma*. doi: 10.1016/S0016-7061(98)00078-0.
- Gortmaker, S. L., Hosmer, D. W. and Lemeshow, S. (1994) 'Applied Logistic Regression.', *Contemporary Sociology*. doi: 10.2307/2074954.
- Griffiths, D. V., Fenton, G. a. and Tveten, D. E. (2002) 'Probabilistic Geotechnical Analysis: How difficult does it need to be?', *International Conference on Probabilistics in Geotechnics Technical and Economic Risk Estimation*, 21(2), p. 19. doi: 10.12788/j.sder.0090.
- Griffiths, D. V., Huang, J. and Fenton, G. A. (2009) 'On the reliability of earth slopes in three dimensions', *Proceedings of the Royal Society A: Mathematical, Physical and Engineering Sciences*, 465(2110), pp. 3145–3164. doi: 10.1098/rspa.2009.0165.
- Griffiths, D. V., Huang, J. and Fenton, G. A. (2011) 'Probabilistic infinite slope analysis', *Computers and Geotechnics*. doi: 10.1016/j.compgeo.2011.03.006.
- Griffiths, D. V. and Lane, P. A. (1999) 'Slope stability analysis by finite elements', *Géotechnique*. doi: 10.1680/geot.51.7.653.51390.
- Guarascio, M. and Turchi, A. (1977) 'EXPLORATION DATA MANAGEMENT AND EVALUATION TECHNIQUES FOR URANIUM MINING PROJECTS.', *Appl of Comput Methods in the Miner Ind, Proc of the Symp, 14th*.
- Guerriero, L., Revellino, P., Grelle, G., *et al.* (2013) 'Landslides and infrastructures: The case of the montaguto earth flow in southern Italy', *Italian Journal of Engineering Geology and Environment*, 2013(TOPIC 5), pp. 459–466. doi: 10.4408/IJEGE.2013-06.B-44.
- Guerriero, L., Revellino, P., Coe, J. A., *et al.* (2013) 'Multi-temporal maps of the Montaguto earth flow in Southern Italy from 1954 to 2010', *Journal of Maps*, 9(1), pp. 135–145. doi: 10.1080/17445647.2013.765812.
- Guerriero, L. *et al.* (2014) 'Influence of slip-surface geometry on earth-flow deformation, Montaguto earth flow, southern Italy', *Geomorphology*, 219(May 2016), pp. 285–305. doi: 10.1016/j.geomorph.2014.04.039.
- Guerriero, L. *et al.* (2015) 'Reconstruction of long-term earth-flow activity using a

hydroclimatological model', *Natural Hazards*, 77(1), pp. 1–15. doi: 10.1007/s11069-014-1578-5.

Guerriero, L., Mascellaro, N., *et al.* (2016a) 'Combined monitoring of earth-flow movement and its environmental drivers, Montaguto earth flow in southern Italy', *Rendiconti Online Societa Geologica Italiana*, 41(Xxxx), pp. 167–170. doi: 10.3301/ROL.2016.120.

Guerriero, L., Mascellaro, N., *et al.* (2016b) 'Combined monitoring of earth-flow movement and its environmental drivers, Montaguto earth flow in southern Italy', *Rendiconti Online Societa Geologica Italiana*. doi: 10.3301/ROL.2016.120.

Guerriero, L., Revellino, P., *et al.* (2016) 'Kinematic Segmentation and Velocity in Earth Flows: A Consequence of Complex Basal-slip Surfaces', *Procedia Earth and Planetary Science*. doi: 10.1016/J.PROEPS.2016.10.016.

Guerriero, L. *et al.* (2016) 'The Montaguto earth flow: Nine years of observation and analyses', in *Landslides and Engineered Slopes. Experience, Theory and Practice*.

Guo, J. and Du, X. (2007) 'Sensitivity Analysis with Mixture of Epistemic and Aleatory Uncertainties', *AIAA Journal*. doi: 10.2514/1.28707.

Guo, J. and Du, X. (2009) 'Reliability sensitivity analysis with random and interval variables', *International Journal for Numerical Methods in Engineering*. doi: 10.1002/nme.2543.

Gustafsson, J. *et al.* (2012) 'Non-deterministic analysis of slope stability based on numerical simulation', *International Journal of Remote Sensing*, 33(01), p. 169. doi: 10.1016/j.eiar.2015.10.002.

Habibnezhad, Z. (2014) 'Stability Analysis of Embankments Founded on Clay', (3).

Hammah, R. E., Yacoub, T. E. and Curran, J. H. (2009) 'Probabilistic Slope Analysis with the Finite Element Method', *the 43rd US Rock Mechanics Symposium and 4th U.S.-Canada Rock Mechanics Symposium*.

Handwerger, A. L., Roering, J. J. and Schmidt, D. A. (2013) 'Controls on the seasonal deformation of slow-moving landslides', *Earth and Planetary Science Letters*. doi: 10.1016/j.epsl.2013.06.047.

Harr, M. E. (1987) 'Reliability-based design in civil engineering', Mc-Graw-H.

Harrison, R. L. (2010) 'Introduction to Monte Carlo Simulation', *AIP Conf. Proc.*, 1204, pp. 17–21. doi: 10.1063/1.3295638.Introduction.

Hasofer, A. M. and N.C., Lind (1974) 'An exact and invariant first order reliability format', *Journal Eng. Mech. Division (ASCE)*.

- Haukaas, T. and Der Kiureghian, A. (2003) *Finite element reliability and sensitivity methods for performance-based earthquake engineering*, *Peer*. doi: 10.1186/s12711-014-0075-3.
- Helton, J. C. *et al.* (2006) 'Survey of sampling-based methods for uncertainty and sensitivity analysis', *Reliability Engineering and System Safety*. doi: 10.1016/j.ress.2005.11.017.
- Heuvelink, G. B. M. *et al.* (2016) 'Geostatistical prediction and simulation of European soil property maps', *Geoderma Regional*. doi: 10.1016/j.geodrs.2016.04.002.
- Hicks, M. a and Samy, K. (2004) 'Stochastic evaluation of heterogeneous slope stability', *Italian Geotechnical Journal*, pp. 54–66.
- Honjo, Y. and Otake, Y. (2011) 'WHICH UNCERTAINTY (OR ERROR) IS THE MOST CRITICAL IN GEOTECHNICAL DESIGN Yusuke Honjo 1', *PWRI*.
- Hsu, H. (2013) *Probability, Random Variables and Random Processes*, *Journal of Chemical Information and Modeling*. doi: 10.1017/CBO9781107415324.004.
- Huang, J. *et al.* (2013) 'Quantitative risk assessment of landslide by limit analysis and random fields', *Computers and Geotechnics*. Elsevier Ltd, 53, pp. 60–67. doi: 10.1016/j.compgeo.2013.04.009.
- Hungr, O., Leroueil, S. and Picarelli, L. (2014) 'The Varnes classification of landslide types, an update', *Landslides*, 11(2), pp. 167–194. doi: 10.1007/s10346-013-0436-y.
- Hutchinson, J. N. (1970) 'A Coastal Mudflow on the London Clay Cliffs at Beltinge, North Kent', *Géotechnique*. doi: 10.1680/geot.1970.20.4.412.
- Iverson, R. M. (1986) 'Unsteady, Nonuniform Landslide Motion: 1. Theoretical Dynamics and the Steady Datum State', *The Journal of Geology*. doi: 10.2307/30081052.
- Iverson, R. M. and Major, J. J. (1987) 'Rainfall, ground-water flow, and seasonal movement at Minor Creek landslide, northwestern California: physical interpretation of empirical relations', *Geological Society of America Bulletin*. doi: 10.1130/0016-7606(1987)99<579:RGFASM>2.0.CO;2.
- Jaksa, M. B. (1982) 'the small- and large-scale spatial variability of the Keswick and Hindmarsh Clays', pp. 372–378.
- Jaksa, M. B. (1995) 'The influence of spatial variability on the geotechnical design properties of a stiff, overconsolidated clay', (December). doi: <http://hdl.handle.net/2440/37800>.
- Jaksa, M. B., Kaggwa, W. S. and Brooker, P. I. (1999) 'Experimental evaluation of the scale of fluctuation of a stiff clay', in *8th International Conference on Applications of Statistics and Probability in Civil Engineering*.

- Jefferies, M. G. and Davies, M. P. (1993) 'Use of CPTu to Estimate Equivalent SPT N60', *Geotechnical Testing Journal*. doi: 10.1520/GTJ10286J.
- Jiang, S. H. *et al.* (2014) 'Slope reliability analysis considering spatially variable shear strength parameters using a non-intrusive stochastic finite element method', *Engineering Geology*. Elsevier B.V., 168, pp. 120–128. doi: 10.1016/j.enggeo.2013.11.006.
- Johari, A., Fazeli, A. and Javadi, A. A. (2013) 'An investigation into application of jointly distributed random variables method in reliability assessment of rock slope stability', *Computers and Geotechnics*. Elsevier Ltd, 47, pp. 42–47. doi: 10.1016/j.compgeo.2012.07.003.
- Johari, A. and Javadi, A. A. (2012) 'Reliability assessment of infinite slope stability using the jointly distributed random variables method', *Scientia Iranica*. Elsevier B.V., 19(3), pp. 423–429. doi: 10.1016/j.scient.2012.04.006.
- Justel, A., Peña, D. and Zamar, R. (1997) 'A multivariate Kolmogorov-Smirnov test of goodness of fit', *Statistics & Probability Letters*. doi: 10.1016/S0167-7152(97)00020-5.
- Kasmaeeyazdi, S. *et al.* (2018) 'How different data supports affect geostatistical modelling: the new aggregation method and comparison with the classical regularisation and the theoretical punctual model', *International Journal of Mining, Reclamation and Environment*. doi: 10.1080/17480930.2018.1507609.
- KATADE, R. and KATSUKI, S. (2009) 'Target Reliability Index Determination Method Based on Burden Risk Concept', *Doboku Gakkai Ronbunshuu A*, 65(1), pp. 42–60. doi: 10.2208/jsceja.65.42.
- Keefer, D.K.; Johnson, A. M. (1983) 'Earth Flows : morphology , mobilization , and movement', p. 56 p.
- Kelley, K. and Bolin, J. H. (2013) 'Multiple regression', in *Handbook of Quantitative Methods for Educational Research*. doi: 10.1007/978-94-6209-404-8.
- Kelsey, H. M. (1978) 'Earthflows in Franciscan melange, Van Duzen River basin, California', *Geology*. doi: 10.1130/0091-7613(1978)6<361:EIFMVD>2.0.CO;2.
- Keough & Quinn (1995) 'Multiple regression and correlation.', *Design and Analysis for Biologists*. doi: 10.1037/0022-3514.90.4.644.
- Kervyn, M. *et al.* (2015) 'Landslide resilience in Equatorial Africa: Moving beyond problem identification!', *BELGEO*. doi: 10.4000/belgeo.15944.
- Kim, J. *et al.* (2004) 'Influence of rainfall-induced wetting on the stability of slopes in weathered soils', *Engineering Geology*, 75(3–4), pp. 251–262. doi: 10.1016/j.enggeo.2004.06.017.
- Kim, J. (2011) 'Improvement of geotechnical site investigations via statistical analyses and

simulation', *Chemistry*, Available at: <http://onlinelibrary.wiley.com/doi/10.1002/cbdv.200490137/abstract%5Cnhttp://smartech.gatech.edu/handle/1853/41218>.

Kim, J., Jeong, S. and Regueiro, R. A. (2012) 'Instability of partially saturated soil slopes due to alteration of rainfall pattern', *Engineering Geology*. Elsevier B.V., 147–148, pp. 28–36. doi: 10.1016/j.enggeo.2012.07.005.

Kim, J. M. and Sitar, N. (2013) 'Reliability approach to slope stability analysis with spatially correlated soil properties', *Soils and Foundations*. Elsevier, 53(1), pp. 1–10. doi: 10.1016/j.sandf.2012.12.001.

Krzykacz-Hausmann, B. (2006) 'An approximate sensitivity analysis of results from complex computer models in the presence of epistemic and aleatory uncertainties', *Reliability Engineering and System Safety*. doi: 10.1016/j.res.2005.11.019.

Kulhawy, F. H., Phoon, K.-K. and Prakoso, W. A. (2000) 'Uncertainty in Basic Properties of Geomaterials', *GeoEng2000 Conference*. doi: 10.1210/jc.82.5.1409.

Lacasse, S. and Nadim, F. (1996) 'Uncertainties in characterising soil properties', *Publikasjon - Norges Geotekniske Institutt*. doi: 10.1016/S1076-6332(05)80514-8.

Lari, S., Frattini, P. and Crosta, G. B. (2014) 'A probabilistic approach for landslide hazard analysis', *Engineering Geology*. Elsevier B.V., 182(PA), pp. 3–14. doi: 10.1016/j.enggeo.2014.07.015.

Lewis-Beck, M. (1980) 'Applied Regression: An Introduction', *SAGE*. doi: 10.1037/020564.

Li, D. *et al.* (2011) 'Stochastic response surface method for reliability analysis of rock slopes involving correlated non-normal variables', *Computers and Geotechnics*. Elsevier Ltd, 38(1), pp. 58–68. doi: 10.1016/j.compgeo.2010.10.006.

Li, L. *et al.* (2013) 'Risk de-aggregation and system reliability analysis of slope stability using representative slip surfaces', *Computers and Geotechnics*. Elsevier Ltd, 53, pp. 95–105. doi: 10.1016/j.compgeo.2013.05.004.

Lilliefors, H. W. (1967) 'On the Kolmogorov-Smirnov-Test for normality with mean and variance unknown', *Journal of the American Statistical Association*. doi: 10.1080/01621459.1967.10482916.

Loh, W. Y. (2002) 'Regression trees with unbiased variable selection and interaction detection', *Statistica Sinica*. doi: 10.5351/KJAS.2004.17.3.459.

Lollino, P., Giordan, D. and Allasia, P. (2014) 'The Montaguto earthflow: A back-analysis of the process of landslide propagation', *Engineering Geology*. Elsevier B.V., 170, pp. 66–79. doi: 10.1016/j.enggeo.2013.12.011.

Lombardi, M., Cardarilli, M. and Raspa, G. (2017) 'Spatial variability analysis of soil

strength to slope stability assessment', *Geomechanics and Engineering*, 12(3). doi: 10.12989/gae.2017.12.3.483.

Loots, C., Planque, B. and Koubbi, P. (2010) 'Spawning distribution of North Sea plaice and whiting from 1980 to 2007', *Journal of Oceanography, Research and Data*, 3, pp. 77–95.

Lopes, R. H. C. (2011) 'Kolmogorov-Smirnov Test', in *International Encyclopedia of Statistical Science*. doi: 10.1007/978-3-642-04898-2_326.

Low, B. K. (2003) 'Practical Probabilistic Slope Stability Analysis', *39th U.S. Rock Mechanics Symposium*, 2, pp. 2777–2784. Available at: http://www3.ntu.edu.sg/home/cbklow/documents/Conference/bkLow_ProbabilisticSlope.pdf.

Lu, H., Shen, G. and Zhu, Z. (2017) 'An approach for reliability-based sensitivity analysis based on saddlepoint approximation', *Proceedings of the Institution of Mechanical Engineers, Part O: Journal of Risk and Reliability*, 231(1), pp. 3–10. doi: 10.1177/1748006X16660489.

Lunne, T., Robertson, P. K. and Powell, J. J. M. (1997) 'Cone Penetration Testing in Geotechnical Practice', *Blackie Academic & Professional*. doi: 10.1007/s11204-010-9072-x.

Mac, H. (2014) 'A posteriori error estimation for stochastic static problems To cite this version : Science Arts & Métiers (SAM)'.

Mancini, F., Ceppi, C. and Ritrovato, G. (2010) 'GIS and statistical analysis for landslide susceptibility mapping in the Daunia area, Italy', *Natural Hazards and Earth System Science*, 10(9), pp. 1851–1864. doi: 10.5194/nhess-10-1851-2010.

Manoj, N. R. (2016) 'First-order Reliability Method: Concepts and Application', pp. 4–12.

Martin-Breen, P. and Anderies, J. M. (2011) 'Background Paper - Resilience: A Literature Review', *The Bellagio Initiative The Future of Philanthropy and Development in the Pursuit of Human Wellbeing*, (November), p. 67. doi: 02/03/2017.

Martino, S., Moscatelli, M. and Scarascia Mugnozza, G. (2004) 'Quaternary mass movements controlled by a structurally complex setting in the central Apennines (Italy)', *Engineering Geology*. doi: 10.1016/j.enggeo.2003.06.005.

Martino, S. and Scarascia Mugnozza, G. (2005) 'The role of the seismic trigger in the Calitri landslide (Italy): Historical reconstruction and dynamic analysis', *Soil Dynamics and Earthquake Engineering*. doi: 10.1016/j.soildyn.2005.04.005.

Marx, J. D. and Cornwell, J. B. (2001) 'What is a QRA and what can it tell you?', *2001 Annual Symposium Beyond Regulatory Compliance, Making Safety Second Nature*.

Massey, F. J. (1951) 'The Kolmogorov-Smirnov Test for Goodness of Fit', *Journal of the American Statistical Association*. doi: 10.1080/01621459.1951.10500769.

- Mater, A. *et al.* (2010) 'Valutazione delle condizioni di stabilit  dell'abitato di succiso (provincia di reggio emilia)'.
- Matheron, G. (1963) 'Principles of geostatistics', *Economic Geology*. doi: 10.2113/gsecongeo.58.8.1246.
- Matheron, G. (1973) 'INTRINSIC RANDOM FUNCTIONS AND THEIR APPLICATIONS.', *Advances in Applied Probability*. doi: 10.1017/S0001867800039379.
- Meshalkina, Y. L. (2007) 'A brief review of geostatistical methods applied in modern soil science', *Moscow University Soil Science Bulletin*, 62(2), pp. 93–95. doi: 10.3103/S014768740702007X.
- Metya, S. (2013) 'Proceedings of the International Symposium on Engineering under Uncertainty: Safety Assessment and Management (ISEUSAM - 2012)', (June). doi: 10.1007/978-81-322-0757-3.
- Meusburger, K. *et al.* (2012) 'Spatial and temporal variability of rainfall erosivity factor for Switzerland', *Hydrology and Earth System Sciences*. doi: 10.5194/hess-16-167-2012.
- Meyerhof, G. G. (1994) 'Evolution of safety factors and geotechnical limit state design', *Texas USA*.
- Muller, R. (2013) 'Probabilistic stability analysis of wind turbine foundation on clay in cyclic loading'.
- Murty, S. D. (2005) 'Probabilistic Site Characterization and Reliability Analysis of Shallow Foundations and Slopes', (December), p. 291. Available at: http://doktori.bibl.u-szeged.hu/1751/3/Girma_Waro_-_Abstract_of_PhD_Thesis_English_03-28.pdf.
- Mustaffa, Z., Gelder, P. Van and Vrijling, H. (2009a) 'A Discussion of Deterministic vs . Probabilistic Method in Assessing Marine Pipeline Corrosions', *The International Society of Offshore and Polar Engineering Conference*, 1(July), pp. 653–658.
- Mustaffa, Z., Gelder, P. Van and Vrijling, H. (2009b) 'A Discussion of Deterministic vs . Probabilistic Method in Assessing Marine Pipeline Corrosions', *The International Society of Offshore and Polar Engineering Conference*. doi: 10.1017/CBO9781107415324.004.
- Myers, D. E. (2005) *Reliability and Statistics in Geotechnical Engineering*, *Technometrics*. doi: 10.1198/tech.2005.s838.
- Nadim, F. *et al.* (2006) 'Global landslide and avalanche hotspots', *Landslides*. doi: 10.1007/s10346-006-0036-1.
- Nadim, F. (2016) 'Accounting for Uncertainty and Variability in Geotechnical Characterization of Offshore Sites', in *Geotechnical Safety and Risk V*. doi: 10.3233/978-1-61499-580-7-23.

Nadim, F., Einstein, H. and Roberds, W. (2005) 'Probabilistic stability analysis for individual slopes in soil and rock', in *Landslide Risk Management*.

Nakileza, B. R. *et al.* (2017) 'Enhancing resilience to landslide disaster risks through rehabilitation of slide scars by local communities in Mt Elgon, Uganda', *Jàmá: Journal of Disaster Risk Studies*. doi: 10.4102/jamba.v9i1.390.

Olea, R. a. (2009) *A Practical Primer on Geostatistics, USGS Open File Report 2009-1103*. doi: <https://doi.org/10.3133/ofr20091103/>.

Oliver, M. A. and Webster, R. (2014) 'A tutorial guide to geostatistics: Computing and modelling variograms and kriging', *Catena*. doi: 10.1016/j.catena.2013.09.006.

Papaioannou, I., Breitung, K. and Straub, D. (2013) 'Reliability sensitivity analysis with Monte Carlo methods', pp. 5335–5342.

Papaioannou, I. and Straub, D. (2012) 'Reliability updating in geotechnical engineering including spatial variability of soil', *Computers and Geotechnics*. doi: 10.1016/j.compgeo.2011.12.004.

Parise, M. (2003) 'Observation of surface features on an active landslide, and implications for understanding its history of movement', *Natural Hazards and Earth System Science*. doi: 10.5194/nhess-3-569-2003.

Park, H. J., Lee, J. H. and Woo, I. (2013) 'Assessment of rainfall-induced shallow landslide susceptibility using a GIS-based probabilistic approach', *Engineering Geology*. Elsevier B.V., 161, pp. 1–15. doi: 10.1016/j.enggeo.2013.04.011.

Pebesma, E. and Graeler, B. (2017) 'Spatial and Spatio-Temporal Geostatistical Modelling, Prediction and Simulation', pp. 1–82. Available at: <https://github.com/edzer/gstat/>.

PESCATORE T; RUSSO B; SENATORE M R; CIAMPO G; ESPOSITO P; PINTO F; STAITI D; (1996) 'La successione messiniana della valle del T. Cervaro (Appennino Dauno, Italia meridionale)', *Bollettino della Società Geologica Italiana*, fascicolo:, pp. 369–378.

Phoon, K.-K. and Kulhawy, F. H. (1999) 'Evaluation of geotechnical property variability', *Canadian Geotechnical Journal*. doi: 10.1139/t99-039.

Phoon, K.-K. and Kulhawy, F. H. (2001) 'Characterization of geotechnical variability & Evaluation of geotechnical property variability: Reply', *Canadian Geotechnical Journal*. doi: 10.1139/cgj-38-1-214.

Phoon, K. (1995) 'RELIABILITY-BASED DESIGN OF FOUNDATIONS FOR TRANSMISSION LINE STRUCTURES Presented to the Faculty of the Graduate School of Cornell University in Partial Fulfillment of the Requirements for the Degree of Doctor of Philosophy by Kok-Kwang Phoon', 105000(May).

Phoon, K. *et al.* (2006a) 'Soil variability analysis for geotechnical practice', *Characterisation and Engineering Properties of Natural Soils*, (December). doi: 10.1201/NOE0415426916.ch3.

Phoon, K. *et al.* (2006b) 'Soil variability analysis for geotechnical practice', in *Characterisation and Engineering Properties of Natural Soils*. doi: 10.1201/NOE0415426916.ch3.

Phoon, K. *et al.* (2006c) 'Soil variability analysis for geotechnical practice', *Characterisation and Engineering Properties of Natural Soils*, (April 2016). doi: 10.1201/NOE0415426916.ch3.

Phoon, K. K. (1999) 'Characterization of geotechnical variability', *Canadian Geotechnical Journal*.

Phoon, K. K. and Kulhawy, F. H. (1996) 'On quantifying inherent soil variability', *Geotechnical Special Publication*.

Pinheiro, H. S. K. *et al.* (2018) 'Prediction of topsoil texture through regression trees and multiple linear regressions', *Revista Brasileira de Ciencia do Solo*, 42, pp. 1–21. doi: 10.1590/18069657rbc20170167.

Pinto, F. *et al.* (2016) 'Structural and lithostratigraphic controls of earth-flow evolution, Montaguto earth flow, Southern Italy', *Journal of the Geological Society*, 173(4), pp. 649–665. doi: 10.1144/jgs2015-081.

Popescu, M. (2001) 'A suggested method for reporting landslide remedial measures', *Bulletin of Engineering Geology and the Environment*. doi: 10.1007/s100640000084.

Popescu, M. E. and Sasahara, K. (2005) 'Engineering Measures for Landslide Disaster Mitigation', *Landslides – Disaster Risk Reduction*, pp. 609–631. doi: 10.1007/978-3-540-69970-5_32.

Popescu, R., Prevost, J. H. and Deodatis, G. (1998) 'Spatial variability of soil properties: Two case studies', *Geotechnical Special Publication*, (75 I), pp. 568–579. Available at: <http://www.scopus.com/inward/record.url?eid=2-s2.0-0031625111&partnerID=40&md5=0be0357d3cb4f9c42efa5ec130eddb93>.

Del Prete, M. and Guadagno, F. M. (1988) 'Observations on landslides in typical flysch sequences of southern Apennines (Italy)', *Landslides. Proc. 5th symposium, Lausanne, 1988. Vol. 1*.

Proske, D. (2008) *Catalogue of risks: Natural, technical, social and health risks, Catalogue of Risks: Natural, Technical, Social and Health Risks*. doi: 10.1007/978-3-540-79555-1.

Quanta Technology (2009) 'Cost-Benefit Analysis of the Deployment of Utility Infrastructure Upgrades and Storm Hardening Programs', *Satellite Communications*, 3021, pp. 1–108.

- Rengers, N. (1973) 'Landslides and their control', *Engineering Geology*. doi: 10.1016/0013-7952(73)90037-9.
- Resume, P. and Robertson, P. K. (2006) 'PETER K . ROBERTSON Technical Director , Gregg Drilling & Testing Inc . Professor Emeritus , University of Alberta SUMMARY INFORMATION', pp. 1–27.
- Rethati, L. (1989) *Probabilistic solutions in geotechnics, Canadian Geotechnical Journal*. doi: 10.1139/t89-047.
- Revellino, P. *et al.* (2010) 'Structurally controlled earth flows of the Benevento province (Southern Italy)', *Bulletin of Engineering Geology and the Environment*. doi: 10.1007/s10064-010-0288-9.
- Ricci, V. and Ricci, V. (2006) *Principali tecniche di regressione con R, Development*.
- Riesch, H. (2013) 'Essentials of Risk Theory', (2009), pp. 29–57. doi: 10.1007/978-94-007-5455-3.
- Robertson, P. K. (2009) 'Interpretation of cone penetration tests — a unified approach', *Canadian Geotechnical Journal*, 46(11), pp. 1337–1355. doi: 10.1139/T09-065.
- Robertson, P. K. (2010) 'Soil behaviour type from the CPT: an update', *2nd International Symposium on Cone Penetration Testing*, (May), p. 8 p.
- Robertson, P. K. (2016) 'Cone penetration test (CPT)-based soil behaviour type (SBT) classification system — an update', *Canadian Geotechnical Journal*, 53(12), pp. 1910–1927. doi: 10.1139/cgj-2016-0044.
- Robertson, P. K. and Campanella, R. G. (1983) 'Interpretation of cone penetration tests. Part I: Sand', *Canadian Geotechnical Journal*, 20(4), pp. 718–733. doi: 10.1139/t83-078.
- Rosenblueth, E. (1975) 'Point estimates for probability moments', *Proceedings of the National Academy of Sciences*. doi: 10.1073/pnas.72.10.3812.
- Rossi, M. *et al.* (2010) 'Optimal landslide susceptibility zonation based on multiple forecasts', *Geomorphology*, 114(3), pp. 129–142. doi: 10.1016/j.geomorph.2009.06.020.
- Rouaiguia, A. and Dahim, M. A. (2013) 'Numerical Modeling of Slope Stability Analysis', *International Journal of Engineering Science and Innovative Technology (IJESIT)*, 2(3), pp. 533–542.
- Sarma, C. P., Krishna, A. M. and Dey, A. (2015) 'Probabilistic slope stability analysis considering spatial variability of soil properties: Influence of correlation length', (August), pp. 1125–1130.
- Schulz, W. H. *et al.* (2009) 'Relations between hydrology and velocity of a continuously

moving landslide-evidence of pore-pressure feedback regulating landslide motion?', *Landslides*. doi: 10.1007/s10346-009-0157-4.

Scolobig, A., Thompson, M. and Linnerooth-Bayer, J. A. (2016) 'Compromise not consensus: designing a participatory process for landslide risk mitigation', *Natural Hazards*. doi: 10.1007/s11069-015-2078-y.

Sidler, R., Prof, S. and Holliger, K. (2003) 'Kriging and Conditional Geostatistical Simulation Based on Scale-Invariant Covariance Models by', *Unpublished Diploma Thesis. Institute of Geophysics, Department of Earth Science, Swiss Federal institute of Technology Zurich*, p. 79. Available at: http://citeseerx.ist.psu.edu/viewdoc/download?doi=10.1.1.126.3499&rep=rep1&rep_type=pdf.

Sigua, G. and Hudnall, W. (2008) 'Kriging analysis of soil properties', *Journal of Soils and Sediments*. doi: 10.1007/s11368-008-0003-7.

Skempton, A. W. and Delory, F. A. (1957) 'Stability of Natural Slopes in London Clay', in *SELECTED PAPERS ON SOIL MECHANICS*. doi: 10.1680/sposm.02050.0011.

van Slyke, R. M. (1963) 'Monte Carlo methods and the PERT problem', *Operations Research*. doi: 10.1287/opre.11.5.839.

Sofianos, A. I., Nomikos, P. P. and Papantonopoulos, G. (2014) 'Distribution of the factor of safety, in geotechnical engineering, for independent piecewise linear capacity and demand density functions', *Computers and Geotechnics*. Elsevier Ltd, 55, pp. 440–447. doi: 10.1016/j.compgeo.2013.09.024.

Song, S. *et al.* (2014) 'The uncertainty importance measures of the structural system in view of mixed uncertain variables', *Fuzzy Sets and Systems*. doi: 10.1016/j.fss.2013.06.002.

Svensson, A. (2014) 'Estimation of hydraulic conductivity from grain size analyses', p. 96.

Tedesco, N. and Sociale, S. (2016) 'Regressione Logistica: un Modello per Variabili Risposta Categoricali', p. 54.

Terra, S. Della *et al.* (2013) 'Integration between radar interferometric monitoring and hydrological modelling for the study of landslide evolution'.

Tsompanakis, Y. *et al.* (2010) 'Probabilistic seismic slope stability assessment of geotechnical structures', *Structure and Infrastructure Engineering*, 6(1–2), pp. 179–191. doi: 10.1080/15732470802664001.

UNISDR (2017a) 'Landslide Hazard and Risk Assessment, In: Words into Action Guidelines: National Disaster Risk Assessment. Hazard Specific Risk Assessment'.

UNISDR (2017b) 'National Disaster Risk Assessment-Part III Hazard Specific Risk Assessment'. Available at: https://www.unisdr.org/files/52828_nationaldisasterriskassessmenthazar%5B1%5D.pdf.

USACE (2006) *ETL 1110-2-561: Reliability Analysis and Assessment for Seepage and Slope Stability Failures Modes for Embankment Dams*, Online.

Uzielli, M. (2008) 'Statistical Analysis of Geotechnical Data.', *Geotechnical and Geophysical Site - Characterization Proceedings of the 3th International Conference on Site Characterization, ISC-3*. doi: 10.1201/9780203883198.ch10.

Valley, B., Kaiser, P. K. and Duff, D. (2010) 'Consideration of uncertainty in modelling the behaviour of underground excavations', *Proceedings Fifth International Seminar on Deep and High Stress Mining (Deep Mining 2010)*, M. Van Sint Jan and Y. Potvin (eds), (November 2015), pp. 6–8.

Vanmarcke, E. H. (1980) 'Probabilistic stability analysis of earth slopes', *Engineering Geology*. doi: 10.1016/0013-7952(80)90005-8.

Vardanega, P. J. and Bolton, M. D. (2015) 'Design of Geostructural Systems', *Journal of Risk and Uncertain in Engineering Systems*. doi: 10.1061/AJRUA6.0000849.

Ventura, G. *et al.* (2011) 'Tracking and evolution of complex active landslides by multi-temporal airborne LiDAR data: The Montaguto landslide (Southern Italy)', *Remote Sensing of Environment*. doi: 10.1016/j.rse.2011.07.007.

Viscarra Rossel, R. A. *et al.* (2010) 'Mapping the information content of Australian visible-near infrared soil spectra.', *Proceedings of the 19th World Congress of Soil Science: Soil solutions for a changing world, Brisbane, Australia, 1-6 August 2010. Working Group 1.5 Soil sense: rapid soil measurements*. doi: 10.1109/tns.2009.2019960.

Wackernagel, H. (2003) *Multivariate Geostatistics: An introduction with applications, Modern Approaches in Solid Earth Sciences*. doi: 10.1111/ntwe.12079.

Wang, L., Hwang, J. H., Luo, Z., *et al.* (2013) 'Probabilistic back analysis of slope failure - A case study in Taiwan', *Computers and Geotechnics*. Elsevier Ltd, 51(3), pp. 12–23. doi: 10.1016/j.compgeo.2013.01.008.

Wang, L., Hwang, J. H., Juang, C. H., *et al.* (2013) 'Reliability-based design of rock slopes - A new perspective on design robustness', *Engineering Geology*. Elsevier B.V., 154, pp. 56–63. doi: 10.1016/j.enggeo.2012.12.004.

Wang, Z. *et al.* (2012) 'An approach to system reliability analysis with fuzzy random variables', *Mechanism and Machine Theory*. doi: 10.1016/j.mechmachtheory.2012.01.007.

Whitney, M. (1911) 'The use of soils east of the Great Plains region', *United States. Dept. of Agriculture; United States. Bureau of Soils; United States. Government Printing Office*.

- William D. Berry & Stanley Feldman (1985) 'Multiple Regression in Practice'. doi: <http://dx.doi.org/10.4135/9781412985208>.
- Willmott, C. J. and Matsuura, K. (2005) 'Advantages of the mean absolute error (MAE) over the root mean square error (RMSE) in assessing average model performance', *Climate Research*. doi: 10.3354/cr030079.
- Wu, T. *et al.* (1997) 'Probabilistic methods in geotechnical engineering', *ASCE GeoLogan*, p. 95. doi: 10.17226/9476.
- Wu, X. Z. (2013) 'Probabilistic slope stability analysis by a copula-based sampling method', *Computational Geosciences*, 17(5), pp. 739–755. doi: 10.1007/s10596-013-9353-3.
- Wu, Z. Y. *et al.* (2013) 'A reliability-based approach to evaluating the stability of high rockfill dams using a nonlinear shear strength criterion', *Computers and Geotechnics*, 51, pp. 42–49. doi: 10.1016/j.compgeo.2013.01.005.
- Xiao, N. C. *et al.* (2011) 'Reliability sensitivity analysis for structural systems in interval probability form', *Structural and Multidisciplinary Optimization*. doi: 10.1007/s00158-011-0652-9.
- Zaman, K. *et al.* (2011) 'A probabilistic approach for representation of interval uncertainty', in *Reliability Engineering and System Safety*. doi: 10.1016/j.res.2010.07.012.
- Zaugg, E. C. *et al.* (2016) 'Differential interferometric SAR at multiple frequencies over the Slumgullion Earthflow', in *2016 IEEE Radar Conference, RadarConf 2016*. doi: 10.1109/RADAR.2016.7485227.
- Zêzere, J. L. *et al.* (2004) 'Integration of spatial and temporal data for the definition of different landslide hazard scenarios in the area north of Lisbon (Portugal)', *Natural Hazards and Earth System Science*, 4(1), pp. 133–146. doi: 10.5194/nhess-4-133-2004.
- Zhang, J. *et al.* (2013) 'Application of the Kriging-Based Response Surface Method to the System Reliability of Soil Slopes', *Journal of Geotechnical and Geoenvironmental Engineering*, 139(4), pp. 651–655. doi: 10.1061/(ASCE)GT.1943-5606.0000801.
- Zhang, J. *et al.* (2014) 'Probabilistic prediction of rainfall-induced slope failure using a mechanics-based model', *Engineering Geology*. Elsevier B.V., 168, pp. 129–140. doi: 10.1016/j.enggeo.2013.11.005.
- Zhang, P. (2010) 'Probabilistic methods used in environmental risk evaluation for groundwater protection', (March).

Appendix 1

Kolmogorov - Smirnov test

In statistics, is a non-parametric test (Massey, 1951) of the equality of continuous, one-dimensional probability distributions that may be used to compare a sample with a reference probability distribution (one-sample K-S test), or to compare two samples (two-sample K-S test). The Kolmogorov-Smirnov test may be used as a goodness of fit test (Justel, Peña and Zamar, 1997).

The Kolmogorov-Smirnov statistic quantifies a distance between the empirical distribution function of the sample and the cumulative distribution function of the reference distribution (Fasano and Franceschini, 1987), or between the empirical distribution functions of two samples.

The null distribution of this statistic is calculated under the null hypothesis (Lopes, 2011) that the samples are drawn from the same distribution (in the two-sample case) or that the sample is drawn from the reference distribution (in the one-sample case).

In each case, the distributions considered under the null hypothesis are continuous distributions but are otherwise unrestricted.

The two-sample K-S test is one of the most useful and general non-parametric methods for comparing two samples, as it is sensitive to differences in both location and shape of the empirical cumulative distribution functions of the two samples (Lilliefors, 1967).

Following the one-sample K-S routine used for two soil parameters:

```
> fit1<-fitdistr(s1$V1,"normal")
> ks.test(s1$V1,"pnorm",fit1$estimate)

      One-sample Kolmogorov-Smirnov test

data:  s1$V1
D = 0.7781, p-value > 1.23

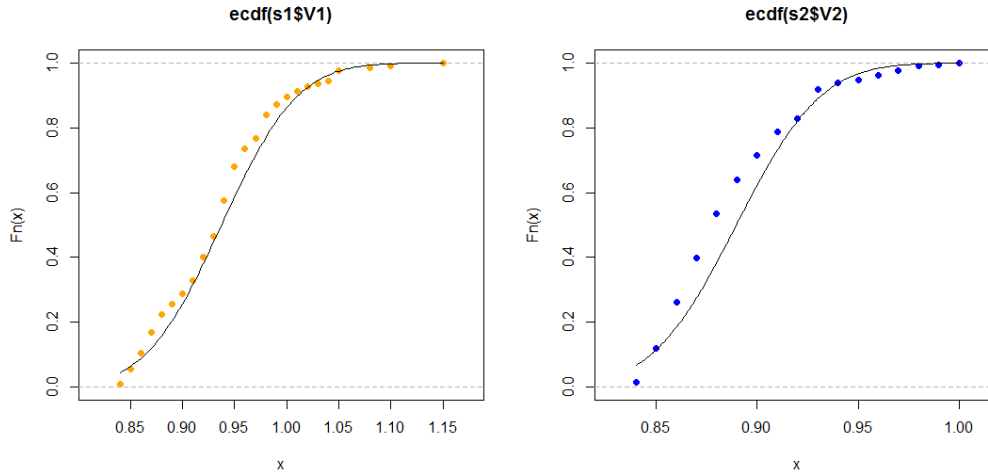
> fit2<-fitdistr(s2$V2,"normal")

> ks.test(s2$V2,"pnorm",fit2$estimate)
```

One-sample Kolmogorov-Smirnov test

```
data: s2$V2  
D = 0.7855, p-value > 3.34
```

Since both $p\text{-value} > 0.05$, we accept the null hypothesis: the vectors are from Gaussian distributions.



Following the two-sample K-S routine used for the two soil layers:

```
> ks.test(s1$V1, s2$V2)
```

Two-sample Kolmogorov-Smirnov test

```
data: s1$V1 and s2$V2  
D = 0.4587, p-value = 1.89
```

Since $p\text{-value} > 0.05$, we accept the null hypothesis: the vectors are from the same distribution (Gaussian distribution).

Appendix 2

Regression model with interactions

Ordinary Least Squares (OLS) or linear least squares (Ricci, 2006) is a method for estimating the unknown parameters in a linear regression model. The goal consists of minimizing the differences between the observed responses in some arbitrary dataset and the responses predicted by the linear approximation (Lewis-Beck, 1980) of the data (visually this is seen as the sum of the vertical distances between each data point in the set and the corresponding point on the regression line - the smaller the differences, the better the model fits the data). The resulting estimator may be expressed by a simple formula, especially in the case of a single regressor on the right-hand side (Kelley and Bolin, 2013).

The OLS estimator is optimal in the class of linear unbiased estimators when the errors are uncorrelated (Loh, 2002). Under these conditions, the method of OLS provides minimum variance mean-unbiased estimation when the errors have finite variances. The primary assumption of OLS is that there are zero or negligible errors in the independent variable, since this method only attempts to minimise the mean squared error in the dependent variable (Loh, 2002).

It is common to assess the goodness-of-fit of the OLS regression by comparing how much the initial variation in the sample may be reduced by regressing onto X (William D. Berry & Stanley Feldman, 1985). The coefficient of determination R^2 is defined as a ratio of "explained" variance to the "total" variance of the dependent variable.

Following the command to perform the OLS regression (*lm* command) to obtain soil indices:

```
> soil.index <-lm(formula = prof ~ (A + L + S + G)^2 + (A + L + S + G)^3 + (A + L + S + G)^4 + (A + L + S + G), data = soil)
```

```
> summary(soil.index)
```

Call:

```
lm(formula = prof ~ (A + L + S + G)^2 + (A + L + S + G)^3 + (A + L + S + G)^4 + (A + L + S + G), data = soil)
```

```
Residuals:
      Min       1Q   Median       3Q      Max
-15.9094  -4.5094  -0.1867   4.3133  20.7523
```

Coefficients:

	Estimate	Std. Error	t value	Pr(> t)	
(Intercept)	9.8303	5.0854	1.933	0.053352	**
A-1.174	38.2221	10.6134	3.601	0.000323	***
A-0.628	12.0649	5.4344	2.220	0.026507	*
A1.556	30.1995	11.7210	2.577	0.010040	**
L-1.603	-33.3298	8.3312	-4.001	6.51e-05	***
L2.225	-22.0024	5.8865	-3.738	0.000190	***
S0.838	-15.7927	4.0439	-3.905	9.67e-05	***
G-0.102	-33.6264	6.5731	-5.116	3.37e-07	***
G1.114	-25.0300	10.4354	-2.399	0.016536	*
A-1.174:L-0.646	-0.4040	4.4419	-0.091	0.927545	***
A-0.628:L-0.646	32.8958	7.2888	4.513	6.70e-06	***
L-0.646:S0.838	16.4173	2.6242	6.256	4.67e-10	***
L1.268:S0.838	13.7643	2.6969	5.104	3.59e-07	***
A-0.628:L1.268:G-0.102	NA	NA	NA	NA	
...					
...					

Signif. codes: 0 '***' 0.001 '**' 0.01 '*' 0.05 '.' 0.1 ' ' 1

Residual standard error: 7.009 on 2375 degrees of freedom
 Multiple R-squared: 0.8326, Adjusted R-squared: 0.825
 F-statistic: 43.83 on 27 and 2375 DF, p-value: < 2.2e-16

If the p-value observed is less than the theoretical p-value (usually 0.05) so the used model explains a significant proportion of the variance of the phenomenon.

Appendix 3

Statistics and probability distribution of soil properties

The results of second-moment modelling of soil properties are generally provided in tabular form. The compilation of descriptive statistics is not an entirely mechanical procedure (Phoon *et al.*, 2006a).

Subsequently, the results of a literature review of second-moment statistics are provided below.

Phoon and Kulhawy (1999) reported the results of an extensive literature review of coefficients of variations of inherent variability for some laboratory-measured geotechnical properties. Unfortunately, not all the data may be classified properly, because the importance of reporting test types with the strength properties is only gradually being recognised.

Table 45 summarizes the soil type, the number of data groups and tests per group, and the mean and COV of the soil property (Phoon and Kulhawy, 1996). A description of soil type is useful because the site-specific COVs tabulated may be extrapolated to other locations, provided the soil deposits are of similar geologic formation and environmental history. The number of tests is a useful indicator of the accuracy of the mean and COV estimates (Phoon, 1999). The number of tests per group typically is large, which implies that the errors in the statistical estimates are minimal. The presentation of the mean in conjunction with the COV also is important to ensure that the COV is not misinterpreted as being applicable to all possible mean values (Kulhawy, Phoon and Prakoso, 2000).

SUMMARY OF INHERENT VARIABILITY OF STRENGTH PROPERTIES

Property ^a	Soil Type	No. Data Groups	No. Tests/Group		Property Value (units ^b)		Property COV (%)	
			Range	Mean	Range	Mean	Range	Mean
s_u (UC)	Fine-Grained Soils	38	2 - 38	101	6 - 412	100.2	6 - 56	33
s_u (UU)	Clay, Silt	13	14 - 82	33	15 - 363	275.9	11 - 49	22
s_u (CIUC)	Clay	10	12 - 86	47	130 - 713	405.4	18 - 42	32
s_u ^c	Clay	42	24 - 124	48	8 - 638	112.3	6 - 80	32
$\bar{\phi}$ ^c	Sand	7	29 - 136	62	35 - 41°	37.6°	5 - 11	9
	Clay, Silt	12	5 - 51	16	9 - 33°	15.3°	10 - 50	21
	-	9	-	-	17 - 41°	33.3°	4 - 12	9
$\tan \bar{\phi}$ (TC)	Clay, Silt	4	-	-	0.24 - 0.69	0.509	6 - 46	20
$\tan \bar{\phi}$ (DS)	Clay, Silt	3	-	-	-	0.615	6 - 46	23
$\tan \bar{\phi}$ ^c	Sand	13	6 - 111	45	0.65 - 0.92	0.744	5 - 14	9

a - s_u = undrained shear strength; $\bar{\phi}$ = effective stress friction angle; TC = triaxial compression test; UC = unconfined compression test; UU = unconsolidated-undrained triaxial compression test; CIUC = consolidated isotropic undrained triaxial compression test; DS = direct shear test

b - units of s_u = kN/m²

c - laboratory test type not reported

1 kN/m² = 0.0104 tsf

Table 45 - Strength properties (mean and COV value) per soil type
(source: Phoon and Kulhawy, 1996)

The inherent variability of some common field measurements is summarized in the following Table 46. There are important sub-divisions within each field test. The soil type, number of data groups and tests per group of the field measurement are also summarized, which reports also typical ranges of mean values and COVs of laboratory and in-situ testing parameters (Phoon and Kulhawy, 1999).

Details and references to original sources may be found in (Phoon, 1995; Phoon and Kulhawy, 1996; Lacasse and Nadim, 1996; Phoon, 1999; Kulhawy, Phoon and Prakoso, 2000).

Table 7. Approximate guidelines for second-moment statistics of soil parameters

Test type	Property	Soil type	Mean	COV (%)
Lab strength	s_u (UC)	Clay	10-400 kN/m ²	20-55
	s_u (UU)	Clay	10-350 kN/m ²	10-30
	s_u (CIUC)	Clay	150-700 kN/m ²	20-40
	ϕ'	Clay & sand	20-40°	5-15
CPT	q_T	Clay	0.5-2.5 MN/m ²	< 20
	q_c	Clay	0.5-2.0 MN/m ²	20-40
		Sand	0.5-30.0 MN/m ²	20-60
VST	s_u (VST)	Clay	5-400 kN/m ²	10-40
SPT	N	Clay & sand	10-70 blows/ft	25-50
DMT	A reading	Clay	100-450 kN/m ²	10-35
		Sand	60-1300 kN/m ²	20-50
	B reading	Clay	500-880 kN/m ²	10-35
		Sand	350-2400 kN/m ²	20-50
	I_D	Sand	1-8	20-60
	K_D	Sand	2-30	20-60
	E_D	Sand	10-50 MN/m ²	15-65
PMT	p_L	Clay	400-2800 kN/m ²	10-35
		Sand	1600-3500 kN/m ²	20-50
	E_{PMT}	Sand	5-15 MN/m ²	15-65
Lab index	w_n	Clay & silt	13-100 %	8-30
	w_L	Clay & silt	30-90 %	6-30
	w_p	Clay & silt	15-25 %	6-30
	I_p	Clay & silt	10-40 %	**
	I_L	Clay & silt	10 %	**
	γ, γ_d	Clay & silt	13-20 kN/m ³	< 10
	D_R	Sand	30-70 %	10-40*** 50-70****
Lab. consolidation	C_c	Not reported	-	10-37
	p'_c	Not reported	-	10-35
	OCR	Not reported	-	10-35
Not reported	k	Saturated clay	-	68-90
		Partly saturated clay	-	130-240
Not reported	c_v	Not reported	-	33-68
Not reported	n	All soil types	-	7-30
	e	All soil types	-	7-30
	e_0	All soil types	-	7-30

* s_u = undrained shear strength; UC = unconfined compression test; UU = unconsolidated-undrained triaxial compression test; CIUC = consolidated isotropic undrained triaxial compression test; ϕ' = effective stress friction angle; q_T = corrected cone tip resistance; q_c = cone tip resistance; VST = vane shear test; N = standard penetration test blow count; A and B readings, I_D , K_D and E_D = dilatometer A and B readings, material index, horizontal stress index and modulus; p_L and E_{PMT} = pressuremeter limit stress and modulus; w_n = natural water content; w_L = liquid limit; I_p = plasticity index; I_L = liquidity index; γ and γ_d = total and dry unit weights; D_R = relative density; C_c = compression index; p'_c = preconsolidation pressure; OCR = overconsolidation ratio; k = permeability coefficient (direction not specified); c_v = coefficient of vertical consolidation; n = porosity; e = void ratio; e_0 = initial void ratio

** COV = (3-12%) / mean

*** total variability for direct method of determination

**** total variability for indirect determination using SPT values

Table 46 - Strength properties (mean and COV value) per test type (source: Phoon *et al.*, 2006c)

Different probability distribution models have been selected, even for the same soil property, by different authors (Phoon *et al.*, 2006a). This suggests that distributions are site- and parameter-specific, and that there is no universally “best” distribution for soil properties. In-situ effects, which may result in a spatial trend, may also be relevant (Phoon *et al.*, 2006a).

Based on cone penetration data from artificial and natural deposits, Popescu, Prevost and Deodatis (1998) observed that the distribution of soil strength in shallow layers were prevalently positively skewed, while for deeper soils the corresponding distributions tended to follow more symmetric distributions. Corotis and Azzouz (1975) investigated whether a number of properties of three groups of soils might be described by the normal or lognormal distribution. Lacasse and Nadim (1996) reported the results of a review of probability distribution selection for some soil properties. It should be noted that best-fit probability distributions may also depend on soil type.

Table 14. Probability distributions for different soil properties (adapted from Lacasse & Nadim 1996)

Soil property	Soil type	Distribution
Cone resistance	Sand	LN
	Clay	N/LN
Undrained shear strength	Clay (triaxial tests)	LN
	Clay (index tests)	LN
	Clayey silt	N
Stress-normalised undrained shear strength	Clay	N/LN
Plastic limit	Clay	N
Submerged unit weight	All soils	N
Friction angle	Sand	N
Void ratio, Porosity	All soils	N
Overconsolidation ratio	Clay	N/LN

Table 47 - Probability distributions for various soil units (source: Phoon *et al.*, 2006c)

As a general observation, points corresponding to the same property for different soil units generally plot in different areas of the chart; this reflects the influence of soil type and in-situ state on data distribution. Hence, it is difficult to associate a specific probability distribution to a soil property *a priori* (Nadim, 2016).

List of Figures

Figure 1 - Slope failure mechanism (source: Wyoming State Geological Survey)	11
Figure 2 - Deterministic and Probabilistic distributions of Load and Strength	12
Figure 3 - Probability of Failure P(FS) (source: Johari and Javadi, 2012)	13
Figure 4 - Drainage system (left) and anchorage grid (right)	14
Figure 5 - Uncertainty diagram in soil property estimates (source: Phoon and Kulhawy, 1999) .	17
Figure 6 - Uncertainty diagram in geotechnical design process (source: Honjo and Otake, 2011)	18
Figure 7 - Variability of soil profile (source: Honjo and Otake, 2011)	25
Figure 8 - Description of Aleatory Function in S domain (source: Kasmaeeyazdi <i>et al.</i> , 2018)	26
Figure 9 - Schematization of S domain and x_i values (source: Famulari, 2013)	27
Figure 10 - Variogram parameters and function (source: Loots, Planque and Koubbi, 2010).....	28
Figure 11 - Theoretical variogram functions (source: gisgeography.com).....	28
Figure 12 - Anisotropy characteristics and discretization (source: spatial-analyst.net).....	29
Figure 13 - Spatial prediction between unsampled point (red) and measured values (black) (source: resources.esri.com)	31
Figure 14 - Three-dimensional joint density function $f(R,S)$	33
Figure 15 - Probability of exceedance (source: daad.wb.tu-harburg.de).....	34
Figure 16 - Earthflow landslide representation diagram (source: Keefer, D.K.; Johnson, 1983) ...	39
Figure 17 - Landslide body and run out after the reactivation in 2006	40
Figure 18 - Landslide toe covering the National Road SS90 after 2006 movement	41
Figure 19 - Landslide body and run out after the reactivation in 2010	41
Figure 20 - Landslide toe covering the road SS90 and railway after 2010 movement	42
Figure 21 - Geological Sheet No. 174 "Ariano Irpinia" (SGd'I, 1964):	43
Figure 22 - Main scarp of Montaguto earthflow (view from the top).....	44
Figure 23 - Geological longitudinal section of the slope in 2006. The Faeto Flysch (brown), the clayey marl unit of Villamaina formation (dark yellow) and the landslide mass (grey).	46
Figure 24 - Longitudinal profile showing the geometry of the basal slip surface of the Montaguto earth flow (source: Guerriero <i>et al.</i> , 2014).....	46
Figure 25 - Slip surface geometry along landslide body.....	47
Figure 26 - Geognostic and geotechnical surveys in 2006 (red and green)	48
Figure 27 - Maps of the Montaguto Earth flow in 2006 (left) and 2010 (right)	50
Figure 28 - Trench channel works.....	51
Figure 29 - Retaining gabions on the toe.....	52
Figure 30 - Aerial view of the landslide toe after reshaping (source: Google Earth)	53
Figure 31 - Survey area in 2006 at 1:5000 scale (left): CPT tests (in blue), geognostic surveys (in red). Carrots extracted during on-site tests up to 10 meters of depth (right)	56
Figure 32 - Survey area at 1:5000 scale (left): old surveys executed in 2006 (in blue), new geognostic surveys in 2010 (in green). Carrots extracted during on-site tests up to 10 meters of depth (right).....	58
Figure 33 - Differences in elevation by comparing 2006 and 2010 reactivations	60
Figure 34 - Sample used for laboratory tests (silt with clayey sand)	61
Figure 35 - A CPT profile: f_s (left) and q_c (right) with depth	62
Figure 36 - Soil texture triangle of soil classes (source: Whitney, 1911)	66
Figure 37 - Comparison of particle size scales (source: Whitney, 1911)	67
Figure 38 - Correlation among soil texture components in 2006:	74
Figure 39 - Correlation among soil texture components in 2010:	74

Figure 40 - Correlation among soil texture components in 2006:	75
Figure 41 - Correlation among soil texture components in 2010:	75
Figure 42 - Variability maps of spatial predictions (left) and variances (right) of I_{CSiSaG} at ground surface in 2006	89
Figure 43 - Variability maps of spatial predictions (left) and variances (right) of I_{CSiSaG} at middle surface in 2006	90
Figure 44 - Variability maps of spatial predictions (left) and variances (right) of I_{CSiSaG} at slip surface in 2006	90
Figure 45 - Variability maps of spatial predictions (left) and variances (right) of I_{CSiSaG} at ground surface in 2010	91
Figure 46 - Variability maps of spatial predictions (left) and variances (right) of I_{CSiSaG} at middle surface in 2010	92
Figure 47 - Variability maps of spatial predictions (left) and variances (right) of I_{CSiSaG} at slip surface in 2010	92
Figure 48 - Variability maps of spatial predictions (left) and variances (right) of I_{CoDS} at ground surface in 2006	93
Figure 49 - Variability maps of spatial predictions (left) and variances (right) of I_{CoDS} at middle surface in 2006	94
Figure 50 - Variability maps of spatial predictions (left) and variances (right) of I_{CoDS} at slip surface in 2006	94
Figure 51 - Variability maps of spatial predictions (left) and variances (right) of I_{CoDS} at ground surface in 2010	95
Figure 52 - Variability maps of spatial predictions (left) and variances (right) of I_{CoDS} at middle surface in 2010	96
Figure 53 - Variability maps of spatial predictions (left) and variances (right) of I_{CoDS} at slip surface in 2010	96
Figure 54 - Variability maps of spatial predictions (left) and variances (right) of I_{Fs} at ground surface in 2006	97
Figure 55 - Variability maps of spatial predictions (left) and variances (right) of I_{Fs} at middle surface in 2006	98
Figure 56 - Variability maps of spatial predictions (left) and variances (right) of I_{Fs} at slip surface in 2006	98
Figure 57 - Variability maps of spatial predictions (left) and variances (right) of I_k at ground surface in 2006	99
Figure 58 - Variability maps of spatial predictions (left) and variances (right) of I_k at middle surface in 2006	100
Figure 59 - Variability maps of spatial predictions (left) and variances (right) of I_k at slip surface in 2006	100
Figure 60 - Variability maps of spatial predictions (left) and variances (right) of I_{soil} at ground surface in 2006	101
Figure 61 - Variability maps of spatial predictions (left) and variances (right) of I_{soil} at middle surface in 2006	102
Figure 62 - Variability maps of spatial predictions (left) and variances (right) of I_{soil} at slip surface in 2006	102
Figure 63 - Variability maps of spatial predictions (left) and variances (right) of I_{geo} at ground surface in 2006	103
Figure 64 - Variability maps of spatial predictions (left) and variances (right) of I_{geo} at middle surface in 2006	104

Figure 65 - Variability maps of spatial predictions (left) and variances (right) of I_{geo} at slip surface in 2006	104
Figure 66 - Variability maps of spatial predictions (left) and variances (right) of I_{geo} at ground surface in 2010	105
Figure 67 - Variability maps of spatial predictions (left) and variances (right) of I_{geo} at middle surface in 2010	106
Figure 68 - Variability maps of spatial predictions (left) and variances (right) of I_{geo} at slip surface in 2010	106
Figure 69 - Translational sliding diagram, infinite slope geometry and parameters	115
Figure 70 - Slope terrain models (β) in 2006 (left) and 2010 (right). Chromatic classes range from 0 degrees (green) up to over 45 degrees (red)	115
Figure 71 - Spatial values of slip surface (left) and friction angle (right) in 2006 and 2010	118
Figure 72 - Spatial values of cohesion (left) and groundwater surface (right) in 2006 and 2010	118
Figure 73 - Spatial values of slope angle in 2006 (left) and in 2010 (right)	119
Figure 74 - Spatial values of FS and P(FS) in 2006.....	123
Figure 75 - Spatial values of FS and P(FS) in 2010.....	123
Figure 76 - Type of uncertainties in soil parameters (source: Vardanega and Bolton, 2015).....	126
Figure 77 - Main components contributing to the total uncertainty of soil properties	128
Figure 78 - Uncertainty in mean values of depth (green) by using survey investigations (red).	133
Figure 79 - Longitudinal profile of the landslide area with stabilization works: draining trenches (pink points) and drainage channels (blue lines)	139
Figure 80 - Variogram and theoretical model for FS and 2010.....	140
Figure 81 - Variability maps of spatial predictions (left) and variances (right) of FS in 2010	140
Figure 82 - Spatial values of FS and P(FS) after stabilization works	143

List of Graphs

Graph 1 - Evolution of the monthly LHC indicator (01/1923 - 05/2010) for the landslide	45
Graph 2 - Frequency of soil texture from surveys in 2006	69
Graph 3 - Frequency of soil texture from surveys in 2010	70
Graph 4 - Frequency of soil compaction from surveys in 2006	70
Graph 5 - Frequency of soil compaction from surveys in 2010	71
Graph 6 - Variogram clouds of I_{CSiSaG} in 2006 (left) and 2010 (right).....	79
Graph 7 - Variogram clouds of I_{CoDS} in 2006 (left) and 2010 (right)	80
Graph 8 - Variogram clouds of I_{Fs} (left) and I_k (right) in 2006	80
Graph 9 - Horizontal variograms and theoretical models for I_{CSiSaG}	82
Graph 10 - Horizontal variograms and theoretical models for I_{CoDS}	83
Graph 11 - Horizontal variograms and theoretical models for I_{Fs} (left) and I_k (right) in 2006.....	83
Graph 12 - Vertical variograms and theoretical models for I_{CSiSaG} in 2006 (left) and 2010 (right) .	85
Graph 13 - Vertical variograms and theoretical models for I_{CoDS} in 2006 (left) and 2010 (right) ...	85
Graph 14 - Vertical variograms and theoretical models for I_{Fs} (left) and I_k (right) in 2006.....	86
Graph 15 - Frequency of I_{CSiSaG} index at different vertical depths in 2006	89
Graph 16 - Frequency of I_{CSiSaG} index at different vertical depths in 2010	91
Graph 17 - Frequency of I_{CoDS} index at different vertical depths in 2006.....	93
Graph 18 - Frequency of I_{CoDS} index at different vertical depths in 2010.....	95
Graph 19 - Frequency of I_{Fs} index at different vertical depths in 2006	97
Graph 20 - Frequency of I_k index at different vertical depths in 2006	99
Graph 21 - Frequency of I_{soil} index at different vertical depths in 2006	101
Graph 22 - Frequency of I_{geo} index at different vertical depths in 2006	103
Graph 23 - Frequency of I_{geo} index at different vertical depths in 2010	105
Graph 24 - Frequency of soil indices at ground surface ($z_{topography}$) in 2006	107
Graph 25 - Frequency of soil indices at ground surface ($z_{topography}$) in 2010	107
Graph 26 - Frequency of soil indices at middle surface between ground and slip surfaces (z_{middle}) in 2006.....	108
Graph 27 - Frequency of soil indices at middle surface between ground and slip surfaces (z_{middle}) in 2010.....	108
Graph 28 - Frequency of soil indices at critical surface (z_{slip} surface) in 2006	109
Graph 29 - Frequency of soil indices at critical surface (z_{slip} surface) in 2010.....	109
Graph 30 - Scatterplot between observed and estimated values of the indices I_{CSiSaG} (left) and I_{CoDS} (right) in 2006.....	110
Graph 31 - Scatterplot between observed and estimated values of the indices I_{Fs} (left) and I_k (right) in 2006	110
Graph 32 - Scatterplot between observed and estimated values of the indices I_{CSiSaG} (left) and I_{CoDS} (right) in 2010.....	111
Graph 33 - Empirical Frequency plots of FS in 2006 and 2010	120
Graph 34 - Cumulative distributions of FS in 2006 and 2010	121
Graph 35 - Probability density curves of FS in 2006 and 2010	122
Graph 36 - Sensitivity of FS in 2006 with different COVs for slip surface	131
Graph 37 - Sensitivity of FS in 2006 with different COVs for groundwater depth	131
Graph 38 - Sensitivity of FS in 2006 with different COVs for slope angle	132
Graph 39 - Sensitivity of FS in 2006 with different COVs for friction angle	132
Graph 40 - Sensitivity of FS in 2006 with different COVs for cohesion.....	133

Graph 41 - Sensitivity of FS in 2010 with different groundwater depths.....	135
Graph 42 - Sensitivity of FS in 2010 with different friction angles.....	135
Graph 43 - Sensitivity of FS in 2010 with different cohesion values.....	136
Graph 44 - Sensitivity of FS in 2010 with different slope angles.....	136
Graph 45 - Sensitivity of FS in 2010 with different ground surfaces.....	137
Graph 46 - Scatterplot between initial and estimated values of FS in 2010.....	141

List of Tables

Table 1 - Causes of soil movement (source: F. Dai, Lee and Ngai, 2002)	11
Table 2 - Terms used in the literature to describe the duality of meaning for "uncertainty" (source: Muller, 2013)	18
Table 3 - Scheme of evaluation methodologies (source: Aleotti and Chowdhury, 1999)	24
Table 4 - Properties of statistical estimators (source: Sigua and Hudnall, 2008)	31
Table 5 - Typical values of the Reliability Index and Probability of Failure	34
Table 6 - Sources of uncertainty (source: Fischer <i>et al.</i> , 2009)	54
Table 7 - Details of geognostic samples in 2006	57
Table 8 - Details of geognostic samples in 2010	59
Table 9 - Details of CPT surveys in 2006	61
Table 10 - SBTn zones per Normalized CPT Soil Behavior Type (SBTn)	63
Table 11 - Estimated soil permeability (k) based on the CPT SBTn	64
Table 12 - Textural class names (source: Whitney, 1911)	67
Table 13 - Soil texture classes and percentage content of sand, silt, clay separates	68
Table 14 - Range of values based on physical characteristics	68
Table 15 - Soil parameters and percentage content converted to numerical coding	68
Table 16 - Range of values for friction ratio and soil permeability by CPTs in 2006	71
Table 17 - Correspondence between some soil lithologies and I _{CSiSaG} classes in 2006	73
Table 18 - Correspondence between some soil lithologies and I _{CSiSaG} classes in 2010	73
Table 19 - Goodness of the regressions applied to soil parameters in 2006 and 2010	77
Table 20 - Empirical values of horizontal variograms for I _{CSiSaG} , I _{CoDS} , I _{FS} , I _k in 2006	84
Table 21 - Empirical values of horizontal variograms for I _{CSiSaG} and I _{CoDS} in 2010	84
Table 22 - Theoretical values of horizontal variograms for I _{CSiSaG} , I _{CoDS} , I _{FS} , I _k in 2006	84
Table 23 - Theoretical values of horizontal variograms for I _{CSiSaG} and I _{CoDS} in 2010	84
Table 24 - Empirical values of vertical variograms for I _{CSiSaG} , I _{CoDS} , I _{FS} , I _k in 2006	86
Table 25 - Empirical values of vertical variograms for I _{CSiSaG} and I _{CoDS} in 2010	86
Table 26 - Theoretical values of vertical variograms for I _{CSiSaG} , I _{CoDS} , I _{FS} , I _k in 2006	86
Table 27 - Theoretical values of vertical variograms for I _{CSiSaG} and I _{CoDS} in 2010	87
Table 28 - Performance criteria between predicted and observed values of the indices in 2006	111
Table 29 - Performance criteria between predicted and observed values of the indices in 2010	111
Table 30 - Constant slope parameters for all tiles	116
Table 31 - Soil parameters and values in 2006 per tile	116
Table 32 - Statistical values of soil parameters in 2006	116
Table 33 - Table 19 - Soil parameters and values in 2010 per tile	117
Table 34 - Statistical values of soil parameters in 2010	117
Table 35 - Empirical Frequency of FS in 2006 and 2010	119
Table 36 - Statistical and Reliability values of FS in 2006 and 2010	122
Table 37 - Sensitivity of FS in 2006 with different COVs	130
Table 38 - Statistical and Reliability values of FS for different COVs in 2006	130
Table 39 - Sensitivity of FS in 2010 with different mean values	134
Table 40 - Statistical and Reliability values of FS for different mean values in 2010	135
Table 41 - Empirical values of FS variogram in 2010	139
Table 42 - Theoretical values of FS variogram in 2010	140
Table 43 - Performance criteria between predicted and observed values of FS in 2010	141
Table 44 - Soil parameters and values after interventions per tile	142

Table 45 - Strength properties (mean and COV value) per soil type.....	172
Table 46 - Strength properties (mean and COV value) per test type (source: Phoon <i>et al.</i> , 2006c)	173
Table 47 - Probability distributions for various soil units (source: Phoon <i>et al.</i> , 2006c).....	174